Making Recycled Carbon Fibres Viable: Enhancement of Thermoplastic Composite Quality & Manufacturing Procedures

INNOVATION REPORT

Christina Froemder

This work is submitted as partial fulfilment of the requirements for the degree of Doctor of Engineering

WMG

University of Warwick

Submitted October 2019.

DECLARATION

I have read and understood the rules on cheating, plagiarism and appropriate referencing as outlined in my handbook and I declare that the work contained in the innovation report is my own, unless otherwise acknowledged.

No substantial part of the work submitted here has also been submitted by me in other assessments for this or previous degree courses, and I acknowledge that if this has been done an appropriate reduction in the mark I might otherwise have received will be made.

Christina Froemder

ABSTRACT

Carbon fibre reinforced polymers are widely applied as a lightweight material with high specific strength in, e.g. wind, automotive and aerospace industry. Production exceeded 150 000 tonnes in 2019 and is expected to grow by 10 % annually. As these materials are used in greater volume, waste increases. Up to 40 % of the waste arises in manufacturing alone. The production and use of recycled carbon fibres (rCF) saves the material from going to landfill and provides a new feedstock source with the same weight reduction and similar fibre qualities, providing further advantages to virgin carbon fibres, such as a lower carbon footprint and significant cost savings. However, the remanufacturing of rCF and closing the loop of carbon composite production faces substantial obstacles: unknown effects of recyclate quality, a lack of interfacial properties and excessive processing time for long rCF applications.

This thesis focuses on commercial composite manufacturing processes and investigates how rCF-reinforced thermoplastics, in the form of commingled nonwoven textiles, can deliver optimised properties. A systematic experimental approach was applied to process the material, which included an extensive number of analytical methods that focused on optical, physical and chemical material characteristics, utilising rCF arising from manufacturing and End-of-life waste in a range of thermoforming processes. The starting point was an isothermal static process with a 110 minute cycle time. Numerous experiments using rapid-isothermal and stamping processes were used to optimise the cycle time and composite properties, targeting industrial applications. The initial focus was on a polypropylene (PP) matrix and this evolved to an investigation of maleic anhydride-grafted PP (MAPP) and modified rCF to enhance interfacial properties.

The results demonstrated that the isothermal process could be improved and produced an optimum process time of 27 minutes. The comprehensive process study enabled cycle times as low as 13 minutes with the rapid isothermal process and down to 1 minute with non-isothermal stamping. Both processes achieved excellent composite properties (maximum tensile strength 225 MPa, tensile modulus 21.3 GPa, 40 wt% rCF in PP), which can outperform glass fibre applications and aluminium. MAPP demonstrated enhanced interfacial characteristics and subsequent mechanical properties (+ 44% in strength) with only a minor increase in production cost (+ 9 %). The results of the rCF treatment highlighted the need for future research into water-based functionalisation.

The research established a comprehensive data set, revealed viable processing methods and proved suitability for mid-volume production, identified significant processing factors, and moved the processing scale of MAPP based nonwovens from lab to pilot scale. This work has improved the understanding of commingled nonwoven material at the industrial sponsor, ELG Carbon Fibre Ltd, in terms of handling and processing. It has also given manufacturers and designers new insight into the material characteristics and demonstrated how it can be used in an economically competitive manner. By making rCF viable, the work contributed to a more sustainable composite industry.

ACKNOWLEDGEMENT

Firstly, I'd like to thank my supervisors, Kerry Kirwan and Stuart Coles, for their help and support throughout the research journey. A huge thanks to my industrial mentor, Mathilde Poulet, for dedicating her time and invaluable feedback. I would also like to acknowledge the Engineering and Physical Sciences Research Council (EPSRC) and ELG Carbon Fibre Ltd. for funding and for giving me the opportunity to conduct such an interesting project within the Centre of Doctoral Training in Sustainable Materials & Manufacturing.

Many thanks to Felipe Cicaroni Fernandes, Peter Wilson, and Neil Reynolds for training, continuous support and technical feedback. Many thanks to WMG's workshop managers and technicians (Luke Millage, Zachary Parkinson, Paul Hadlum, Martin Worrall), their helpful and most competent apprentice technicians and the BUEHLER team (Evans Mogire, Lewis Curry, Mike Green) for their continuous support with material preparation and testing in the best atmosphere. Also, many thanks to the continuous support of Daniel Lester, David Hammond and their team at the Polymer Research Technology Platforms (RTP) at the University of Warwick.

Many thanks to the research teams at Deakin & Swinburne University for the possibility to conduct the international placement at their facilities. Special thanks go to the best research team under the lead of Luke C. Henderson. I enjoyed the time very much at Carbon Nexus and working with James D. Randall, as well as Filip Stojcevski and Andreas Hendlmeier. Thanks to the team for their outstanding research support, and fun times!

I would like to continue with some inspirational people, which I met on this journey and would like to thank Steve Evans, Mark Jolly, Ian Bamford, Fiona, Charnley, Gunter Pauli, Cynthia Adu, Curie Park and Vi Kie So for their inspiration towards a greener future and their insights into circular economy practice.

I am also thankful to my colleagues and in particular Felipe, Peter, , Cynthia, Marco Cinelli, Maryam Masood, Sharron Wilson, Rachael Kirwan, Dan Carlotta-Jones, Lavinia Bianchi and Sue Gibson for their words of encouragement whenever I needed it, continues support on this journey and special coffee breaks.

Also, special thanks to my friends and family. And finally, and most importantly, mum and dad, I could not have done this without you. Vielen lieben Dank!

TABLE OF CONTENTS

TABLE OF FIGURES

LIST OF TABLES

ABBREVIATIONS

ABS	Acrylonitrile butadiene styrene
CA	Chronoamperometry
CAD	Computer-aided design
CD	Cross direction
CF	Carbon fibre
CFRP	Carbon fibre reinforce polymer
CH_3CN	Acetonitrile
CO_2	Carbon dioxide
CV	Cyclic Voltammetry
DIM	Di-iodomethane
DOE	Design of Experiment
DSC	Differential Scanning Calorimetry
ELGCF	ELG Carbon Fibre Ltd.
EoL	End-of-Life
EU	European Union
FTIR	Fourier transform infrared spectroscopy
FVF	Fibre volume fraction
FWF	Fibre weight fraction
GF	Glass fibre
GMT	Glass matt thermoplastic
GMTex	Glass matt thermoplastic textile
GPC	Gel permeation chromatography
HCl	Hydrogen chloride
H_20	Hydrogen dioxide (Water)
IFSS	Interfacial Shear Strength
IM	Intermediate modulus
LCA	Life cycle assessment
LF	Long fibre
MA	Maleic anhydride (e.g. MA5 stands for 5 wt% MA content)
MeCN	Acetonitrile
MAPP	Maleic anhydride-grafted polypropylene
MD	Machine direction

$NaNO_3$	Sodium nitrate
NH_2	Amine group
NMR	Nuclear magnetic resonance spectroscopy
NO_2	Nitrogen dioxide
OVAT	One-Variable-at-the-Time
OWRK	Owens, Wendt Rabel and Kaelble's approach
PA	Polyamide
PAN	Polyacrylonitrile
PE	Polyethylene
PEEK	Polyether ether ketone
PH	Pre-heating
PP	Polypropylene
PPS	Polyphenylene sulphide
Prepreg	Pre-impregnated Fibres
PS	Polystyrene
PU	Polyurethane
rCF	Recycled Carbon Fibre
R	Functional groups (in chemistry)
RTP	Research Technology Platforms
SEM	Scanning electron microscope
SF	Short fibres
SFTS	Single fibre tensile strength
SFPT	Single fibre pull-out test
SG	Surface Generation
SM	Standard modulus
SMC	Sheet moulding compound
$TBAPF_6$	Tetra-n-butylammonium hexafluorophosphate
TGA	Thermal Gravimetric Analysis
TP	Thermoplastic
UP	Unsaturated polyester
UV	Ultraviolet
vCF	Virgin carbon fibre
WMG	Warwick Manufacturing Group
XPS	X-ray Photoelectron Spectroscopy

1 INTRODUCTION

Carbon fibre reinforced polymers (CFRPs) are one of the most used and in demand lightweight materials with high strength to weight ratio. The possibilities of applications seem endless. Rotor blades are developed to be wider and longer, where wind parks can almost achieve the heights of the Eiffel Tower in Paris. But what happens when these materials reach the end of their product lifecycle?

The recycling of carbon fibre (CF) waste is tremendously important for environmental and economic reasons. Up to 40 % of off-cuts can arise at a manufacturing state using CF material [1]. 36 000 t of CF waste, including End-of-Life (EoL) products, was generated in 2015 and is expected to double by 2020 [2, 3]. Losing this considerable amount of high-tech material represents a high loss in value but also a high amount of inherent chemical products on landfill at the expense of the environment. Closing the loop of the carbon fibre composite production is essential to design out waste and make the recycled feedstock viable [4].
Today, carbon fibres can be recovered on a commercial scale [5]. However, with the recycling treatment and due to its waste origin, e.g. textile off-cuts, the fibre strength decreases, hence the composite structure changes from mainly continuous fibre reinforcement to discontinuous applications. Even though the material loses performance, this also opens up new opportunities. New markets have been developed where the virgin material has not been considered before due to the high cost. There is a general trend visible to move away from a linear economy towards a circular approach. The material will be shifted from one sector to another to exploit its full capability.

There is a general concern about the quality of the reclaimed fibres and re-manufactured composites, which results in a lack of demand from industry and therefore an unstable market and price for recyclers. By providing semi-finished products such as pellets, pre-impregnated fibres (prepreg) and carded textiles in addition to the recycled feedstock, the recyclers can show the actual performance with quality control standards and re-insure the industry about the quality of recyclates and products that contain recycled fibres .With this in mind, new areas of expertise need to be covered, including processes for manufacturing composites using different kind of recycled feedstock.

1.1 INDUSTRIAL SPONSOR & AIM OF THE PROJECT

The research covered in the Engineering Doctorate project is about modifications of thermoplastic using recycled carbon fibre and is sponsored by ELG Carbon Fibre Ltd. (ELGCF). ELGCF started in 2003 as an established R&D company, Milled Carbon, and patented the pyrolysis process to reclaim carbon fibre. It started with a pilot-scale furnace to prove the concept. In 2009, the company began the commercialisation of the recycling process under the new name Recycled Carbon Fibre. The installation of an industrial-scale furnace led to the first sales to market. ELG Haniel bought the company in 2011 and from that point it has been known as ELG Carbon Fibre. Nowadays, there is a focus on high volume carbon fibre recovery by mechanical and thermal recycling, conversion to recycled carbon fibre products and quality control. The recycling capacity of the plant exceeds 10 000 tonnes per annum. The company has established several projects looking at how the recovered fibres can be reintroduced to the supply chain. By 2015, ELGCF had already developed a diverse product range of semi-finished materials for the compounding and composite industry, as shown in Figure 1-1, which includes milled and chopped recycled carbon fibres (rCF), from 80 µm up to 50 mm fibre length. The extension of the recyclate market to semi-finished products adds value to the base material but also develops a bridge between recycler and customers.

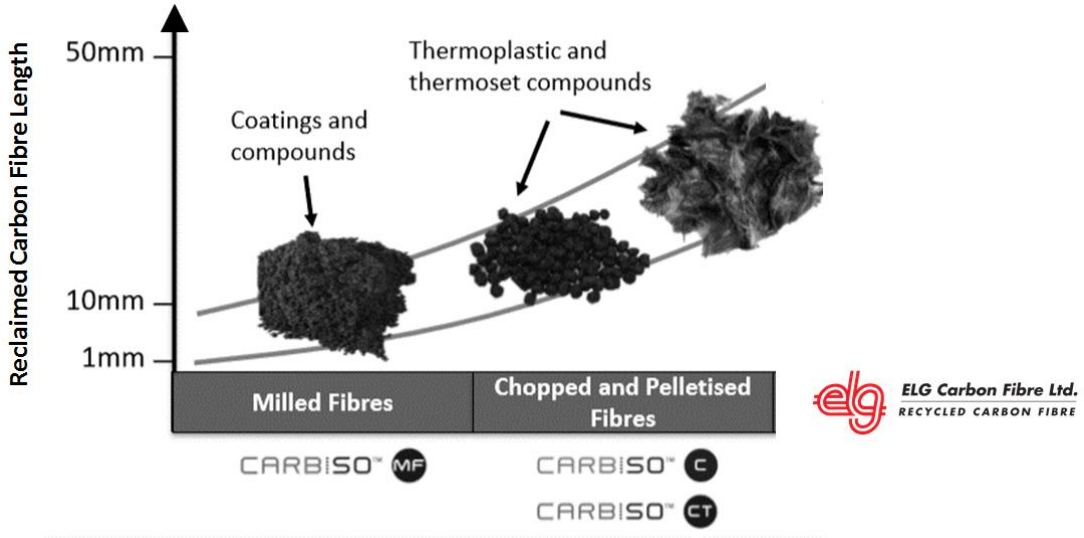

Figure 1-1: Product range of recycled carbon fibres in the form of milled or chopped fibres, as well as nonwoven textiles as semi-finished products developed by ELGCF [6].

Recycled carbon fibre (rCF) has many potential applications in the composites industry. The material can provide a cost-effective replacement for expensive virgin carbon fibres (vCF) as well as modify the electrical, thermal and mechanical properties of base polymers. Nevertheless, long-fibre applications are still missing to use the fibre characteristic for more

advanced composite applications. Secondly, processing rCF and manufacturing composites is still challenging.

In 2015, the company started working with products to offer applications using long fibres (fibre length up to 100 mm) in the form of nonwoven textiles. These textiles would be available in a pure form of 100 % rCF fibres for thermoset applications but also, secondly, commingled version with polymer fibres for thermoplastic applications. To ensure short cycle times and cost-effective reprocessing, thermoplastic polymers are extensively utilised in the automotive industry [7]. Therefore, commingled nonwoven textiles, a mix of thermoplastic polymer fibres and rCF feedstock, form the focus of this project.

The project partner ELGCF is currently processing their in-house manufactured commingled nonwoven textiles by static pressing. The manufacturing trials lead to long cycle times, describing the length of the applied composite manufacturing procedure (e.g. the automotive industry is looking for cycle times below 3 min [8]), of a minimum of 110 min due to slow cooling and heating rates. Other projects reported up to 130 min for the whole process [9], which turns thermoforming of thermoplastics into a time-inefficient process method. By avoiding long cycle times, the production of thermoplastic composites can be further optimised and should make the use of recycled fibre reinforced composites economically viable.

The goal of this research project is to find the most time-efficient processing method of thermoplastics using recycled carbon fibres which is present as a commingled nonwoven textile supplied by ELGCF. Thermoforming of thermoplastic composites is the preferred option to maintain fibre length and reuse long fibres to achieve semi-structural composite properties.

When using thermoplastics, the interfacial adhesion between the matrix and the fibres is moderate compared to thermosets. As such, similar to the production of vCF, rCF is required to undertake a surface treatment to chemically alter the fibre surface before interacting with the target matrix system. Fibre activation or adapted sizing of the fibre is therefore used to both protect the fibre through the production process and also add chemical functionality to the fibre surface that should interact with the thermoplastic matrix [10]. Another method is the modification of the matrix material surrounding rCF, which has been shown in connection with maleic anhydride-grafted polypropylene (MAPP), a chemically modified polypropylene (PP) version [11]–[13]. This modification enables the polymer to increase its polarity and functionality in order to enhance the interfacial performance with the

embedded rCF. Both material modifications, matrix enhancement and fibre treatment, are additionally exploited in this research programme.

1.2 STRUCTURE OF THE RESEARCH PROGRAMME

An in-depth analysis of the carbon fibre supply chain forms the basis of the project. Chapter 2 focuses on the vCF production to understand all process steps and treatments involved, which leads to excellent vCF composite performance. Related economic and environmental challenges are highlighted. It is followed by an overview of recycling strategies and current rCF applications with a focus on thermoplastic composites. Thereby, the benefits and challenges of the use of rCF material are pointed out, which form the research objectives of the project. Further details of the project structure and especially the EngD portfolio with the related submissions are given at that point (Chapter 3), followed by the work developed around the processing of rCF commingled textiles (Chapter 4) and potential material enhancement (Chapter 5). At the end of the innovation report, the outcomes are summarised, and key points highlighted.

The innovation report represents a summary of the performed research undertaken and reported in the attached submissions. The report structure is shown in Figure 1-2, where the submissions are assigned to each chapter. For further details of each sub-project, a reading order is suggested following the submission numbering. Further explanation of the research journey is given in section 3.2. describing the portfolio plan of the research project, after the research objectives have been developed.

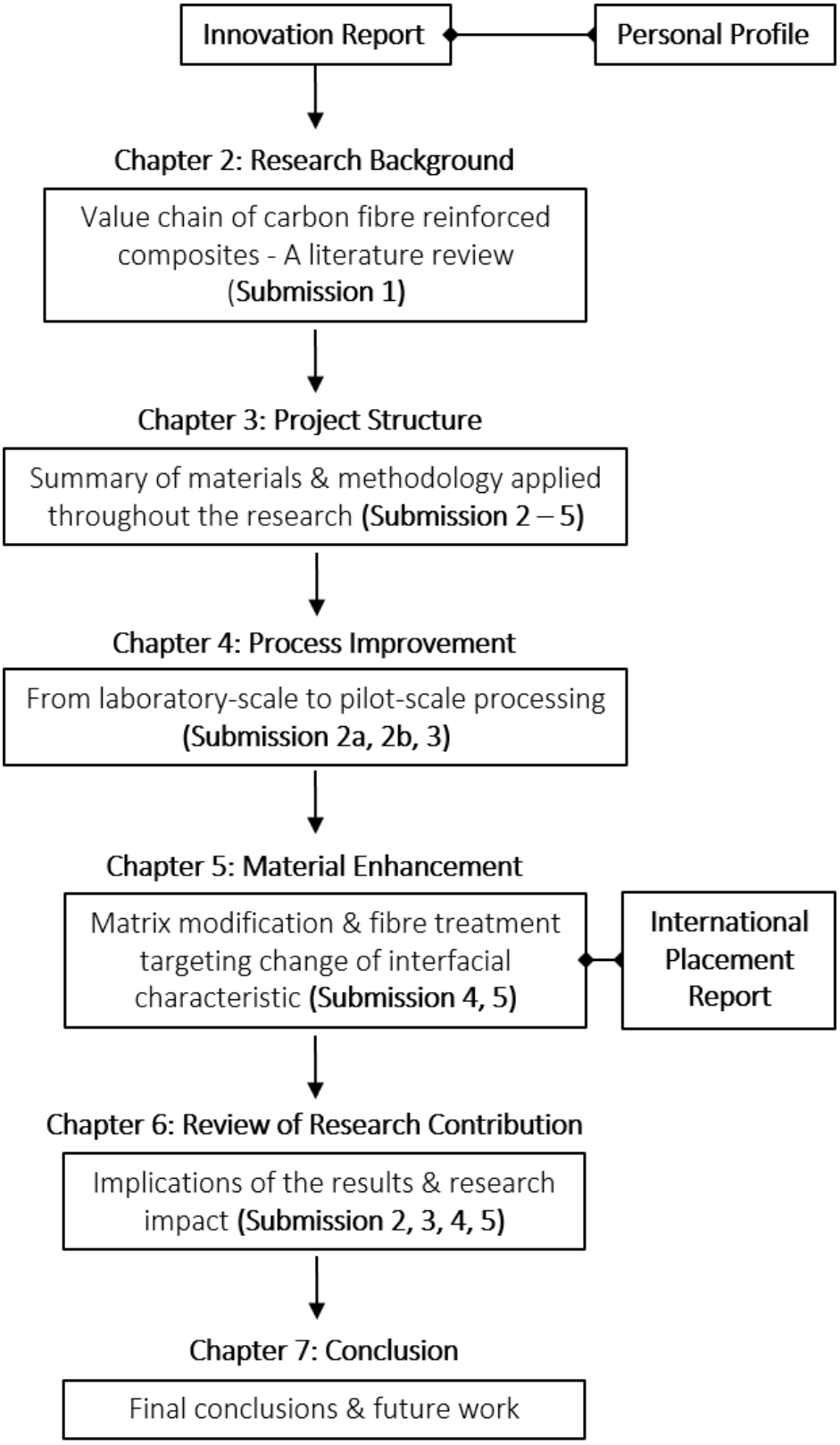

Figure 1-2: Project frame and structure of the innovation report, including a personal profile of the EngD researcher and the international placement report.

2 RESEARCH BACKGROUND

2.1 CARBON FIBRE AS HIGH-TECH MATERIAL

With a growing global population and limited natural resources (specifically fossil fuels) and increasing emissions linked to climate change, the global community is being required to use its resources more efficiently. Nowadays, carbon fibres are renowned worldwide as the "wonder material" [14], a lightweight material driving a greener economy, where the production capacity exceeded 150 000 tonnes in 2019 and is expected to grow by 10 % annually [15]. CFRPs are comprised of the reinforced fibres surrounded by a matrix system. The material is equipped with a unique high strength-to-weight ratio which leads the textile and lightweight material market. The material's mechanical properties and composite quality depend on several factors [16], [17], where the most important are the following:

- Fibre length
- Fibre volume fraction (FVF) and void content
- Fibre orientation
- Matrix type
- Interfacial characteristic

Each factor can be varied and tailored to the target properties, where its manufacturing process from the base material to the final composite is an additional and important parameter to bear in mind.

The reinforcement length can be divided between short, long and continuous fibres of different material e.g. glass, ceramic, natural fibres and carbon. When embedding the fibres in the matrix system, the FVF and fibre orientation play a key role in the level of load transfer, mechanical properties and direction of loading. The CFRP material design is optimised when the fibres are aligned to the direction of loading and contain the maximum possible FVF. It can be distinguished between isotropic (homogenous material properties in all directions) and anisotropic (different material properties in all directions, directional dependence) textile-based material. The final mechanical properties can be estimated using linear equations assuming a simple unidirectional fibre-matrix system. The FVF is the result of the fibre mass, m_f, and the fibre density, ρ_f, as well as the matrix density, ρ_m:

$$FVF\ [vol\ \%] = \frac{1}{1 + \frac{\rho_f}{\rho_m} * \left(\frac{1 - m_f}{m_f} - 1\right)} * 100 \qquad (1)$$

An estimate of the optimum stiffness of the composite can be determined by the rule of mixtures (ROM) [16]. The mechanical performance of applied base feedstock can be predicted under the assumption that fibres are homogeneously oriented in the overall specimen and optimum impregnation without any defects is obtained. It also helps to level the performance of the manufactured samples. Most potential triggers for lack of performance are voids and a weak adhesion between matrix and fibre. The optimum stiffness of a composite E_C (E_f - fibre modulus, E_m - matrix modulus) can be well predicted using the Cox-Krenchel' model [16]. It describes the ROM including fibre length distribution factor η_l and fibre orientation distribution factor, η_o, as shown in Equation (2):

$$E_C = \eta_l \, \eta_o \, E_f \, \mathrm{FVF} + E_m(1 - \mathrm{FVF}) \qquad (2)$$

The fibre length distribution factor can be neglected and therefore is set to η_l = 1. Following the guideline for components targeting no voids can be calculated using the fibre architecture correction factor of $\eta_0 = 1$ for unidirectional composites and $\eta_0 = 0.2$ describing a random orientation of the fibres in 3D direction [18].

The matrix material's function includes initiation and transmitting the applied forces between the reinforcement, fastening the position of the fibres and protecting these from environmental impacts [16]. As the stress properties of the matrix system are limited, the polymer characteristic will determine the appropriate application. The type of matrix material can be distinguished between thermoset and thermoplastic applications. The type of suitable polymer is chosen depending on the potential application of the final component, the target properties and also the level of production volume and consequent cycle time. Thermoset based composites require a curing process to be converted from fibres embedded in a liquid phase to a solid coherent component [16]. The polymer is very durable due to the chemical cross-linking, which takes place during the manufacturing process. However, the final composite cannot be reshaped due to its chemical structure. On the other hand, thermoplastics give the advantage of low-density products, which are simply reprocessed and are gaining increasing popularity for CFRP applications due to their recyclability and shorter manufacturing cycles [19].

The third essential part of the composite is the interface between fibre and matrix, where the load stress should be efficiently transferred between the two components. Damage and fracture in the material are most likely to occur at an imperfect interface and result in undesirable interfacial deboning and cracks [20]. To transfer the properties efficiently from

the fibre throughout the composite it requires not only a suitable matrix material but also an optimum interfacial characteristic between the fibre and the matrix, which can be adjusted by fibre activation or matrix modification. So, the overall composite properties depend highly on the individual material components but also its interface on a micro scale to obtain the best possible target properties on a macro scale. In general, the following three main aspects need to be considered during manufacturing and the quality of the composite needs to be analysed to reach optimum performance:

- Complete distribution of matrix and impregnation of the fibres within the composite to ensure effective load transfer;
- Full wetting of the fibres shows sufficient interfacial properties and promises impactful stress transfer within the composite;
- Aiming for high volume fraction to achieve high strength properties and meet high-performance standards.

Industries such as aerospace, the automotive sector for luxury and sports cars and the energy industry take advantage of the composite material to overcome barriers in weight and size indirectly driven by legal regulations to lower their carbon footprint. Aircraft and other transport vehicles can be made lighter and more fuel-efficient, by moving from steel and aluminium to the usage of composite material. Additionally, their lifespan can be increased by improved durability and corrosion-resistance. Also, wind turbines can exceed their current size with a simultaneous drop in weight compared to the traditionally used fibreglass composites, aiming for higher energy output using plates of up to 88.4 m (type Adwens AD 8-180, [21]). Figure 2-1 visualises a size comparison of the dimension of turbine blades on the market, developed over five years from 2014 and ranging from 164 m (type Vestas V164 8.0 MW, [22]) to potentially 252 m in diameter (type EWEA, [21]). In addition, the Airbus A380 is shown in comparison, which represents the largest aircraft type to date and includes 25 % composite material, with its successor A350 XWB comprising of up to 53 % CFRP material [23].

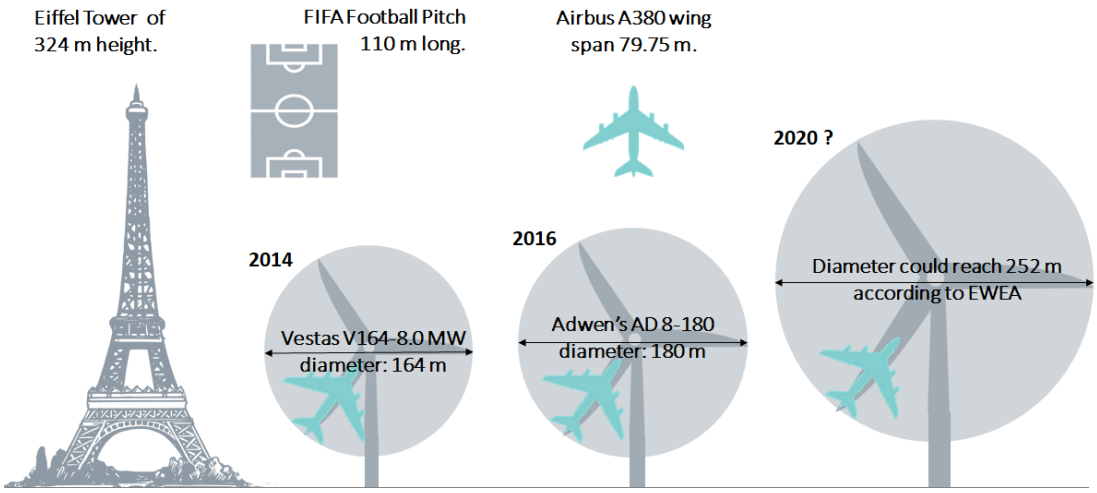

Figure 2-1: Size comparison of the largest wind turbines and aircraft type A380 ccompiling composite material on a larger scale (adjusted from [21]**).**

This image shows the size of exemplary products containing a high amount of carbon fibre material. However, the production, manufacturing and disposal of carbon fibre based products, including semi-finished products (e.g. prepreg, textiles), involves major challenges which are discussed in the following sections.

2.2 THE MATERIAL'S DRAWBACKS

Next to the materials' advantages described in Section 2.1., the composite material production, manufacturing and waste management exhibits considerable disadvantages:

- Production causes high embodied energy
- Inefficient composite manufacturing
- Limited end-of-life strategies

The three main points are described in the next sub-sections.

2.2.1 PRODUCTION CAUSES HIGH EMBODIED ENERGY

A very energy-intense production process is required to develop durable and strong CFs, especially manufacturing polyacrylonitrile (PAN) based CFs. The procedure encompasses an energy-intensive polymer production step from fossil fuels followed by an even more intense series of carbonisation and graphitisation steps obtaining a chemically inert fibre. The long production process, which involves high energy consumption, not only results in high market prices, but also a carbon footprint larger than any other competitive material e.g. steel and aluminium.

Carbon fibres are an industrially manufactured high-performance material made from organic compounds, transformed into a high strength graphite structure by thermal

treatment. The aim of the manufacturing process is a high carbon content using the thermal breakdown of the precursor material at high temperature and to remove most of the constituents other than carbon. The result is the lightest and strongest filament material at micron-scale on the market, resistant to heat, light, chemicals and water.

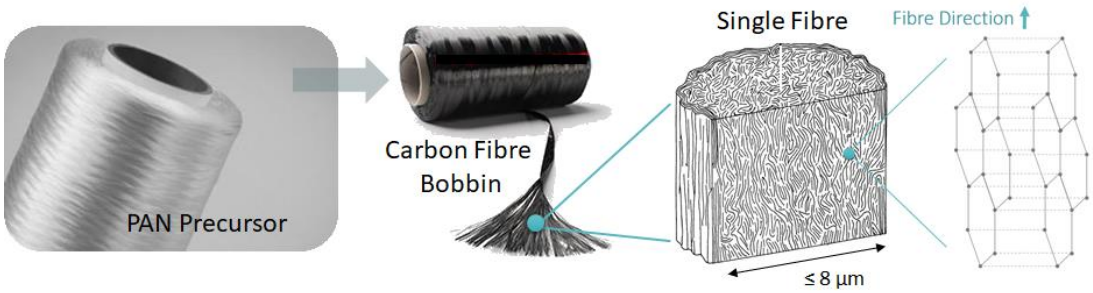

Figure 2-2: Showing origin PAN polymer (left, [7]), developed CF (middle, [26]**) and specific atomic structure of the final vCF.**

Embedded in a matrix, it turns into an advanced lightweight composite with the highest specific strength compared to aluminium and steel. Due to its manufacturing process, PAN-based carbon fibres are composed of a turbostratic structure containing aromatic benzene rings with mostly carbon in-plane [27], as shown in Figure 2-2. Commercially available untreated carbon fibres have a low surface tension, an extremely hydrophobic nature and nonpolar surfaces. Surface treatment and/or sizing is applied at the end of the production line (mainly Epoxy compatible sizing, which includes Polyurethane, PU) to enhance fibre characteristic by functionalizing the surface.

Despite the outstanding material performance of carbon fibres in manufactured composites, researchers and environmental authorities have revealed several downsides, which make them less attractive. One of the main environmental drawbacks can be identified in the carbon fibre production line. Researchers compared the manufacturing process of several advanced materials, as shown in Table 2-1 regarding their embodied energy [28].

Table 2-1: Energy analysis of several different advanced material manufacturing processes (virgin material) [28]

Material	Embodied Energy [MJ/kg]	Material	Embodied Energy [MJ/kg]
Carbon Fibre	183 – 286	Epoxy Resin	76 – 80
Glass Fibre	13 – 32	Aluminium Alloys	196 – 257
Polyester Resin	63 – 78	Stainless Steel	110 – 210

The calculated embodied energy for several advanced materials highlights the impact of the energy-intensive manufacturing process of virgin carbon fibres with it reaching 286 MJ/kg exceeding virgin aluminium with maximum 257 MJ/kg and steel production up to 210 MJ/kg

[28]. It further demonstrates the low energy required for the production of glass fibres (13 – 32 MJ/kg) as well as unsaturated polyester (UP) and epoxy resin. The production of the pristine fibres is cost and energy-intensive exceeding the energy consumption from steel production with the added drawback of not being re-meltable and reusable. When classified as rejected, by-product or having reached end-of-life, only efficient waste management can make the carbon fibre supply chain economically viable and environmentally acceptable

2.2.2 INEFFICIENT COMPOSITE MANUFACTURING

Carbon fibres were developed at the end of the 19th century and since the industrial-scale production of PAN fibres in the 50s the demand has been growing steadily. The main breakthroughs were driven by Airbus and Boeing, both of which are market leaders in the aerospace sector. Their emphasis on novel engineering has reached a carbon composite fraction of over 55 wt% in their latest aircraft models. Boeing B777 (12 wt%) in 1995, Airbus A380 (25 wt%) in 2007, B787 (50 wt%) in 2009and A350 (53 wt%) in 2013 have been noted for exceptional properties and high-quality standards[11, 12]. In 2014, BMW launched the electric car model i3 and first introduced carbon fibre applications as roof panel in the chassis structure to the automotive market for exceptional weight and subsequent power savings [31]. It prompted many to consider carbon fibre composites for high volume production.

However, up to 40 % of the material ends up as industrial by-products throughout the production in the automotive and aerospace sectors and others [32]. The significant volumes of waste arise on a daily basis, making the manufacturing process inefficient and creating a considerable loss in value throughout the supply chain.

To justify these values, the demand for ecologically and economically efficient waste management routes is high and must cope with the 36 000 t of waste generated globally today [33]and a rising amount in future.

2.2.3 END-OF-LIFE STRATEGIES

Continuing with the aerospace sector as an example, the first Boeing 747s manufactured in the late 60s were decommissioned in 2017 [34]and the first A380 Airbus were retired in August 2019 [35] after its first flight in 2006 [36]. These aircrafts and other types of similar age found their way to aircraft recyclers like Aircraft Salvage International (ASI, UK), a company working on aircraft disassembly based at Cotswolds Airport UK. A visit in March 2018 as part of the research programme showed the different steps involved in the complex engineering of extracting valuable components from an aircraft, composed of mostly aluminium parts, after it reaches the end-of-life. After removing parts like turbines for reuse,

or door and cockpit parts for training purposes, the rest of the structure is demolished and, with relative ease, recycled by material type in special facilities. With the new composites technologies being adopted by the aircraft industry as highlighted before, the resulting composite waste is constantly increasing.

The materials placed in landfill remain unchanged for a very long period, maybe forever. With the present pressure on landfill space, this is undesirable [37]. Moreover, due to the advanced nature of its dense carbon structure, the materials are a non-degradable product and requires sustainable waste management solutions. Disposal to landfill was permitted when the material was first introduced to the market. With the implementation of new legislation, carbon fibre waste is banned from landfill in most composite manufacturing countries in the world. In addition, limited recycling facilities exist to recycle the large amount of waste arising globally.

Therefore, there is a demand for waste management and recycling techniques that can keep up with the latest developments. Techniques such as re-melting (the method used for aluminium components) is not always an option when dealing with thermosets which cannot be reshaped due to their chemical structure [19]. Common sources of waste include production scrap fibres, out-of-date prepregs, manufacturing cut-offs, testing materials, production tools and the final EoL components. Carberry [38] estimated the amount of retired commercial aircraft to be 8500 in 2025. Airbus aims to bring 39000 new aircraft to market by 2039 [39] and more will undoubtedly follow. Additional waste will arise from the wind power industry [24, 25], as well as automotive, both with an even shorter lifespan. The general waste hierarchy released by the European Union`s (EU) Waste Framework Directive is shown in Figure 2-3.

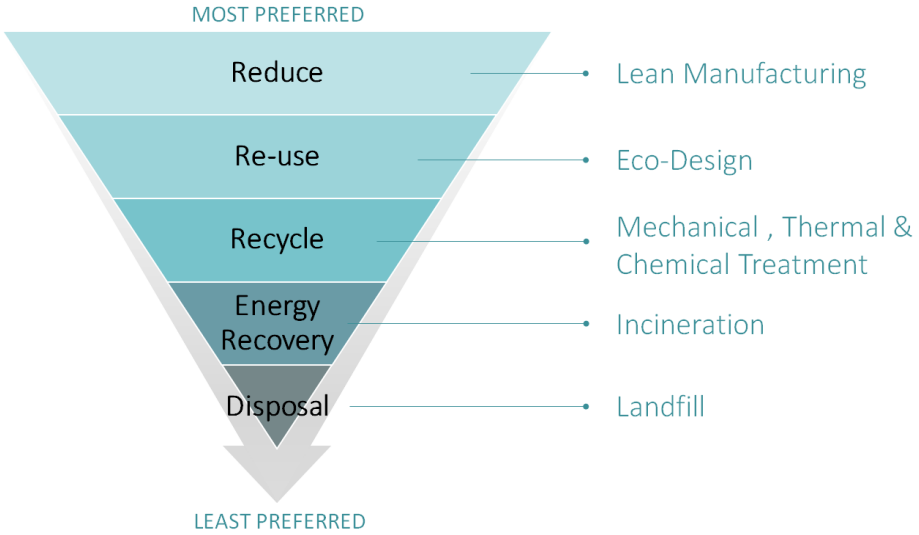

Figure 2-3: EU Waste Hierarchy (modified from [11, 12]) applied on CFRPs.

It classifies disposal as the least sustainable waste treatment and clarifies the importance of prevention [42]. The waste treatment policy also includes a new viewpoint by treating waste as a resource and initiates a comparison between different waste routes. Starting from the least preferred waste management option, carbon fibre and composite waste is banned from landfill in Europe [44] and further restrictions became effective at the turn of the millennium regarding incineration by the EU commission to encourage industry for the recycling route [45]. The potential of energy recovery is based on the type and amount of combustible material[46]. The remaining ash contains residual fibre and fillers, which shows not only limitation in energy recovery of the actual carbon fibre but also the impossibility of clean fibre recycling at an incineration plant. Nonetheless, energy recovery can be implemented in thermal recycling methods to reduce total energy consumption and raise efficiency.

However, because the waste origin is mainly offcuts or demolished parts the fibre size is automatically decreased. From originally being continuous it becomes a discontinuous material with reduced strength. The waste material will be shifted from one sector to another to fully exploit is capability. Regarding the environmental guidelines above, another incentive is the EoL[a] vehicles directive [47] forcing industry to limit their non-recyclable material used in automobile manufacture to 15 %. At maximum, a third of this remaining part can be disposed in landfill whereas two-thirds are allowed to be treated at an incineration plant. Overall, a total recovery of 95 % from an entire vehicle is the manufacturing guideline resulting from the initiative in 2015. In summary, all types of carbon fibre waste mentioned before should be converted into various new products which meet their technology requirements, guidelines and help to make CFRPs more affordable. Reuse and reduce strategies are the most preferred options of waste management, following eco-design and lean principles, respectively. Nevertheless, the alternatives alongside reducing and reusing the waste are not able to eliminate waste. The EoL Directive is, therefore, encouraging the industry to consider effective recycling strategies for their used resources. In the following section, several potential recycling methods are investigated in detail.

2.3 RECLAIMING CARBON FIBRE

At the time of writing, the largest amount of waste is generated during the manufacturing process and includes mainly dry and impregnated fibres. Almost half of the materials used in

[a] Can be between 2 and 40 years.

the manufacture of a product can arise as waste for a complex part, which traditionally was sent to landfill until 2008 [37]. The relation between manufacturing waste and end-of-life components will change over the next decades, whereby end-of-life products will predominate, and manufacturing waste will decrease to almost one quarter. Carbon fibre waste can be treated differently per waste type. There are dry fibres (e.g. offcuts, roll end), fibre from prepreg and fibre from composites (e.g. failed prototypes, end-of-life parts) as categorised in Figure 2-4.

Dry fibre waste (type I) is created during the production and manufacturing process of carbon fibres and carbon fibre textiles. Spool ends, offcuts and off-spec contain similar surface chemistry to the origin and therefore do not require an essential recycling process.

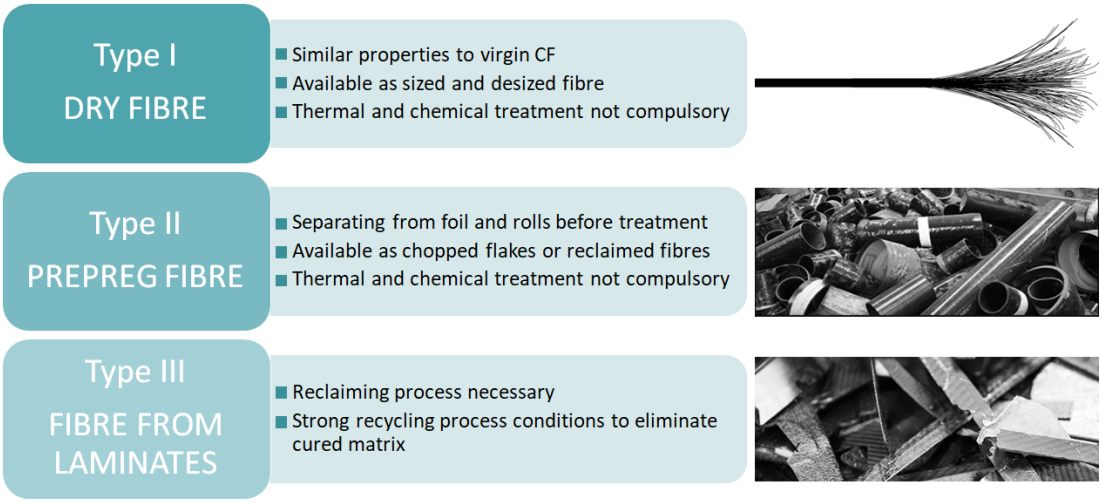

Figure 2-4: Categorising Carbon Fibre Waste in three types, dry fibre, impregnated prepreg fibre and fibre from laminates

Nevertheless, additional treatment, e.g. mechanical recycling, can be used for the standardisation of fibre batches and new sizing applications. Impregnated fibres (type II) can have a similar origin to dry fibre waste but have already been through an impregnation process. In this case, offcuts can be additionally produced after the impregnation of standard rovings or as a production residue during tape laying. Waste also arises during quality control. In all cases, apart from general mechanical recycling, a reclaiming process to separate fibre from sizing and/or matrix is required [5]. Laminate waste includes plain sheets, complex 3D structures, sandwich panel or honeycomb structures, metal integrated composites and other commingled composites (type III). Recycling of composites from prototype production, damage occurrence or EoL parts and reclaiming the reinforced carbon fibres make it more complex but the principle is the same. In the next decade, there will be a shift towards EoL parts dominating the feedstock, but at the moment, manufacturing waste, including dry and impregnated waste dominates the waste bins. Carbon fibre waste

type I and II for re-use and recycling can be either treated in-house or all waste types can be sent to commercial external recycling plants. Apart from ELGCF in the UK, there are also CFK Valley Stade Recycling (DE), Carbon Conversions (US), Karborek (IT), Procotex S.A. (BE) and Carbon Fiber Recycle Industry (JP) as main plants to be mentioned [48], where mechanical treatment and pyrolysis are the main standardised recycling processes.

What happens at the recycler before the actual recycling process starts? All the different feedstock must be sorted and separated. In contrast to virgin fibre production, the feedstock of waste material does not usually have a batch number which can be tracked and used to identify the exact resource and process conditions including fibre type, surface treatment and applied coating. This is one of the main challenges for the recycler, as the required information is usually unknown or remains confidential.

At ELGCF suppliers' premises, the feedstock is segregated by waste type I, II and III manually or automatically. Dry fibres (type I) can be processed immediately. Prepreg fibres (type II) need to be separated from foil and rolls. To process composite waste (type III), several different separation procedures have been developed. After removing the ferromagnetic components with a magnetic separator, small non-ferromagnetic metals can be sorted out using an eddy current separator and its alternating magnetic field. The sink float separator uses the density characteristics of the materials and facilitates an additional refined analysis. Other common types of separating can be highly innovative and automated by implementing detection signals and sensors to detect and analyse chemical or physical characteristics of specific polymers [49].

2.3.1 MECHANICAL & THERMAL RECYCLING ON COMMERCIAL SCALE

Mechanical recycling processes compromise size reduction of dry and prepreg fibre for standardisation, as well as the pre-recycling procedure for cured composite components (EoL products, prototypes). Already known from the plastic industry, high throughput can be achieved using relatively little energy [50]. The waste material is cut, chopped and milled in required sizes from 100 mm down to particles less than 50 µm using shredding and milling machines for all waste types I, II and type III. It can then be further re-processed to e.g. pellets or textiles. The recycled material, called recyclate, is sieved and afterwards classified into powder and fibrous products which contain resin, filler and a proportion of reinforcements (Figure 2-5) [51]–[53].

Figure 2-5: Recyclates from ELGCF in powder, chopped sized short or long fibre form after mechanical recycling process [6]

The recyclate's surface properties are not changed during this procedure and contain coatings, which were applied during the original carbon fibre production process (mainly epoxy compatible sizings). The robust production cycle breaking up the waste material is called downcycling [46]. The resulting fibre breakage can cause both size reduction and an additional decrease in the fibre material properties (if it goes below critical fibre length).

Thermal and chemical recycling procedures require a mechanical recycling step as a pre-treatment to achieve consistency in input material dimension for homogenous further processing (e.g. pyrolysis) and/or due to a limitation in the reactor size, total energy consumption and to decrease logistic effort. These procedures are both described in the following sections.

Thermal recycling processes entirely reclaim fibres from the composite scrap using high temperatures. The thermal breakdown decomposes the resin and separates the fibres and fillers diminishing the original fibre properties as little as possible. Depending on process type the matrix combusts, were this complies with environmental standards or gets broken down to a low weight molecule structure for further use [5]. Thermal treatment can involve a pyrolysis process as well as an extension by using microwaves or the fluidised bed process.

The pyrolysis process is the only available recycling process on a commercial scale at the time of writing other than mechanical recycling. Pyrolysis results in a thermal split of the resin while a high temperature leads to the breakdown of the long molecule chains into smaller particles in a furnace in the absence of oxygen. The recycled carbon fibre feedstock will be cut and ground into manageable pieces. In the case of ELGCF, the furnace is a linear continuous transport system which the material is conveyed through. It comprises a tunnel with two heating portions, a cooling part and a closing spot. The first heating part covers the main chemical decomposition at a high temperature (higher compared to the second stage), which can be tailored to the type of matrix or composite being processed. The resin is converted mainly into gas and removed from the fibres. The second heating part is used to select and control the char removal from the treated fibres at about ~ 500 °C, which is called

polishing. In the end, the recycled material is cooled before the residual fibres will be collected in receptacles.[23, 39]

Even so, the pyrolysis process, which is currently considered to be the only commercial thermal recycling process, has difficulty retaining efficient energy consumption and uniform treatment of fibre feedstock [46]. As the coating type and amount of fibre feedstock are sometimes unknown, the residual fibre differentiates in surface quality. Inefficient treatment or overtreatment can occur, which results in either remaining sizing, char, or oxidation damage [55]. Therefore, it is the responsibility of the recycling company to set up a proper contract with their waste suppliers, so all that information can be known, and the recycling treatment can be optimised and adjusted to the input feedstock. With regards to the affected single fibre it can cause a decrease in interlaminar shear strength with the matrix or a general decrease in mechanical performance. Regarding composite properties, it can, therefore, increase the variance and inconsistency of test results. Nevertheless, a recently published review of currently available recycling methods highlighted the pyrolysis process as the most advanced waste management options [43].

2.3.2 OTHER RECYCLING METHODS (LAB & PILOT-SCALE)

An advanced version of the pyrolysis process involves microwave heating instead of an energy-intense burn-off. The electro-conductivity of carbon fibre causes absorption of microwaves in the scrap material. There is a potential to recover the matrix and reduce the energy input compared to the general used pyrolysis process due to the fast heating rate[56]. Similar to the original pyrolysis process, residual char worsens the final mechanical properties in composite due to low adhesion and high fibre length distribution appears [5], where the residual fibre quality depends on process time and strength. Researchers from the University of Cranfield (UK, [43]) ranked the upgraded process on the lower TRL scale 3, meaning the concept has been proven to have value but the pilot-scale has not yet been established.

The fluidised bed process is a type of gasification where preheated air is constantly blown through an air distributor plate followed by a sand bed which gets fluidised. Once a temperature of approximately 500°C is reached, shredded CFRP fills the bed. After several cycles, the matrix combusts in the hot stream of air and the reclaimed fibres blow out to be collected afterwards in a connected cyclone. The process is used for mixed and contaminated composites, including metal parts and sandwich constructions. Organic contaminants such as mineral oils and facing paints are volatilised with the polymer matrix while inorganic solids

such as metal inserts sink in the fluidised bed and will be removed during the cleaning process [57]. The hot combustion products pass another combustion chamber where the polymer is fully oxidised [51]. This process was developed by Pickering and his research team at the University of Nottingham in 2008 and has proven to be suitable for commercialisation using an up-scaled pilot plant, which has involved Boeing since 2012 [58]. The main advantage is that the fluidised bed method can treat all types of waste, especially EoL parts. Currently, the challenging obstacle is the somewhat destructive process which impacts final fibre length and performance passing three size reduction steps before the actual reclaiming process.

Solvolysis describes a chemical recycling process where a solvent is used to break down the coating and/or matrix including their chemical bonds and reclaim the embedded fibres. Alcohols (e.g. propanol, ethanol), nitride acid and also water, neat or with catalyst, are used as potential solvents in the supercritical phase and have been discussed in the last decade [59]. In principle, the solvent flows through the reactor and the waste material is continuously heated up to a process temperature of around 250 - 400°C under pressure from 5 - 30 MPa. At this stage, the fluid is in a critical condition, between the liquid and gas phase [5]. At this point, the polymer matrix is split into lower molecular weight constituents, which can be further processed and the fibres are released intact. Supercritical fluids have received much attention in the industry because of their tuneable properties depending on operating conditions including temperature, pressure and volume.

2.3.3 RECYCLATE FIBRE QUALITY

As well as the need to be economically sustainable, fibre quality and easily processable output material are the key requirements for future recycling methods. Table 2-2 gives a summary of the three main types of thermal recycling in respect of the loss in single fibre tensile strength (SFTS) and fibre modulus. It can be shown that pyrolysis performs in the least harmful way and protects the fibre strength characteristic most, compared to microwave heating and the fluidised bed process. However, it was reported by Oliveux *et al.* [5] that the surface quality is more uniform when processed with the fluidised bed technique than using only pyrolysis and there is a potential for improvement and commercialisation. Whereas microwave heating can have a negative impact of up to 20 % loss in strength, there is a loss in fibre strength from the fluidised bed process of over 25 % of its initial strength. In general, limited comparable data has been reported in previous projects for the fibre modulus characteristic.

Table 2-2: Overview of SFTS Test results comparing the impact of recycling methods (values in brackets refer to the compared untreated fibre properties).

Process	Fibre Type	Fibre Modulus	Fibre Strength	Reference
Microwave Heating	Grafil 34-700	**- 13 %** (242 GPa)	**-20 %** (4.09 GPa)	Lester [56]
Fluidised Bed	Grafil 34-700	**+ 4 %** (242 GPa)	**-25 %** (4.09 GPa)	Lester [56]
	Toray T800	**+ 8 %** (308 GPa)	**-18 %** (5.986 GPa)	Pickering [58]
	Toray T600SC	**- 4 %** (232 GPa)	**-33 %** (4.098 GPa)	Wong [60]
Pyrolysis	Toho-Tenax	n/a	**-4 %** (3.712 GPa)	Meyer [55]
	HTA	n/a	**-4 %** (4.55 GPa)	Pimenta [4]
	Hexcel AS4	**- 7 %** (242 GPa)	**-10 %** (3.19 GPa)	Akonda [61]
	Cytec TR505	**+ 4 %** (356 GPa)	**-15 %** (6.965 GPa)	Jiang, Pickering
	Toray T800s	**- 7 %** (356 GPa)	**-2.5 %** (6.965 GPa)	[62]

The available data on fibre modulus before and after undergoing different recycling treatment shows less impairment and occasionally improved modulus properties by the recycling process than shown for SFTS. The exclusive focus on fibre strength properties, in of the majority of the reviewed projects, could indicate that this property requires closer attention as it subsequently will have a more significant effect on the mechanical composite properties for new applications. The microwave heating method promises more a eco-efficient process performance as well as added value in the form of recovered matrix vapour. However, future research needs to focus on optimising process parameters and subsequent fibre performance. The fluidised bed method loses most of the single-fibre-tensile-strength due to the aggressive process. A new way to replace the destructive mechanical recycling method has been developed by applying high voltage fragmentation [63]. Prepreg tapes are electrodynamically treated and fibre fragments detach from EoL parts successfully but this has only been studied on a laboratory scale for now. The solvolysis process promises uniform and good fibre quality as well as retained fibre length (Table 2-3).

Table 2-3: Overview of single-fibre-tensile-strength test results comparing the impact of solvolysis recycling methods.

Process	Fibre Type	Fibre Modulus	Fibre Strength	Reference
Water + O_2	Toray T300	n/a	**±0 %** (vCF: 3.11 GPa)	Bai [64]
Acetone + H_2O_2	Toray T700	n/a	**-5 %** (2.81 GPa)	Li [65]
n-Propanol	Grafil 34-700	**- 5 %** (242 GPa)	**-5 %** (4.09 GPa)	Hyde [66]

However, the associated equipment can be very expensive as it must withstand the exceptional conditions. Solvents and catalysts can be toxic and impede separation and eco-friendly waste management. Additionally, residual contaminants such as the remaining solvent on fibre surface can inhibit interphase impairment and final mechanical performance. Adherent Technologies (US) combines pyrolysis with solvolysis but do not count as an official recycling plant and currently only supply the machinery commercially. The inventor of the process has been developing an improvement and is close to commercialisation, as reviewed in the latest report by Composite UK and partner universities [48].

2.4 GENERAL BENEFIT OF USING RECYCLED FEEDSTOCK

The previous sections presented the unique properties of CF and its life cycle from the virgin material to recycled feedstock. The man-made chemical structure of carbon fibres leads to its subsequent high-end performance but also prevents from possible natural decomposition as an option for waste disposal at the end of its life cycle. Instead, it provides the base for reusing the material and closing the material's loop for numerous life cycles.

After the recycling process, the recycled feedstock can be distinguished between milled and ground particles (≤ 1 mm), short (≤ 40 mm) and longer (≥ 40 mm) fibres, giving a wide range of available products and possible future applications. Looking at applications of successfully reclaimed fibres into new thermoplastic composites, which promised simply processability and recyclability, the following material characteristic were identified:

- Small CF particles, ranging from milled feedstock to ground composites, were successfully applied as polymer filler using injection moulding to boost its mechanical properties, e.g. acrylonitrile butadiene styrene (ABS) [67], [68], polyethylene (PE) [69] or PP [68], [70].
- Short fibres used as ground or chopped prepreg, mechanically recycled dry tow or reclaimed from CFRP were successfully implemented to outperform neat polymer properties from PP [11], [12], [71], polyphenylene sulfide (PPS) [72] to advanced polyether ether ketone (PEEK) [73], but also keeps up with short fibre composites using glass [74] or virgin carbon fibres (discontinuous) [11], [12], [72], [73], [75], [76].
- Long fibre applications showed high potential towards advanced performance and can achieve almost continuous fibre composite performance [73], [77]–[79]. Long fibres in the form of commingled textiles were processed exclusively using compression moulding with the difference of having chopped tow, prepreg or manufactured yarns as a base material.

The examples above show the large variety of potential applications reusing recyclates. These come with several benefits, which are summarised in the following:

- Saving the material (which can be supplied as new feedstock source) from landfill
- Providing the same weight reduction as using virgin carbon fibre feedstock
- Gaining a lower carbon footprint for using the recycled material than relying on virgin feedstock material for any new product life cycle
- Experiencing up to 98 % of virgin fibre quality when looking at the fibre strength properties after the material has gone through the recycling process. The fibre strength properties are more affected by the reclaiming procedure than its stiffness as highlighted in Section 2.3.3.
- Extensive cost saving of up to 40 % compared to virgin material.

2.5 CHALLENGES TO OVERCOME

Looking at the application of recyclates in new components, the final number of products which can be found today on the market, is still limited. It shows a low acceptability of recycled material by engineers and designers, who are the initiators in the supply chain to use the material as alternative to virgin carbon fibres. The knowledge gap and missing expertise in processing thermoplastic composites containing recycled feedstock within this young industry might be the reason and need to be addressed.

The carbon fibre production itself can be traced back to the 1940s with the first mass production at the Nemours Foundation, now known as DuPont [16]. However, the recycling and reutilisation of industrial by-products from the entire supply chain started shortly before millennium, where the first documented research project looked into the potential of thermoplastic applications in the form of long fibre and chopped prepreg in PEEK dealing with waste from the aerospace industry [73]. Reclaiming CF was commercialised in 2003 by ELGCF. Since then, the interest in this field is has increased, as measured by the published papers on the subject. This can be traced back to the increased penalties which were introduced to prevent carbon fibre waste from landfill, but also shows a commitment to a more sustainable industry closing the loop of the carbon fibre supply chain.

As summarised in Chapter 2.4, researchers initially investigated small particles and short fibre thermoplastic applications. Subsequently, the focus included long fibre applications. Taking advantage of the fibre length and its strength, the thermoplastic composite performances could then be levelled in intermediate to the highest category when using long reclaimed fibres.

Generally, the subsequent use of thermoplastic matrix systems gives the advantage of low-density products. With fast production cycles high volume output would be guaranteed. An additional opportunity to use low-cost polymers with recycled carbon fibres could turn composite production into a viable manufacturing process. However practically speaking, the remanufacturing of recycled carbon fibre and closing the loop of carbon composite production is still a huge challenge even when considering recycled carbon fibres as a viable feedstock. The following three main things have been identified as barriers to the successful implementation and market launch:

- Excessive process stages of processing long fibre rCF applicable in industry,
- Unknown effect of recyclate quality on processing and composite performance,
- Poor to moderate interfacial characteristic between rCF and thermoplastic polymers.

Further details are given in the following subsections and form the overall base of the research conducted in this project.

2.5.1 EXCESSIVE PROCESSING TIME FOR LONG FIBRE APPLICATIONS

A lack of industrially applicable process methods was identified as a primary challenge facing recyclates to, firstly, turn the reclaimed chopped long rCF into textiles and, secondly, manufacture composites.

Currently, only the production of nonwovens, as developed by ELGCF, demonstrate cost-efficient processing possibilities. An alternative is re-spun yarn from discontinuous fibres, where the material takes advantage of the aligned fibre orientation and the final composites show comparable higher level of performance than the general nonwoven applications [80]. Nevertheless, the costs involved in the yarn production are higher due to more involved process steps (preparing nonwoven, spinning nonwoven, yarn development). Additionally, brittle fibre structure can lead to increased failure modes in the preparation of yarns and subsequently in the component which can be traced back to lack of extensive industry experience.

When examining the processing of such nonwovens, extensive cycle times in the composite production creates obstacles. Here, further investigation is needed to consider material processing and composition and to provide the opportunity to optimise the properties of the final component, targeting low cost products, by applying high volume manufacturing. The general use of thermoplastic fibres is a common approach to reduce the polymer flow distance [81]and was adopted in this research programme with the use of ELGCF's

commingled thermoplastic nonwoven products. The production process is kept simple and cost-efficient and the composite manufacturing process theoretically only involves a quick consolidation process. Compression moulding is the most preferred option to maintain fibre length and reusing long fibres achieves semi-structural composite properties [82].

The project partner ELGCF is currently processing their nonwoven textiles themselves into semi-finished products. However, the static pressing trials produced cycle times of a minimum of 110 min due to slow cooling and heating rates. Also other projects reported substantial cycle times above 50 min [83] and up to 130 min [9], which turns compression moulding of thermoplastics into an inefficient process method. By avoiding such long cycle times, the production of thermoplastic composites can be further optimised and should make the use of recycled fibre reinforced composites economically viable.

2.5.2 UNKNOWN EFFECT OF RECYCLATE QUALITY

Knowing the wide range of composite applications (prepreg, laminates, dry fibre etc.) and several possibilities to recycle industrial by-products coming from the carbon fibre supply chain, the variety of recycled products is steadily increasing. So, due to the different waste origins and treatment levels, fibre quality varies between recycling plants. Researchers are working on more efficient recycling processes where the fibre properties can be fully retained and the matrix material can be recovered, but no recycling process can yet achieve these conditions on a commercial scale. However, the main obstacle towards efficient reuse of rCF feedstock is the limited information given about the source of processed rCF material and their specific base material characteristics. With limited information given, the learning outcomes from reviewed academic research projects may not be comparable to one another thereby casting a question mark over adaption and further development. In addition, residual char has been reported on pyrolysed fibres [69], [79], the effects of which are still unknown. Researchers assume that it can negatively impact the interfacial characteristic between the recycled fibre and the new matrix, leading to loss in macro-mechanical composite properties. However, these need to be further investigated and research might confirm the opposite. When working with any kind of recycled feedstock, a comprehensive base material characterisation helps to understand its nature and subsequently any effect of future modification of the base material and final composite system. Working closely with a recycler, like in this research project, gives the advantage of being able to investigate different waste streams and compare the overall composite performance in relation to the rCF base material and processability.

2.5.3 THERMOPLASTIC COMPOSITE INTERFACE

Thermoplastics were chosen as matrix system for this work to reduce the manufacturing conditions to a minimum in terms of cycle time and subsequently enlarge the possible production volume. However, thermoplastic composite applications are still limited as the matrix material has a limited amount of reactive functional groups (e.g. polyolefin group, especially polypropylene) available to interact with the fibre. A lack of interfacial bonding and general wetting can lead to insufficient interfacial properties and stress transfer, which impact the macro-mechanical composite performance [16]. This can be explained by polarity and surface energy imbalances between CF and thermoplastic polymers. This challenge can be overcome by introducing missing functional groups on the fibre surface to attract the matrix material or the use of more advanced polymers (e.g. grafted polypropylene). Both options are further investigated in the following subsections to find possibilities applicable to rCF thermoplastic applications.

2.5.3.1 MATRIX MODIFICATION

The modification of the matrix material surrounding rCF is often shown in connection with maleic anhydride-grafted polypropylene (MAPP), a chemically modified polypropylene (PP) version [11]–[13]. The modification enables the polymer to increase its polarity and functionality in order to increase the interfacial performance with the embedded rCF. MAPP possesses a hydrophilic characteristic and good wettability and is therefore used commonly as coupling agent or compatibilizer of natural fibres [84]–[87], glass fibres [88], recycled carbon fibres [11], [12], [89], [90] and mixed recycled plastic (e.g. PP/PET [91], PS/PP [92] and PA12/PP [93]). With improved processability and polymer flow it can decrease the void content of the final composite part and prevent penetration of water and other fluids, like chemicals or gases and subsequent crack initiation. In choosing the application of the material, tensile strength properties were paramount, but tensile modulus also shows a sufficient increase with the addition of 5 wt% coupling agent. The optical investigation is often used to show a clear trend towards increased wetting using the MAPP as coupling agent (Figure 2-6, adapted from [12]).

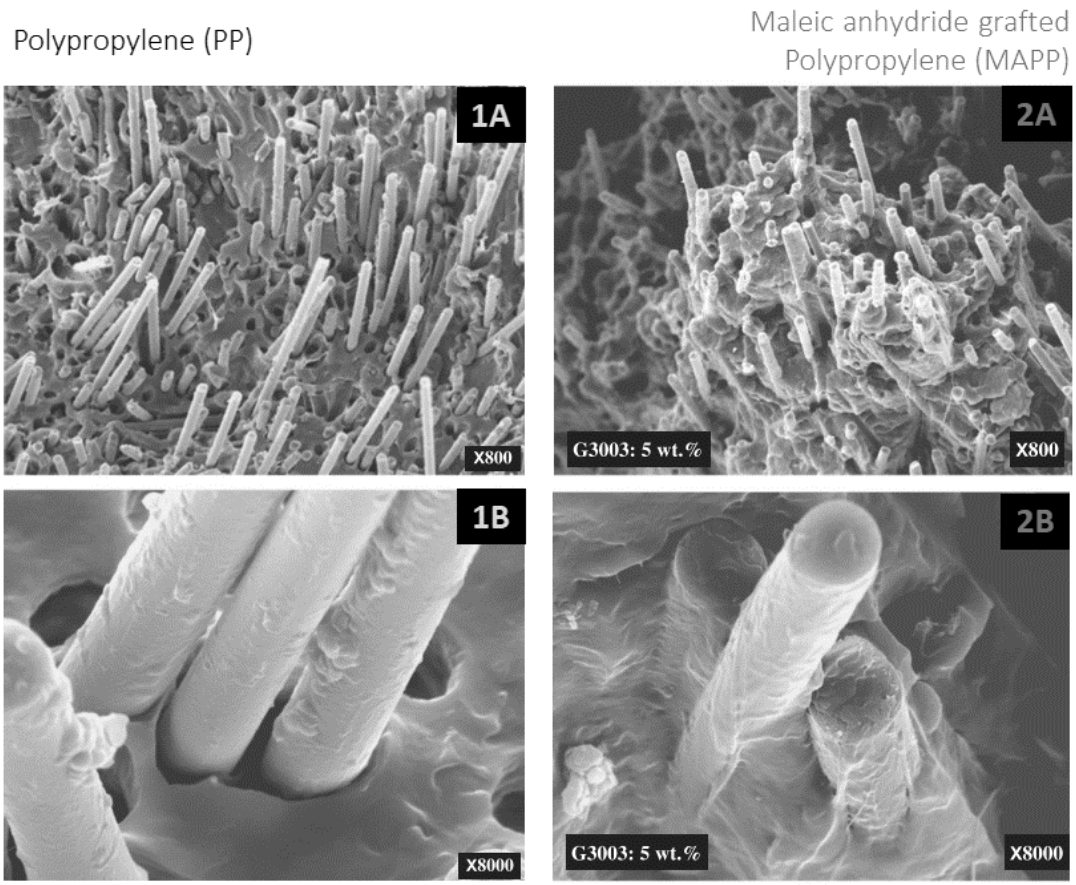

Figure 2-6: SEM images of the fracture surface of tested composite tensile samples showing a comparison of the interfacial characteristic of neat polypropylene/ rCF (1A, 1B) and polypropylene coupled with MAPP/ rCF (2A, 2B), here 5 wt% of G3003 coupling agent on different magnification [12].

The sample without coupling agent (Figure 2-6, 1A) shows only slight bonding between matrix and fibre (called debonding), and the relatively long fibre pull-out (1B) indicates a low adhesion. Using a coupling agent, the fibres are entangled by the matrix efficiently (2B) and the fracture after mechanical testing appears to be through the matrix as desired.

Therefore, using MAPP shows a good alternative for rCF applications to enhance the interfacial characteristic between the matrix and the fibres. However, the actual effect can depend on the rCF quality and need to be proven with any new material source, like rCF from ELGCF. In addition, the increased cost accompanied with the use of more advanced polymers was not mentioned in the above studies but is an important criterion for the choice of material applied in industry and will be further investigated in this project. The effort of efficient recycling and re-treatment must lead to revenue using waste material. By achieving the target and enhancing the interfacial and thus final composite performance of remanufactured carbon fibre composites to its optimum, the balance between expenditure and revenue was targeted.

2.5.3.2 FIBRE TREATMENT

An alternative to the matrix modification is the fibre treatment. As such, similar to the production of vCF, rCF require surface treatment to chemically alter the fibre surface before interacting with the target matrix system. Fibre activation or adapted sizing, which describes a thin layer covering the fibre, are used to protect the fibre through the production process, but it also adds functional groups to the surface that should interact with the thermoplastic matrix [10].

Generally, in the carbon fibre industry, an electrochemical treatment is followed straight after the carbonisation process when producing virgin carbon fibre material to bias the chemically inert and smooth surface. The electrochemical treatment is commonly applied for vCF in the form of an oxidative treatment using nitric acid (HNO_3), ammonium sulphate ($(NH_4)_2SO_4$), or ammonium bicarbonate (NH_4HCO_3) as electrolyte [94]–[96]. The sizing is a separate and sequentially placed process after rinsing in water and drying (Figure 2-7). Here, the relationship between the electrochemical surface treatment and sizing need to be considered, whilst its complexity and efficiency depend on each treatment as well as the compatibility with the fibre and the targeted matrix system [97].

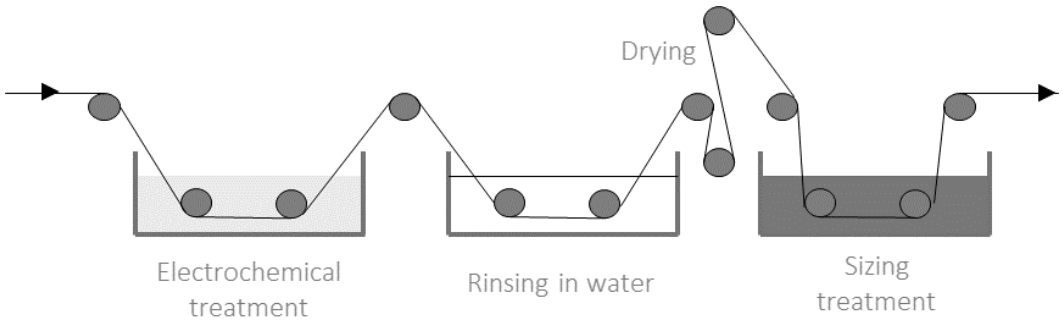

Figure 2-7: Schematic of the applied surface treatment for vCF after the oxidation and carbonisation process.

Particularly rCF need to be handled with care because they have already undergone a recycling treatment to recover from its primary state after a certain life cycle and before possible re-treatment. Here, an overlapping of functionalising effect (from possible surface treatments and/or applied sizing) leading to undesirable offsets need to be investigated for both processes. For example, the epoxy compatible sizing, detected on mechanically recycled fibres, impedes this phenomenon in thermoplastic applications but can be traced back to its original purpose as virgin fibre, where the fibre surface was modified for mainly thermoset applications.

Overall, the improved processability and interfacial properties, as well as involved cost should be in line with the sustainable aspect of the applied treatment targeting a thermoplastic matrix system, as mentioned earlier. These aspects narrowed down the current available rCF treatments dramatically [98], [99] and initiated further research to find additional alternatives like the use of ionic liquids and electrochemical grafting:

- **Sizing** consists mainly of a polymer solution (water or solvent-based), which can be applied continuously e.g. in a bath or as a spray [100]. Satisfactory results were achieved when the sizing was a similar polymer to the target matrix system [101]. Epoxy sizing on rCF works well with functional polymers like PA6 [98], if not handled with care this can lead to the opposite effect hence weakening the interface and subsequently increasing the potential susceptibility to fracture of the final composite [102]. Silane coupling agents are a common sizing used for natural and glass fibres to protect and functionalise the surface [16, 17] [19, 20]. Small polyester particles enhanced the chemical bonding [107]. Bio-based content of PU and PEI sizings can be increased when modifying the sizing [108], [109]. General drawback when applying to low-cost rCF feedstock the cost-intense sizing.
- Applying **ionic liquids** (e.g. a salt in liquid state at room temperature) was proven to be successful for direct fibre-matrix interface [110] and shows potential as green chemistry for the future [111], [112]. A combination of surface grafted amines and ionic liquid does not negatively affect each other's functionalisation effect and rather synergistically results in increased interfacial performance [96]. However, ionic liquids were not further investigated at the time of writing due to the rarity and price of raw materials. However, despite the high cost of the ionic liquids today, the effect of treating recycled fibres could be explored in future projects by replacing virgin material with ionic liquids recovered from outsourced batteries or wastewater [113]–[115].
- **Electrochemical grafting** describes a common method applied in industry, as mentioned earlier. The treatment is used as preconditioning when manufacturing vCF to functionalise the chemicals inherent in the fibre surface to support a good adhesion to selected matrix systems [16]. Research by Gnaedinger *et al.* [10] has shown that the electrochemical treatment removes the upper inert layer of vCF and simultaneously activates the surface by adding functional groups. After a successful reaction, functional groups like -COH, -COO or -COOH can be detected on the carbon fibre surface. The actual treatment takes only a few seconds and is a huge advantage

to other new developments. However, the high energy consumption related to this process and potential reduction in single fibre tensile strength are exclusion criteria to be applied for rCF. Here, the level of salt concentration and type, as well as the applied current are the main parameters which can be configured for optimum results.

The latter treatment, electrochemical grafting, showed the highest potential for rCF applications New alternatives, like water-based grafting methods, are investigated in this research project to prove their viability and applicability to industry.

2.6 POTENTIAL OF THERMOPLASTIC COMPOSITE APPLICATIONS USING RCF

Overcoming all the challenges listed in Chapter 2.5. and turning the waste into a cost-advantageous light-weight material, we would avoid landfill and produce lower emissions compared to the use of virgin material. The successful implementation of rCF material back into the materials loop could open new market opportunities and contributes to the economic efficiency and environmental sustainability of the carbon fibre supply chain. Figure 2-8 shows a summary of mechanical performances using rCF material in thermoplastic composites showcasing the potential of these thermoplastic composite applications.

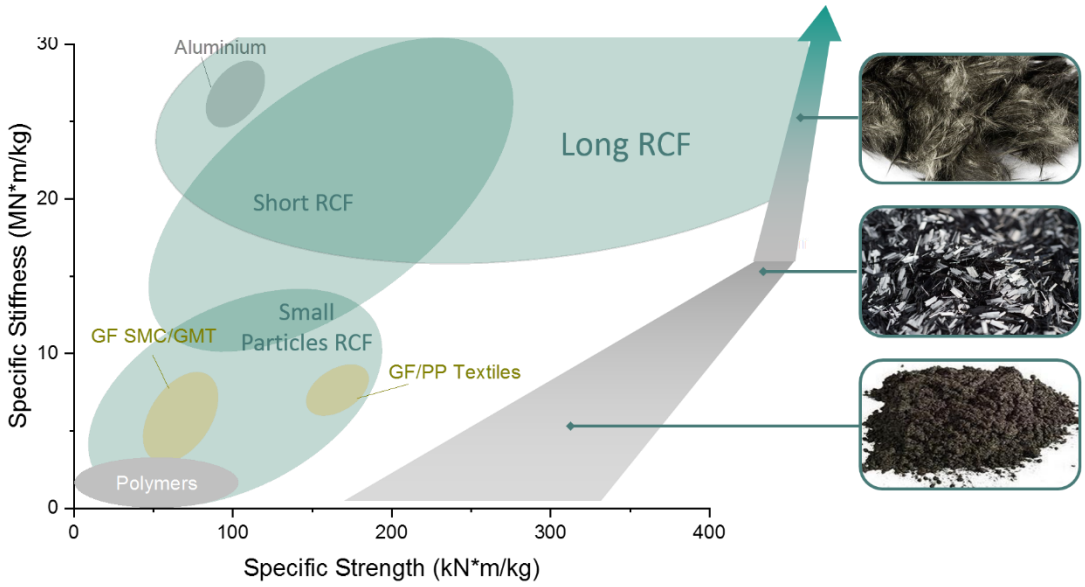

Figure 2-8: Comparison of examples of rCF thermoplastic composite performance regarding tensile strength and stiffness using various polymers (figure derived from literature review [Appendix A]).

Regardless of the waste source, it shows that the recycling and subsequent use in new composites is a viable alternative to the use of advanced polymers and virgin feedstock. The fibres and fragments are used as a filler to boost the mechanical performance of the virgin

polymer and simultaneously decrease the cost. The filler can enhance the electrical conductivity of the virgin polymer [69]. Short fibre composites using recycled feedstock demonstrate remarkable characteristics in combination with PP and polyamide 6 (PA6) matrix, and representing the main polymers applied in the automotive industry for non-structural to semi-structural applications [116].

Depending on the fibre length, the re-utilisation of rCF ranges from filler, to wet-laid and dry-laid nonwovens or further processing to staple yarns and subsequent textile. However, thermoplastic composites utilising long fibres show great potential for high-performance applications. A wider range of research projects focused on short fibre composites underlining the primary market focus when introducing the reuse of rCF as feedstock. Chopped fibres are easier to process and achieve tensile properties of comparable performance when using chopped virgin feedstock and can also outperform glass or natural fibre applications with additional weight savings. The rCF reinforced thermoplastics may find uses in many applications such as body panels in the transport industry, where modular design, quick manufacturing for mid-volume production, low carbon and cost-efficient material usage are the main drivers for innovative and more sustainable developments. Converted electric bikes for delivery purposes or fully recyclable motorcycle are just two examples of many (Figure 2-9).

Figure 2-9: Modular e-mobility design with examples showing Gogoro VIVA motorbike (left, [117]**) and the EAV cargo bike (right,** [118]**).**

EAV Cargo's body structure is based on natural fibre thermoset composites [119]and the Gogoro motorbikes contain 100 % PP in their exterior design [117]. Replacing these with rCF thermoplastic composites would produce weight saving and cost reduction which would lead to higher revenue. The potential properties using long fibre rCF could provide highest stiffness and strength of the lightweight material and forms the focus of this research project.

3 PROJECT STRUCTURE & METHODOLOGY

3.1 RESEARCH OBJECTIVES

The summary of current recycling processes, their different outputs in quality and chosen remanufacturing processes with final performance was given in Chapter 2. It was noted that the commercialised pyrolysis process is mainly used as a reclaiming process and it achieves the highest volume throughput and least losses in final fibre strength. The reported projects using the reclaimed feedstock almost exclusively work on a laboratory-scale and lack pilot-scale development which would close the carbon fibre composites supply chain and bringing the recycled feedstock back to market. With a focus on manufacturing using recycled carbon fibre, simple and cost-efficient processes are required to limit extra expenses and promote profit. A short cycle time for high volume applications is targeted for industrial applications. The ideal composition of the nonwoven textiles and their processing route formed the starting point of this project. A combination of nonwoven textile production followed by a fast thermoplastic manufacturing process promised a cost-efficient production route for recycled carbon fibre reinforced composites.

The research question, which has been developed during this review and was considered during this research project, is the following:

How can the commingled thermoplastic nonwoven material be processed and modified to compete in a competitive market environment?

Long fibre applications show the highest potential for high-end applications and were the focus of this study. The following main research objectives of the project were developed:

(1) The nonwoven, as semi-finished product, showed the highest potential for cost-efficient processing in mid to high volume applications. The initial focus of the research project will be their process conditions:
   - How can the textiles be best processed targeting a fully impregnated composite and optimum distribution of matrix and rCF within the composite to ensure effective load transfer?
   - Aiming for high volume fraction and low void content to achieve high strength properties, what are the shortest cycle times achieved in this context?

(2) An addition of maleic anhydride leads to significant increase in tensile strength performance of rCF/PP composites. A general variation in the final composite quality can be traced back to the variation in recyclate quality, which were undergone different recycling treatment. Therefore, future work needs to establish a benchmark on ELGCF feedstock properties when processed to laminates. Additionally, the following questions need to be answered:

- How does the feedstock from ELGCF perform in conjunction with MAPP and what is the optimum amount of MA towards the highest composite properties?
- How does residual char affect the composite properties?
- How does the material composition affect cost and performance?
- Does a possible fibre treatment targeting several matrix systems open wider opportunities?

3.2 PORTFOLIO PLAN

The developed portfolio plan provides guidance through the report and attached submissions (Figure 3-1).

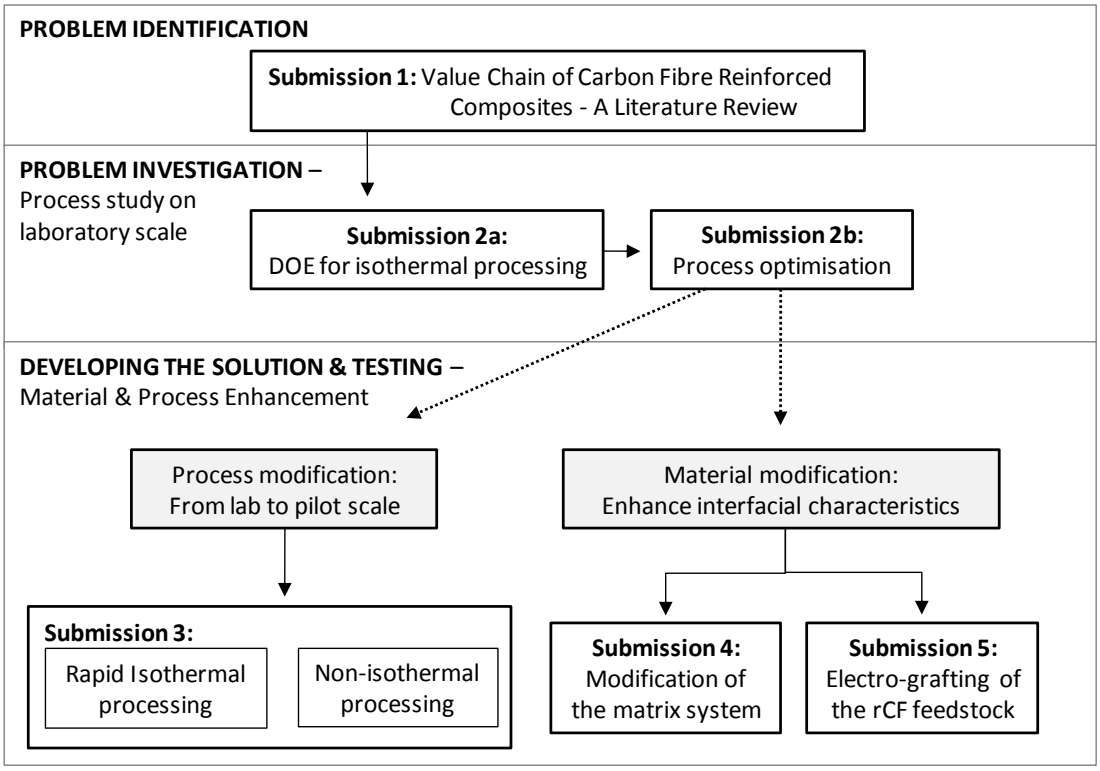

Figure 3-1: Established portfolio plan for this project relating to the attached submissions.

The research background in Chapter 2 defined the base for initial process studies on laboratory scale where the material is investigated under isothermal conditions (Submission 2A, 2B). Further process improvements have been developed in Submission 3, where the process was upscaled from lab to pilot scale.

Investigations regarding material enhancement with a focus on the matrix system are discussed in Submission 4and the fibre treatment study is summarised in Submission 5. These submissions both look at material enhancement and refer to process standards developed in previous submissions (2B, 3). Therefore, it is suggested to go through the submissions applying the portfolio plan.

3.3 SYSTEMATIC EXPERIMENTAL APPROACH

The experimental work was based on two different methods, design of experiments (DOE) and one-variable-at-a-time (OVAT). The principle of both methods is explained in this section.

The DOE approach is a statistical method which limits the number of samples required by using several specified process parameters. This is an efficient experimental procedure and produces reliable outcomes. The technique helps to understand and gain knowledge about a specific manufacturing process and shows its impact on the process itself.

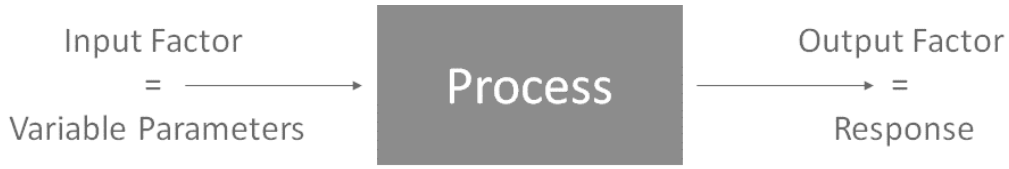

Figure 3-2: Schematic of the DOE approach.

The DOE approach can screen through variations of parameter combinations and identifies the key input process variables for an optimum output performance with only a limited amount of experimental runs [120], [121]. For the initial set of experiments, it is necessary to screen the identified variable parameters (input) , where the level of impact on the quality (output) of the manufactured composite is analysed (Figure 3-2).

Therefore, the aim is to decrease the total amount of reviewed process parameters in the first phase using a fractional (1/2) factorial design with two levels (-1, +1). It is also known as the Placket-Burman Screening and helps to eliminate insignificant variables [122]. The interaction order for the DOE analysis is limited to two. For the applied screening design repeats are desired but not required, as it was developed to gain a fast overview of process variables. Later, a focus on residual parameters with significant influence on two or more levels (-1, 0, +1) is advised for a more comprehensive study to find the optimum settings for the best output performance.

An alternative way of studying several parameters on a new machine or process is the principle of OVAT, which changes one variable at the time and keeps all the other parameters fixed [123]. In contrast to the initial DOE approach, this requires a considerable amount of testing material, time and depends on experience, but allows detailed analysis to see a trend in behaviour change by varying the parameters step by step.

3.4 CHOICE OF MATERIALS

Project partner ELGCF produces several types of raw material at their facility, which include milled fibres, short tow and longer fibres. Longer fibres are further processed in-house to nonwoven textiles providing a semi-finished product with a variety of possible applications. The textiles are available as a pure rCF product, but also commingled versions including polymer fibres (Figure 3-3).

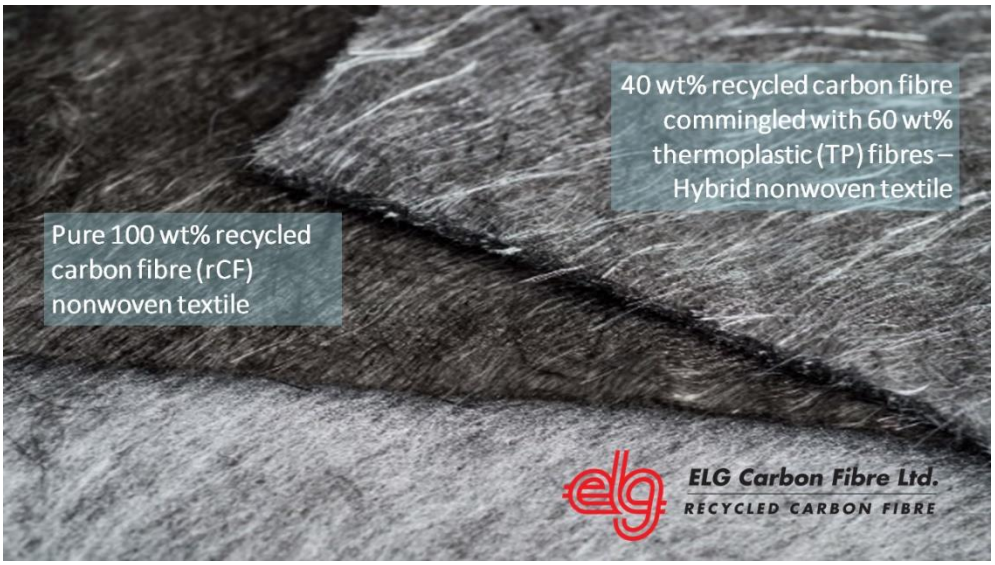

Figure 3-3: ELGCF nonwoven textile range from pure rCF to commingled textiles versions [6]

The 100 % rCF textiles are used for thermoset applications, whereas the commingled textile is exclusively applied for thermoplastic composites. This project focuses on the commingled thermoplastic nonwovens which is a semi-finished product with the potential to be recyclable and processed within short cycle times. When heat and pressure are applied, the commingled textiles can be processed to composite components. The distributed polymer fibres within the textiles promise short impregnation distance for the more viscous polymer to penetrate the entire textile efficiently, targeting a high quality and void-free component. The process and material investigations in this project looked at a variety of different recycled carbon fibre feedstock and types of thermoplastic, which is summarised in the next two sections, 3.4.1 and 3.4.2.

3.4.1 RECYCLED CARBON FIBRE FEEDSTOCK

Repurposed recycled material was supplied by ELGCF. The feedstock ranges from dry chopped fibre, which was mechanically recycled, to pyrolysed feedstock derived from the same origin and cured laminates. SM45D, IM56D, IM56R and IM56L fibre types were considered for comparison representing the main feedstock currently processed in volume by ELGCF. A fibre classification matrix established by ELGCF [124] is adopted and summarises the essential characteristics of the carbon fibre types given by the supplier ELGCF in Table 3-1. In addition, the experimentally determined fibre diameter was added.

Table 3-1: Fibre Feedstock Categories supplied by ELGCF with its specifications [124]**.**

Fibre Type	Recycling Method	Feedstock Source	Fibre Length [mm]	Fibre Diameter [µm]	Tensile Strength [GPa]	Tensile Modulus [GPa]
SM45D	Mechanical	Dry fibre, sized	60 - 100	5.42 ± 0.29	4-5	≤ 270
IM56D	~	~	60 - 100	4.96 ± 0.11	5-6	270 < E < 330
IM56R	Thermal	~	60 - 100	5.39 ± 0.07	5-6	270 < E < 330
IM56L	~	Cured laminate	60 - 100	5.54 ± 0.16	5-6	270 < E < 330

The types can be grouped by recycling method, source, tensile strength and modulus ranging from standard to intermediate modulus and tensile strength between 4 and 6 GPa respectively. Chopped tow, indicated by abbreviation D (dry fibre), are mechanically recycled fibres and contain an Epoxy compatible sizing covering the fibre. Fibre classification containing the abbreviation R (pyrolysed dry fibres) and L (pyrolysed prepreg laminates) are chopped fibres which have been thermally recycled. The SM45D fibre category describes fibres with standard modulus and a tensile strength of 4 to 5 GPa. The waste stream originates from dry fibres and textile off cuts. The material is chopped to a standard length of 60 – 90 mm in fibre length, where the fibres are covered with a certain sizing depending on the fibre origin and its previous purpose and application as shown in the Figure 3-4 below.

Figure 3-4: Schematic of mechanically recycled fibre feedstock SM45D and IM56D from textile source to chopped fluffy fibres, which are covered by a sizing.

Also, the IM56D fibre category describes a mechanically recycled fibre type, which is chopped to the same standard length. However, it`s fibre properties are more advanced, having higher modulus (intermediate level) and a tensile strength of 5 to 6 GPa. The optical investigation of the fibre types shows a smooth surface finish of sized SM45D and IM56D fibre feedstock. (Figure 3-5).

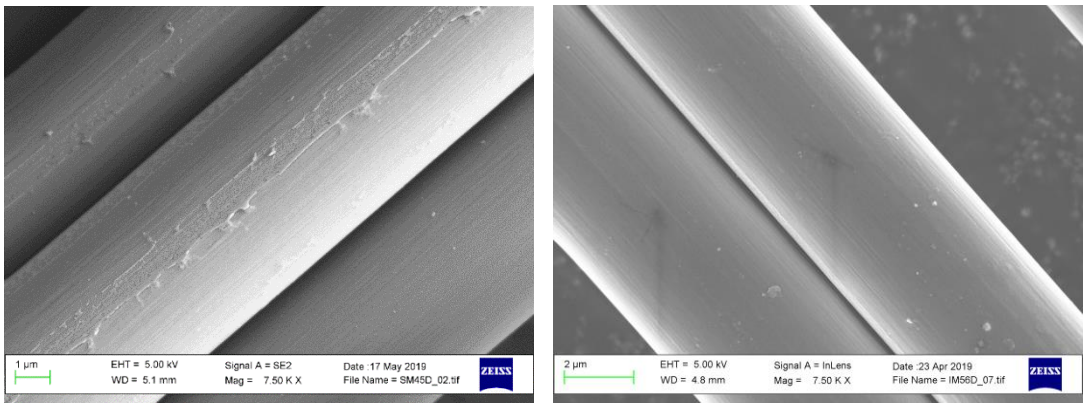

Figure 3-5: SEM images showing mechanical recycled CF covered with epoxy compatible sizing: (A) SM45D and (B) IM56D fibre.

The IM56R fibre category describes pyrolysed fibres which arise from the same waste stream as IM56D fibres (Figure 3-6). The thermal treatment (pyrolysis) removes the sizing from the fibres, so the fibre surface can be modified afterwards and targeted to a new matrix system or other application.

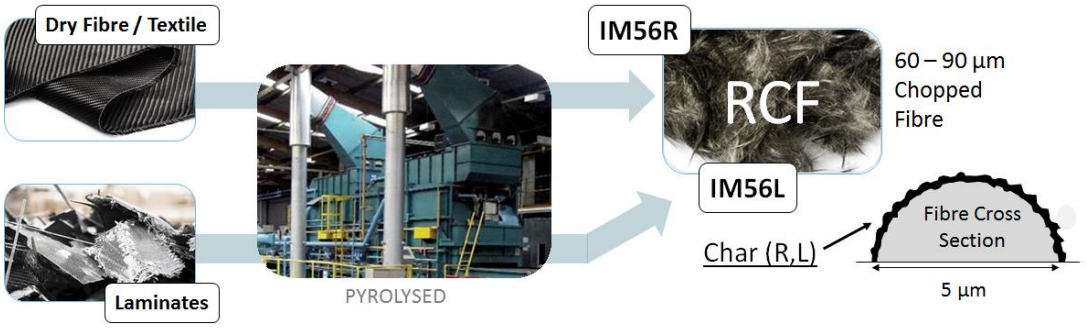

Figure 3-6: Schematic of thermally recycled (pyrolysed) fibre feedstock IM56R and IM56L from textile source to chopped fluffy fibres, which are occasionally covered by char residuals.

The predominant samples of IM56R fibres showed a clean and grooved surface, but also sometimes excess quantities of residual char (Figure 3-7).

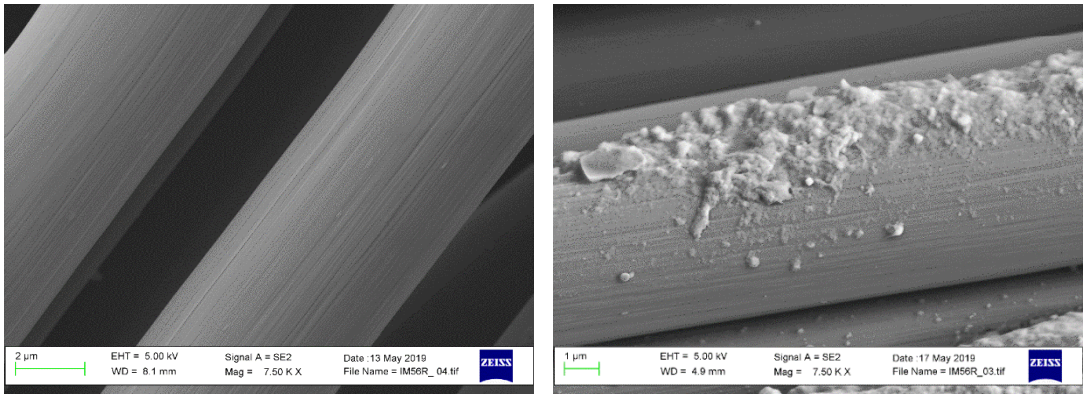

Figure 3-7: SEM images showing pyrolysed IM56R recycled carbon fibre with the varied appearance of (A) clean and low grooved fibres or (B) with excess quantities of residual char.

The fibre category IM56L is also thermally treated. But due to a different waste origin, in this case cured laminates, the recycling treatment requires higher temperature and a longer process to remove the cured matrix system and reclaim the fibres. Similar appearance to IM56R showed the microscopic evaluation of IM56L fibre batches, where mainly clean fibres can be seen. But from time to time fibres were covered with excess quantities of residual char (Figure 3-8).

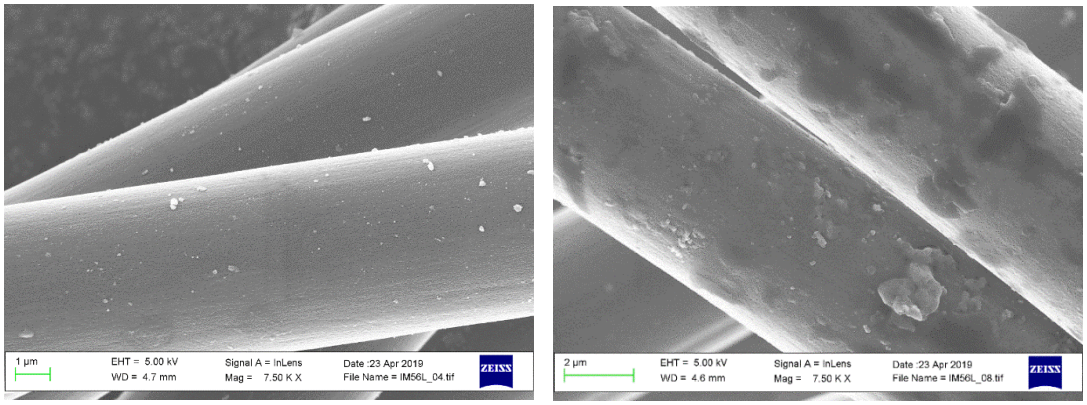

Figure 3-8: SEM images showing pyrolysed IM56L recycled carbon fibre with the varied appearance of (A) clean and smooth fibres or (B) with excess quantities of residual char.

3.4.2 THERMOPLASTIC MATRIX

The polypropylene (0.905 g/cm^3) matrix material was present in forms of filaments (60 mm, 3.3 dtex, homopolymer), supplied by a European supplier. Further information regarding the MAPP polymer is given in Chapter 5.1. The same PP matrix material in the form of filaments is applied in all process and material studies.

3.4.3 COMMINGLED NONWOVEN TEXTILE

To date of research, most of the recovery processes of rCF on an industrial scale yield discontinuous fibre feedstock for further processing, development and application [2]. Targeting advanced mechanical performance for future applications, especially high strength materials with a specific alignment of fibres within the composite (Figure 3-9) is fundamental to fully utilise the fibre properties [16]. Composites oriented in directions additional to the axial fibre direction can promote multi-directional properties. With a focus on thermoplastic composites, the commingled textile structures can be distinguished in (1) commingled mixtures of thermoplastic and reinforcement fibres or homogenous yarns, (2) plied matrix around the reinforced fibre, (3) thermoplastic powder impregnation and (4) commingled yarns in specific woven fabric form [81].

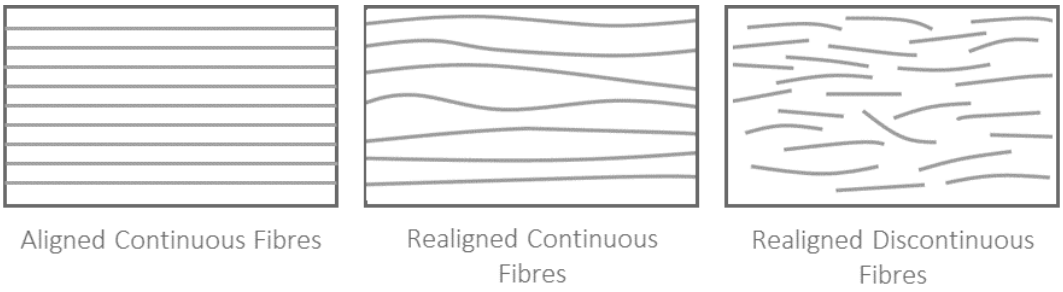

Figure 3-9: Reinforcement fibre architectures showing aligned continuous fibres, realigned continuously and realigned discontinuous in a composite (adapted from [125]**).**

All types target a low flow distance of the relatively high viscosity of thermoplastic matrix systems for optimum impregnation when processed into a composite. Nonwovens are textiles with random or aligned filament orientation joined by physical (e.g. interlocking, friction) or chemical bonding mechanism. Filaments can be single fibres, or a bundle of fibres joined to yarns. The large variety of possible process combinations are leading to a wide range of nonwoven textile types.

Project partner and material supplier ELGCF is manufacturing dry-laid carded nonwovens based on physical bonding mechanism which is post-processed via needle punching. Figure 3-10 highlights the process schematic of the carding process on a laboratory scale at ELGCF. The thermoplastic filaments are dispersed homogenously in the textile and promise a short flow path when melting to subsequently fully impregnate the carbon fibre web. The general industrial mechanical nonwoven formation can be distinguished in the opening, the carded web formation and the cross-lapping process [27].

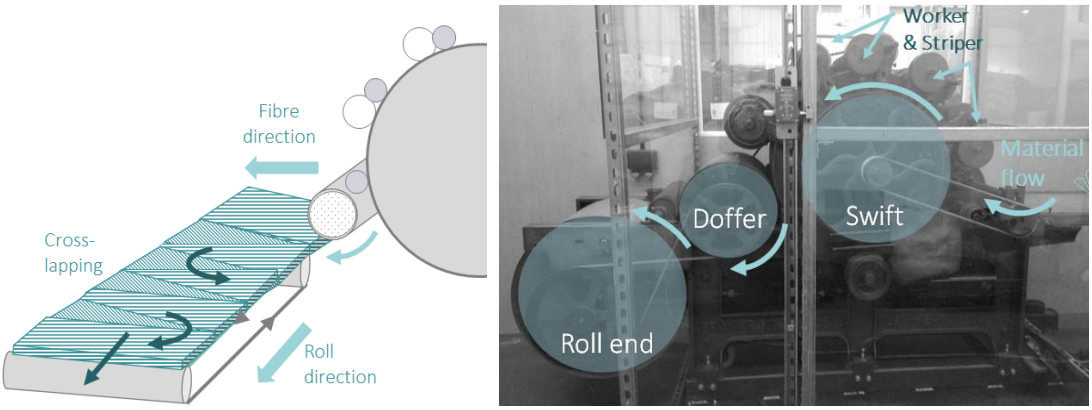

Figure 3-10: Schematic of the carding process to produce nonwoven textiles at ELGCF for research purpose. Green arrows indicate the material flow.

The initial opening stage separates single fibres for a homogenous mixture throughout the textile process. Subsequently, all feedstock passes through the blender to be mixed with thermoplastic fibres before transferring to the carding organ. At the beginning of the research project, all material was collected from the roll end. During the study, an additional step was introduced to the process with further development on the process by ELGCF, the cross-lapping. The cross-lapping allows the surface area to be adjusted according to customer demand. Subsequently, a change of the main fibre direction perpendicular to the final roll direction occurs, as demonstrated in Figure 3-10 (left). With the cross-lapping method, the textile web is turned by 90 degrees and therefore the carding direction makes the transverse textile direction.

When looking at the textile itself, derived from the laboratory scaled line at ELGCF, a first observation showed a general accumulation of carbon fibres or polymer fibres in the form of grey to white areas on the surface of the textiles (Figure 3-11, left). Zooming in closer using a stereo microscope, fibre bundles were detected throughout the samples in the textiles produced on the laboratory scaled line (Figure 3-11, right).

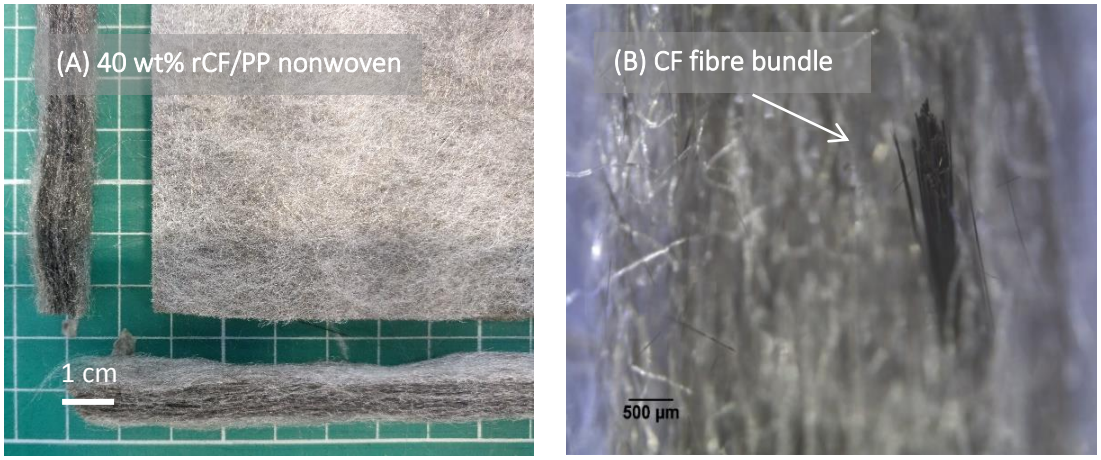

Figure 3-11: Representative textile probes from laboratory scaled textile line at ELGCF containing (A) 40 wt% rCF/PP with (B) occasional fibre bundles in between.

The accumulation of fibres can lead to stress concentration in this particular fields. It can impede the composite analysis where equal distribution is a key when analysing the effect of different process conditions. In the course of the research project, ELGCF also acquired a new textile line on an industrial scale (Figure 3-12). In this case, slitters are in place to cut off the edge for a perfect finish after the needling step. Metal detectors help to clean the textile and prevent future composite tooling from damage by needles enmeshed into the web. A final fibre areal weight – in-line measurement system (gram per square meter, calculates the textile weight) and does quality control and the accumulator at the end of the process line is placed to secure a continuous production line.

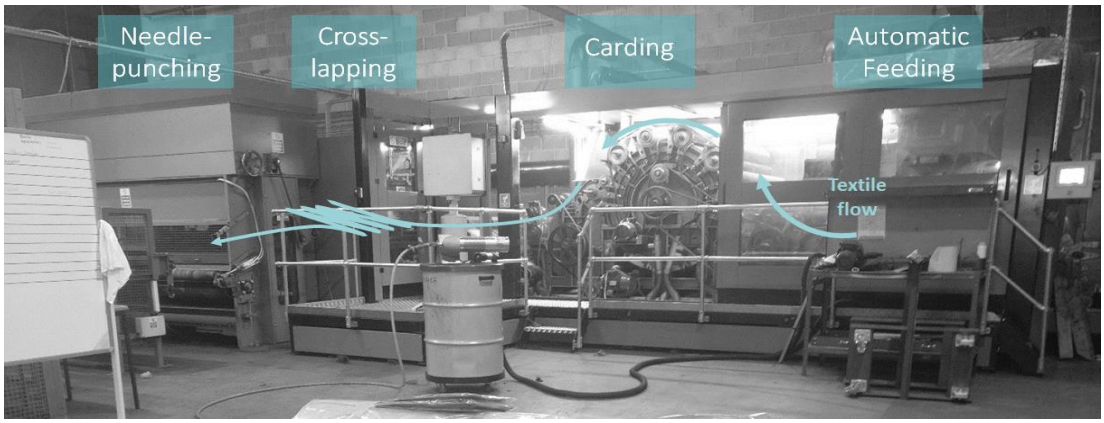

Figure 3-12: Industrial scaled textile production at ELGCF for nonwovens using a dry carding process including automatic feeding, cross-lapping and needle punching.

A homogenous and uniform nonwoven textile is targeted for the surface area, weight fraction and feedstock composition. A representative textile structure is shown in Figure 3-13, where the material distribution between rCF and the polymer fibres seems equal and the stitches are clearly shown from the needle punching process.

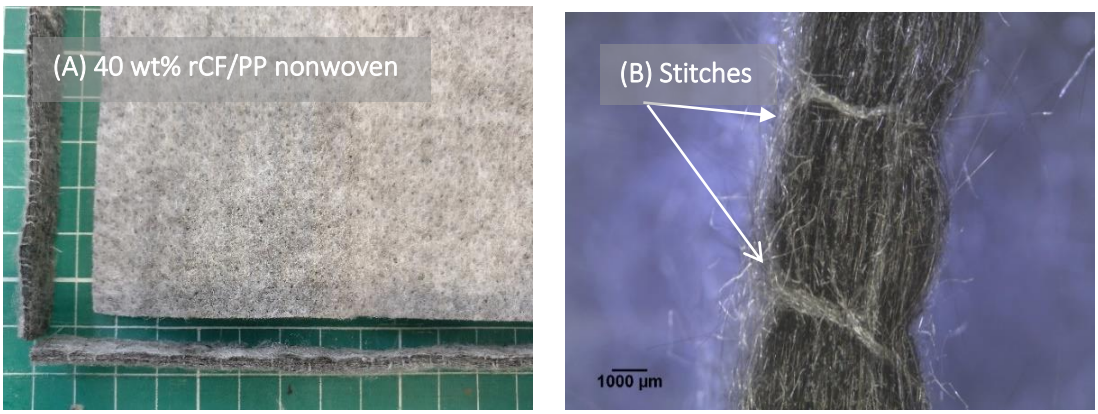

Figure 3-13: Representative textile probes from pilot scaled textile line at ELGCF containing (A) 40 wt% rCF/PP with (B) visible stitches from needle punching.

Knowing the difference in textile quality when deriving from different scaled processes is important when analysing the composite material properties after manufacturing. The textiles properties will be further investigated throughout the project.

3.5 SELECTION OF CHARACTERISATION METHODS

This section describes the selected characterisation methods for the base material, the textiles, its interfacial characteristic and the final composite. An overview of the comprehensive material characterisation is given in Table 3-2.

Table 3-2: Overview of investigated material characteristics within this study ranging from base material, and textile properties to the composite performance including its interface.

	OPTICAL	PHYSICAL	CHEMICAL
Fibre	Morphology & Topography (SEM)	Fibre Strength, Stiffness (SFTT), Density	XPS, Surface Energy (CA)
Matrix	Polymer process window	Thermal Analysis, Tensile Testing	MW, Surface Energy, MA Concentr.
Interface	Wetting	Pull-out Test (SFPT)	Surface Energy
Textile	Topography, Fibre Orientation	Weight, FWF, Loft Factor	-
Composite	Morphology	Mechanical Testing, FWF, Voids	-

3.5.1 TESTS ON CARBON FIBRE

3.5.1.1 SURFACE MORPHOLOGY & TOPOGRAPHY

The microscale fibre feedstock morphology was analysed using a Scanning Electron Microscope (SEM) type Zeiss Sigma FEG with a field emission gun as the electron source. The method involves electron beams that scan the surface and can give a resolution image down to nanoscale. The samples were silver-coated prior to testing (30 s, current of 25 mA), which resulted in an approximate coating thickness of 30 nm. The acceleration voltage was set to 5 kV for all analysed samples. SEM images were taken with a magnification range of between 100 - 20000 (20 K). The fibre diameter taken from the SEM images was evaluated quantitatively using ImageJ software.

3.5.1.2 FIBRE DENSITY

To analyse the fibre density an AccuPyc 1330 gas pycnometer was used. Carbon fibres were weighted and filled in the sample chamber. The chamber was evacuated and filled with helium, from the reference chamber. With the known volume from the reference chamber

and analysed pressure in the sample chamber, the relevant volume and density were subsequently calculated.

3.5.1.3 SINGLE FIBRE TENSILE STRENGTH

A TexTechno FAVIMAT+ machine was used at the research facilities of Deakin University (Carbon Nexus, Geelong, Australia) to evaluate the SFTS of control and modified fibres. In each test batch a minimum of 75 filaments were tested (gauge length of 25 mm and an extension rate of 1mm /min). The samples of the mechanically recycled fibres (SM45D, IM56D) were taken from the waste batches as delivered and prior chopping to have a sufficient fibre length for testing. Initially, fibres were loaded to the rug for robotic input in the machine. However, fine fibres were not able to be fed into the machine automatically to achieve a success rate of 95 % or above. Therefore, the feeding was done manually, giving a 100 % success rate To determine the strength distribution and probability of fibre failure, a statistical analysis was performed of the obtained fibre strength data following the approach by Weibull for brittle material [16], also known as the Weibull analysis. The two-parameter Weibull probability equation below describes the probability of fibre failure, P_f, at an applied tensile strength, σ, where the Weibull modulus m and the predicted strength or scale parameter, σ_O, can be estimated by linear regression:

$$P_f = 1 - exp\left[-\left(\frac{\sigma}{\sigma_O}\right)^m\right] \quad (3)$$

$$ln\left[-ln\,(1-P_f\right] = m * ln(\sigma) - m * l\,n(\sigma_O) \quad (4)$$

Figure 3-14 shows exemplary the Weibull distribution of a fibre strength data set including the rearrangement of Equ. 3 to Equ. 4 in the form of y= *m* x + n for linear curve fitting. The coefficient of determination (R^2) is used to understand the proportion of variance between the predicted and experimental data, targeting 100 % for full agreement. OriginPro is used to plot the data and perform the statistical analysis.

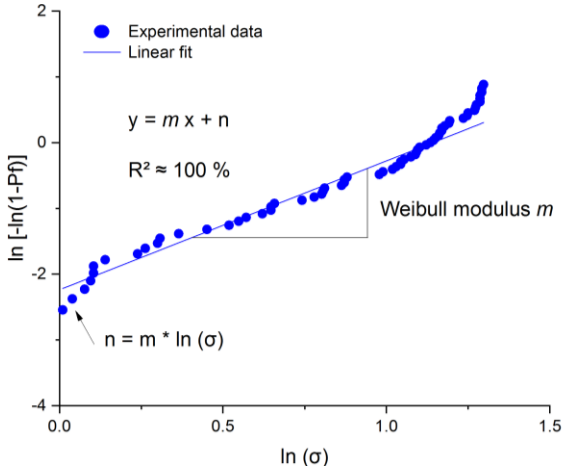

Figure 3-14: Exemplary Weibull distribution analysis of an obtained fibre strength data set.

3.5.1.4 CONTACT ANGLE MEASUREMENT

The contact angle method is applied to fibre tows to evaluate the surface polarity and potential wetting behaviour with the target matrix system. The relation between the surface free energy of the solid σ_{SG} (e.g. fibre or composite), the surface free energy of a liquid σ_{LG} (e.g. test liquid, matrix, sizing) against its interfacial tension σ_{SL} and the measured contact angle θ can be described by Young's principle (Figure 3-15).

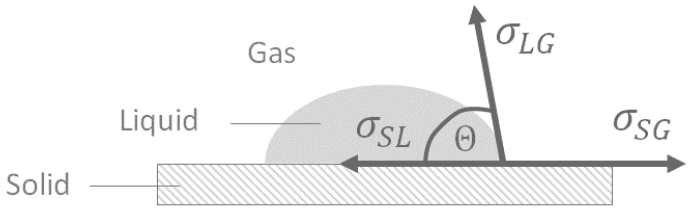

Figure 3-15: Schematic relation between surface energies of liquid (σ_{LG}), solid (σ_{LG}) and solid-liquid interface (σ_{LG}) to calculate the residual contact angle Θ.

The relation shows that the surface energy of the solid is equal or greater than the surface energy of the liquid including the interface energy to be wetted easily [16]. Further correlations can be determined [126]:

- No wetting takes place, if $\theta \approx 180\ ^{o}$
- Low wetting takes place, if $\theta > 90\ ^{o}$
- Insufficient wetting takes place, if $\theta \approx 90\ ^{o}$,
  - where $\cos 90\ ^{o} = 0$.
- Ideal wetting is taking place if $\theta \ll 90\ ^{o}$,
  - where $\cos 0^{o} = 1$.

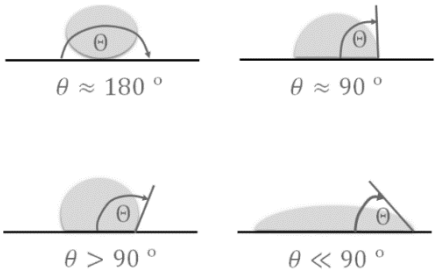

With the obtained contact angles, the surface energy (sum of a polar σ^{p} and dispersive σ^{d} component), interfacial tension and work adhesion are calculated following Owens, Wendt, Rabel and Kaelble's approach (OWRK) [127]–[129], which describes the most common method found in the literature for fibre characterisation.

A description of each characteristic and implication is summarised below:

- the dispersive proportion of the surface energy describes the Van der Waals interaction
- the polar part is composed of dipole-dipole interactions and hydrogen bonds
- Energetic surfaces are defined as solid surfaces, where the polar fraction outweighs the disperse fraction. The ratio is described by the surface polarity X^{p} [130].
- The interfacial tension σ_{SL} describes the level of incompatibility of the fibre-matrix system. A low interfacial tension is targeted for good adhesion between the fibre and the matrix.

- The adhesion energy ψ_{SL} describes the physio-chemical bonding, and how energetically favourable the initial formation is [131]. For good interfacial adhesion properties within the composite, low interfacial tension and high adhesion energy were targeted [129], [131].

In conjunction with the obtained surface energies, the capillary effect describes the movement of liquids within thin spaces (capillary) due to the surface tension between the liquid-solid-interface [132]. The effect is commonly used in impregnation models when simulating the polymer flow within textiles [126], [132], [133] and was also explored in this study. It shall be noted, that all these effects only describe a possible characteristic on micro-level and should be handled with care when evaluating the composite performance on macro level. The sessile drop method was applied to analyse the contact angles, whereby deionised water and Di-iodomethane were used as test liquids, which are in contrast strongly polar (deionised water) and strongly dispersive (Di-iodomethane, DIM). The Theta Lite Optical tensiometer device by Biolin Scientific was used to analyse the contact angles of the two test liquids on the sample surface using their known surface energies γ (including its polar γ_p and dispersive γ_d component, Table 3-3).

Table 3-3: Surface free energies of applied test liquids (γ_p – polar component of surface energy, γ_d – dispersive component of surface energy, γ – total surface energy, X_p – surface polarity)

Test Liquid	γ_p [mN/m]	γ_d [mN/m]	γ [mN/m]	γ_p/γ_d	$X_p = \gamma_p / \gamma$	Reference
H_2O	51	21.8	72.8	2.34	0.70	[134]
DIM	2.3	48.5	50.8	0.05	0.05	[134]

A drop volume of 2 µl test liquid 1 and 2, with a rate of 20 µl/s was dispersed on each sample with four repetitions. The drop shape was captured and analysed by the tensiometer's camera when in contact with the probe surface. The software *OneAttention* was used to evaluate the measured values and to calculate the resulting surface energies and its polar and dispersive component. All reported contact angle values are the average values of five measurements per sample batch using a different fibre tow for each test.

3.5.1.5 SURFACE CHEMISTRY

X-Ray Photoelectron spectroscopy (XPS) was used to analyse functional elements and certain carbon groups on the carbon fibre surface. It is a standard method to investigate the efficiency of fibre treatment as well as a quantitative examination of elements on the fibre surface with a comparison to its control [135], [136], [137]. With the control fibres, detection of oxygen containing groups, like alcohol or ether groups (C-O) and carbonyl groups (C=O),

and carboxylic acid groups (COOH) is assumed with regard to sizing and residual char. The method was applied to all control fibres (SM45D, IM56D, IM56R, IM56 L) and modified fibres as part of the fibre treatment project carried out at Deakin & Swinburne University. All samples were kindly tested at the Swinburne University of Technology (Melbourne, Australia) using an AXIS Nova (Kratos Analytical Ltd, UK) XPS system. The samples were prepared by fixing on carbon and silica tape to the sample plate.

Table 3-4: C1 spectra binding energies for organic samples derived by J.C. Vickerman & I. S. Gilmore [138] **with applied constraints for curve fitting of the functional groups in the obtained spectra if not otherwise noted.**

Functional Group	Molecule Structure	Binding Energy (Ev)	Constraints In Casaxps Software
Hydrocarbon	C-C, C-H	285.0	285.2 eV < X < 284.8 eV
Alcohol, Ether	C-O	286.5	286.7 eV < X < 286.3 eV
Carbonyl	C=O	288.0	288.2 eV < X < 278.8 eV
Acid, Ester	COOH	289.0	289.2 eV < X < 288.8 eV

The obtained curves were analysed using Casa XPS software. A survey spectrum was used for an initial overview, where detected elements are quantified (e.g. oxygen, nitrogen). With an additional high-resolution C1 spectrum functional groups can also be detected by curve fitting. A general charge correction was applied for all obtained curves. In this regard, the main peak shown for the C-C bonds was aligned to 285.0 eV following the standard suggested by J. C. Vickerman & I. S. Gilmore [138]. The other spectra (O 1s, N1s) are adjusted accordingly. Main binding energies of C1 spectra are summarised (including constraints) in Table 3-4.

3.5.2 TESTS ON THERMOPLASTIC MATRIX

3.5.2.1 THERMAL STABILITY

The thermal properties of the polymer were analysed by Thermal Gravimetric Analysis (TGA) and Differential Scanning Calorimetry (DSC). All thermal characterisation methods involve one repetition of the sample with a maximum sample weight of ≤10 mg for each measurement. The samples were taken from a larger batch of ~ 100 g material, which was cryogenically milled to ensure good distribution of fibre and matrix material and a closer representation of the entire batch. The cryogenic milling was performed using a 6875 Freezer/Mill from SPEX Sample Prep Inc. Two runs of at least 7 min with a 5 min pre-cooling and cooling time in between the cycles were required to turn the samples into powder.

The TGA (Mettler Toledo TGA 1 STARe System) identified that the weight loss of the tested samples was due to thermal degradation. The method was used to analyse the limits of process temperature whilst moulding. The following test methods were applied:

- Thermogravimetric curves were obtained from a temperature range 25°C to 600 °C at a heating rate of 10 °C/min. Tests run first in a nitrogen atmosphere according to standard [139]. However, real process conditions could be simulated with additional runs in air atmosphere.
- Isothermal treatment was done on pure PP samples as well as a commingled material composition containing 40 wt% SM45D fibres. The samples were exposed to a specific temperature from 200 °C to 260 °C in air and nitrogen for 60 min to understand the thermal stability overtime at certain temperature levels and varied atmosphere.

The DSC (Mettler Toledo DSC 1 STARe System) was used to evaluate the crystallisation (T_C) and the melting points (T_m) of the polymeric matrix. Processing includes a thermal cycle with a heating and cooling rate of 20 °C/min, from -50 to 250 °C in nitrogen atmosphere [3, 4]. Two cycles are run on the DSC, whereas the first cycle sets the blank curve to eliminate the thermal history and the second cycle is used for evaluation.

3.5.2.2 SURFACE ENERGY

The contact angle method was also used to evaluate the surface energies of the different polymers using the sessile drop method. In conjunction with the fibre data (Section 3.5.1), the interfacial tension and adhesion energy between the fibre and target matrix system PP can be calculated following OWRK's approach.

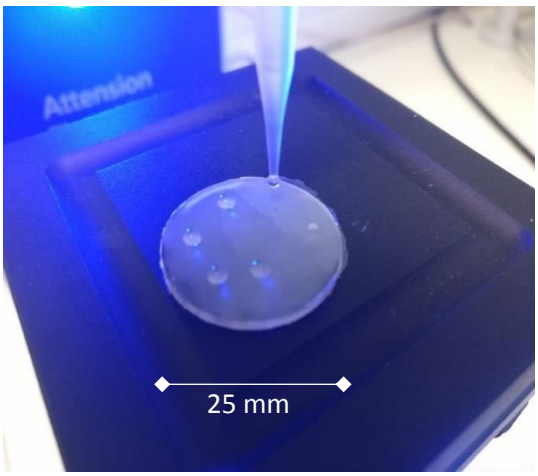

Figure 3-16: Experimental set up for the contact angle measurement applying the sessile drop method on polymer sheets.

To achieve consistency in the characterisation, the fluffy polymer fibres, as received from the supplier, were processed to thin sheets (Figure 3-16). This is a common approach taken from the literature [13], [142]. The same process parameters were applied as in baseline projects on laboratory scale: 200 °C, 10min, 20 °C/min cooling.

3.5.2.3 QUANTIFICATION OF MALEIC ANHYDRIDE CONTENT

One way to analyse the MA content is to use Nuclear Magnetic Resonance Spectroscopy (NMR). This technique can be used to qualitatively and quantitatively determine the presence of MA in the material, but requires dissolving the polymer filaments in a chemical solvent such as toluene-d8, chloroform-D and nitrobenzene-d [143], or D-acetone or ethanol

or chloroform [144], [145]. The polymer used in this project could not be dissolved in the mentioned solvents. As a result, Fourier Transform Infrared Spectroscopy (FTIR) was used, which was able to identify functional groups and chemical bonds with an FTIR spectrum. The peak heights of the given spectra for each polymer type could give an estimation of MA in the supplied MAPP.

The FTIR spectra were recorded on a Perkin-Elmer FTIR Spectrometer 1760-X from 4000 to 400 cm^{-1} with a 0.5 cm^{-1} resolution. The quantitative analysis was performed after the Roover method [146], where the poly (maleic anhydride) concentration [µeq/g] was calculated by the ratio of specific absorbance bands of the determined infrared (IR) scans:

$$[\text{Anhydride}] = 51.3 * (Abs\ 1784\ cm^{-1} / Abs\ 1100\ cm^{-1}) + 52.5 * (Abs\ 1715\ cm^{-1} / Abs\ 1100\ cm^{-1}) \quad (5)$$

The $Abs\ 1784\ cm^{-1}$is the absorbance of the poly(maleic anhydride) symmetric C=O stretch, $Abs\ 1715\ cm^{-1}$is the absorbance of the carboxylic acid symmetric C=O stretch, and $Abs\ 1100\ cm^{-1}$ is the PP reference absorbance [146].

3.5.2.4 MOLECULAR WEIGHT

The chemical resistance and limitation in dissolving the polymer samples under correct safety conditions limited the experimental analysis. Therefore, the samples were prepared and analysed externally by the Polymer RTP team (University of Warwick) using the Gel Permeation Chromatography (GPC) method:

- Determining nominal concentrations in di-chlorobenzene and solubilised overnight on an Agilent PL-SP 260 VS device at 140 °C
- Samples were filtered through 10 µm stainless steel frits before injection.
- All samples were run on an Agilent Infinity II HT GPC system equipped with Agilent Olexis column set, at 140 °C at 1 ml/min.

3.5.3 TESTS ON COMMINGLED NONWOVEN TEXTILE

3.5.3.1 FIBRE ORIENTATION

The arrangement of needles on the textile carding machine, both lab and industrial scale, can cause realignment of discontinuous fibres, perpendicular to the roll direction [27]. The nonwoven material was treated as a randomly oriented textile in the first instance, which resulted in similar mechanical characteristic independent from test orientation of composite samples. The latter phenomenon describes an orthotropic material behaviour and needs to be proven.

No image analysis method could be applied successfully for the nonwoven material to identify the fibre orientation in the textile or composite state. This led to an investigation of

the fibre orientation within the manufactured composite by varying the composite test direction and evaluating the gained tensile properties. If fibres are aligned, the mechanical performance of the composite is dependent on the test direction parallel to the fibre orientation. The exceeded performance in a specified test direction can be as attributed to aligned fibre orientation. Therefore, composite plaques have been manufactured and tested in different directions; the roll direction, cross-plied and in carding direction to investigate the influence of the possible fibre alignment on the tensile strength and modulus.

3.5.3.2 OPTICAL QUALITY CONTROL & LOFT FACTOR

With the known fibre weight fraction (FWF) of the evaluated composites, the loft factor can be calculated using the equation (6) established by Jordan *et al.* [147] describing a quantitate method to evaluate the voluminosity of the textiles:

$$L_F = \frac{d}{m_A}\rho_{theor} \tag{6}$$

where d describes the thickness of the textile, m_A the textile weight and ρ_{theor} the fibre density (all fibres including polymer). Textiles with a loft factor $L_F \geq 40$ of textiles thicker than 3 mm are described as “highloft”[147]. An optical microscope was used to analyse the textiles (including quality in terms of fibre-matrix distribution) on macroscale (Stereo microscope, type Nikon SMZ18). The textile thickness taken from the microscope images were evaluated quantitatively using ImageJ software.

3.5.4 TEST ON THE INTERFACE

3.5.4.1 HOT STAGE MICROSCOPE

A hot stage microscope device was used to observe the base material in the melted stage on a small scale and predetermine the interfacial behaviour between rCF and the polymer. The qualitative analysis showed a tendency for hydrophobic or hydrophilic behaviour from the matrix material when melted. A LINKAM hot stage microscope was used to process the material. The heating cycle of the compression moulding process can be simulated without the actual compression operation. Sections of the commingled nonwoven textile are placed between two glass slides on the hot stage device. The heating rate of 20 °C/min and temperature level (180 – 220 °C) is set in the temperature controller, which is connected to the hot stage. The sample is then heated in a controlled environment above the melting point of the polymer. Whereas the connected microscope is only able to observe but not save images, the samples were transferred subsequently to a transmitted light microscope, type Zeiss AXIO Imager, to capture image data.

3.5.4.2 SINGLE FIBRE PULL-OUT TEST

In this study, the SFPT was chosen as the preferred method for a thermoplastic system [129]. The test was kindly performed by the Leibniz Institute Dresden. MAPP was used as the target matrix system, which was suggested by the project partner to obtain a higher success rate than a rCF/PP system possessing a general weaker interface. The test temperature sits slightly above the composite processing temperature due to large test chamber, where temperature sensors are not directly located next to the test device. Target melt temperature was 200 °C. 15 – 20 single tests were performed per batch as shown in Figure 3-17 (right).

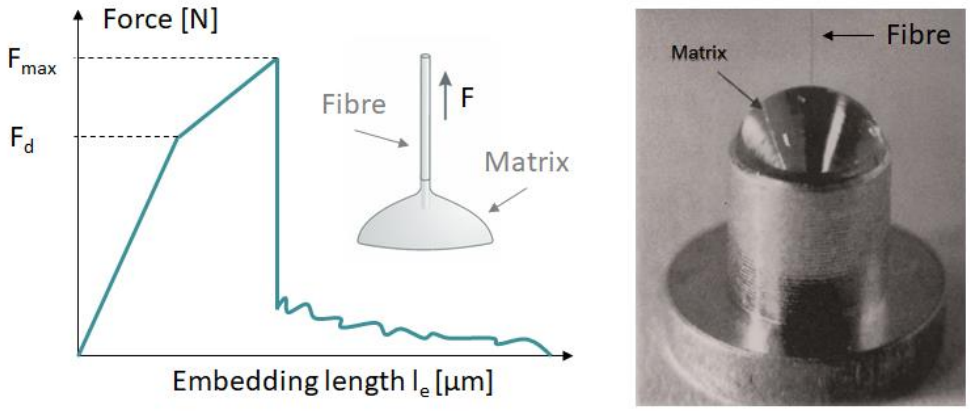

Figure 3-17: Schematic principle of the fibre pull-out test method shown with a work-displacement curve (left) and exemplary sample set up (right), modified from [148], [149]**.**

The determination of the interfacial parameters is based on [150], [151] where the apparent interfacial shear strength (τ_{app} , $IFSS$) is dependent on the maximum achieved force (F_{max}) and describes the adhesion between fibre and matrix affected by interfacial friction. The ultimate (local) interfacial shear strength (τ_d) is based on the debonding force (F_d) and is independent from any friction between fibre and matrix.

3.5.5 TESTS ON COMPOSITE

3.5.5.1 SAMPLE PREPARATION USING PANELS FROM COLLIN PRESS

The samples were cut into shape and correct test dimension with an abrasive cutter *Abrasimatic 300* (Buehler, water-cooled). Samples were taken from the centre with limitation in length (150 cm), having a total amount of five samples for each process condition.

3.5.5.2 SAMPLE PREPARATION USING PANELS FROM DASSETT PRESS

The sample preparation for tensile testing included several steps due to its large size. For each tested condition (in regard to moulding temperature etc.) two composite panels were

manufactured, where the second panel was used primarily for testing. This is due to two reasons:

- Temperature adjustment when changing process conditions
- Compensation panel as back up

The manufactured composite panels were first cut to smaller pieces by a band saw due to size restrictions for the water jet cutter. Afterwards, the samples were cut into shape and correct test dimension with an abrasive cutter *Abrasimatic 300* (Buehler, water-cooled), following the standards. The tensile samples are taken from the middle of the panels, marked as 1, 2, 3, 4, in Figure 3-18. Trials of testing samples from section 20, 30, 21 and 31 (Figure 3-18) showed lower performance due to texture on the backside marked from the tooling. Therefore, samples were taken from the centre with limitation in length (150 cm) to gain a minimum sample number of four for each process condition.

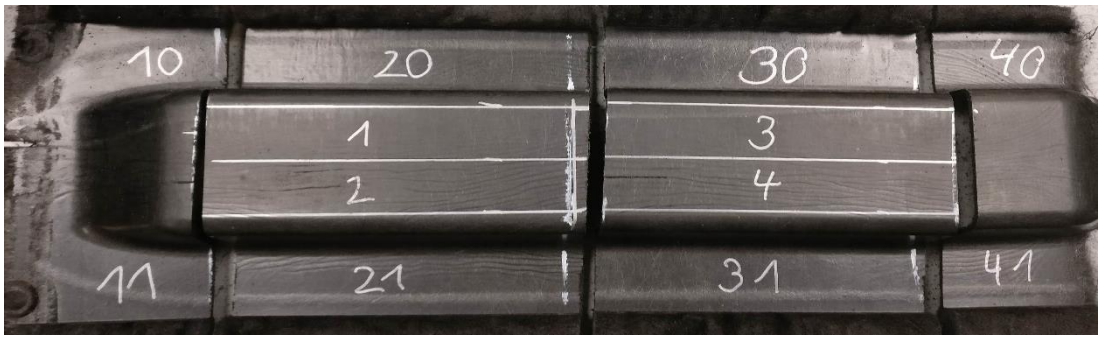

Figure 3-18: Exemplarily moulded composite part with marked test sample regions. The part was cut by a band saw prior further sample preparation with a water-cooled cutter.

3.5.5.3 MECHANICAL TESTING

The tensile properties were investigated using an INSTRON 5800R universal test frame [152] with a 30 kN load cell and a test rate of 2 mm/min. An extensometer was used to record the actual extension depending on the applied load. Specimen type 2 (2 mm thick) of the ISO 527-4, describing a rectangular shape, was used with end tabs. Flexural testing was performed on the INSTRON machine equipped with a 100 kN load cell following ISO Standard 14125/II [153]. 5mm/min is the speed of testing until failure (drop in load). Sample dimension was 80 mm x 15 mm x 4 mm unless otherwise stated.

3.5.5.4 OPTICAL INVESTIGATION

The optical investigation on the manufactured panels prior to cutting and testing was captured using a digital camera, type CANON EOS 700D. The panels were observed regarding dry spots, overall appearance and mould coverage (e.g. fully or partially filled). The optical analysis helped to qualitatively evaluate the level of impregnation after processing and to

adjust the experimental plan accordingly. Figure 3-19 shows examples of phenomena which led to process window restrictions caused by: polymer degradation, low level of impregnation and deformation happening after de-moulding at high temperature.

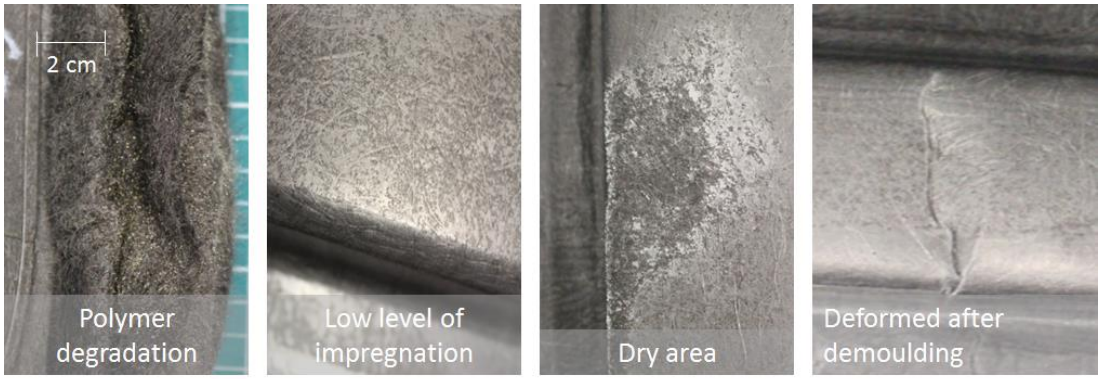

Figure 3-19: Optical investigation of moulded parts and its partial level of good impregnation and deformation at the limit of the process window.

The actual level of impregnation was assessed on the level of void content and surface finish of the manufactured panels. A very good level of impregnation exhibits void content close or equal to zero as well as good surface finish. SEM is used for fracture surface analysis of the tested samples. Fibre surplus obstructed the matrix material and prevented from further analysis. Therefore, an artificial cryogenic manual break was performed in liquid nitrogen. The level of thermoplastic melting, fibre distribution and possible wetting behaviour were of interest for the specific base material characterisation.

3.5.5.5 FIBRE WEIGHT FRACTION & VOID CONTENT

The initial constituent analysis was carried out and included density measurements of fibre and composite samples using gaspycnometry and the Archimedes principle. The (FVF) was calculated in the early stages of the project using a set FWF ratio:

$$FVF\ [vol\ \%] = \frac{1}{1 + \frac{\rho_f}{\rho_m} * \left(\frac{1}{FWF} - 1\right)} * 100 \quad (7)$$

where ρ_f, ρ_m are the determined densities of the fibre and matrix respectively. The theoretical density ρ_{theor} and final void content V_v in the of the composite sample can be calculated using the following equation:

$$\rho_{theor} = FVF * \rho_f + (1 - FVF) * \rho_m \quad (8)$$

$$V_v = \left(1 - \frac{\rho}{\rho_{theor}}\right) * 100 \quad (9)$$

A more in-depth constituent is carried out in the following studies and turns FVF into a variable factor obtained from an additional thermal analysis study. For variable values of actual FVF fraction, the burn-off method was used to identify material composition within

the manufactured samples. The TGA method identifies the weight loss of the tested sample, here the solidified composite, on a determined heat cycle at 10 °C/min from 25 °C to 600 °C in a nitrogen atmosphere (to prevent from the degradation of the carbon). The characterisation method involves one repetition of each probe using cryogenically milled composite parts from tested samples. The actual FWF was calculated precisely, whereas the residual polymer chard (in wt%) from a pure polymer sample can be utilised as a correction factor for the final calculation. The following formula is applied:

$$FWF\ [wt\ \%] = (w_{remTotal,i} - w_{remPolymer,std} * w_{remTotal,i}) * 100 \qquad (10)$$

With $w_{remTotal,i}$ describing the remaining weight fraction after degradation (derived from the deviation of leftover char mass m_{char} by total mass m_{total}) in a total of the composite sample (i) and $w_{remPolymer,std}$ (= 5 wt%) describing the remaining weight fraction of the only polymer after degradation in pure polymer sample set as standard value throughout the experimental study.

$$w_{remTotal,i} = \frac{m_{char}}{m_{total}} \qquad (11)$$

This method was applied to all manufactured samples throughout the project, comparing achieved consistency in the set material ratio (and additional parameters when mentioned) between batches but also within a batch.

4 PROCESS IMPROVEMENT

The use of recycled carbon fibres in the production of high strength components presents a cost-efficient alternative to virgin material. However, the lack of information about their performance and efficient production methods are significant barriers to uptake, which was highlighted earlier (Section 2.5). The main purpose of this study is to gain expertise in manufacturing composite material using a new commingled nonwoven textile and generate knowledge about the processing and handling of this specific material. Furthermore, different manufacturing processes were investigated, targeting short cycle times which could be applicable in industry. These new textiles were developed with the aim that the polymer is able to impregnate the carbon fibre over a short distance equally and quickly throughout the entire textile mat when heat and pressure are applied, to form the composite material. As such the first investigation of this research project focused on the characteristics of the base material, in regard to the rCF feedstock and nonwoven textiles (Section 4.1.). This is followed by an examination of the process conditions of commingled thermoplastic nonwoven textiles on a laboratory scale, applying an isothermal process. The supplied textiles were produced first on a small textile line for research trials by ELGCF, with a further upscale to an industrial line at a later stage during the project (timeline schematically shown in Figure 4-1). With the applied process adjustments, on a laboratory scale, of the composite manufacturing process, the material source (SM45D) was kept consistent at the beginning. The final, optimised process parameters and set process conditions were then applied to other material feedstock (IM56D), including pyrolysed fibres (IM56R, IM56L), for performance comparison and form milestone 1.

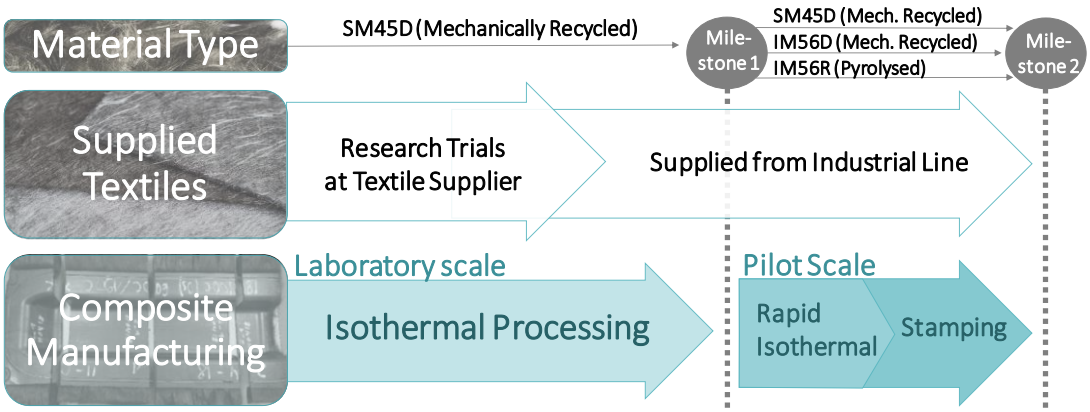

Figure 4-1: Schematic timeline of process improvement with regards to supplied textile type, material feedstock and composite manufacturing level from laboratory to pilot scale.

In general, working on a laboratory scale (Section 4.2.) gave certain benefits, such as continuous access to small batches of textile material produced on ELGCF`s research line, but also involved further limitations, such as a lack of material consistency between the batches which was due to manual feeding (further details in Section 4.2.5.). A similar phenomenon can be seen in the isothermal processing approach, which describes the manufacturing process applied on a laboratory scale. The small-scale process set-up provided the possibility to develop knowledge about the handling and processing of the material. On the other hand, limitations arose regarding component size, cycle time and applied pressure and prevented the upscale of the research and development towards an industrial application.

From that point onwards, each material type was processed independently (Section 4.3.). Pilot-scale work enabled a more advanced case study of manufacturing conditions and used supplied textiles produced on ELGCF`s industrial line with increased material consistency. A comprehensive process study was developed to understand how these processing parameters can be optimised to maximise the mechanical performance of the manufactured components with a simultaneous reduction in cycling time to reach milestone 2.

4.1 RANGE OF MATERIAL CHARACTERISTICS

4.1.1 RECYCLED CARBON FIBRES

Different rCF fibre feedstock was used for processing. The general classification of the rCF feedstock was highlighted in Chapter 3.4.1., a summary is given in Table 4-1 below. Fibre type SM45D and IM56D are covered with a coating, which was epoxy compatible according to the supplier. In contrast, IM56R and IM56L fibres, which describe a thermally recycled feedstock, are occasionally covered with char which is a residual of the pyrolysis process.

Table 4-1: Fibre Feedstock Categories (60 – 100 mm fibre length) supplied by ELGCF

Fibre Type	Feedstock Source	Recycling Method	Surface Characteristic after Recycling	Tensile Strength [GPa]	Tensile Modulus [GPa]
SM45D [2]	Dry fibre, sized	Mecha-nical	Clean fibre, sized	4-5	≤ 270
IM56D [3]	~	~	~	5-6	270 < E < 330
IM56R	~	Thermal	Unsized	5-6	270 < E < 330
IM56L	Cured laminate	~	~	5-6	270 < E < 330

[2] SM - Standard modulus
[3] IM – Intermediate modulus

When investigating the process conditions of the textiles with different types of rCF, the fibre surface chemistry and level of surface energy is also of importance. To gain an increase in polar groups, vCF material is commonly treated with plasma or other functional sizing . In general, a positive linear correlation is given between an increase in nitrogen, oxygen or hydrogen, due to functionalisation of the polar component of the surface [154], [155]. The chemically inert CF surface can be modified to the target application ranging from a very polar, describing a surface with a high number of functional groups, to a very non-polar surface.

The surface energies of each fibre type were measured using the contact angle method (more information in Section 3.5.1.4.) to understand the specific surface characteristics and the potential effect on the level of interfacial interaction with the target matrix system as well as the processability when moulding. Furthermore, the type of sizing applied to SM45D and IM56D fibres was estimated by comparing surface characteristics with reported values from the literature.

The contact angle method was used to determine the contact angles of the two test liquids, deionised water (H_2O) and DIM, and the tested substrates. The results are stated in Table 4-2. A high standard deviation of the obtained contact angles was detected. This could be due to the fact that the fibres are industrial by-products and were rejected due to inhomogeneous sizing and subsequent uneven pyrolysis treatment. Additionally, there could be errors in the testing method. Fibre bundle testing may not be the optimum technique, but it does allow interpretation of a trend in fibre performance. The deviation may also have been triggered by the uneven surface topography of the tows, where the single fibre test describes a more precise alternative [156]. However, the applied method using tows shows a clear trend of detected hydrophobic and hydrophilic fibre surface characteristics between SM45D and all other fibre types.

Table 4-2: Contact angle measurements of all fibre samples applying the sessile drop method and using deionised water and DIM as the test liquid.

Fibre Type	Surface Characteristic	θ (H_2O)	θ (DIM)
SM45D	Sizing 1	2.55° ± 1.89°	2.64° ± 2.05°
IM56D	Sizing 2	59.75° ± 12.77°	3.51° ± 2.41°
IM56R	Pyrolysed	77.97° ± 15.01°	0°
IM56L	Pyrolysed	67.95° ± 1.79°	0°

The fibre feedstock SM45D showed a strong hydrophilic surface characteristic with similar contact angles for the polar and non-polar test liquid. A fully wetted fibre occurs when the

angle becomes 0°, to which the SM45D (2019) fibre type came close when tested by DIM. Fibres IM56R and IM56L also came close to full wetting when tested with the non-polar DIM test liquid. Conversely, the fibre tows showed very high contact angles when tested with the polar test liquid, which indicates a strong hydrophobic characteristic. The IM56D fibre, which is a sized type, showed high contact angles when tested with water and contact angles close to 0° when tested with DIM. This was in line with IM56R and IM56L fibres.

No direct relation was shown between the contact angle measurement and the processability of the nonwovens on its own. With the measured contact angle and OWRK's approach, the surface free energies including its polar and dispersive part were calculated subsequently and listed in Table 4-3. From the ratio between the polar fraction and the total energy, the polarity was determined.

Table 4-3: Surface energies γ of all fibres including its polar γ^{p} and dispersive γ^{d} part, with the polarity X^{p} describing the ratio between the polar and the total surface energy.

Fibre Type	γ^{p} [mJ/m²]	γ^{d} [mJ/m²]	Total Surface Energy γ [mJ/m²]	Surface Polarity X^{p} [%]	Processing
SM45D	39.98 ± 0.70	34.97 ± 0.09	74.95 ± 0.16	53.34 ± 0.23	Good
IM56D	11.44 ± 6.67	42.92 ± 3.32	54.35 ± 3.36	21.04 ± 0.51	Limited
IM56R	2.63 ± 2.62	48.19 ± 4.81	50.81 ± 2.19	5.17 ± 0.84	Limited
IM56L	6.83 ± 0.88	45.23 ± 0.51	52.06 ± 0.37	13.12 ± 0.42	Limited

The SM45D fibre types showed the highest measured fibre surface energy with 73.12 mJ/m², compared to IM56D, IM5R and IM56L fibres in the range of 50.81 – 54.35 mJ/m². Alongside this, the SM45D material also showed the highest polar components which result in a polarity of 53 % which describes an energetic surface characteristic. The other fibre surfaces outperformed with regard to its dispersive fraction. From the analysis of the polarity level of the fibre surfaces, and from a review of the literature, it can be assumed that the sizing of the IM56D fibres will be Epoxy-based [130]. From the more hydrophobic characteristic of the pyrolysed IM56R fibres and their low polarity it could be assumed that residual char on the surface contains less active groups after the pyrolysis process as reported before by Gonçalves *et al.* [157].

Following on that, an additional XPS analysis, which was conducted in conjunction with the fibre treatment study presented in Chapter 5.2., proved the presence of elements other than carbon on SM45D fibres with the lowest measured amount of carbon of 82.80 % between all rCF fibres. All results are stated in Table 4-4. In general, a very low or amount or no nitrogen was detected when measuring the elemental composition of all fibre surfaces.

Table 4-4: Elemental composition of C1s survey spectra of evaluated fibre types including functional groups [Appendix C].

Fibre Type	C [at%]	O [at. %]	N [AT. %]	O/C RATIO	N/C RATIO
SM45D	82.80 ± 0.53	16.86 ± 0.68	0.00	0.20	0.00
IM56D	88.11 ± 1.13	10.45 ± 0.48	0.68 ± 0.33	0.12	0.01
IM56R	84.60 ± 0.74	13.47 ± 0.36	1.80 ± 0.16	0.16	0.02
IM56L	83.68 ± 0.59	11.23 ± 0.62	1.09 ± 0.18	0.13	0.01

A comparable high oxygen concentration of 16.86 at% was determined on SM45D fibres. It is notable that the (occasional) char covered fibres also have oxygen available on their surfaces (IM56R, IM56L). Figure 4-2 highlights again the highest atomic percent of oxygen detected for the SM45D and IM56R fibre type and shows it in conjunction with the previously calculated surface polarity. Here, the highest oxygen concentration correlates to the highest surface polarity among the rCF fibres.

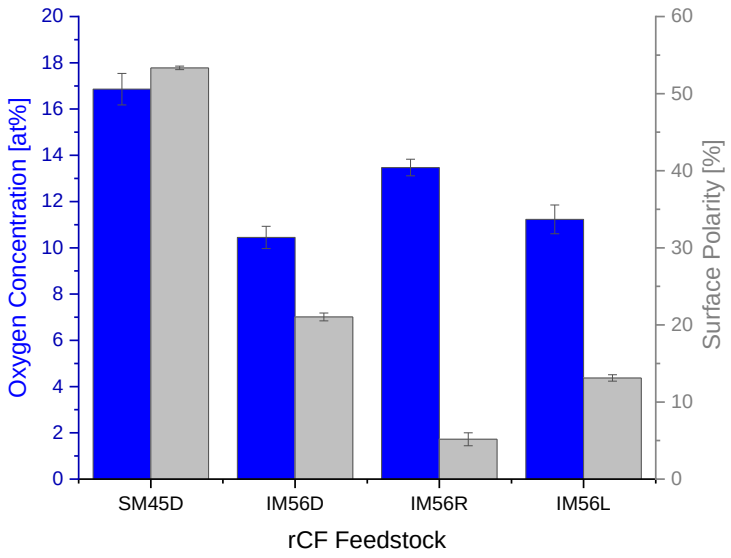

Figure 4-2: Oxygen concentration of the surfaces for range of observed rCF fibres (evaluated from the survey spectra) in relation to the calculated surface polarity.

However, a direct correlation of the lower oxygen concentration and surface polarity is not given. The reason for this is that it is assumed that the increased surface roughness (due to the char) contributes to the decrease in surface energy obtained for IM56L and IM56R fibre types and therefore a more hydrophobic behaviour [36, 37].

Looking at the distribution of oxygen in the different functional groups (Table 4-5), the sized fibres (e.g. SM45D and IM45D) contain predominantly ether groups within the functional

polymer sizing. Whereas for IM56R rCF surfaces next to ether groups also more carboxylic acid groups are present.

Table 4-5: Detailed breakdown of evaluated functional groups detected on the fibres by XPS with performed curve-fitting on the C1s spectra.

Fibre Type	C-C, C-H [at%]	C-O [%]	C=O [%]	COOH [%]
SM45D	82.80 ± 0.53	31.12 ± 3.65	1.80 ± 1.52	1.68 ± 0.71
IM56D	88.11 ± 1.13	23.48 ± 1.92	0.83 ± 0.24	1.97 ± 0.21
IM56R	84.60 ± 0.74	18.91 ± 0.76	5.73 ± 0.92	14.79 ± 0.9
IM56L	83.68 ± 0.59	8.01 ± 0.99	3.02 ± 1.36	2.64 ± 0.21

No further relation to the possible processability of the material can be shown. However, the information forms a basis for the later fibre modification.

4.1.2 COMMINGLED NONWOVEN TEXTILES

All textiles processed in this study were provided by ELGCF. In the early stages of the work, the textiles were produced on ElGCF`s research line (more information given in Section 3.4.3.), also referred to as a laboratory scaled textile line. When looking at the cross section of these nonwoven textiles in longitudinal and transverse direction to the textile roll direction (Figure 4-3), a bundled mat hold by few stitches is visible.

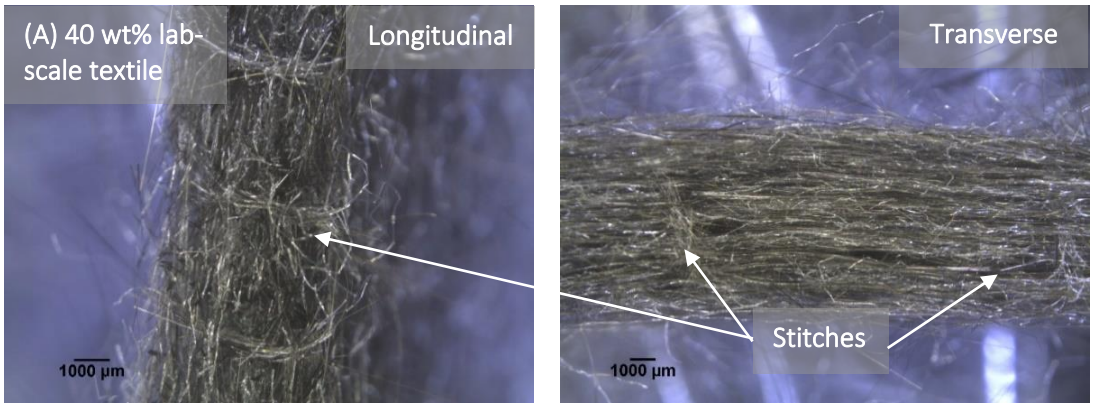

Figure 4-3: Representative enlarged cross section images of nonwoven textiles from a laboratory scaled line at ELGCF.

The research textile line gave the possibility to produces a large variety of new nonwoven textiles in a short amount of time and in a small volume. At later stages, only material from the industrial line was used to demonstrate the capability of the newly developed textile quality for industrial relevant applications (the source of textile is indicated in each subproject). On the industrial line a fibre opening stage prior to carding is in place and aims for equal properties throughout the material rather than stress concentration which occurs

by fibre bundles in the textile. Exemplary, nonwoven material supplied by ELGCF`s industrial line is shown in Figure 4-4. When comparing the textile from the early stage of the implemented industrial textile line with textiles produced at later stage, an increase in compactness is visible. In the below images, predominantly polymer fibres are shown which function as stitch that hold the textile together. This leads to the assumption of an unlimited flow of carbon fibres when melting and pressing the final composite rather than holding the textile compact and prevent from distribution and possible aligning in the mould.

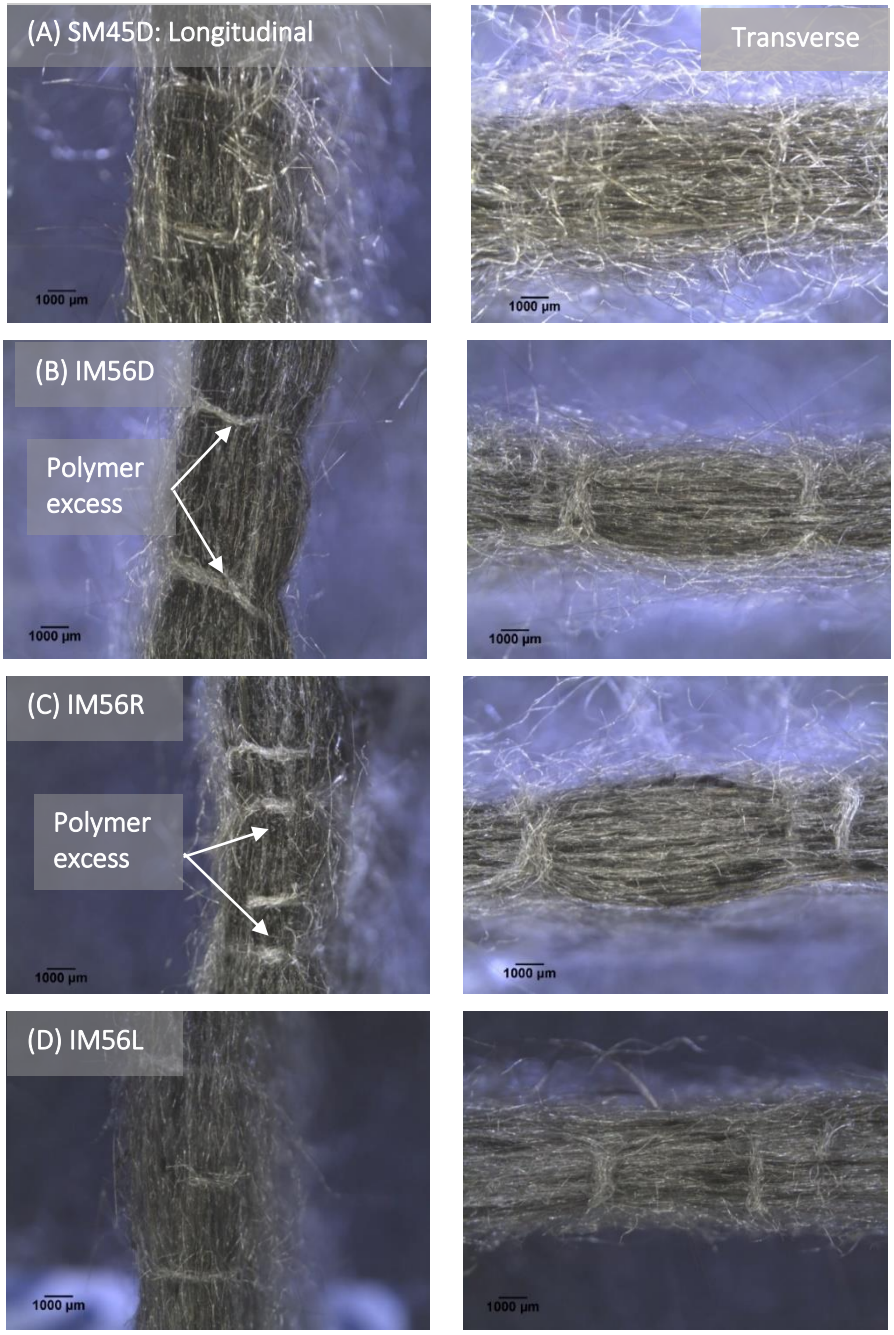

Figure 4-4: Representative enlarged cross section images showing (A) SM45D/PP nonwovens 40 wt% produced at early stages on ind.-scale, (B) IM56D/PP, (C) IM56R/PP, and (D) IM56L/PP from latest textile production on industrial line from ELGCF.

In general, textiles like IM56D/PP, IM56R/PP and IM56L/PP are produced at later stage of the development on the industrial line and show a more compact textile, where the same textile weight (200 gsm) is bundled to a thinner layer with clear stitching in z-direction of the upper polymer fibres. From a qualitative analysis of the textile thickness, compactness and stitch form, a quantitative evaluation is completed at a later stage when the effect of the processing of the material on the final composite quality was investigated.

In summary, the textiles containing SM45D (industrial line) and IM56D feedstock showed a very similar parameter range of comparable textile topography for further processing. However, IM56R and IM56L textiles resulted in a heavier weight with a thinner final textile thickness resulting in a more compact form. Therefore, it is assumed that the denser textile structure leads to more difficult process conditions when moulding the material.

4.2 LABORATORY-SCALE PROCESSING

This section describes the experimental methods applied on a laboratory scale with focus on the controlled process conditions of commingled thermoplastic nonwoven textiles and explore the process boundaries of the isothermal process. Initially, the focus is on one material type, specifically the mechanically recycled fibres SM45D. At the time of writing this represented the largest feedstock volume at ELGCF and there was, therefore, a great deal of interest in its re-processability for future applications. When the optimised conditions are defined, the final process parameter conditions will be applied to the other available feedstock to benchmark their performance.

The experiments conducted at this stage involved:

- Preliminary process investigations to define the DOE process window (4.1.1.)
- Performing and evaluating the DOE (4.1.2.)
- OVAT study to receive further details about the material, e.g. consistency, textile quality, fibre orientation (4.1.3.)

4.2.1 ISOTHERMAL COMPOSITE MANUFACTURING

Isothermal process conditions were used for the initial experiments. An isothermal process is when the mould is directly and constantly heated and cooled throughout the experiment simultaneously with the processed material (schematically shown in Figure 4-5). A moulding cycle, which entails the manufacturing process from the textile to the composite, is over when a part is removed from the press and the machine start conditions are reached again to process further parts [160].

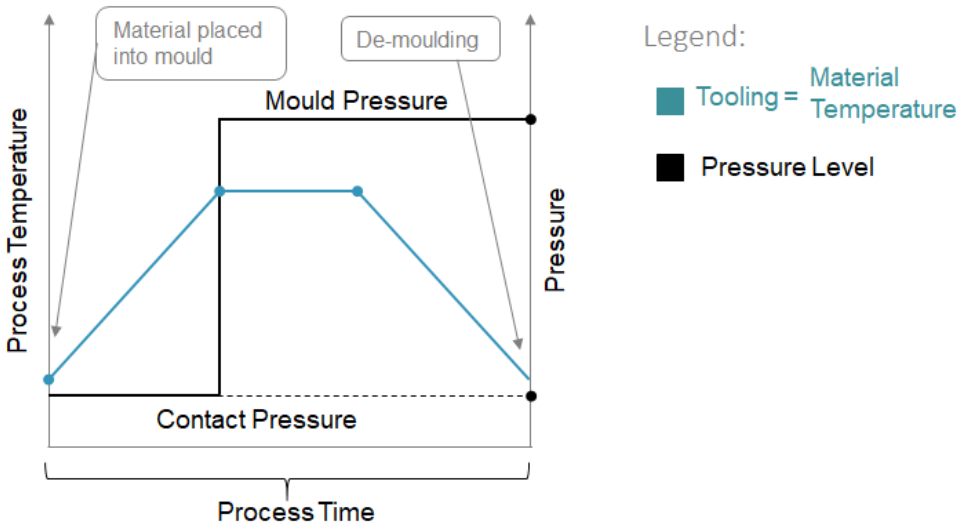

Figure 4-5: Schematic of the isothermal process with heating and pressure cycle applied for compression moulding, where material and tool temperature are the same.

For the experiments a hydraulic platen press, type COLLIN P200P/M, was found applicable to this study and has the following machine requirements:

- maximum mould size: 400 cm^2
- maximum applied temperature of 300 °C
- maximum 125 kN pressing force
- heating- / cooling rate of 5 – 20 °C/min.

The textile was cut into squares of 15 cm x 15 cm and then laid in the roll direction, cross-plied and in the carding direction, depending on the experiment. At this stage, the fibre orientation within the textile was not yet known. Consequently, the material was tested in all directions to asses if the fibres were randomly oriented or if there is a specific fibre alignment present. The alignment of the fibres can be identified by comparing the mechanical properties in the different test directions, where the mechanical properties of the samples tested parallel to the fibres (fibre test direction) exceed the properties of the transverse test direction as illustrated in Figure 4-6.

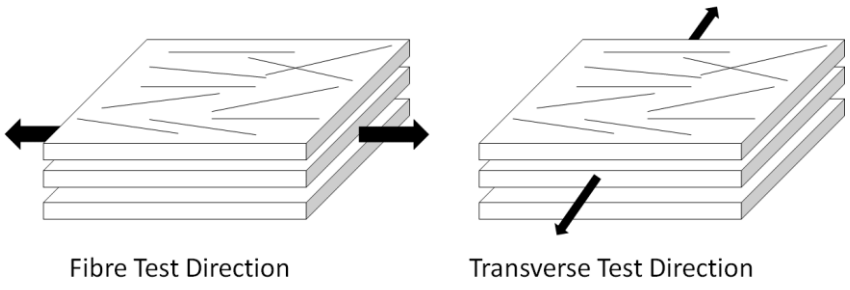

Figure 4-6: Illustrating the test direction of the specimen with direction parallel to the fibres and in transverse direction.

The material was then placed in-between a steel mould frame with targeted thickness of 2 mm (thickness of steel frame) in the designated moulding area (Figure 4-7).

Figure 4-7: Experimental set-up showing (A) the nonwoven textile lay-up and mould frame and (B) the platen press with designated moulding area on a COLLIN P200P/M machine.

A range of tests were conducted prior to composite moulding to reveal further information about the material and behaviour when moulding:

- Thermal analysis of the thermoplastic polymer was conducted to obtain its process window for the subsequently applied process cycle. The evaluated onset temperature of 350 °C for degradation of the PP material tested in a nitrogen atmosphere sets the upper boundary for the process conditions in the first part of study until otherwise noted.
- Analysis of the fracture surface of single-layered and moulded textiles were evaluated from a qualitative perspective to evaluate the fibre distribution with a change in FWF. Compression trials of single layers with pure polymer showed optimum melt behaviour at 200 °C.
- The heating cycle of the moulding process was simulated with a hot stage microscope. The base analysis revealed a small degree of a hydrophilic characteristic when simulating the fibre-matrix (SM45D/PP) interaction whilst melting and cooling on a hot stage microscope. After solidification, the effect is not visible anymore. The hydrophobic tendency can be confirmed with SEM images of the composite fracture surface showing no indication of wetting as expected between a non-polar polymer and the sized material. This shows that the simulation was suitable for this material characterisation and could be used for other material compositions to understand the behaviour of the material prior to the composite production.

4.2.2 DESIGN OF EXPERIMENTS (DOE)

The following parameters can be modified for the isothermal processing and were taken into consideration in this study:

- Heating rate
- Moulding temperature (Dwell time)
- Cooling rate
- Start & end temperature
- Contact pressure
- Moulding pressure
- Moulding time
- Mould fill

Alongside the adjustable process parameters associated with heating and cooling the level of mould fill is of importance in order to achieve void-free composites. With regard to processing, the machine is loaded with the material to a certain level before processing. The process starts when the set temperature is reached. When the heating rate has been obtained, the contact pressure is applied to the material. The contact pressure compresses the mould to the final plaque thickness and optimises the heat transfer between the press plate and the compound [16]. When compressing the textile, the air within the nonwoven layers is expelled. The moulding pressure is applied when the moulding temperature is reached and is maintained for the entire moulding process to prevent deformation [83].

As described above, there are eight variable parameters within this experimental investigation. A common way of studying several parameters on a new machine or process, in general, is the OVAT method which changes one variable at a time and keeps all the other parameters fixed [123]. To identify the individual impact of multiple parameters (k) on the composite performance with a minimum of two levels – low and high (n) -the following equation can be used to determine the total number of a two-level permutations [161]

$$n^k = 2^8 = 256 \quad (12)$$

This results in a minimum of 256 total experiments to run when varying two or more levels per parameter and considering all adjustable parameters on the COLLIN press. The high number of runs not only requires a high amount of material but also exceeds the time available for the project. Based on the literature and standardised processing, the following section gives more information on the process window development.

4.2.2.1 PROCESS WINDOW DEVELOPMENT

Current and past research projects working on compression moulding, particular the isothermal process, using polypropylene-based composites reinforced by rCF were reviewed in Chapter 1 and the stated process conditions are summarised in Table 4-6 divided by process parameters. Apart from the heating rate, which is set to 9 °C/min by Caba *et al*. [83] for processing carbon fibre mats, there is no particular method to follow when it comes to

processing the specified material. The moulding temperature varies between 15 °C and 46 °C above the melting temperature of PP, with no degradation issues reported on the higher end of the process window of Giannadakis' work [162]. The moulding time was reported from 1 minute to 10 minutes before cooling down with 11 °C/min or very quickly by 40 °C/min. Also, the moulding pressure shows a wide range from 20 bar to 172 bar, all applied on a laboratory scaled press with a maximum applied force of 667 kN [83].

Table 4-6: Overview of Process Parameters for Thermoplastic Composites (rCF/PP)

Parameter	Specific Condition	Manufacturer
Heating Rate	9 °C/min	Caba [83]
Moulding Temperature	180 °C ($T_{m,PP} = 165\ ^{o}\mathrm{C}$)	Caba [83]
	200 °C ($T_{m,PP} = 164.5\ ^{o}\mathrm{C}$)	Akonda *et al*. [61]
	210 °C ($T_{m,PP} \approx 164\ ^{o}\mathrm{C}$)	Giannadakis *et al*. [162]
Moulding Time	1 min	Wölling *et al*. [79]
	7 min	Giannadakis *et al*. [162]
	10 min	Caba [83]
Cooling Rate	11 °C/min	Caba [83]
	40 °C/min	Giannadakis *et al*. [162]
Moulding Pressure	20 bar	Akonda [61], Wölling [79]
	135 bar	Giannadakis *et al*. [162]
	172 bar (667 kN press)	Caba [83]

There is a high variation of process conditions in the reviewed projects. Therefore, information about precise process conditions was collected from ISO standards of polymer and composite processing and used as additional guidance (Table 4-7). Furthermore, a thermal analysis of the supplied polymer was carried out to further clarify the polymerisation process window. The process window of PP was set between 163 °C - 300 °C for heating the polymer which is cooled to below 111 °C before further processing or handling to prevent deformation.

Table 4-7: Given ISO standards as recommended process parameters for polymer processing

Process Parameter	Specific Condition	Reference
Pre-heating Time	5 – 15 min	ISO 1873-2 [163],
Moulding Temperature	210 ^{o}C	ISO 1873-2 [163]
Moulding Time	2 min	ISO 293 [164],
Demoulding Temperature	≤ 40 ^{o}C	ISO 1873-2 [163]
Cooling Rate	15 ± 5 °C/min	ISO 1873-2 [163]
	5 - 20 °C/min	ISO 293 [164]
Moulding Pressure	50 bar	ISO 1873-2 [163]
Mould Type	Picture frame	ISO 1873-2 [163]

The preheating time, heating rate and de-moulding temperature were neglected to minimise the total number of variables. The pre-heating time is set to 5 min at 30 °C [163] to restore the tool temperature before every run (not included in the total measured cycle time). The heating rate can influence the surface finish depending on the specific heat capacity of the resin [165]. However, the focus lies on the mechanical performance and is therefore not included in this investigation. The heating rate is set to the machine's maximum limit, here 20 °C/min, to speed up the process. The suggested picture frame was applied as mould type. The main input parameters to be investigated in the DOE were reduced from eight to five, with a yet unknown level of impact on the process, are:

- Moulding temperature
- Moulding time
- Cooling rate
- Moulding pressure
- Mould fill

Further initial experiments were performed to define the initial process window using these five parameters. The trials showed that a minimum contact pressure of 5.2 bar (derives from 40 bar pistol pressure on a 384 cm^2 sample including frame) and moulding temperature of 200 ^oC are necessary, when operating the COLLIN platen press, to close the mould for the given material lay-up and to obtain a visible fully melted polymer and acceptable composite surface finish. The effect of moulding time is unspecified in the literature. So, the lower edge of the process window was chosen from the listed ISO Standard, which indicates 2 min. The maximum dwell time of 10 min is adopted from Caba *et al.* [83]. The influence of crystallinity on the mechanical properties requires the implementation of the proposed values for cooling rates of 5 – 20 °C/min by the ISO standard for thermoplastic processing [164] The entire isothermal process with chosen process parameters results in process cycles between 20 - 40 min. Assuming that an optimum calculated mould fill gives the best behaviour (set to minimum), an additional level with overload (set to maximum) is added to prevent a high level of porosity by applying relatively low compact pressure. The factors of DOE and their levels are given in Table 4-8.

Table 4-8: Initial Process Window with process parameter factors and their levels for DOE

Factor	Low level (-1)	High Level (+1)
Moulding Temperature	200 °C	240 °C
Moulding Pressure	5.2 bar	15.7 bar
Moulding Time	2 min	10 min
Cooling Rate	5 °C/min	20 °C/min
Mould Fill	Optimum (100 %)	Overfill (130 %)

4.2.2.2 SELECTED DESIGN

The final DOE describes a two-level fractional factorial design with a maximum of five factors and a total number of 16 runs. The general design matrix is given in Table 4-9. Output parameter for statistical analysis is the tensile performance, separating between strength and modulus properties, which represent the mechanical performance of the manufactured composite and can be determined quantitatively. The void content of the manufactured panels was measured for additional quality control of the composite. In addition, a qualitative fractural analysis of tested samples by SEM was carried out and shows the level of fibre-pull out, matrix distribution and wetting behaviour. For statistical analysis, the run order is randomised by the software, to prevent any impact from other machine conditions and additional noise variables. For validation of the findings of the DOE approach, the response values are plotted against its error (standard deviation) [123].

Table 4-9: Experimental matrix showing combinations of applied input factors investigating two levels, with its low level (represented by -1) and high level (represented by +1) for a screening design based on a ½ factorial model.

NO.	INPUT FACTORS					RESPONSE VALUES		QUALITY
Run	Moulding Temp. [°C]	Moulding Time [min]	Cooling Rate [K/min]	Moulding Pressure [bar]	Mould Fill [%]	Tensile Strength [MPa]	Tensile Modulus [GPa]	Porosity [vol%]
1	-1	-1	-1	-1	+1	Y1-1	Y2-1	P-1
2	-1	-1	-1	+1	-1			
3	-1	-1	+1	-1	-1			
4	-1	-1	+1	+1	+1			
5	-1	+1	-1	-1	-1			
6	-1	+1	-1	+1	+1			
7	-1	+1	+1	-1	+1			
8	-1	+1	+1	+1	-1			
9	+1	-1	-1	-1	-1			
10	+1	-1	-1	+1	+1			
11	+1	-1	+1	-1	+1			
12	+1	-1	+1	+1	-1			
13	+1	+1	-1	-1	+1			
14	+1	+1	-1	+1	-1			
15	+1	+1	+1	-1	-1			
16	+1	+1	+1	+1	+1	Y1-16	Y2-16	P-16

With a set confidence level of 95 %, a normal distribution of errors is targeted, which can be visible in normal probability plots or a histogram generated by the software. When the data points follow a straight line in a normal probability plot, the distribution can be seen as confirmed. The histogram shows one peak and further columns accumulated around with lower frequency. Additionally, an equal distribution of the plotted values in a versus fit plot

above and below the fitted line is targeted. The residual analysis is performed prior to the factor evaluation of the design of experiments. A non-conformance from the normal distribution in plotted values gives information about the experiments not performing as expected [122] or being incomplete in terms of evaluated factors [166]. In the following, the design outcome and robustness of the model is discussed.

4.2.2.3 DESIGN OUTCOME

Following a six-sigma approach, the design of experiments was chosen to identify the most relevant process parameters. The composites were manufactured following a screening approach of the design of the experiment. 16 runs of randomly selected parameter combinations of moulding time, moulding temperature, pressure, cooling rate and mould fill were performed to understand which parameters most affect the tensile strength and modulus most before going further into detail. Two design of experiments were performed, because the pressure level was adjusted after DOE to exploit the maximum possible pressure on the hot press device with DOE2 [Results given in Appendix B].

A response analysis was conducted prior to the DOE analysis. It showed a bimodal distribution of DOE traced back to the material source, which can be caused by a machine or human failure which may lead to material inconsistency (Figure 4-8).

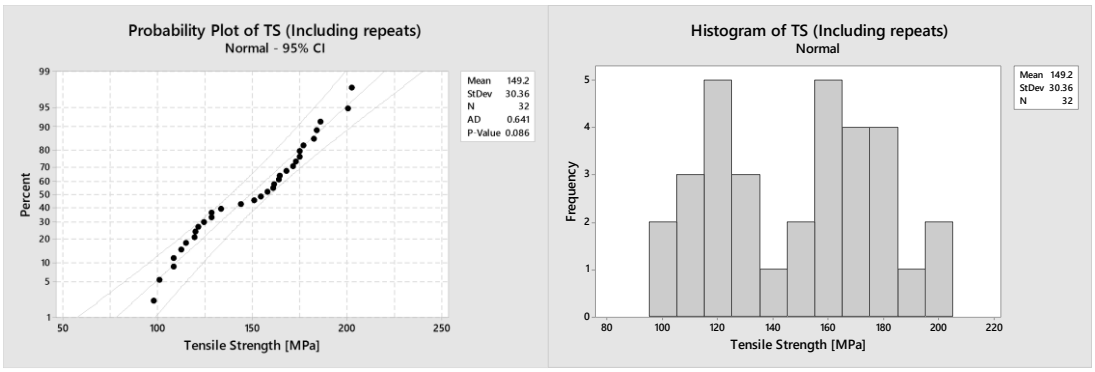

Figure 4-8: Histogram and probability plot of all response values Y1 (tensile strength) with 32 data points for DOE showing slight divergence from a normal distribution, obtained from the calculation in Minitab 18 software.

The repeated histogram plot with a sample size of 32 gives a bimodal distribution, which indicates that important variables were not yet accounted for or the data was collected from two sources [7, 14]. It could be, for example, the test temperature, machine conditions on a specific test day or the material batch, which was not considered as an input variable and affects the analysis so much as to create two populations.

In Figure 4-9, histograms are shown where the material was considered as one of these factors. The histogram grouped by batch number (delivered material roll) showed no correlation to the bimodal distribution (Figure 4-9, left).

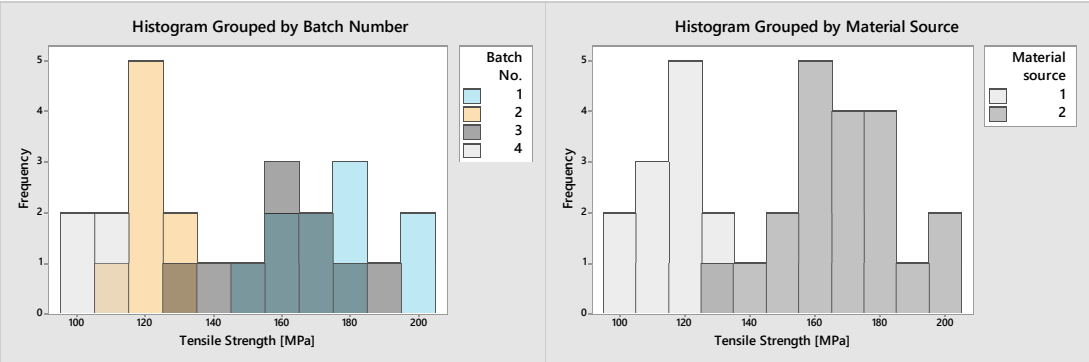

Figure 4-9: Histograms of response values Y1 (tensile strength) for DOE1 with 32 data points, calculated in the Minitab 18 software. The histograms were grouped by batch number and material source.

However, the histogram grouped by material source, where batch 1 and 3 and batch 2 and 4 are considered to be from the source, clearly demonstrates two different populations within the distribution (Figure 4-6, right). In addition, the use of material source 1 results in composites from 98 to 128 MPa, whereas material source 2 achieved performances between 130 and 200 MPa in strength. The difference in the material source (with regard to the supplier) can be traced back to the textile production and shows a batch-to-batch variation as significant factor, which was not considered in the model before. It shows that the textile material is not yet as consistent as the textile producer thought (processed in the early development stages at EGLCF). The identified outcome can have the following reasons:

- Varied material composition and/or FWF,
- Different production date or another machine related variation
- Workers related variation (e.g. different handling, manual feeding speed)

Whereas the FWF can be analysed, specific information regarding production, machine and workers are undisclosed and cannot be clarified at this point. Therefore, a final conclusion cannot be drawn yet. At this stage it should be highlighted that the consistency of the material, the workers and machine related configurations are important to be able to identify the impact of the changes in processing conditions when manufacturing the composites. Nevertheless, the total number of runs is below the recommended data points for a fully robust system and the correlation between the bimodal distribution and the material source shows the importance of working with the same material batch to ensure material consistency. It should be noted that the uncertainty regarding the effect of the material

source on the response values for DOE1 and the proof that material consistency is very significant. Due to the given inconsistency in DOE1, only the additional modified DOE (DOE2) was further analysed.

For DOE2, the material refers to the same batch for one series of experiments. Subsequently, the DOE2 showed a normal distribution as targeted, yet the applied processing conditions led to poor composite quality. As a result, no significant effect of parameters on the composite performance could be evaluated from this study. Reasons were the following:

- General excessive long fibre pull-out, visible by eye after testing, indicated a low level of consolidation and lack of matrix proportion in the samples. The supplementary microscopic analysis confirmed loose fibre arrangement and unequal matrix distribution in the composite samples
- This study started by conducting the DOE based on a literature review and available ISO standards. Since the applied material was not used in this form for this process type before, recommendations are based on short fibre composites, general plastic processing and glass mat thermoplastics (GMT) manufacturing.

In conclusion, the outcome of the DOEs showed that the process window development was limited, and the approach not suitable for the textile material. Therefore, new alternatives in terms of methodologies are needed to fully explore the capacity to process the commingled nonwoven material. A more traditional approach was taken, using the OVAT method, to explore one variable at the time, and is explained in the next section.

4.2.3 ONE-VARIABLE-AT-A-TIME (OVAT)

Another methodology was applied to determine the missing information about handling and processing the nonwoven material. The polymer characterisation formed the starting point to examine the polymer processing window and the thermal resistance of the polymer. Furthermore, the mould set-up was checked to establish a reason for the poor composite quality reported in the previous described DOE trials. Overall, the following process adjustment were investigated using the OVAT approach:

- Effect of mould set up (vacuum bag, frame, tape)
- Effect of moulding parameters (e.g. temperature, time, pressure)

4.2.3.1 EFFECT OF MOULD SET-UP

Applying an additional vacuum bag system showed less effect on the reduction in void content than simply avoiding the use of the metal picture frame. Nevertheless, it presented a positive outcome when looking at the amount of circumvented material applied for

potential future setups when using the vacuum bag method. Heat-resistant technical foam tape (known as Tack tape) was used for further experiments as frame compensation and to prevent polymer overflow. Trials achieved constant plaque thickness with this new experimental set-up and accomplished the targeted standard thickness of 2 mm and 4 mm (Figure 4-10).

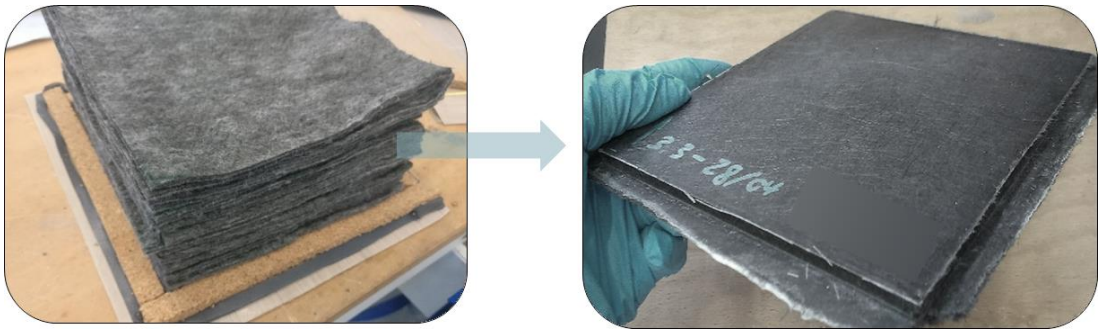

Figure 4-10: Adjusted mould set up moving from a steel frame a softer mix of tack tape and cork frame.

The crucial point here is that the presence of the steel frame prevented a full distribution of applied pressure on the actual composite which resulted in highly porous panels of up to 17 vol%. Also, comparing the achieved values with a variety of applied process modifications to the results from the DOE shows a successful reduction of the void content to a minimum of 1 vol% when using the adjusted mould set-up. However, where a maximum of 213 MPa in tensile strength was achieved in the set-up with a picture frame (DOE2) resulting in 12.2 vol% porosity, the modifications only achieved a maximum strength of 149 MPa with 3.7 vol% respectively. At this stage, no correlation was detected between the lowest porosity values and strongest samples in regard to the tensile strength. This leads to the assumption that other factors, which could not be identified at this stage, affected the performance significantly.

4.2.3.2 EFFECT OF MOULDING PARAMETERS

The analysed isothermal process types in DOE/DOE2 resulted in cycle times exceeding 40 min. The long process time could have led to degradation of the polymer during the process and subsequently a low composite quality. Further trials focusing on the process parameters were performed as follows:

- The thermal stability of the matrix material
- Processing parameters applied to textiles with varied FWF.

The thermal stability of the polymer was further investigated in artificial (N_2) and ambient conditions (air) to prove the set process window for manufacturing nonwoven material in the hot press [90]:

- Isothermal test condition: resulted in a maximum dwell time for material exposed to temperatures between 240 °C and 260 °C for 15 min. With a process temperature of 220 °C or 200 °C moulding times of 32 min and 60 min are within scope respectively (loss of greater than 5 % is unacceptable.).
- Dynamic test condition: showed that the onset temperature varies more greatly with the type of atmosphere. The new evaluated onset temperature of 223 °C for degradation of the PP material in N_2 (air: 354.25°C) sets the upper boundary for the process conditions in this study

Further trials looked into two levels of FWF to further investigate the material composition and the possible relation to the low composite quality detected in the DOE studies. A decrease in fibre weight fraction from 40 to 30 wt% could lead to a more satisfactory balance between fibre and matrix material, an improved impregnation of the textile and subsequent enhanced stress transfer throughout the samples. The different textiles containing either 30 wt% or 40 wt% were processed at two different temperature levels (200 °C, 220 °C) for up to 20 min, excluding heating and cooling (Figure 4-11). The isothermal process carried out on a laboratory scaled press delivered a consistent thermal and pressure cycle with 19 – 63 min long runs.

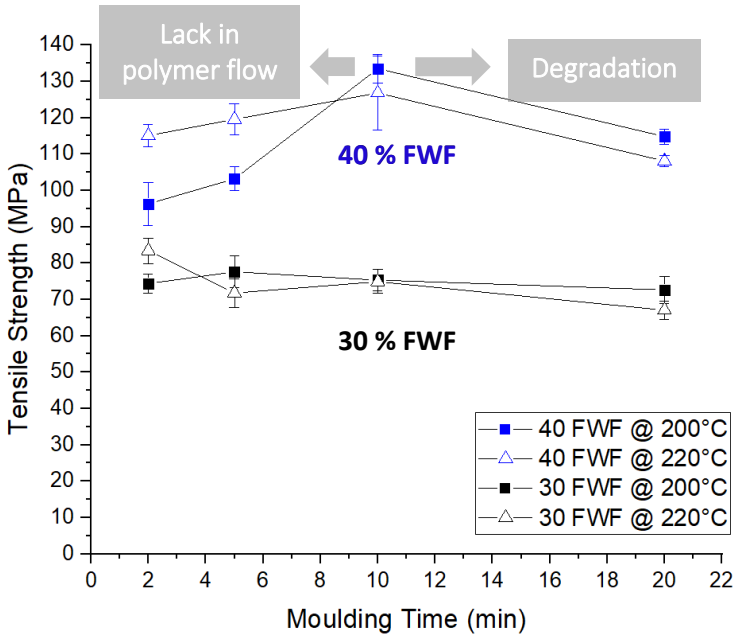

Figure 4-11: Analysed tensile strength performance versus moulding time and moulding temperature (SM45D / PP) containing a different level of fibre weight fraction, 30 wt% and 40 wt% textiles derived from ELGCF`s lab line.

Overall, it can be seen that the material processed with 30 wt% rCF led to lower mechanical performance which therefore prevents the successful application for 30 wt% textiles. Furthermore, it should be noted that for 40 wt% composites processed at 200 °C and 220 °C below 10 min, the composites did not reach a level of good consolidation, which reflects the increase in void content. The subsequent decrease in strength and may have been caused by a lack of polymer flow. In addition, when manufacturing plaques at 220 °C at 10 min moulding time, the smell of degraded polymer occurred. The thermal degradation was neglected in the DOE to the detriment of the researcher and long-term stability of the parts but is from now on treated as 'failed' experiment. The drop in tensile strength with a simultaneous increase in moulding temperature and time (40 wt% composites) shows a similar trend to the thermal analysis on isothermal conditions, where a weight loss was detected when exposed for a longer time that increases with simultaneous higher temperature.

Optimum conditions were obtained when processing the commingled 40 wt% SM45D/PP material at 200 °C for 10 min with the same heating and cooling cycle of 20 °C/min. Processing below or above this condition resulted in polymer degradation or was restricted by inefficient polymer flow. These process conditions were set at this stage and not further modified.

4.2.3.3 EFFECT OF FIBRE ORIENTATION & PRODUCTION BATCH

Throughout the experimental study, a noticeable change in values whilst repeating selected parameters was detected. The reasons for this were inconsistency in material or differences in material batches (as identified in the DOE) and manufacturing conditions. In general, it was observed that laminates manufactured for the DOE2 achieved higher mechanical performance in strength and Young's modulus than in the OVAT study applying similar process conditions but were limited by the frame which resulted in high porosity. In addition, a relatively low mechanical performance, but sufficient void content, let assume potential alignment in the samples and possible incorrect test direction for mechanical composite performance analysis. Fibre alignment is one of several issues which needs to be addressed when it comes to manufacturing composites with discontinuous fibres, which nonetheless require the highest mechanical performance. Here, the nature of the textile manufacturing process and the method of preparation influence the final performance. If the fibres are aligned, the mechanical performance of the composite is dependent on the test direction parallel to the fibre orientation. The exceeded performance in a specified test direction can be detected as aligned fibre orientation. Therefore, composite plaques have been manufactured and tested in different directions; the roll direction, cross-plied and in carding

direction to investigate the influence of the possible fibre alignment on the tensile strength and modulus. The following experimental study compared textiles derived from to different textile batches. The textiles were piled with different orientation (roll direction, cross-ply, carding direction) and were tested accordingly. The results are shown in Figure 4-12.

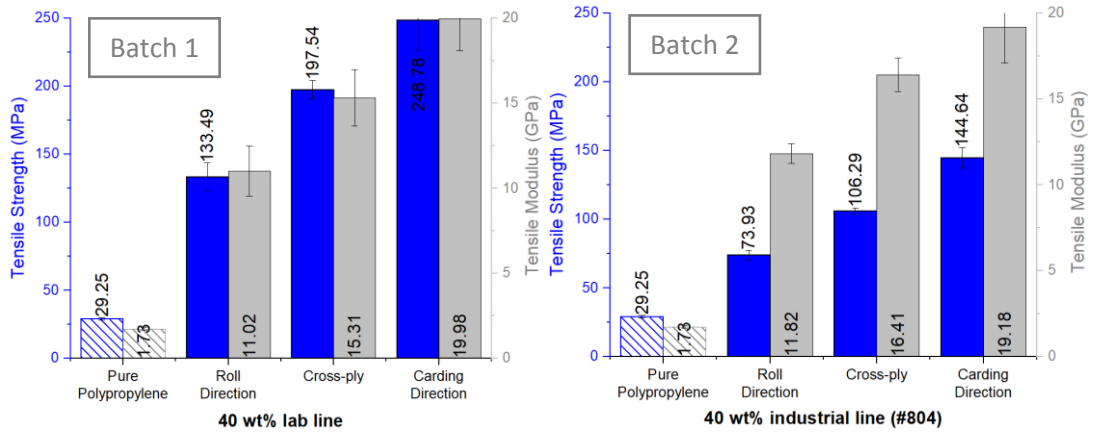

Figure 4-12: Mechanical performance dependent on the textile direction for two different batches: (A) batch 1 supplied from research line at ELGCF and (B) batch 2 derived from industrial line at ELGCF.

An increase of 86 % and 96 % in tensile performance, tested strength and stiffness respectively for both batches, from roll to carding direction underlines a clear trend towards fibre orientation in the nonwovens along the carding, which orients perpendicular to the roll direction of the textile. Considering the textiles supplied from the research line at ELGCF (Figure 4-9, left), up to 248 MPa in tensile strength and 20 GPa in modulus can be obtained respectively for samples tested along the main fibre direction, which represents the cross direction (CD). In comparison, only 134 MPa and 11 GPa were obtained respectively in the machine direction (MD) for manufactured 40 wt% SM45D/ PP laminates. This underlines that the previously manufactured samples in the OVAT study were tested in the weaker direction and the assumption of random orientation in the composite probe can be shown to be false. It demonstrates a quasi-alignment of the fibre arrangement within the nonwoven textile manufactured at ELGCF`s laboratory line and subsequently in the composite materials. When comparing properties of textiles supplied from the industrial line at ELGCF, a certain decrease was detected in composite strength. With a similar level of measured tensile modulus, a decrease in maximum tensile strength from 249 MPa to 145 MPa was observed when comparing the two textile batches processed on a laboratory scale and an industrial scale. A detectable difference in fibre diameter between the processed material batches is assumed to be the cause of the decrease in composite strength. With the change of textile machines thinner fibres were fed into the machines when processing SM45D/ PP webs which were

manufactured on an industrial scale. Obtaining the same level of Young's modulus, the overall process conditions can be shown to be homogenous. Nevertheless, this demonstrates that the material range of each fibre class given by the supplier is too large to predict the optimum behaviour. It can be assumed, that with the composite performance obtained from the processed textiles supplied from the industrial line (batch 2) the lower range is reached. Whereas the textiles from the research line (batch 1) showed the upper range of possible composite performance.

4.2.4 BENEFITS AND LIMITATIONS OF PRODUCTION ON LAB SCALE

4.2.4.1 TEXTILE PRODUCTION

A high deviation in the materials ratio was detected within the textiles derived within and from different batches. A range of 23.4 – 33.1 wt% of FWF was measured for supplied textiles set to 30 wt%. The measured deviation sits above the 5 wt% allowance set by the supplier. A slightly lower range was obtained for 40 wt% textiles: 33.0 – 44.5 wt%. Whereas the nonwoven material has a slight, natural uneven distribution of carbon and polymer filaments within the probe which can be traced back to the machine equipment, additional manual failure of hand-feeding (on a laboratory scale) the feedstock into the machine could be the reason for a higher deviation. In addition to the detected inconsistency in material ratio within the commingled nonwoven textiles, inconsistency in material type within manufactured batches was also detected when evaluating the fracture surfaces. Figure 4-13 gives an example of a contaminated material batch containing two different material types, which vary in surface topography when manufacturing composites using SM45D fibres only.

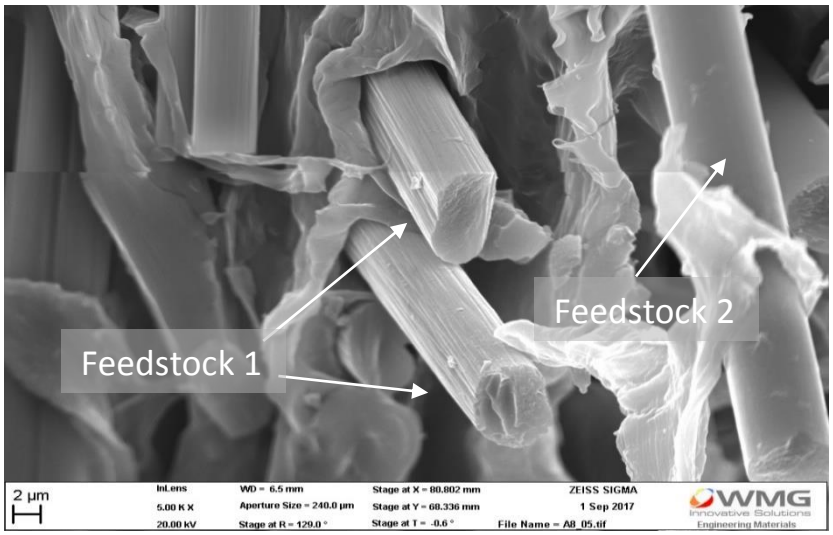

Figure 4-13: SEM image shows fracture surface of a manufactured sample showing pyrolysed (Feedstock 1) and sized (Feedstock 2) fibre feedstock in the same sample.

The preceding analysis in Section 4.1.1. showed the difference in fibre topography between sized and pyrolysed fibres differing in a smooth and carved surface respectively (inclusive of textiles supplied before 2018). The detected material inconsistency in terms of weight fraction and material contamination could be the trigger for uncertainty in processing conditions throughout the experimental study. The variety in material ratio (determined FWF) and mix of fibre feedstock from contamination between material changeovers are two factors which need to be constant when the effect of processing conditions is analysed to identify significant effects on the process line. With an ELGCF internal upgrade from laboratory scale to an industrial textile line, the process runs inclusive which automatically eliminates any manual intervention of. hand feeding and variance of FWF.

4.2.4.2 COMPOSITE PROCESSING

The composite processing on a laboratory scale, using the COLLIN platen press, was carried out to gain knowledge and expertise about the processing of commingled nonwoven material. It forms the first section of the investigations, including the DOE and OVAT studies, throughout this project. The small-scale application provided opportunities to vary the final composite thickness. Also, a simple preparation with only few materials required allowed a large number of experiments to be conducted, based on a controlled process cycle. However, a certain restriction of processing was found with the isothermal processing approach on the COLLIN machine which indicated limitations regarding component size, cycle time and applied pressure and prevented research into and development of industrial applications.

4.2.5 MILESTONE 1: BASELINE MANUFACTURING CONDITIONS

This section summarises the first set of experiments with their findings considering DOE and OVAT studies on a laboratory scale and forms milestone 1. The defined and optimised process window obtained from comprehensive experimental work using a laboratory-scaled press resulted in a total cycle time of 27 min. After an in-depth analysis of the process parameters at isothermal process conditions, the optimised process window for manufacturing SM45D/PP composites using commingled nonwovens was set to the following:

- Start processing at room temperature,
- Heating and cooling cycle rates of 20 °C/min,
- Dwell time of 10 min at 200 °C and
- De-moulding at room temperature.

The isothermal process type simulated the manufacturing conditions of the industrial partner ELGCF. The applied systematic approach reduced the cycle time to a quarter of the starting point of 110 min (schematically shown in Figure 4-14).

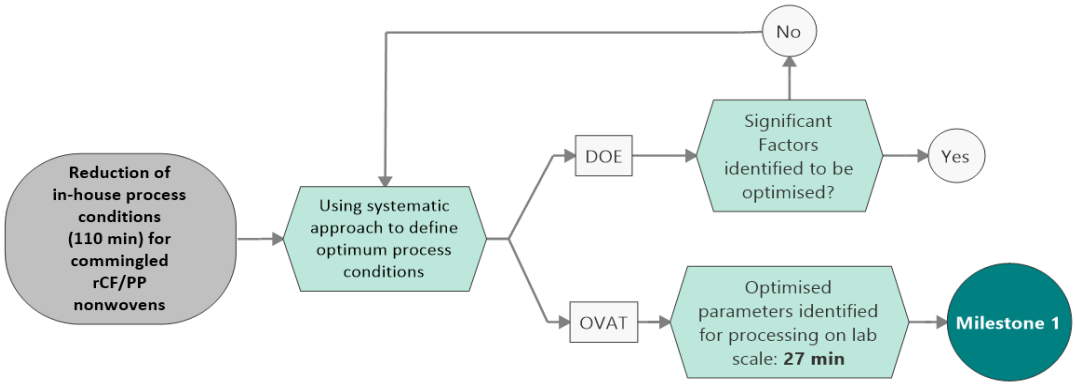

Figure 4-14: Schematic of the initial experimental steps on laboratory scale to be conducted using different systematic approaches to identify the optimised process conditions.

The more efficient process was applied to other material combinations. In this case, the processed nonwovens varied in fibre type (IM56D, IM56R, IM56L), but the ratio and type of the polymer composites were kept identical to 40 wt% rCF for direct comparison. A summary of obtained mechanical performance with a focus on tensile and flexural properties is given in Figure 4-15 divided by fibre type. This gave the first indications of possible composite quality for further modifications.

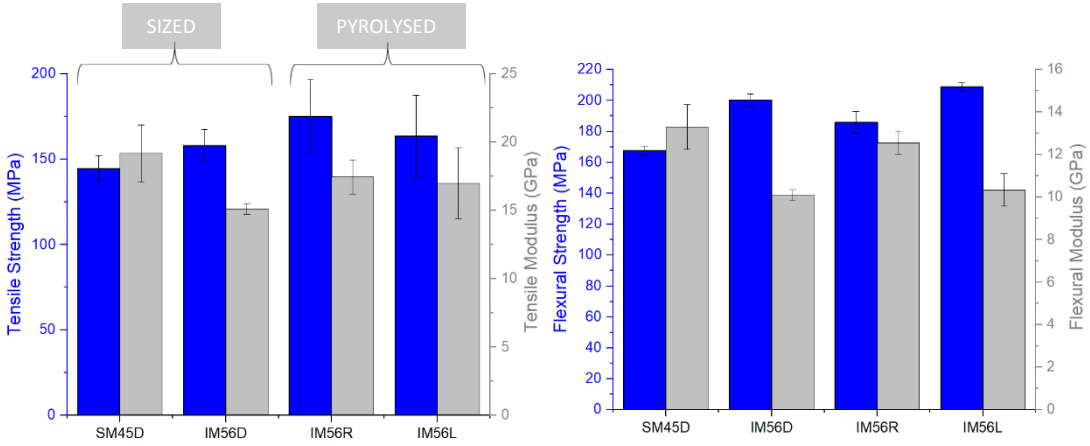

Figure 4-15: Summary of fibre dependent tensile performance of 40 wt% composites with different rCF feedstock[4]. Test direction along the fibre direction. All evaluated composite

[4] SM – standard modulus, IM – intermediate modulus; numbers stand for strength level, e.g. 45: 4 – 5 GPa in fibre strength; recycling method is indicated by abbreviation D (dry fibre, mechanically recycled), R (pyrolysed dry fibres) and L (pyrolysed prepreg laminates).

types can be classified in the top-range of rCF/PP applications when comparing these to other recycled carbon fibre projects given in Chapter 2. This underlines the market competitiveness regarding their mechanical properties. In addition, the direct comparison of rCF feedstocks processed with the same polymer under same conditions, as given in this project, highlights the rCF fibre type-dependent characteristic for the first time. Fibre type SM45D, representing a sized and chopped fibre with the lowest fibre modulus and strength, resulted in the weakest composite regarding tensile and flexural strength) which was, surprisingly, the stiffest. In this case, a homogenous impregnated textile resulted in an almost void-free composite where efficient stress transfer is given. SM45D/PP reached comparable properties as obtained by Wölling *et al.* [79] using the same fibre class. Furthermore, the IM56 fibre type generally resulted in a similar or lower evaluated stiffness, where IM56D/PP showed the lowest. The lowest stiffness of IM56D/PP panels can be directly related to the higher void content (Table 4-10). This led to the assumption of low interfacial characteristics, in regard to the chemical interaction, and subsequent weak adhesion between IM56D fibre surface and matrix (PP).

Table 4-10: Summary of evaluated FWF and void content for each manufactured composite panels for tensile testing.

Fibre Type	Recycling Method	FWF [wt%]	Void Content [vol%]
SM45D	Mechanical	40.22 ± 0.46	0.05 ± 0.00
IM56D	Mechanical	43.45 ± 0.27	13.23 ± 0.21
IM56R	Thermal	34.38 ± 0.0	2.39 ± 0.01
IM56L	Thermal	29.77 ± 0.24	0.21 ± 0.01

Looking at the pyrolysed feedstock, the measured void content varied between 0.21 and 2.39 vol% which falls in the range of low porous composites. The lower composite modulus could be traced back to a higher polymer fraction. But the composites containing pyrolysed fibre IM56R and IM56L, behaved similar or better in composite strength (tensile and flexural), compared to the composites containing sized fibres. This could be explained as follows:

- Residual char may behave as a positive trigger promoting the interfacial adhesion, in regard to physical interaction, between the fibres and the non-polar matrix. However, the data cannot prove this assumption.
- Through an additional chemical composition analysis of the fibre surfaces, which was included in a later subproject to increase the knowledge about the fibre characteristic from the chemical point of view (Section 5.2.3), it was shown, that the pyrolysed feedstock behaved slightly better in terms of interfacial bonding compared to the sized feedstock.

- The permanent sizing covering IM56D fibres created a barrier and behaves contradicted to a smooth stress transfer within the composite. The opposite was visible for SM45D fibres.

In summary, a starting point was given for the process study on a laboratory scale. The results from this chapter were taken as a baseline for further process investigations. The obtained cycle time needs further research to obtain not only good mechanical properties but also achieve market competitiveness in terms of process conditions and subsequent process cost.

Further process investigations could focus on understanding the suitability of different process types for each feedstock and the possible adaption of characterisation techniques to identify trend prior to processing.

4.3 PILOT-SCALE PROCESSING

The gained knowledge about processing nonwoven textiles under isothermal conditions on a laboratory scale, uncovered benefits and limitations. Working on a small scale required fewer materials for the research trials but the applied isothermal process continued to lead to long cycle times. An adverse effect of a wide range in FWF was detected. It was not clear if the change in composite performance occurred due to modifications of the process conditions or varied material composition. The textile thickness and detected feedstock contamination within the supplied textiles from the research line at ELGCF showed further limitations on a laboratory scale.

The objectives of this research were to determine the achievable composite characteristic with state-of-the-art material supplied by ELGCF from the industrial textile line and the processing of textiles into composite components on a pilot scale. Two new processing methods were investigated to achieve the target to further decrease the process cycle time and enabling time-efficient processing. Here, given the baseline in the previous chapter, a range of rCF/PP material (please refer back to Chapter 4.1. for an overview) will be processed and evaluated separately to understand their process characteristics and subsequent composite properties.

4.3.1 RAPID-ISOTHERMAL & NON-ISOTHERMAL MANUFACTURING

Using a thermoplastic composite press on pilot-scale (100 t) gave the opportunity to apply a wider range of pressure (100 - 950 kN) and increase the cooling rate to up to 60 °C/min in a rapid-isothermal process. The DASSETT Process Engineering 950 kN composite press (Figure 4-11) includes a variothermal tooling system from Surface Generation (SG) with a 32-channel system (16 Channels per mould half, 600 W heating per channel).

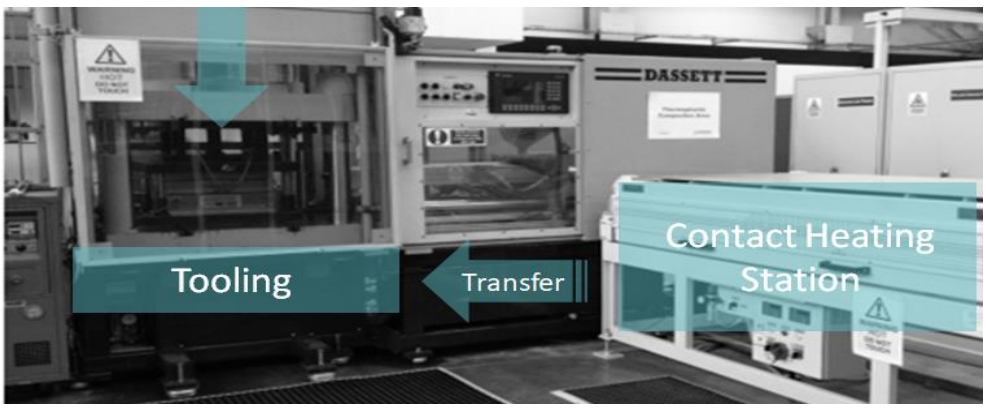

Figure 4-16: DASSETT composite process equipment (left) with external pre-heating stage (right)allowing continuous heating but requiring manual transfer to the mould.

The process consists of two stages, where the material is first pre-heated at an Elkom mikotherm-optimal contact heating station (Figure 4-16, right) and then quickly transferred to the closed mould system (Figure 4-16, left), where the moulding takes place. The mould is manufactured for 2 mm thick panels and curved on the sides to demonstrate drapeability throughout the part (Figure 4-17). A release agent was used to simply remove the parts after processing from the hot moulds.

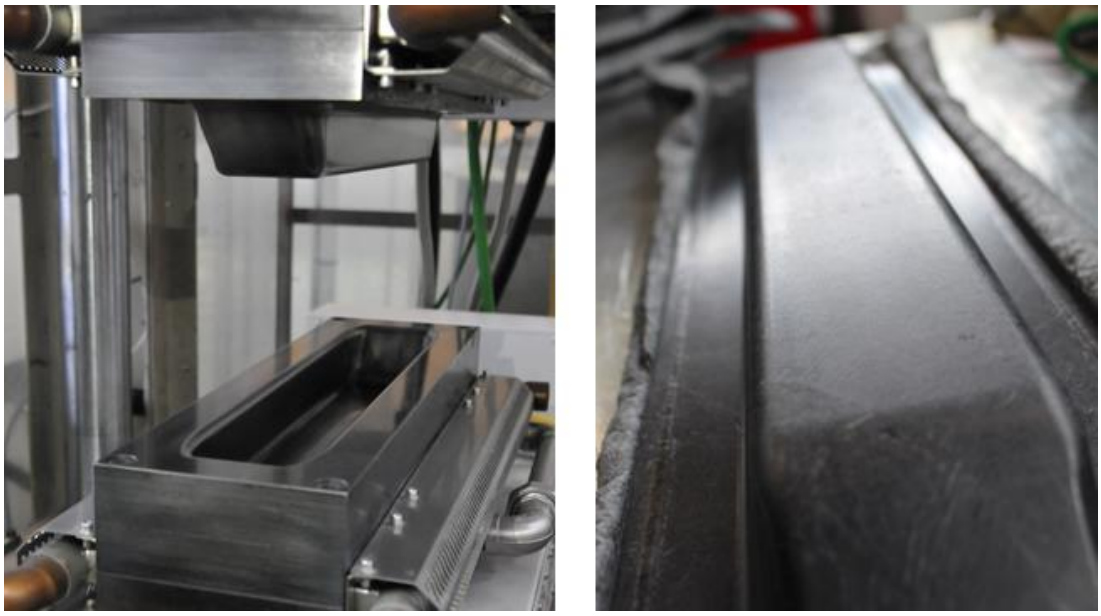

Figure 4-17: Mould system for part design of 2 mm thick manufactured panels using an 864 cm^2 steel tooling with the final composite on the left (developed and design protected by a WMG & SG internal project [167]**)**

To apply a comparable pressure of 3.13 MPa as with the isothermal process used on laboratory scale, a minimum force of 270 kN for the 0.0864 m^2 (864 cm^2) current tool size has to be applied and can be converted to 27 t of the applied load. The project trials in this study initially used an applied force of 200 kN (20 t applied load), which resulted in an applied pressure of 2.32 MPa, and represents a more cost-efficient process. There is the potential to increase the pressure in the future. The textiles are folded from the roll and plied in one direction with fibre orientation along the long axis (transverse direction) of the tool and subsequent test direction. The same machine set-up is used for both processes.

A potential alternative to the isothermal process is Rapid Isothermal Stamp Forming (RISF, Figure 4-18). Material is heated separately from the moulding device and placed in a hot tool, and is subsequently fast cooled below the crystallisation temperature before de-moulding [167]. In this instance the tool temperature is continuously undergoing a temperature change by circulating from moulding to de-moulding temperature, which is rather cost-intensive.

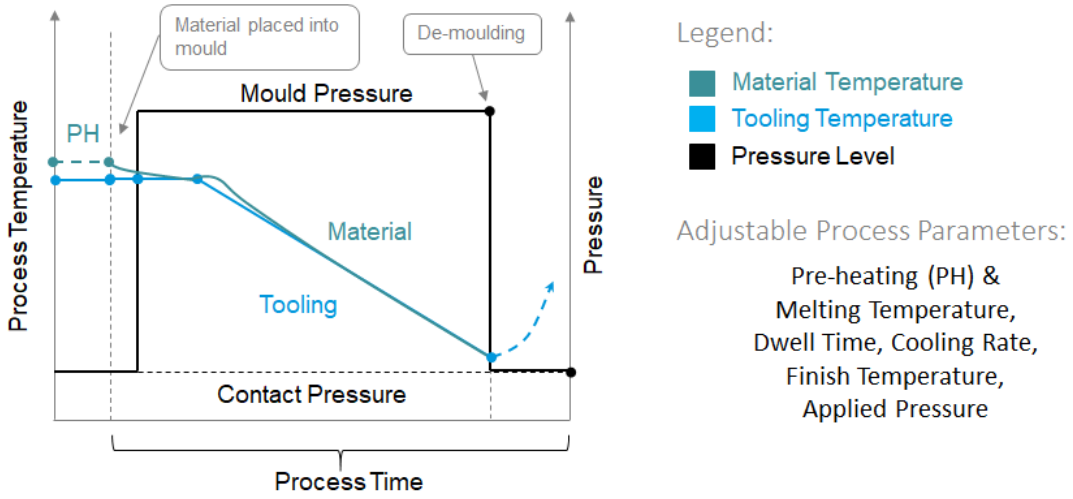

Figure 4-18: Schematic of the rapid-isothermal process with possible adjustable process parameters.

The second process which was investigated applies a non-isothermal method, also known as stamping [7]. The non-isothermal process promises the shortest cycle times and therefore the lowest cost [82]. The same machine set up was used as with the rapid-isothermal process. The material was also pre-heated in the separate heating system until above the melting point. After pre-heating (PH), the material was placed in a 'cold mould' (80 – 120 °C) and the material was forced to cool down under applied pressure to the tool temperature (Figure 4-19). One advantage of this is the unchanged tool temperature, which leads to savings in energy and operation cost, and the short cycles are suitable for a semi to high volume production [168].

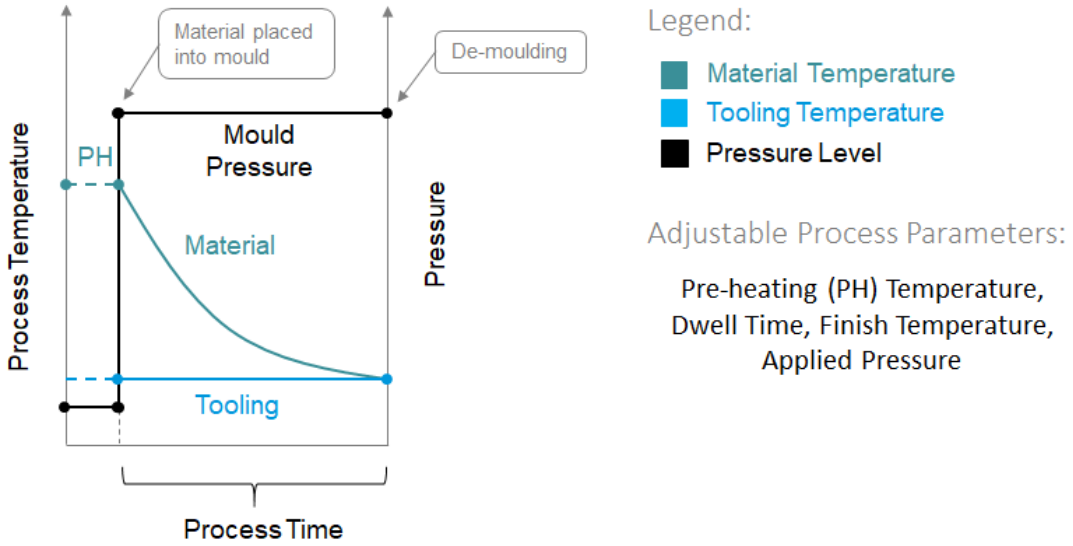

Figure 4-19: Schematic of the conventional non-isothermal process with summarised possible adjustable process parameters.

A trial performed by Davis *et al.* [160] showed that GMT can be manufactured using pre-consolidated sheets, which are thermoformed within 30 – 60 s of the final composite. Similar to the RISF method, the pre-heat temperatures vary with the polymer grade and are approximately 50 °C above the melting point of the polymer [120]. A comprehensive process study was developed by Trudel-Boucher *et al.* [169] to understand how all the adjustable processing parameters could be optimised and to maximise the mechanical performance of the manufactured components. The study showed that higher temperature and longer moulding times allowed for prolonged material flow before being fully consolidated, thus resulting in higher mechanical performance. In general, to reduce the void content, higher pressure is applied to the composite during processing which can potentially lead to fibre breakage [170]. The moulding temperature is required to be high enough to decrease the matrix viscosity and impregnate all fibres, but it must be below the degradation point. Lower temperatures and pressures would reduce capital costs [171]. All investigated processes can potentially be automated and, importantly, the non-isothermal process opens new possibilities for lower cycle times and cost-efficient processing [170], [172].

4.3.2 PRELIMINARY PROCESS INVESTIGATIONS

To investigate the process boundaries and set/ actual parameters of the pre-heating temperature, an interim process study was carried out. Thermocouples were placed in the approximate mid-plane of the material stack to record the actual material temperature while processing. Comparing different set and actual temperatures for the pre-heating process gives an average difference of 5.5 °C to the target value. To ensure a consistent softening stage (semi-soft) of the commingled nonwoven textile, the pre-heating window was fixed to 300 s (5 min) and performed before the moulding cycle.

By applying both the rapid-isothermal and the stamping process, the target was to shorten the processing time compared to the standard isothermal process but with a level of quality remaining (e.g. low void content, good impregnation level), which would be applicable in industry. A fast cooling cycle is essential when it comes to shortening the entire process. Hence, the monitored temperature profiles of the entire processes are given to understand the effect of the process sections next to the moulding procedure. It was noted that, the re-heating cycle of the rapid process stayed unchanged with the temperature level from the de-moulding process back to moulding temperature at 14.5 °C/min for the applied steel tooling. The start temperature was reached when the upper and lower mould reached the set temperature level again (Figure 4-20, left).

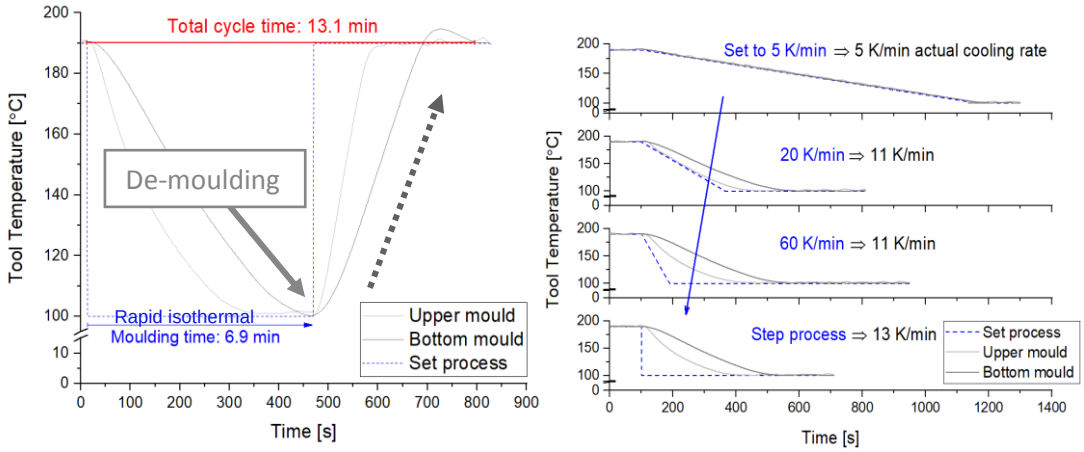

Figure 4-20: Monitored temperature profile for processing material using the rapid isothermal process from 190 °C to 100 °C showing (left) the entire cycle including re-heating the tools subsequently to the start temperature for the next part and (right) the varied cooling cycle with set process window.

When calculating the total cycling time of the process, 6.2 min was assigned to the re-heating section to start temperature, which is dependent on the machinery and its tooling material. Therefore, only the moulding section was the focus of the following process study for a potential optimisation and reduction in moulding time and subsequent total cycle time.

In the beginning, the aim was to eliminate as many process parameters as possible to focus only on the essential processing conditions during the process study. Preliminary trials observed the capability of the machine to quickly cool down the parts before de-moulding, where the correlation and effect on the mechanical performance were considered. It is known that the cooling rate can affect the degree of crystallinity of the polymer and with that, the composite stiffness [173]. Whether the effect also occurs for rCF/PP composites, is discussed in the following section.

The moulding temperature was set at 10 °C above the pre-heating level assuming a minor heat loss during the transfer from one device to another but avoiding overheating and possible oxidation of the material with applied pressure. The cooling started directly after closing the tool when the softened material was transferred to the mould. First of all, a significant difference in programmed/set and the actual cooling rate of the variothermal tooling system was discovered (Figure 4-20, right). Cooling rates of 60, 20, 5 and 0 °C/min were evaluated. The latter was simulated with a so called ‘step process’, where a change in temperature level was programmed and the actual cooling rate eliminated. In general, the following observations were made during the experiments:

- The cooling system (airflow) achieved the most precise cooling rate for both moulds, upper and bottom mould, with **5 °C/min** below 200 °C, but the associated moulding time of 18 min runs against the interest of short process cycles
- The programmed cooling rate of **20 and 60 °C/min** resulted equally in an actual cooling rate of 11 °C/min.
- The quickest cooling rate measured **13 °C/min**, which was achieved by the step process where the temperature cycle of the upper mould runs behind the lower mould part.
- Faster cooling rates were restricted by the cooling system's original purpose of processing at temperatures above 200 °C (designed for processing PA at ~ 250 °C).

Here, the tooling material showed a temperature-dependent thermal heat capacity [174]. Process windows above 230 °C have the advantage of enhanced heat exchange due to lower heat capacity, however, the process window of PP lies between 165 °C and 220 °C. The effect of different cooling rates on the composite properties is summarised in Figure 4-21 (samples prepared and tested following standards stated in Section 3.5.5.). In addition, the void content measurement determined 7.9 ± 0.1 vol% for composites process using a cooling rate of 5 °C/min, and 3.9 ± 0.1 vol% for 11 °C/min and 3.5 ± 0.1 vol% for 13 °C/min cooling rates respectively. Conversely, a reduction in moulding time from 18 min to 6.9 min was reached by increasing the cooling rate from 5 °C/min to a maximum of 13 °C/min, which did not significantly decrease the composite strength and stiffness nor increased the porosity.

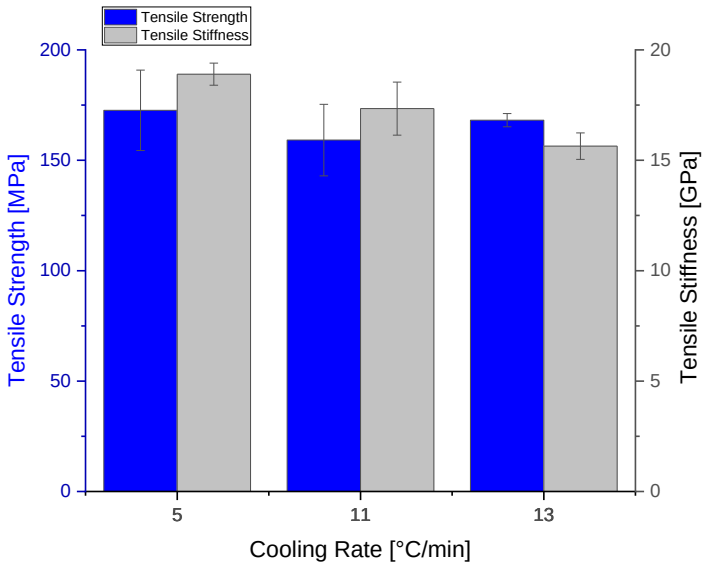

Figure 4-21: Rapid Isothermal processing at 190 °C, no dwell time and 5, 11 and 13 °C/min cooling rate (SM45D/PP).

A slight drop in composite stiffness was recorded for the analysed samples from a 5 °C/min cooling rate up to 13 °C/min which can be traced back to the semi-crystalline characteristic of PP. It was also noted that an imbalance of upper and lower mould temperature when cooling (Section 4.2.) did not seem to affect the composite quality negatively when considering the mechanical performance of differently cooled composite parts. Overall, a tensile strength of 168.2 MPa and modulus of 15.6 GPa can be achieved for the shortest cycle applying a cooling rate of 13 °C/min, which exceeded the performance measured in the isothermal approach on the COLLIN press for a cycle time of 27 min with a cooling rate of 20 °C/min.

It should be noted that this performance is similar to a comparable study by Wölling *et al.* regarding its applied recycled feedstock, but quicker processing [79]. 7.9 vol%, 3.9 vol% and 3.5 vol% in void content were measured for the panels from 5K/min, 11 °C/min and 13 °C/min respectively, moulded at 190 °C with a pre-heating temperature of 180 °C. The adequate level of void content correlated to an overall good level of surface finish when visually analysing the manufactured panels after moulding (Figure 4-22).

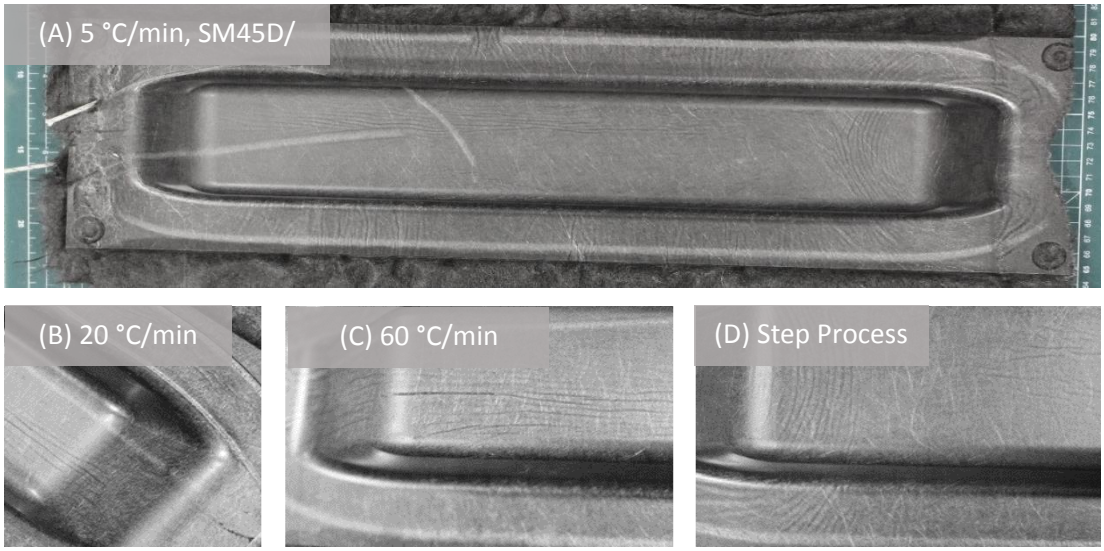

Figure 4-22: Illustrating exemplary manufactured composite parts with the outstanding surface finish for rapid isothermal process type processed at 190 °C (SM45D/PP) varying in set cooling rates of (A) 5 °C/min, (B) 20 °C/min, (C) 60 °C/min and (D) the step process.

For all cooling rates, a few wrinkles were observed which could be prevented by using an additional clamping frame when moulding [4, 30]. However, good drapeability was noted for all manufactured samples. Overall, composites manufactured under the shortest possible cooling rate at this temperature level (realised by the step process) resulted in an overall good composite quality and was therefore used as standard cooling rate for the following trials.

Further preliminary investigations focused on the transfer time and resulting stamping cycle when processed non-isothermally. The monitored temperature cycle for a representative process cycle is shown in Figure 4-23 (left). A temperature drop of 30 °C prior the stamping could be traced back to the material transfer between the heating system and the press, as well as the closing time.

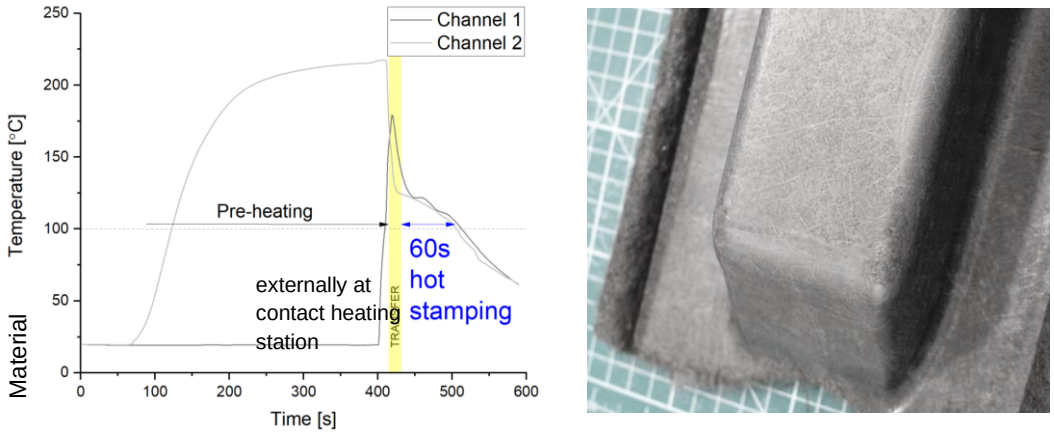

Figure 4-23: Logged temperature cycle of the material during pre-heating, transfer and the stamping process (left) and first processed SM45D/PP panel with good surface finish (right).

In this time range, the material cooled down by 93 °C to 124 °C, resulting in a very fast cooling rate of 186 °C/min. The actual stamping gives the form and final consolidation of the part and brings the material temperature below the crystallisation point for de-moulding. In 60 s the processed material was rapidly cooled down to the de-moulding temperature of 100 °C. Within this short period, the material was pressed, impregnated, formed to shape, and simultaneously cooled down below the soft stage. The developed process parameter levels within the preliminary investigation are summarised below and were not modified in the following experimental work:

- Pre-heating material temperature was set to 10 °C above moulding temperature,
- The pre-heating was set to 5 minutes to reach the target temperature,
- 30 s were allowed for material transfer and tool closure,
- The cooling rate was set to 13 °C/min, achieved by the 'step process'.

4.3.3 PROCESS STUDY

4.3.3.1 RAPID-ISOTHERMAL PROCESSING

With the learning outcome in mind, the following Table 4-11 summarises the mechanical properties of the textile manufactured under rapid-isothermal conditions on pilot-scale with a shortened cycle time compared to the isothermal process on a laboratory scale. The SM45D

feedstock was successfully processed within 6.9 min (13.1 min total cycle time) on a lower moulding temperature of 190 °C, whereby IM56D and IM56R lacked efficient polymer flow which resulted in dry surface finish and high void content.

Table 4-11: First trials applying the rapid Isothermal process on low conditions with no dwell time and 13 °C/min cooling rate.

Feedstock Type	Moulding Temp. [°C]	Dwell Time [s]	Moulding Time [min]	Tensile Strength [MPa]	Tensile Modulus [GPa]	Void Content [vol%]
SM45D (36 wt%)	190	0	6.9	168.2 ± 4.0	15.6 ± 0.6	3.5 ± 0.0
	200	0	8.7	187.9 ± 2.0	19.2 ± 0.9	1.0 ± 0.1
IM56D (36 wt%)	190	0	6.9	163.0 ± 8.5	14.7 ± 1.3	11.9 ± 0.1
	200	0	8.7	197.9 ± 4.6	16.0 ± 0.2	13.3 ± 0.0
IM56R (37 wt%)	190	0	6.9	119.6 ± 4.6	12.2 ± 0.9	11.6 ± 0.2
	200	0	8.7	189.4 ± 9.8	18.2 ± 1.1	9.9 ± 0.1

Further process modifications and increase in moulding temperature eliminated voids in SM45D/PP composites showing optimised process conditions, but the level of void content measured for IM56D and IM56R composites stagnated between 10 -13 vol%, even though an increase in mechanical properties could be recorded. The additional adjustments showed that IM56D and IM56R material needed more impregnation time, and the processability was improved with higher temperatures and longer dwell times of 60 – 120 s. Higher pressure would be the last alternative to efficiently force the air out of the textiles before fully consolidating IM56D and IM56R composites. Overall, the modification of the temperature and dwell duration led to similar moulding times of approximately 9 minutes and subsequent total process cycle of 15 – 18 minutes (depending on temperature) resulting in more enhanced properties compared to the 27 minutes cycle on a laboratory scaled press.

The influence of moulding temperature and dwell time for the RISF process were largely exploited, where the applied pressure was set to 200 kN at time of research. Only a small further increase in moulding temperature was possible before polymer degradation limited further process modification to increase the polymer viscosity. Thermal degradation of the polymer was observed when the set pre-heating temperatures of ≥ 225 °C (actual 220 °C) were applied.

A thermal analysis of the unprocessed textile in an air and nitrogen atmosphere was performed and showed the onset point above this phase at 223 °C. In this case, additional pressure and humidity can change the process environment, accelerating the thermal

degradation process that ultimately leads to degradation in material performance. Therefore, panels manufactured in these conditions presented low levels of impregnation (Figure 4-18). Consequently, the upper process temperature limit was set to 215 °C (set 220 °C) for further processing of PP based composites. This highlights the small option of only further increasing moulding temperature within the identified polymer process window but also underlines the need for additional consideration of the applied pressure level. Lower boundaries were given due to lack in polymer flow, whereby extreme conditions showed unmolten polymer fibres in the evaluated fracture samples processed at 180 °C (Figure 4-18 A) or degraded polymer in the powdery state (Figure 4-24 B).

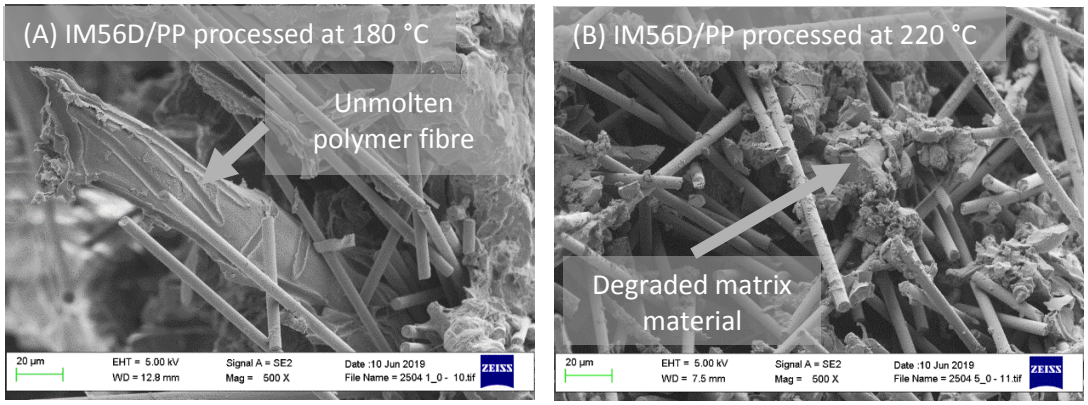

Figure 4-24: SEM images showing fracture surface of IM56D/PP samples processed at (A) 180 °C where unmolten polymer filaments are visible and (B) at 220 °C with powdery matrix material caused by degradation.

Independent from the process type, the moulded part temperature has to drop below the glass crystallisation temperature of 110 °C to prevent deformation during de-moulding in a soft stage of the composite. Therefore, a tool temperature of 100 °C was chosen for the non-isothermal process and is also recommended for the de-moulding temperature when further processed in rapid-isothermal mode.

4.3.3.2 STAMPING PROCESS

This section summarises the work where the processability of the textiles is investigated, applying the second processing type on a pilot scale, the stamping process. The process describes a very short and therefore economically favourable process. At the same time, the material was processed under extreme conditions with regards to no dwell time and the highest cooling rates. The material was pre-heated separately above the melting point, followed by a quick transfer to the mould where the textile in softening stage was stamped to its final shape within minutes. Whilst the tool temperature stayed unchanged at 100 °C, the effect of the pre-heating temperature on the composite properties was investigated. A

summary of the obtained mechanical properties depending on the investigated parameter combinations, of the pre-heating and tool temperature, is given in Table 4-12.

The tensile strength properties range from 163 MPa – 175 MPa measured for the SM45D/PP material, to 124 MPa – 146 MPa obtained for the IM56D/PP composites and down to 95 MPa – 118 MPa strength for the IM56R/PP material combination. Similar results were recorded for the modulus properties, where the values obtained for the SM45/PP material outdo the other materials with 15 – 15.6 GPa against 13 – 14 GPa measured for IM56D/PP and 10 – 12 GPa measured for IM56R/PP. Here, the low values correlate to the highest measured void content for IM56D/PP (14 – 16 vol%) and IM56R/PP (15 – 18 vol%) panels compared to 6 – 9 vol % determined for SM45D/PP composites.

Table 4-12: Optimised non-isothermal process conditions for different feedstock types showing benefits and limitations.

Feedstock Type	Pre-heating Temp. [°C]	Tool Temp. [°C]	Tensile Strength [MPa]	Tensile Modulus [GPa]	Void Content [vol%]
SM45D (36 wt%)	195	100	163.4 ± 15.6	15.6 ± 0.3	8.5 ± 0.1
	210	100	175.2 ± 3.5	15.0 ± 0.3	5.7 ± 0.1
IM56D (36 wt%)	195	100	145.5 ± 2.5	13.1 ± 0.8	15.6 ± 0.1
	210	100	124.1 ± 17.6	13.6 ± 0.4	13.7 ± 0.1
IM56R (45 wt%)	195	100	94.8 ± 2.9	10.3 ± 0.4	14.5 ± 0.6
	210	100	117.7 ± 6.6	11.6 ± 0.9	17.5 ± 0.1

The non-isothermal process follows the trend and underlines again the good processability for SM45D/PP textiles, compared to IM56D/PP or IM56R/PP types, showing a higher quality panel with lower void content (Table 4-9). The level of mechanical properties, as well as porosity, showed similarity to recorded values for unimproved parameter combination at an early stage of rapid isothermal processing. The very short cycle time of 60 s does not always allow the polymer to sufficiently spread throughout the component, impregnate and consolidate in sequence within an extremely short time frame. Satisfactory properties were only recorded when applying the optimised conditions to the SM45D/PP textiles and demonstrated quick manufacturing with the shortest recorded process time (to date) for thermoplastics using recycled carbon fibres.

An increase in applied pressure has the potential to force the air from the yet fully unconsolidated textiles prior consolidation (as reported before), which could lead to a further drop in void content to obtain increased tensile strength and modulus. But when the pressure is too high, it can also lead to void formation caused by agglomeration of fibres where the polymer is inhibited from impregnating to its centre [170]. No clear statement can

be made about the wetting behaviour of the fibre-matrix systems from the fracture surface analysis (Figure 4-18). It was expected that no chemical reaction between all fibre types and the non-polar matrix system would be observed. Nevertheless, occasionally fibre-matrix adhesion was detected on the fracture surface images on a micro-scale.

4.3.3.3 SUMMARY

Producing high quality products which showcase the potential of future applications of the material, under short cycle times was the main objective of this work. As previously mentioned, the quality of a composite is characterised by the highest possible strength and stiffness, void-free components and demonstrable good interfacial adhesion for efficient load transfer (more detailed information is given in Chapter 2.1.). Here, a relation between composite quality, with regards to strength and void content, and moulding time was detected.

A summary of the obtained porosity in the processed composites versus process type and processed material is given in Figure 4-25. The lowest void content was expected for the longest process, which was obtained for SM45D/PP and IM56R/PP composites. When applying the rapid isothermal process, the moulding time could be reduced from 27 min to 7 – 9 min, and a composite with a void content of 0 – 4.5 vol% was still obtained for SM45D/PP composites. When processing IM56R/PP composites rapid- isothermally the polymer flow was hindered and produced porosity of approximately 10 vol%. A further reduction in moulding time down to 1 min stamping sequences resulted in higher void content for both material types but SM45D/PP composite quality showed superior quality compared to the other materials. In contrast, the IM56D/PP material seemed to be unaffected by the length of moulding time and level of process temperature, where all process settings led to low composite quality components (15 – 16 vol% porosity).

Initially, it proved the technical feasibility to process commingled nonwovens. However, the porosity and final composite quality seemed to be affected by material and process type. Having exploited different process conditions for the commingled nonwovens, no sufficient outcomes have been obtained when repeating the best process conditions for IM56D/PP and IM56R/PP commingled nonwovens, which makes pressing below 27 min inapplicable at the moment. Nevertheless, the processability of SM45D/PP material was proven to be successful for all process types.

Further investigations were rolled out to understand the cause for the large variety in obtained composite quality, where a significant effect of the material (e.g. textile quality, recyclate characteristic) was assumed.

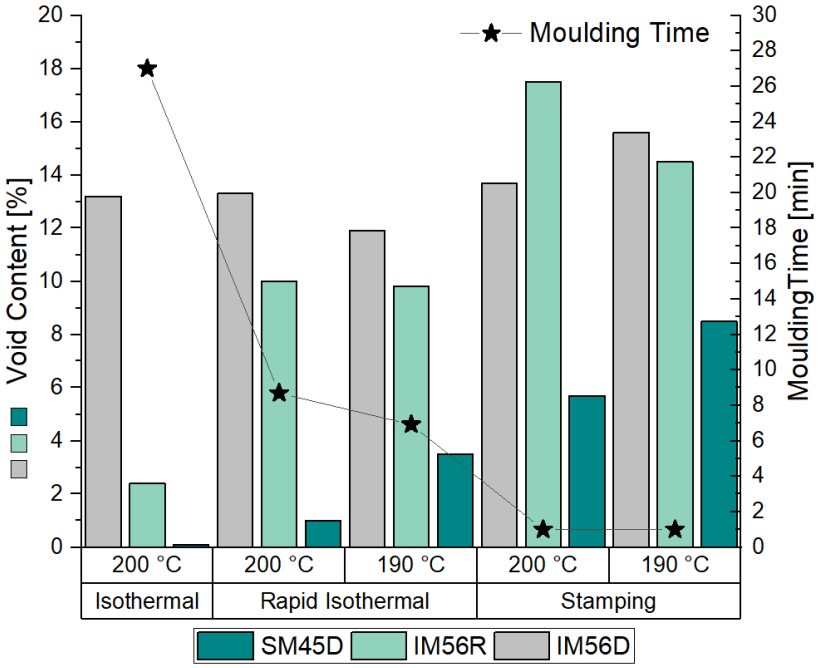

Figure 4-25: Showing process depending composite quality versus cycle time with regards to the measured void content of panels containing different recyclate type.

4.3.4 SIGNIFICANT PARAMETER CONTRIBUTION

Throughout the experiments it was noted, that for certain materials, like the SM45D/PP textiles, the different types of processing worked better for some than for others, e.g. IM56D/PP. In the following section, the results are summarised, and the factor that contributes most to the processability (fibre type or textile dependent) is determined. The investigated criteria are summarised in Table 4-13. The analysis follows the criteria comparing the physical properties of the fibres, and the textile, including the textile thickness, loft factor and its level of fibre weight fraction. The second investigation focused on the surface characteristic and interfacial behaviour of the fibre to the matrix.

Table 4-13: Analysed criteria when comparing the processability of different feedstock and textile types.

Fibre Characteristic	Textile Characteristic
Physical Properties - Fibre stiffness - Fibre Strength - Diameter, length	Physical Properties - Uniform/ uneven FWF - Loft factor (Carding setting might differ)
Surface Characteristic - Aerospace-grade: SM45D & IM56D fibres sized with an epoxy compatible sizing - Pyrolysed: IM56R & IM56L are covered by residual char - Surface energy, tension, Capillary effect	

4.3.4.1 EFFECT OF PHYSICAL FIBRE & TEXTILE CHARACTERISTIC

With regard to the physical properties of the fibres, there are three fibre classes which were processed in the study:

- SM45D: less stiff and strong fibres
- IM56D: higher stiffness and strength than SM45D
- IM56R, IM56L: similar stiffness to IM56D but lower in strength, could lead to fibre breakage when processing (textile production and/or pressing)

All fibre types have been analysed by fibre diameter before to understand the possible effect on the flow capability when moulding (Section 3.4.1.). The measurement showed a similar level of 5.3 µm in fibre diameter for all fibres. Additionally, the supplier ELGCF noted, that the fibre length is unchanged with the fibre type when fed into the carding machine. However, fibre breakage throughout the textile process or composite manufacturing cannot be excluded, whereby the pyrolysed feedstock (IM56R, IM56L) could be prone to break earlier than the mechanically recycled feedstock. Further work should include an additional investigation of the effect of the processing steps on the fibre length (textile process, composite moulding) to initiate proceedings to prevent breakage.

The loft factor was calculated to understand the cause for the good or poor processability of the different textiles, using the textile thickness, weight and level of fibre packaging. Investigating the possible relationship between loftiness and the processability of the textiles will help to clarify whether the polymer flow was inhibited by a low loft factor (less air within the textiles, stronger carded) or the processability was enhanced with a high loft factor, where it might be better to remove the air before consolidation. The record textile thickness for all applied batches was used for further evaluation of the loft factor (Figure 4-26). It can be noted, that SM45D textiles showed a looser fibre arrangement than the IM56D or IM56R textiles.

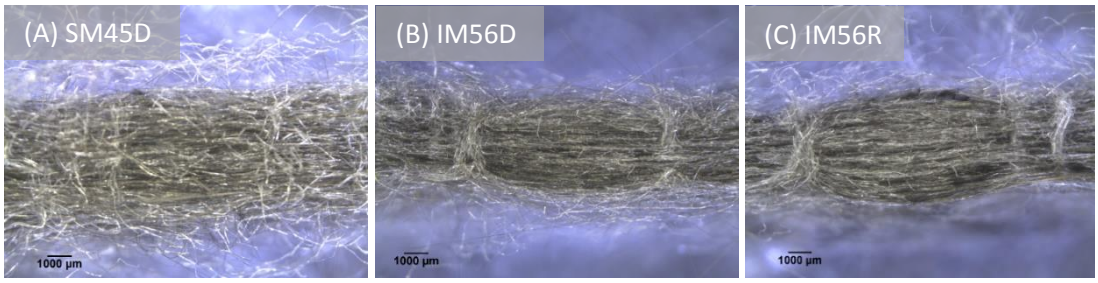

Figure 4-26: Microscopic image of the textile's transverse section of (A) SM45D textile from early stages of industrial production at ELGCF, (B) IM56D and (C) IM56R textiles from latter stages of Industrial textile line.

However, due to a variation in textile thickness and fibre weight fraction, the evaluated loft factor shows only a significant difference for the IM56R textiles in relation to the thinnest reported textile thickness and relatively high measured FWF (Table 4-14).

Table 4-14: Summary of evaluated textile parameters in relation to processability

Textile Parameter	RAPID ISOTHERMAL PROCESS			NON-ISOTHERMAL PROCESS		
	SM45D	IM56D	IM56R	SM45D	IM56D	IM56R
Processing	Good	Poor	Good	Good	Poor	Poor
Voids [vol%]	1.8 ± 1.4	12.6 ± 0.9	5.0 ± 3.8	7.1 ± 2.0	14.7 – 1.3	16.1 – 2.2
FWF [wt%]	35.9 ± 0.6	32.3 ± 4.0	37.3 ± 1.2	35.6 ± 4.1	35.5 ± 0.4	45.0 ± 0.4
FVF [vol%]	21.7 ± 0.3	19.0 ± 2.0	22.7 ± 0.6	21.4 ± 2.1	21.4 ± 0.2	28.8 ± 0.2
Density [g/cm^3]	1.11 ± 0.0	1.11 ± 0.1	1.12 ± 0.0	1.10 ± 0.1	1.10 ± 0.0	1.17 ± 0.0
Loft Factor [-]	21.1 ± 0.3	20.6 ± 2.6	14.7 ± 0.4	21.0 ± 2.4	21.0 ± 0.2	15.7 ± 0.2

Whereas SM45D and IM56D textiles have a similar level of loft factor, IM56R textiles are less voluminous containing less air within the nonwoven. It means that the textile characteristic might contribute to the level of processability, but a primary textile dependent processing was eliminated.

4.3.4.2 EFFECT OF SURFACE ENERGY ON IMPREGNATION LEVEL & MOULDING

When working with vCF, the chemical inert fibre surface is modified, ranging from non-polar to polar surface chemistry, depending on the target polymer and subsequent application. In this study, it worked the other way around. The research project focused on different recyclates from different suppliers with unknown surface characteristic, where the processability of the different feedstock was evaluated accordingly. The process study showed, that the processability and impregnation level when moulding was dependent on the fibre characteristic. which can be distinguished by its rCF surface energies. In the following, the analysed fibre properties are summarised by fibre type (taken from Section 4.1.1.):

- SM45D: unknown sizing showed highest surface energy, and subsequent high surface polarity
- IM56D: unknown sizing with lower surface energy and subsequent lower surface polarity
- IM56R, IM56L: pyrolysed fibres with occasional char cover showed low surface energy with low surface polarity.

Therefore, a relation between a high fibre surface energy and enhanced impregnation level of the textiles when moulding can be deduced, as was visible for the SM45D feedstock, in conjunction with the best processability when moulding and which resulted in the lowest measured void content. It is assumed that a higher surface polarity of the fibre is the reason for an enhanced spreading of the polymer and therefore homogenously advanced impregnation level. The direct correlation is traced back to the induced forces by the capillary effect, whereby the polymer flow is enhanced to spread and impregnate the porous textile mat [177].

In summary, it is important to tailor the processing conditions of all the different applied techniques to the recyclate type, because not all processing techniques are applicable to the differently processed nonwoven material. A rCF type dependent processability and properties were identified.

- SM45D/PP: Commingled textiles with fibres containing sizing showed best processability for all techniques down to 1 min cycle time; good composite properties (strength, stiffness), few voids where higher rCF surface polarity related to good impregnation level ↔ low porosity

- IM56D/PP: Commingled textiles with fibres containing sizing (different to SM45D) resulted in low quality for all processing technique, where low rCF surface polarity led to low impregnation ↔ high porosity
- IM56R/PP: Commingled textiles with thermally recycled fibres resulted in highest mechanical properties, good to semi-good porosity level as well as processability down to 9 min, where pyrolysed rCF and its rough surface prevents from efficient flow ↔ longer impregnation time is required to overcome the friction.

4.3.4.3 EFFECT OF SURFACE ENERGY ON FIBRE-MATRIX ADHESION

Comparing the surface energies of the fibres with the matrix system can determine the compatibility between both. The potential interaction between the fibre surface and PP was studied, where the interfacial tension σ_{SL} and adhesion energy ψ_{SL} is given in relation to PP ($\gamma^{\mathrm{p}} = 0.91$ mJ/m², $\gamma^{\mathrm{d}} = 29.49$ mJ/m², γ = 30.4 mJ/m² at ambient temperature [178], [179], [180]) in Table 4-15. In general, when good adhesion properties between the fibre and the matrix are targeted, then low interfacial tension and high adhesion energy are desired. A low adhesion was generally described between carbon fibres and PP from the previous microscopic analysis, therefore relatively high-tension levels and low adhesion energies are expected. The surface tension between SM45D fibres was rather high and showed a certain incompatibility to the non-polar matrix as described above. This can be traced back to the different polar ratio of the fibre and the matrix. The closer the ratio matches in polar content, the lower the interfacial tension between the components, which agrees with the literature [181]. However, low interfacial tension was calculated for IM56D, IM56R, and IM56L fibres, which shows potential compatibility with the PP matrix, which was not expected.

Table 4-15: Interfacial tension σ_{SL} and adhesion energy ψ_{SL} is given in relation to PP.

Fibre Type	Interfacial Tension σ_{SL} [mN/m]	Adhesion Energy ψ_{SL} [mJ/m²]
SM45D	29.05 ± 0.49	76.30 ± 1.02
IM56D	7.15 ± 2.50	77.61 ± 1.45
IM56R	2.73 ± 1.54	78.48 ± 1.09
IM56L	4.43 ± 0.26	78.03 ± 0.42

The residual char detected on the IM56R and IM56L fibres using microscopic technique might affect physical interlocking and chemical interaction to support the interfacial adhesion, but low values for IM56D cannot be explained. Another surface characteristic describes the surface adhesion, and in this study, it showed that the bond to PP was favoured for all fibre types.

The reported surface energy values of the polymer were obtained at ambient temperature. However, the obtained results could be different when considering that the impregnation took place at a temperature level of 200 °C. Research shows that, the surface energy decreases with an increasing process temperature, and as a result the polarity changes [154], [182], [183]. Therefore, only a trend in adhesion properties within the composite can be concluded from the obtained interfacial tension and adhesion energy values at this stage of research. Further analysis should consider characterising the polymer at process temperature to represent the actual process conditions.

4.3.5 MILESTONE 2: PROCESS & RECYCLATE DEPENDENT COMPOSITE PERFORMANCE

This section summarises the findings of the process work at pilot scale and includes the following learning outcomes:

- Importance of tailoring the process conditions of all techniques to rCF type
- Not all techniques are applicable to each rCF/PP nonwoven material
- rCF type dependent processability & properties
- Process cycle times can be shortened to 13 min for specific material when processed rapid isothermally, and down to 1 min when applying stamp forming.

The mechanical properties of the processed material were obtained by conducting an OVAT study which focused on the effect of the pre-heating and processing temperature as well as the dwell time as schematically shown in Figure 4-27.

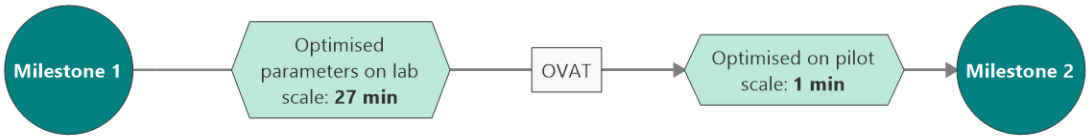

Figure 4-27: Schematic of the initial experimental steps on laboratory scale leading to further process studies applying OVAT method to identify the optimised conditions on pilot scale.

The results are categorised by recyclate and process type and the benefits and limits of the processability of each material are highlighted below.

Three forming processes were compared, isothermal processing, rapid-isothermal processing and stamp forming of commingled nonwoven textiles. Results for the isothermal process were obtained in a previous study using the COLLIN press on laboratory scale where comparable process conditions in terms of process temperature (200 °C) and pressure (270 kN) were applied (Section 4.1.6). Overall, a high variety in matrix-fibre distribution was

detected ranging from 34 wt% to 54 wt%. Therefore, the obtained composite properties were normalised to 40 wt% in FWF (example shown for the strength properties below):

$$Normalised\ Strength\ (GPa) = \frac{Experimental\ Strength\ (GPa)}{Experimental\ FWF\ (wt\%)} * 40\ wt\% \qquad (13)$$

The isothermal process was taken as a baseline, where the process seemed to be optimised for SM45D/PP textiles and the final established process parameters were applied to IM56D/PP and IM56R/PP textiles. Moderate composite strength was obtained for SM45D and IM56D composites, whereas IM56R/PP outperformed both. However, the material includes pyrolysed fibres (Figure 4-28).

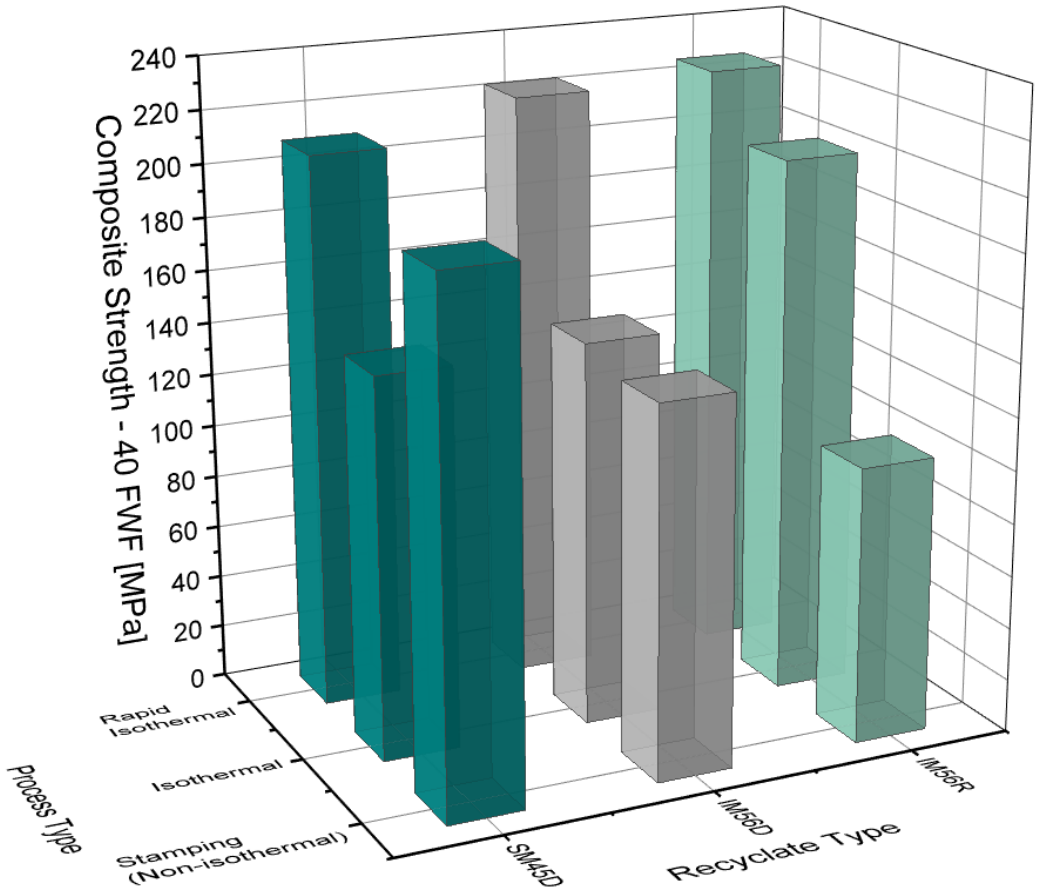

Figure 4-28: Comparison of the composite strength for different processing and fibre types, where the material temperature was set to 200 °C with the start of the moulding process, each textile type originating from the same material batch.

A similar phenomenon was detected for the composite stiffness, but here also SM45D/PP material showed good properties, both with low void content (Figure 4-29). Still, IM56D/PP panels showed lowest stiffness directly relating to a very high void content. The process conditions for the rapid isothermal process were adjusted according to the fibre type. Even so, the process and moulding cycle was shorter, compared to the isothermal process, an increase in strength and stiffness was noted for all material types.

This was related to:

- Pressure differential between the two types of press at laboratory (small platen press) and pilot-scale (curved mould).
- Measured FWF was 5 wt% lower for SM45D and IM56D material processed in rapid-isothermal conditions allowing better polymer flow and impregnation process.

One exemption was the IM56D/PP material, which again recorded the lowest modulus for the rapid-isothermal process. The sizing type of IM56D fibres formed a permanent barrier for efficient polymer flow resulting in repeated high void content.

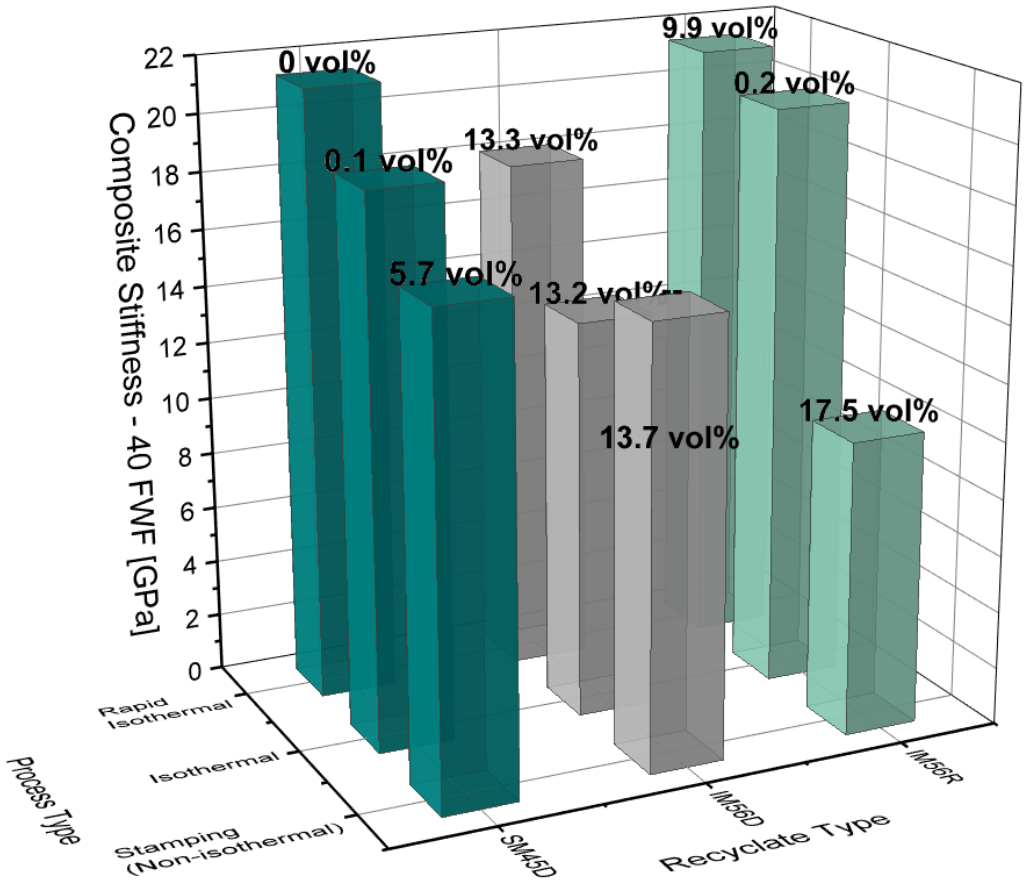

Figure 4-29: Comparison of the composite stiffness for different processing and fibre types, where the material temperature was set to 200 °C with the start of the moulding process, each textile type originating from the same material batch.

The more extreme conditions during the stamping process, where impregnation and consolidation happened within 1 minute, showed only successful application for the SM45D/PP material. Nevertheless, moderate strength and stiffness were experimentally determined for IM56D and IM56R based material, the high void content (~ 15 vol%) and

poor impregnation and consolidation level (dry, not consolidated) showed a limitation of the stamping processing for this particular material.

To predict the level of impregnation and suitability of material type for each process prior to thermoforming, the contact angle method was successfully applied. Here, a direct relationship was determined between the degree of wettability, impregnation level and the fibre surface energies. The simple characterisation technique supported the exploitation of the material characteristic and its link to the processability of the nonwoven textiles. A summary of the evaluated interface characteristic, how it affected the composite properties and the correlation to the processability of the textiles is given below:

- The more the surface energy of the recyclate exceed the polymer's, the better the impregnation level (and subsequently less porous composites -summarised from the surface energy study of the different rCF feedstock and the final composite characteristics).
    - The determination of the surface energy of fibre tows with test liquids, made it possible to relate the level of processability to the surface characteristic of the recyclate type.
    - SM45D feedstock was able to be processed successfully, incompatibility of SM45D fibres and PP (high interfacial tension) was detected which causes weak long-term composite properties.
- The more hydrophobic characteristic of IM56D, IM56L and IM56R fibres created a barrier for efficient polymer flow when moulding:
    - For IM56L and IM56R fibres (pyrolysed feedstock), this was related to the residual char on the surface. However, the char is attached temporarily to the surface by Van-der-Waals forces and as a result the initial interfacial repulsion can be overcome by allowing longer impregnation time (isothermal or rapid-isothermal conditions) or applying higher process pressure.
    - The IM56D feedstock is covered with a sizing, which created a permanent blockage. The proven incompatibility to the applied PP polymer indicated unsuitability for all process types due to friction. The material is recommended for thermoset applications.
- The fracture analysis of rCF/PP composites showed in all cases no wetting behaviour and it can be assumed that the chemical interaction is only visible for more polar polymers.

The energetic SM45D fibre surfaces were sufficiently impregnated by the matrix when manufactured to composites resulting in void-free composites within 9 - 27 min processing and low void content when processed between 1 – 8 min. In contrast, the other fibres are affected by the micro-effects described by the capillary pressure, where the flow of the polymer is hindered and fails to impregnate the textiles sufficiently within the applied process window. This leads to the conclusion that the contact angle method can be used as batch testing for the project partner to separate waste streams but also indicates possible matrix system and processing methods. In summary, several options for processing rCF/PP were given, where good properties were obtained, and low cycle times and possible industrial adaption was demonstrated.

4.4 MARKET COMPETITIVENESS

This chapter gives an overview of the experimental results in relation to other research projects and commercially available lightweight material at time of research. It also examines the industry criteria for potential implementation in terms of part costs and volume of production.

4.4.1 TECHNICAL COST ANALYSIS

Thermoplastic composites offer the potential of reducing component weight and improved recyclability while at the same time enhancing the manufacturing economy through a reduction in processing time [184]. It has been demonstrated that the chosen material and processing conditions have a significant impact on the composite quality and also determine the annual production volume and subsequent part cost [185]. A technical analysis was performed to investigate the economic aspects of the three different process types, which were optimised in this project; the isothermal, rapid-isothermal process and stamping procedure. It was assumed that the same hydraulic press was used for all three processes.

The cost-benefit analysis focused on manufacturing cost to identify the difference in cycle times and production volume for all the comparable processing types. There are two main approaches for the technical cost analysis; process-flow simulation [186] and parametric cost models (also known as a static approach [184], [187]–[189]. The process-flow simulation is when machines are directly connected, and the capacity of machinery and workers is examined to identify possible bottlenecks. The approach is useful for an entire process flow optimisation but in the case of this project the focus lies on the comparison of processing type and material usage. Therefore, a static approach was applied to simplify the cost model, where an independent process flow is assumed between machines. The cost model excluded

the maximum capacity of the single process stations. The overall cost-per-part is compiled of several factors [189]:

$$\text{Cost} = \sum [raw\ materials + labour + energy\ + depreciation + interests + maintenance + floor\ spce + equipment] \quad (14)$$

In general, manufacturing costs are divided into variable and fixed costs. Fixed costs are independent from the manufacturing volume and period [185]. Variable costs are dependent of the production volume of the final product and remain generally constant with the component (raw material cost, labour, scrap, energy). However, the variable cost can differ with material choice and process type. The fixed costs are allocated to one-off capital expenditures e.g. machinery, tooling, maintenance, building costs. The following sub-sections give more details about the calculation of each cost factor.

4.4.1.1 VARIABLE COST

The raw material, energy and labour cost are calculated as follows [189]:

$$\text{Raw material [£]} = \text{part size [kg] x material cost } \left[\text{£}/_{kg}\right] \quad (15)$$

$$\text{Labour cost [£]} = \text{operators x labour rate } \left[\text{£}/_{h}\right] \text{ x operation } [h/part] \quad (16)$$

$$\text{Energy cost [£]} = \text{consumption [kW] x cost } \left[\text{£}/_{kWh}\right] \text{ x operation} \quad (17)$$

Table 4-16 summarises the key information to obtain material costs per part. The information was obtained from the experimental process study (Chapter 4.1/4.2). The textile layers were folded and cut manually resulting in 14.7 wt% off-cuts. The use of an automated ply cutter and precise adaptation of textile to part dimension could significantly reduce the off-cuts in future applications. The final part weight was as low as 0.29 kg.

Table 4-16: Material data based on experimental work.

Description		Unit	Notes
Optimum fill: textile area	0.12	m^2 / ply	
Textile weight (200 gsm roll)	24	g / ply	
Optimum mould fill	283	g / part	2 mm thick
Textile layers	12	Ply	
Textile area (over-dimensioned)	0.14	m^2 / ply	For better handling
Total textile area (12 plys)	1.8	m^2 / part	
Total textile weight	0.34	kg / part	
Wastage	- 14.7	wt%	Included in material cost

Composite part weight	0.29	kg / part	After trimming

The textile material cost decreases with the purchase of greater quantities (information from supplier). The price list is summarised in Table 4-17, including estimated part quantity and total raw material cost-per-part relating to 0.29 kg and 0.34 kg per part excluding and including waste respectively. The industrial textile production is limited to 10 000 kg per line, which is equivalent to a possible maximum of ~ 30 000 composite parts for the case study.

Table 4-17: Textile material cost in relation to production volume of textile line and the final composite parts.

				Including waste	
Textile quantity (kg)	Nonwoven Textile[5]	Estimated part quantity	Material cost per part	Estimated part quantity	Material cost per part
< 100	£26.34	≤ 350	£7.64	≤ 295	£8.96
100 - 500	£21.05	351 < 1725	£6.10	296 < 1470	£7.16
500 - 1000	£17.58	1726 < 3450	£5.10	1471 < 2940	£5.98
1000 - 2500	£17.37	3451 < 8600	£5.04	2941 < 7350	£5.91
2500 - 5000	£16.88	8601 < 17200	£4.90	7351 < 14700	£5.74
5 k – 10 k	£16.43	17201 < 34400	£4.76	14701 < 30000	£5.59

The following assumptions (based on the literature) were made regarding operator and energy costs:

- One operator is used at a rate of 30 £/h (for skilled workers) [185], [189], [190]
- The operation time was estimated as 1 minute additional to the cycle time (to transfer the material including filling the mould and de-moulding the part)
- The energy consumption and subsequent cost are estimated to 77 kW for the press including heating zones of the tool [184], as well as 15.8 kW for the simultaneous running pre-heating system [191].

A summary of the labour and energy costs is given in Table 4-18.

[5] Pricing is given indicative numbers only.

Table 4-18: Variable cost summary per part and process type for one skilled operator (These values are calculated from literature-based data).

Process Type	Cycle time	Operation / Event [h / part]	Operator cost [£ / part]	Energy Cost [£ / part]
Isothermal	27 min = 0.45 h	0.47	14.1	5.67
Rapid Isothermal	13 min = 0.22 h	0.23	6.9	2.77
Stamping	1 min = 0.02 h	0.03	0.9	0.36

For the isothermal process, which includes heating and cooling of the material in the tool, only the energy consumption of the press was considered. In future calculations, lower energy consumption could be assumed for thermoforming processes at 190 – 200 °C to the stamping process temperature of 100 °C. Limited data regarding energy cost was available at time of research. Energy costs are estimated at 0.13 £/kWh, which represents the average unit rate in the UK in October 2019 [192].

4.4.1.2 FIXED COST

The fixed costs were split into depreciation, interest, flooring and building as well as maintenance and tooling cost, which are all amortised by the total part number produced per year. The equipment costs differ between the process types, whereas the pre-heating process was included in the capital cost and energy consumption but not modelled as an extra event as it runs simultaneously with the thermoforming process. The rapid isothermal and stamping process types involved separate pre-heating of the processed material, being able to process several parts per sequence. Only the isothermal process includes heating of the material in the tool and therefore no extra cost is allocated for the heating device for this particular process type. Depreciation, interest, floor space and tooling cost are calculated following the approach of Turner *et al.* [189]:

$$\text{Depreciation [£]} = \frac{\text{equip. [£]/(equipmen life [h] x equipment time [h/a])}}{\text{parts per annum}} \quad (18)$$

$$\text{Interest [£]} = \frac{\text{0.5 x equip. [£] x interest rate [\%]/(euqip. time [h/a] x parts [1/h])}}{\text{parts per annum}} \quad (19)$$

$$\text{Maintenance [£]} = \frac{\text{0.05 x equipment cost [£]}}{\text{parts per annum}} \quad (20)$$

$$\text{Tooling [£]} = \frac{\text{tooling cost [£]}}{\text{parts per annum}} \quad (21)$$

$$\text{Floor cost [£]} = \frac{\text{equipment space } [m^2] \text{ x building cost } \left[{}^{£}/_{m^2}\right]}{\text{parts per annum}} \quad (22)$$

The purchase cost of processing equipment considered is given in Table 4-19. Hereby, the costs for the applied hydraulic press (DASSETT Process Engineering Ltd., built 1997) and pre-heating station are based on updated quotes. The maintenance cost was set to 0.5 % and 5 % of the machine cost per year suggested by Wakeman *et al.* [185] including installation and production tests for smaller and more complex machinery respectively. The cost of the tooling generally depends on several parameters, such as component complexity, heating zones and applied process window [184]. In this case study, , a small mould with simple geometry is considered. As actual cost data was limited, cost estimation was taken from modelled mould cost for a steel tool with dimensions of 250 mm x 500 mm [184]. The floor space was estimated to £ 72.90 / m² [185] with a machine area of 6 or 11 m^2 excluding or including the pre-heating station respectively.

Table 4-19: Equipment cost and energy consumption including building.

Equipment	Cost [£]	Platen size [mm²]	Floor Space [m²]	Power [kW]
DASSETT Hydraulic Press (950 kN)	150 000	1000 x 1000	6	77 [184]
ELKOM Mikutherm Pre-Heating Station	21 800 [191]	1100 x 2100	5	15.8 [191]
Steel mould	31 500	250 x 500	-	-

The equipment time is estimated for 19 days working month, with 12 months a year and one 8h shift per day resulting in 1824 h per annum. An interest rate of 7.5% was used [189]. Table 4-20 summarises the total part number per processes and time range, were calculate part number per day and year are rounded down to include only finished part numbers.

Table 4-20: Part rate overview using one press and heating station simultaneously.

Process Type	Rate [h/part]	Parts per hour [1/h]	Parts per day [1/day]	Parts per annum [1/a]
Isothermal	0.47	2.13	17	3876
Rapid Isothermal	0.23	4.35	34	7752
Stamping	0.03	33.33	266	60 648

4.4.1.3 RESULTS

The technical cost model was used to estimate the part cost in relation to a different level of volume production per year where the three process types were compared. Figure 4-30 shows the predicted part cost for the investigated processes. If the textile production reached full capacity of 10000 kg/annum per textile machine, which is equivalent to about 30000 parts (no rejection), a possible part price of £174.27 (£173.44 excl. waste), £49.59 (£48.76) or £8.01 (£7.18) would be obtained under isothermal, rapid-isothermal and stamping process conditions respectively. Lowest part prices for the isothermal and rapid isothermal processes can only be obtained for a lower production volume of a maximum part number of 3876 (£35.86 per part) and 7752 (£20.56 per part) per annum. Higher production rates are only attainable when the work is carried out simultaneously using multiple machineries and labour resulting in a cost increase.

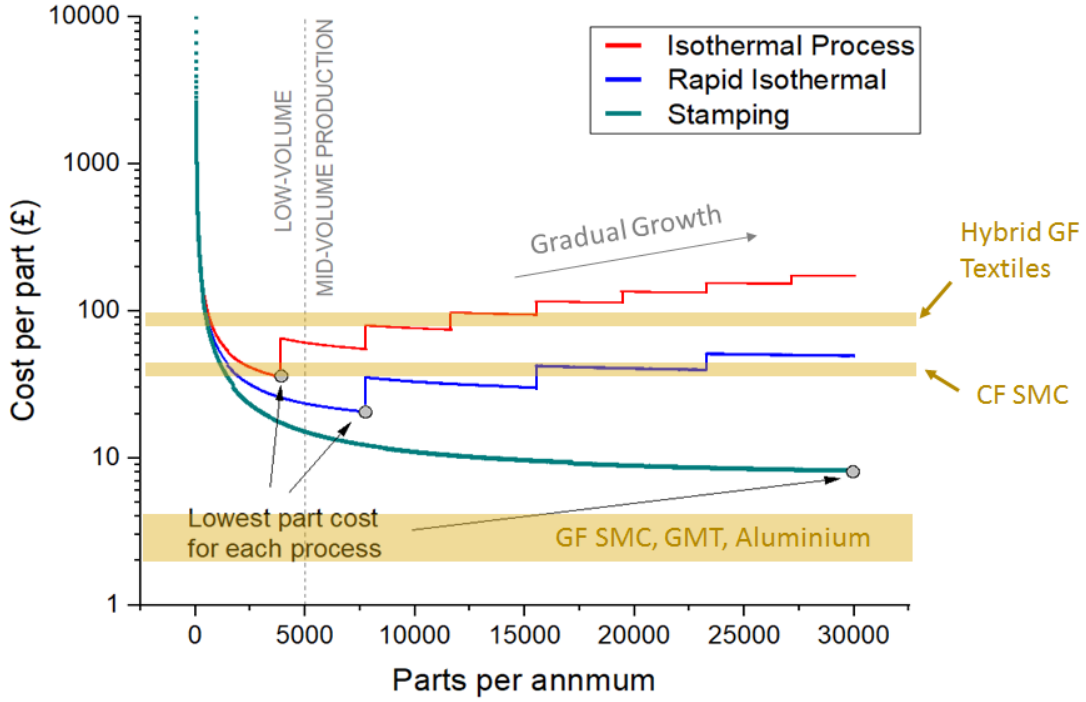

Figure 4-30: Estimated part cost versus annual production volume under different process conditions.

The stamping procedure shows the lowest cost solution due to the lower manufacturing cycle time. The estimation of parts per annum exceeds the maximum capacity of the hydraulic press for the isothermal and rapid isothermal process. The more detailed cost estimation given in Figure 4-31 shows the contribution of the cost categories and level of impact when purchasing multiple pieces of equipment to reach a higher part volume per annum.

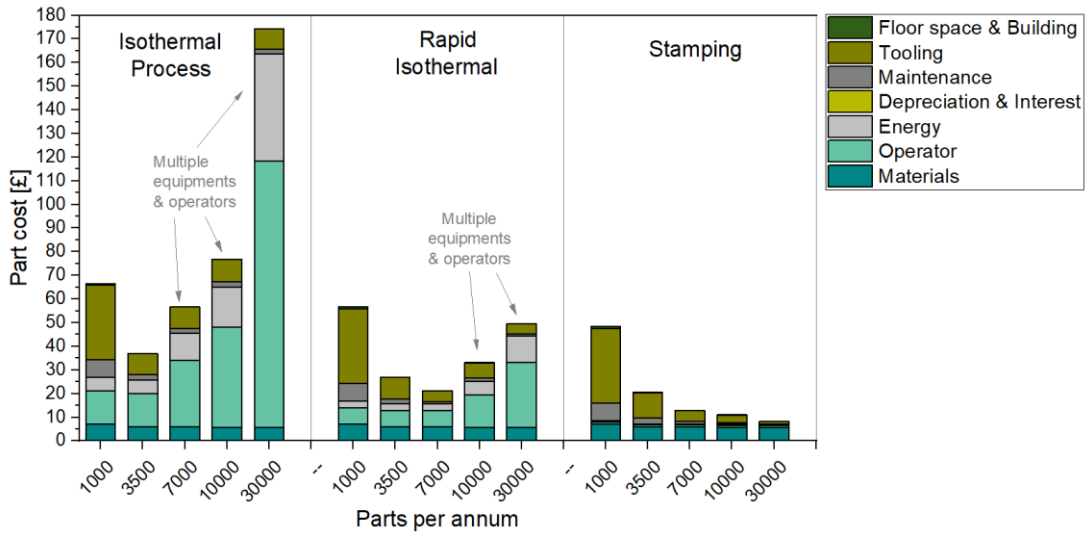

Figure 4-31: Contribution of cost categories to total part cost versus production volume per annum and process type.

The most significant factors with additional machinery are the operator cost, energy consumption and equipment cost including tooling. The relatively long cycle times for the rapid-isothermal and isothermal process makes the operation cost-intensive using skilled operators. A robotic system could be used to eliminate the variable operator cost in the first instance. The extra machine cost and process flow simulation should be considered before purchase. In addition, when working with higher production volumes and longer process cycles it is also important to optimise energy consumption. With the demonstrated decrease in cycle time, e.g. applying the stamping process successfully for the SM45D material type (Section 4.2), the operator cost shrinks. For the stamping process in particular, the main cost contribution is limited to the material choice. Overall, the stamping process represents the most energy-efficient and the best utilisation of the equipment, with a possible volume production of 30000 parts per year.

4.4.2 BENCHMARKING

The material price of all three cost estimates can be compared to competitive material, like glass fibre (GF) applications, and is given as overview in Table 4-21. In this case, sheet moulding compounds (here polyester, UP, based SMC), glass mat thermoplastics (GMT) and more advanced glass fibre applications were added for comparison of thermoset and thermoplastic applications as they represent the main competitor for rCF thermoplastic applications at time of research.

Table 4-21: Material properties and cost for selected competitive material (40wt% FWF).

Material Type	Fibre Type	Polymer Type	Price [£/kg]	Tensile Strength [MPa]	Tensile Modulus [GPa]	Density [g/m³]
GMT [193]	GF, chopped short fibres	PP	2.4	75	5.27	1.22
GMT [194]	GF, chopped long fibres	PP	2.8	110	6.4	1.24
GMT Textile (GMTex) [195]	GF, chopped & continuous	PP	3.0	195	9.9	1.23
Commingled Textile [185]	GF, commingled	PP	91	300	13	1.7
Stamped Nonwoven	SM45D	PP	8.0	192	16.4	1.01
Rapid isothermal processed	SM45D	PP	20.6	219	19.4	1.09
	IM56D	PP	20.6	227	17.5	0.92
	IM56R	PP	20.6	225	21.3	1.01
Isothermal processed	SM45D	PP	35.9	144	19.1	1.14
	IM56D	PP	35.9	145	13.9	1.01
	IM56R	PP	35.9	204	20.3	1.07
SMC [5], [196]	GF	UP	2.7	130 - 150	12-15	1.87
SMC [197]	CF	UP	36.5	300	30-45	1.55
Aluminium [198]	-	-	2.5	240 - 310	69 - 75	2.7

The obtained mechanical properties of rCF/PP composites processed under the different applied process conditions were benchmarked. The comparison with other rCF thermoplastic composite and the competitive material properties from literature (Table 4-21) are shown in Figure 4-32.

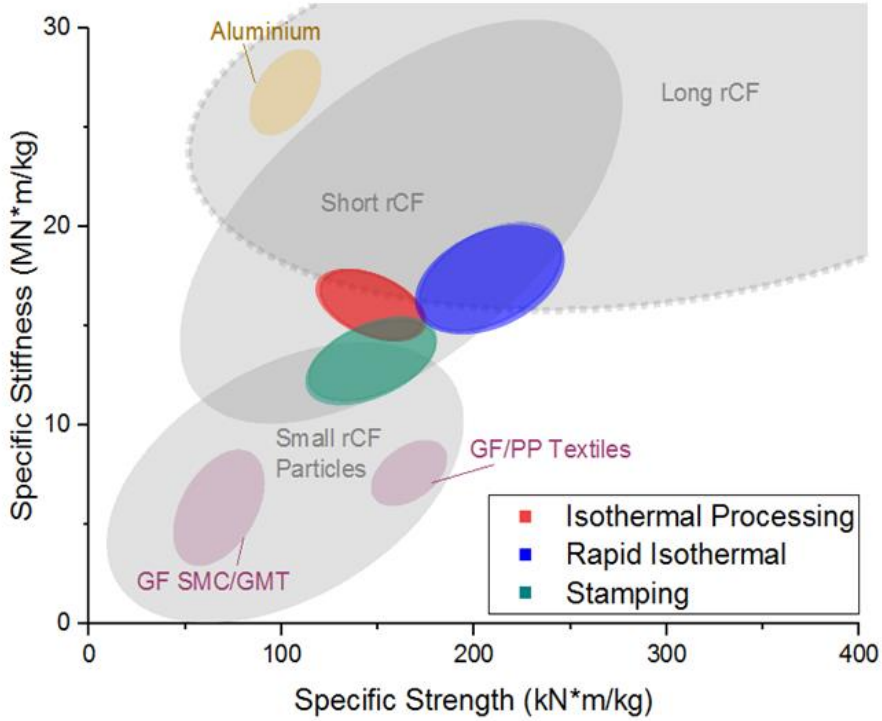

Figure 4-32: Benchmarking using specific composite properties of the processed material (was developed from experimental data and data taken from literature, see Appendix A).

The experimentally processed SM45D, IM56D and IM56R/PP material can clearly outperform several commercial available GMT applications including GF or Carbon as reinforcement. With an additional weight saving, potential applications for rCF/PP could range from interior to exterior components within the automotive car industry, exemple shown in Figure 4-33.

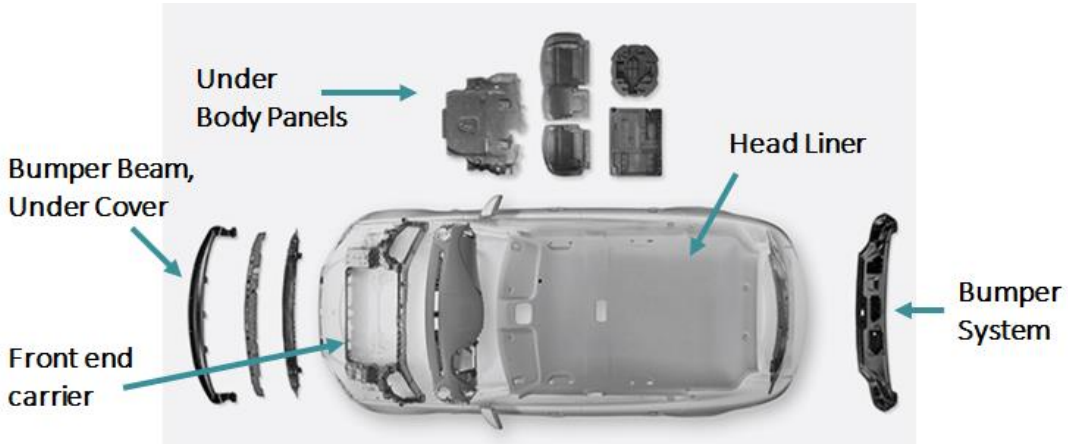

Figure 4-33: Potential application within a car for rCF/PP composites using the commingled nonwoven textiles as a material replacement for e.g. GMT applications (adjusted from [199]**).**

5 MATERIAL ENHANCEMENT

To ensure shorter cycle times in the manufacturing of lightweight components, thermoplastic resins are commonly utilised [7] and are the focus in this project. Even though they are widely used, problems exist regarding the interfacial adhesion between the matrix and rCF (Figure 5-1).

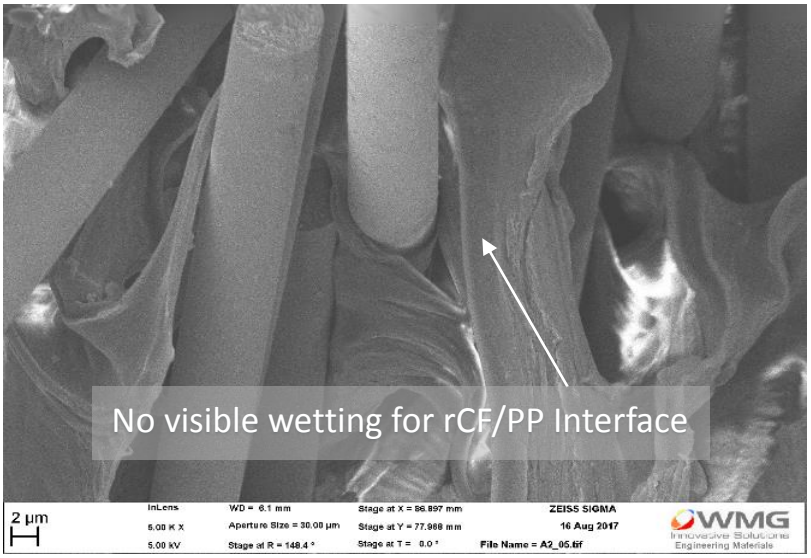

Figure 5-1: Fracture surface analysis representing rCF feedstock surrounded by PP matrix without visible wetting behaviour.

As such, similar to the production of vCF, rCF require a surface treatment to chemically alter the fibre surface before interacting with the target matrix system. Fibre activation or adapted sizing of the fibre is used to, firstly, protect the fibre during the production process, and also to add functional groups to the surface that interact with the thermoplastic matrix [10].

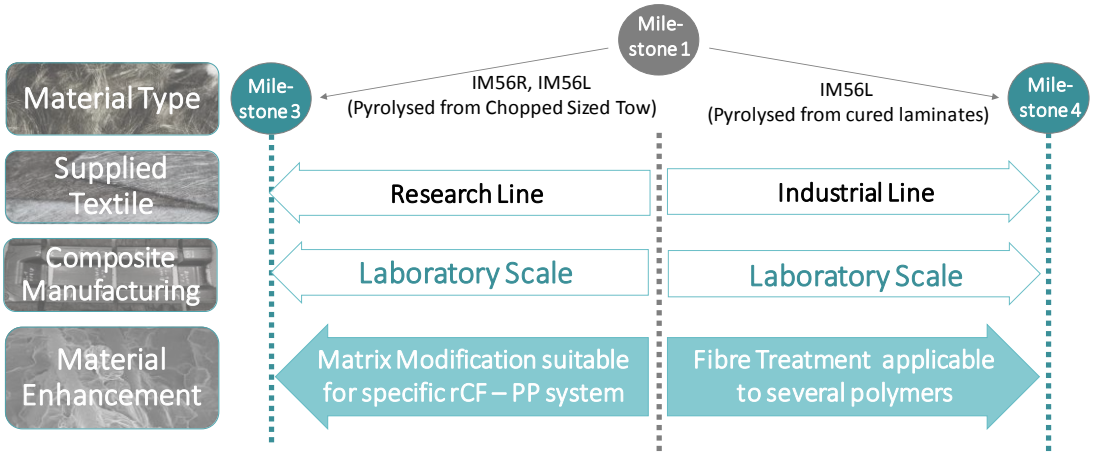

Figure 5-2: Schematic shows the procedure of conducted material modifications with regards to supplied textile type, material feedstock and composite manufacturing level.

Another method which is used to overcome the moderate interfacial adhesion of the matrix and rCF is the modification of the matrix material surrounding rCF, which has been shown in connection with MAPP, a chemically modified PP version [11]–[13]. The modification enables the polymer to increase its polarity and functionality in order to increase the interfacial performance with rCF. These options are considered in further investigations.

Both options with potential to increase the composite performance are considered in further investigations. The processed material differs between the two studies, which is schematically shown in Figure 5-2) and can be explained by different production volume at the time of research. Nevertheless, all obtained data could be compared to the benchmark developed in previous studies (Chapter 4) and is discussed in this section.

5.1 MATRIX MODIFICATION

The effect of a modification of non-polar polypropylene using commercially available maleic anhydride-grafted PP was studied. The nonwovens were manufactured using the same process conditions as the benchmark on lab-scale under isothermal process conditions for a direct comparison i.e. 200 °C, 10 min dwell time and 20 °C/min applied for the heating and cooling cycle resulting in a total cycle time of 27 min with insert and de-moulding applied at room temperature. The processing of these materials was previously reported in [200], [201] using a varied amount of maleic anhydride (MA) in the supplied commingled rCF/MAPP nonwovens and are summarised in the following:

- No significant effect of a different level of MA on crystallisation or melting temperature
- Decrease in the onset of degradation for MA content of 1 – 5 wt%
- Increased composite strength and stiffness (tensile, flexural) with the addition of MA up to 5 wt%
- Decrease in impact strength with increased MA content was traced back to decreased plastic deformation at failure
- Difficulties in moulding material containing > 5 wt% MA
- Improved wetting when using MA as expected
- Reported FWF ranged from 37.6 – 47.1 wt% for targeted 40 wt% (lab textile line).

These results formed the sub-project baseline.

5.1.1 POLYMER PROPERTIES

Having established the project baseline, an in-depth analysis was conducted regarding the applied polymer types with regards to the MA concentration and molecular weight and prediction of interfacial properties of the matrix-fibre system.

FTIR analysis was used to quantify the MA content in the samples. The quantitative analysis was performed using the Roover method [146], where the poly (maleic anhydride) concentration [µeq/g] was calculated by the ratio of specific absorbance bands of the determined infrared (IR) scans. When dried for 24h at 130 °C the carboxylic acid could be detected on the IR scan of MAPP samples after volatilising unreacted MA, which gives the baseline for the calculation [202]. IR scans were completed for all polymer samples including a pure PP reference. By heating the samples for 24h prior testing, the absorbance peak at 1715 cm^{-1} was well noted in the IR scans, which represents the anhydride concentration correlating to the MA concentration in the MAPP samples.

Apart from the value measured for sample TP0082, the given and calculated anhydride concentration matches for sample TP0080 and TP0081 (Table 5-1). Therefore, the following characterisation methods will refer to the range of measured anhydride concentration.

Table 5-1: Determined total anhydride concentration with respect to the given anhydride concentration by the supplier.

Sample No.	Peak Concentration [µeq/g]	Calibrated Anhydride Conc. [µeq/g]	Measured Anhydride Concentration [%]	Given Anhydride Concentration by Supplier [%]
PP	98.54	0	0	0
MA1001	100.05	1.51	0.43	- (Low)
MA1002	110.68	12.14	3.46	- (Medium)
MA1003	114.60	16.06	4.58	- (High)
TP0080	116.21	17.67	5.04	5
TP0081	123.10	24.56	7	7
TP0082	122.62	24.07	6.86	10

Comparing the calculated weight fraction of the MA to the mechanical data reported in the project baseline led to the assumption of different MA types used for the formulation MA1001,1002,1003 (described in the following as type 1) and TP0080, TP0081, TP0082 (type 2). In the GPC analysis the number-average molar mass (M_n), weight-average molar mass (M_W) and the dispersity (Đ) of the neat PP were evaluated and one sample of each MAPP

supplier to compare the physical polymer characteristic. The results of the analysis (data was provided by the Polymer RTP laboratory, University of Warwick.) are summarised as follows:

- The molecular weight of the two MAPP types showed similar levels of weight-average molar mass (M_W), but they differ in number-average molecular mass.
- All samples showed good quality in dispersion, showing the lower range of typically dispersion rates of 2-20 [203].
- The dispersion rates differed between the different MAPP types and were examined further.

A lower dispersion (M_w/M_n) leads to increased melt viscosity and, therefore, a higher flow rate, which may be due to lower entanglement within the system [204].It may also produce different physical properties [205]. The schematic shown in Figure 5-3 underlines the difference in the measured molecular masses and its effect on the possible properties of the composite. The molecular weight of the two MAPP types, with type 1 (MA1001) representing the MA series and type 2 (TP0081) representing the other type of modified thermoplastic (TP) series, show similar levels, but they differ in number-average molecular mass.

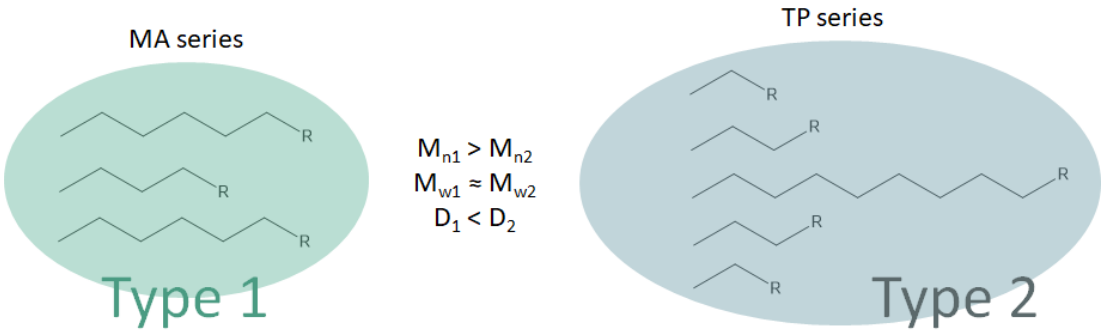

Figure 5-3: Developed schematic showing the difference in molecular mass distribution (Đ) for polymers having a similar molecular weight fraction (M_w) with varied number-average molecular mass (M_n).

As shown in the schematic above, type 1 consists of fewer and medium-length molecular chains, whereas type 2 contains more chains, a mixture of short chains and a single long chain. It is assumed that fewer longer chains (as in type 2) can create a more compact network with larger coverage throughout the composite. On the other hand, type 1 - consisting of a good dispersion of similar medium length chains - could lack in penetration depth within the system and its physical size prevents it from tightly bonding. This phenomenon is called “steric hindrance”, where the bulk polymer is hindered from creating a tight network [205]. In summary, having a MAPP type with a lower dispersion rate results in enhanced polymer flow, which subsequently leads to a lower overall void content. But at

the same time, with a decreased level of penetration due to fewer longer chains, the polymer network can lack in bonding properties throughout the composite.

Further analysis included the contact angle measurements were the effect of the addition of anhydride concentration on the surface energy and subsequent wettability characteristic was analysed. An increase in the contact angle of water was detected when comparing the PP sample with the MA series, which was against expectation and seemed to decrease the wetting behaviour of the polar liquid on the tested surfaces (Table 5-2).

Table 5-2: Contact angle measurements (sessile drop method) of all-polymer samples applying the sessile drop method and using deionised water and DIM as the test liquid.

Polymer Type	Anhydride Concentration [%]	θ (H_2O)	θ (DIM)
PP	0	99.78° ± 1.59°	65.30° ± 8.96°
MA1001	0.43	106.81° ± 2.25°	62.55° ± 5.45°
MA1002	3.46	100.66° ± 1.48°	58.68° ± 6.23°
MA1003	4.58	106.66° ± 1.52°	61.59° ± 4.73°
TP0080	5.04	99.91° ± 6.28°	66.68° ± 2.31°
TP0081	7	93.13° ± 1.78°	57.02° ± 4.44°
TP0082	10	85.08° ± 3.02°	41.86° ± 7.27°

However, when looking at the level of contact angle above 5 wt% of anhydride concentration a certain decrease is visible for the TP series. A similar phenomenon was obtained for the measurements using DIM; the measurements of MA1001, MA1002, MA1003 fluctuate, but measurements for TP0080, TP0081 and TP0082 samples showed a clear decrease in hydrophobicity and subsequent increase in wetting behaviour with increased MA content. Given these results, the contact angle measurement is not a suitable method to identify differences in matrix polarity smaller than 5 wt% of MA concentration level. However, Kim *et al*. were able to measure the difference in contact angles and surface energies from a very low range of 0.1 to 2 wt% of MA, which showed a more sensitive analysis technique using the same method [13]. Therefore, it is further assumed that the analysis was hindered more by the MAPP type than by the weight fraction. The calculated surface energy levels derived from the measured contact angles are plotted in Figure 5-4. Following OWRK's method (Section 3.5.1) the total measured energy can be divided into polar and dispersive content. The polar content is directly related to the functionality of the material in terms of chemical groups, whereas the dispersive part can be related to Van-der-Waals forces [206]. In the case of the tested samples (PP and MAPP), an increase in polarity was obtained with an increase in functional groups, which correlates with findings in the literature [13].

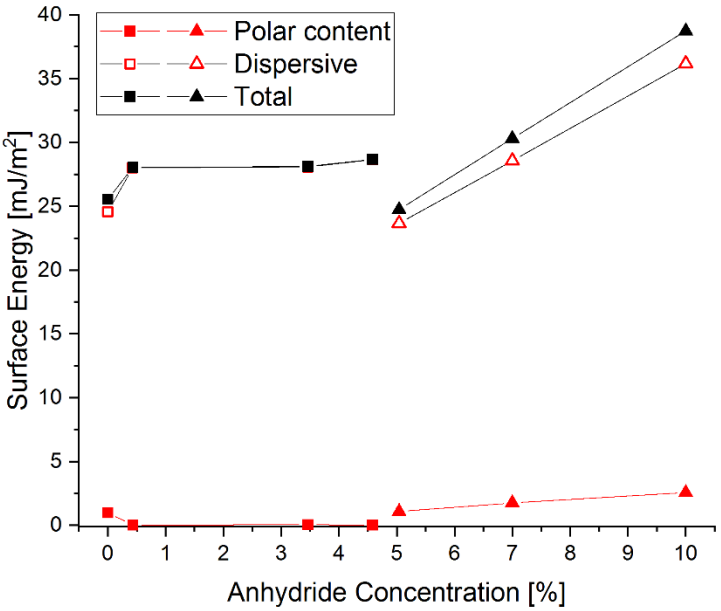

Figure 5-4: Calculated surface energy following OWRK principles; total surface energy was divided into polar and dispersive content. Different MAPP types are distinguished as supplier 1 (■), supplier 2 (▲).

The rise in surface energy (with the addition of and the following increase of anhydride concentration) compared to the control PP was lower when looking at samples with < 5 wt% than above 5 wt% MA content. Also, the addition of MA content showed a more intensive effect on the dispersive part than the increase in polar groups linked to the polar fraction, where the latter can be only detected above 5 wt% of MA content. An estimation of interfacial properties between the matrix and the target fibre can be obtained from a further calculation of the adhesion energy (ψ_{SL}) and interfacial tension (σ_{SL}).

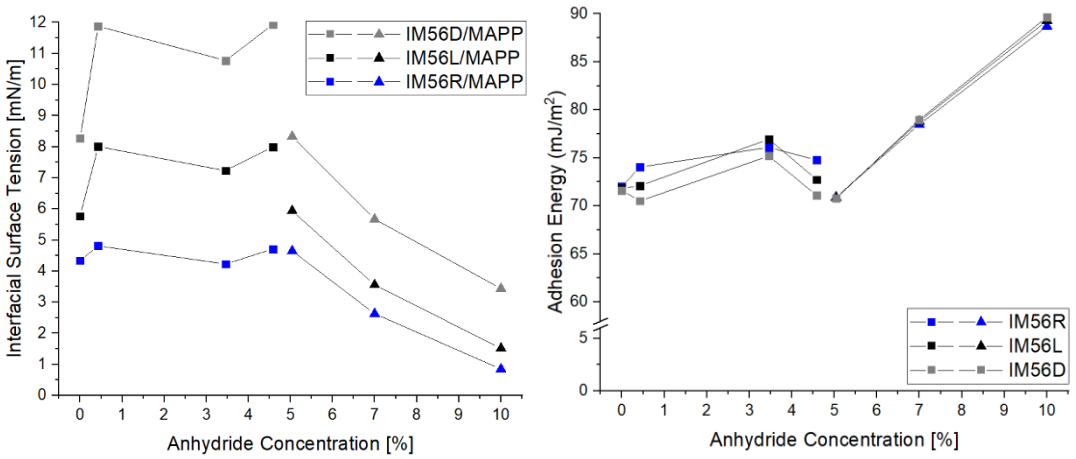

Figure 5-5: Calculated interfacial tension σ_{SL} and adhesion energy ψ_{SL} is given in relation to IM56R fibre types. Different MAPP types are distinguished by the symbol: supplier 1 (■), supplier 2 (▲).

Figure 5-5 displays the results in relation to all evaluated fibre types and their surface characteristic. The interfacial tension describes the level of incompatibility. Therefore, low tension is targeted (equal to the low difference between polar fraction) to increase the wetting behaviour between rCF fibre and matrix. For MAPP type 1 (< 5 wt%) no significant change in tension is detected with an increase of anhydride concentration. However, the desired case of reduced interfacial tension was obtained for all systems with an increased anhydride concentration (> 5 wt%) for all fibre-matrix systems. The level of compatibility improved between fibre types. The highest tension level was observed between the matrix and sized fibre type IM56D, underlining the incompatibility between fibre (covered by Epoxy compatible sizing) and PP. The greatest compatibility with PP was shown for the IM56L and IM56R fibre types which had the lowest calculated interfacial surface tension. The same increase in adhesion by raising the MA content was reported by Novak *et al*. [207].

The adhesion energy describes the physio-chemical bonding, and how energetically favourable the initial formation is between the fibre and the matrix system. In the case of the fibre-matrix interface, high adhesion energy is targeted. The increase of the anhydride concentration leads to the desired properties, again, with a more significant effect visible above 5 wt% of MA content.

5.1.2 EFFECT OF MAPP ON MECHANICAL COMPOSITE PERFORMANCE

To evaluate the effects of the matrix modification on the composite properties, the previously reported results of the project baseline were normalised to a fibre weight fraction of 40 wt%. The results of the calibration shown in Figure 5-6 emphasise the effect of the addition of MA on the composite strength performance, which is the focus of the project.

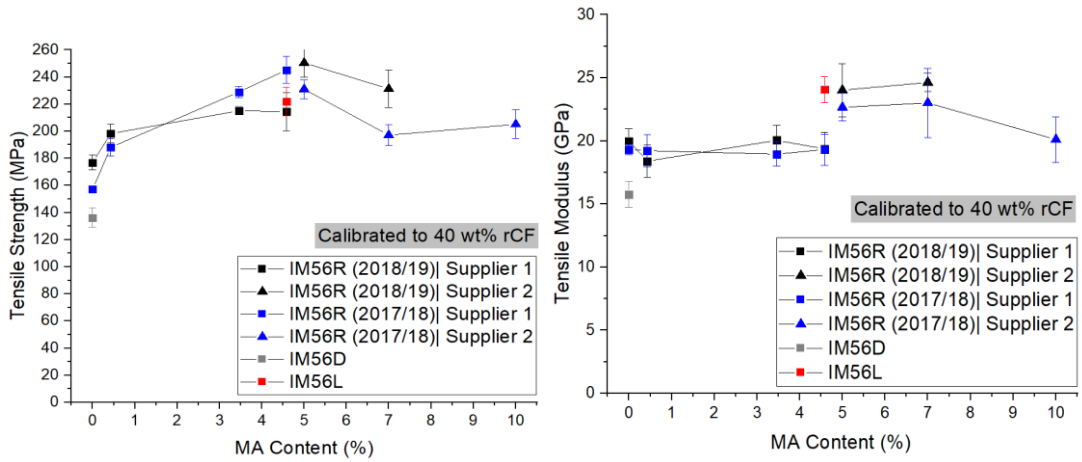

Figure 5-6: Re-processed tensile strength and stiffness data from project baseline containing different amount of MA and 40 wt% recycled fibres. Different MAPP types are distinguished by the symbol: supplier 1 (■), supplier 2 (▲).

A clear increase in tensile strength with the addition of MA was detected for IM56R/PP/MA composites, with a maximum reached at around 5 wt% addition of MA (optimum at 4.5 wt% of the MA1003 tested in 2017/18 and 5.5 wt% of the TP0080 sample in 2018/19). As highlighted earlier, the supplied modified polymer was manufactured differently, which was detected with a variety in molecular weight (Section 6.1.2). However, the trend of an increase in strength with the addition of MA compared to neat PP, leading to a maximum of affective MA content (optimum reached) followed by a drop in performance shows a similarity between the two compared materials as well as the different testing period. In addition, by testing one year after the date of manufacture, it was shown that the materials could be stored for one year without a loss in performance.

Examining other fibre-matrix systems, the IM56L/MAPP sample behaves similarly in strength compared to the IM56R/MAPP samples containing 4.5 wt% MA. The comparable performance shows similar good compatibility with the MAPP and sufficient transfer of strength throughout the composite.

A different trend was detected when evaluating the level of composite stiffness of the tested samples compared to the different level of anhydride concentration in the polymer. The level of stiffness does not show a difference with the addition of MA when looking at IM56R/PP/MA samples containing 0.5 – 4.5 wt% (Supplier 1) compared to the neat PP from the same supplier. Samples with an MA content of 5.5. -7 wt% (from Supplier 2) show a generally higher stiffness for IM56R/PP/MA composites before a drop occurs at 10 wt% MA content. The phenomenon of different levels of stiffness for different types of MA added to the composite can be explained by better compatibility between fibre and polymer supplied by Supplier 2, which has been reported by Wong *et al*. [12]. A further drop in moduli was also detected in Sanadi's study, which was explained by an excessive amount of MA resulting in a drop in performance and reducing the overall level of adhesion with the target fibre surface [208].

A statistical verification was conducted to underline the significance of the results using OriginPro / T-test, where a 95 % confidence level was allowed ($P > 0.05$). If the p-value drops below 0.05, it can be concluded with 95% confidence that there are significant differences between the measured composite stiffness properties. As the results in Table 5-3 show, this was observed in measurements from 2017/18 and 2018/2019 and also a comparison was made between the modified material (adding MA) and the control material (unmodified).

Table 5-3: Verification of the statistical difference in measured composite properties in regard to the composite stiffness of unmodified and modified material series (values below the specified p-value of 0.05 are highlighted in bold showing a significant difference to the control)

	Polymer Supplier 1				Polymer Supplier 2		
Material Series	Control IM56R/ PP	IM56R/ MA0.5	IM56R/ MA3.5	IM56R/ MA4.5	IM56R/ MA5	IM56R/ MA7	IM56R/ MA10
2017/2018	-	0.9190	0.5806	0.9895	**0.0075**	**0.0458**	0.4954
2018/2019	-	0.1562	0.9606	0.0981	**0.0393**	**0.0025**	-

All statistical tests which were run for the material provided by polymer supplier 1 indicate that there is no significant evidence for a difference in mechanical performance in the composite stiffness with p-values below 0.05 when comparing the results from material series 2017/2018 between the control and modified material until 4.5 wt% MA. Similar behaviour was observed for the material series 2018/2019. When comparing the stiffness levels between both suppliers, a significant difference in values was confirmed in the form of p-values below 0.05, for material IM56R/MA5 and IM56R/MA7 independent from the test date. This conclusion cannot be applied to the material IM56R/MA10, which could be traced back to the excessive amount of MA, as mentioned previously.

A relation between the molecular weight and the composite moduli and consequent drop in moduli with increased molecular weight has been described in the literature before [12], [204], [205], but without a reasonable explanation. A similar weight-average molecular mass but a slightly different level of dispersity was measured for MAPP samples derived from the MA series and TP series (Section 6.1.2). The dispersion was calculated from the relation between the number-average molar mass and the weight-average molar mass. It is assumed that a decrease in the particular number-average molecular weight, comprising of fewer longer molecular chains, could create a more compact system and network with higher penetration depth throughout the composite than a higher amount of semi-long molecular chains. However, a lower number-average molecular weight measured for the TP series of MAPP samples results in an increase in composite moduli. The measured molecular weight of the MA1000 series (≤ 4.5 wt% MA) lies 52 177 g/mol above the TP8000 series (≥ 5.5 wt%), which showed a molecular weight of 41 500 g/mol (Section 6.1.2).

A further reason for a lower modulus for samples containing 0.5 – 4.5 wt% could also be the decreased thermal resistance of the MAPP shown in the project baseline (Section 3.1). The lower onset of degradation temperature was evaluated, which could lead to unintentional degradation of the material at the processed temperature of 200 °C.

Considering once more different fibre-matrix systems, the IM56L/MAPP sample showed better stiffness characteristic compared to the IM56R/MAPP samples containing 4.5 wt% MA. The increased performance showed enhanced compatibility with the MAPP and more sufficient transfer of strength throughout the composite.

5.1.3 EFFECT OF FIBRE QUALITY ON COMPOSITE PERFORMANCE

To assess the feasibility of processing commingled rCF/MAPP nonwovens, a case study was performed on a pilot scale. The aims were a reduction of total cycle time and a rise in composite performance by applying the improved process conditions of milestone 1 (Section 4.1.6) to the modified material. Previous trials reported in Chapter 4 demonstrated that with the reduction of the processing time, sufficient impregnation of the textiles before consolidation is limited. It was also demonstrated that the interfacial properties have a significant effect on the processability of the material. With the use of rCF/MAPP textiles it was assumed that due to an optimised fibre-matrix interface both process types (rapid-isothermal stamping) could be applied and would lead to high composite quality.

However, using over-pyrolysed feedstock decreased the fibre quality significantly and led to low overall composite quality compared to milestone 2 (Section 4.2.4.). Firstly, the composite panels were processed on the DASSETT under rapid-isothermal conditions (final part thickness: 2mm) with the following mechanical properties:

- Maximum obtained composite strength of 124.2 MPa and stiffness of 13.4 GPa at pre-heating 170 °C, Moulding temp. 190 °C, 30 s dwell time
- Close to void-free composites (≤ 2 vol%) for conditions recorded above and all other process conditions at pre-heating temperature of 180 °C, mould temperature of 180 – 190 °C and dwell time varied between 30 – 90 s.

This shows that not only an optimised interface but also good quality of the base material after recycling is required to obtain good quality composites. Nevertheless, a high level of impregnation was obtained for all processed textiles using the rapid-isothermal process settings. It is assumed that similar levels of impregnation can be obtained for all further mixtures processed in conjunction with MAPP in future.

The total process time was calculated and maintained an average of 7.24 minutes. However, the temperature level changed slightly. It was noted that the cooling process had a higher effect on the total process time than re-heating back to the start temperature, which on average took 1.8 minutes for all the different investigated temperature levels. A further investigation of the process feasibility of rCF/MAPP nonwovens applying the stamping

process led to unexpected results. Low flowability of the polymer made the moulding and consolidation in such short time (60 – 120 s) impossible and resulted in highly porous unconsolidated parts with composite strength values below 50 MPa and stiffness levels between 4.2 and 5 GPa independent from variation in pre-heating temperature and cycle time (Figure 5-7).

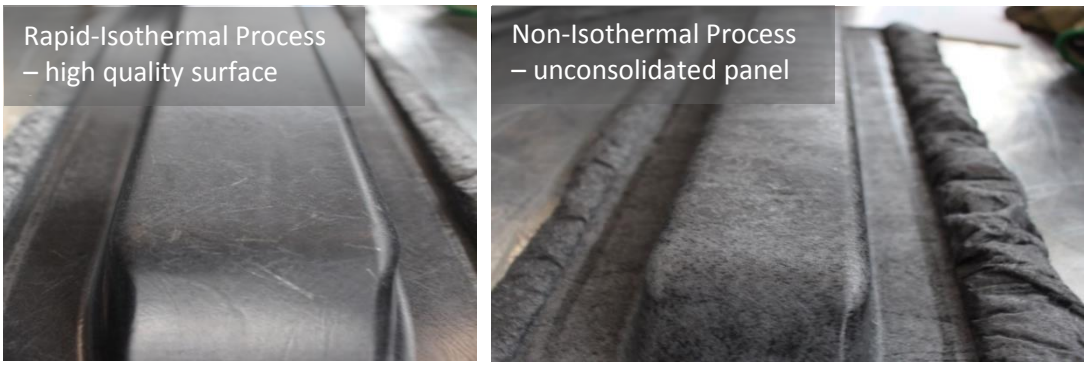

Figure 5-7: The surface finish of manufactured composite panels showing superb quality for material processed under rapid isothermal conditions (left) & low quality and unconsolidated panel processed in non-isothermal / stamping conditions (right).

The overall messages from this case study are the following:

- The feasibility of processing the MAPP based nonwovens on a pilot scale by applying a rapid isothermal process type was proven. However, the extremely low overall composite properties showed the need for good quality recycled carbon fibres in the first instance. Any process adjustments become irrelevant when the base material consists of poor quality. A gentle pyrolysis process is key for maintaining good physical fibre properties for possible re-processing of the recycled material. Without maintaining the material characteristic, closing the material loop becomes challenging and instantaneous down-cycling occurs, which subsequently affects the revenue stream.
- The application of MAPP was used to increase the wetting behaviour between the rCF feedstock and the polymer to ensure a rigid interfacial characteristic for optimised composite properties. In relation to the improved wetting, and the decrease in residual voids in the manufactured composite panels, an overall reduction in viscosity was assumed. With this in mind, the processability of the nonwovens was thought to perform perfectly when processed under non-isothermal conditions (stamping). However, the material solidified immediately when moulding without visible polymer flow. It is therefore assumed, that the advantages involved

with the use of MAPP can be only applied to process types with longer impregnation time to ensure sufficient flow before the chemical reaction occurs.

The limitation in processability regarding the stamping process showed unsuitability of the rCF/MAPP with the gathered knowledge at the time of research. Further trials suggest applying the different MAPP types from different suppliers where the focus should be on the effect of base characteristic (e.g. molecular weight, melt flow index) in relation to its wetting behaviour and flowability in the targeted fibre-matrix system.

5.1.4 ENVIRONMENTAL & ECONOMIC CONSIDERATIONS FOR POLYMER USAGE

The PP production is a refined process and is the simplest and most efficient polymer production process when analysing its life cycle [209]. The polymer is derived from propane gas or crude oil followed by polymerisation of propylene [210]. The subsequent low cost of PP brings advantages and disadvantages.

5.1.4.1 ENVIRONMENTAL BURDEN

The recycling of PP is not yet economically viable due to the low cost and small revenue of the virgin material. If no economic incentives linked to environmental concerns are given, the material is more likely to be dumped onto landfill, if possible, than recycled [211]. Neither PP nor MAPP are UV resistant and require a modification of the polymer for automotive applications e.g. additional UV-resistant top layers or inserts of different material decreasing the potential of recyclability, when manufacturing the composite [212]. Furthermore, Gupta *et al*. reported a loss in tensile strength of ≤ 70 % when exposed to more than six days direct sunlight [213], which underlines the lack in durability and longevity.

The MAPP derives from neat PP and the separate produced maleic anhydride which is, so-called, maleated to the final product by grafting the maleic anhydride groups onto the PP chain [205]. Maleic anhydride itself can be prepared by oxidation of benzene or n-butanes, whereby the latter version is nowadays preferred due to higher efficiency rates (up to 99 %) and lower environmental burden using less process water, and generating less waste [214]. The oxidation process takes place at temperatures of 400 – 430 °C [215]. During the production of MA, small amounts (~ 1 %, [216]) of CO_2 and CO, as well as water, are generated and the intermediate product acts as corrosive, irritant and health hazard, which classifies the material as danger [217].

The grafting process itself is described in patents as follows:

- The MA and peroxide reagent are dissolved in low molecular solvents (e.g. pentane, heptane) and dispersed on the molten PP at a temperature of 180 – 220 °C. The MA is mixed in powder form with the peroxide and PP applying a batch process. (Exxon Chemical Patents Inc., US, 1989 [218])
- A molten mixture of PP and MA is processed continuously on a twin-screw extruder, where peroxide is used as an initiator at 190 - 205 °C. The process is described as an efficient method on an industrial scale with 49 - 93 % conversion (at 85 % highest reported efficiency) under a vacuum to remove any unstable chemical compounds when manufacturing the end product. Due to specific molten process type, reportedly, no solvents or water remains after the process. (Eastman Chemical Company, US, 2008 [219])

From the description of the few available patents describing an industrial process, it can be seen that the first method has been further developed to decrease the use of input material and industrial by-products aiming for a highly efficient process with a lower environmental impact. However, the additional process steps of the MA production and grafting using further petroleum-based input material subsequently leads to a greater environmental impact. Furthermore, the prolong production cycle and cost of solvents and initiator also increases the final material cost of MAPP compared to the pure PP production[219]. Further research has been reported regarding replacing the raw material production of n-butane derived from food waste and other waste sources but drawbacks like a low material recovery and by-product formation, e.g. acetone and ethanol, prevent primary applications currently [220], [221]. Thermal analysis data shown in the project baseline detected a difference in thermal stability between PP, MA series and TP series. Whereas PP and MAPP polymers from the TP series have an onset degradation of 200 °C or higher, polymer degradation for MAPP samples from the MA series is seen at 180–195°C. The initial process temperature of 200°C can lead to degradation of the polymer when processed and the development of gases which are toxic for workers around the machine when exposed in the long term. Therefore, the process temperature needs to be adjusted. Furthermore, a lower process temperature implies less energy usage for processing the material which leads to lower total energy consumption. A polynomial fit was performed using OriginPro to predict the highest

composite strength from the experimental data. With the mathematical analysis, an optimum amount of 5.57 wt% of MA concentration was estimated for the maximum possible composite strength.

5.1.4.2 ECONOMIC BENEFIT

The total increase in composite performance is compared to the increase in cost and plotted in Figure 5-8. The highest average strength is measured for samples containing 5 wt% MA content (TP0080) from supplier 2, which also display lower standard deviation and additional enhanced composite stiffness. An increase of 44 % in strength and 19 % in modulus were reported respectively. Therefore, it is recommended to use 5 wt% MA content in conjunction with IM56R fibres to achieve replicable and optimised composite performance. With the modification and use of the TP0080 polymer type, the cost increases by 14.3 % (polymer price) compared to pure PP base composites with lower mechanical performance, which corresponds to an increase of 8.6 % for an exemplary 40 wt% nonwoven textile. Against expectation and outcome from the project baseline, TP0081 was shown to be more effective in terms of increase in composite strength and stiffness properties.

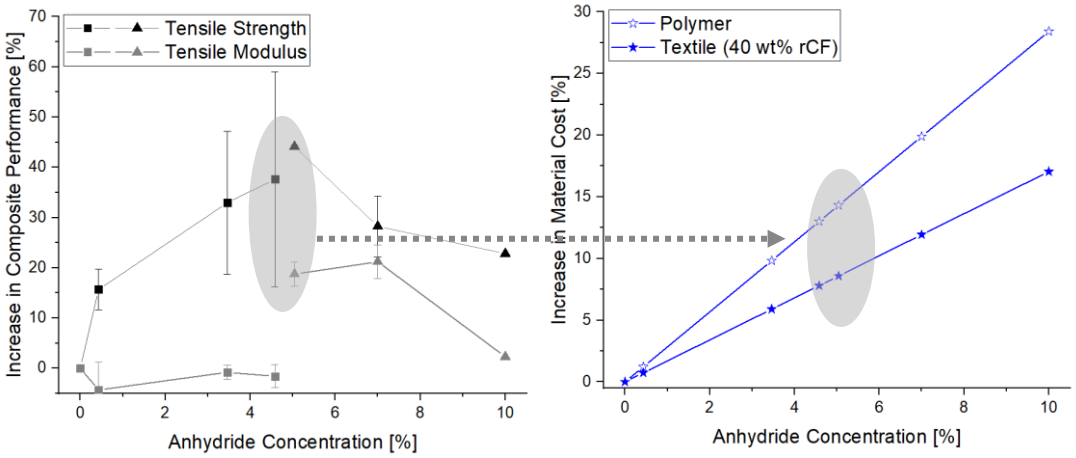

Figure 5-8: Comparison of achieved increase in composite strength and stiffness with relation to an involved cost increase including polymer cot only.

A significant lower expense is given when using MA1001 type with only 0.5 wt% MA content leading to enhanced mechanical performance in strength and stiffness with subsequent minimum cost increase of 1.22 %. The highest increase in composite stiffness (+35 %) was obtained by using polymer type TP0081 with 7 wt% MA content. The extra cost involved to enhance the tensile modulus was almost 20 %. The calculation is only based on the polymer price and does not involve the nonwoven cost, which is assumed to stay unchanged.

In addition to the cost analysis, the following processing guide derived from the material characterisation gives further suggestion for the preferred polymer choice for processing

nonwoven textiles by thermoforming. The system was optimised for PP/IM56R material composition and the same process conditions were applied to the modified version. Further process optimisation with given data from this project report could further decrease process cycle time and moulding temperature, as well as pressure due to varied melt flow which leads to further cost reduction:

- The process temperature could be further reduced and optimised for each material combination due to varied thermal resistance for modified matrix systems. The adjustment automatically reduces the total process time and process cost including part volume per annum and machine usage.
- With an increased melt flow, the applied force when moulding could be further optimised and balanced. The pressure could be reduced to its minimum but still ensure void-free components and efficient bulk flow when moulding, which also results in cost savings.
- A comparison to other MA types with increased molecular weight could further enhance the polymer flow and ensure sufficient matrix percolation whilst moulding.

Both material systems contain advantages and disadvantages with each usage. However, when following the process guideline with modified moulding time and temperature adjusted to each MAPP type, the environmental risk for workers can be reduced and material quality can be improved. Furthermore, the long-term resistance for PP and MAPP can be ensured with a thin extra outer layer of UV resistance shield for the manufactured composites. With this in mind, applying MAPP to enhance composite properties regarding its tensile strength and stiffness can clearly outperform the neat PP based material when processed in isothermal conditions. Nevertheless, the environmental impact of the polymer production of both types needs to be considered to further reduce the environmental impact and provide a sustainable counterpart to the recycled fibre reinforcement.

5.1.5 MILESTONE 3: MODIFIED MATRIX MATERIAL BOOSTS COMPOSITE PROPERTIES

The investigated effect of a modified polymer matrix type, using maleic anhydride-grafted polypropylene included the evaluation of the composite performance and thermal stability and also possible economic and environmental drawbacks. The study focused on IM56R/MAPP nonwovens, which extended the range of examined material from ELGCF to improve expertise in this emerging technology and analyse its market competitiveness.

Improved performance was observed within the project baseline, which set the starting point for further experimental studies. Showing a high variance in fibre weight fraction, also shown in other work when working with textiles supplied from the ELGCF lab line, a subsequent complementary study was performed where the data was calibrated to 40 wt% for direct comparison. The re-calculation supported the analysis of the effect of the addition of MA compared to the neat PP. Working with different polymers varying in anhydride concentration, and possible production routes due to sourcing from different suppliers, led to further investigation of the matrix material characteristic. The exact anhydride concentration was successfully determined by a quantification method using the obtained IR spectra. A difference detected in the dispersion and number-average molecular weight, resulting from the GPC measurement at the RTP lab, led to the assumption of different polymer production routes applied by polymer supplier 1 and 2.

After the in-depth characterisation of the base materials, the evaluation of the calibrated data of the composite performance was followed. The successful enhancement of the composite strength was confirmed. A different trend in composite strength and stiffness performance was obtained:

- The composite strength increases with the addition of 5 wt% MA content to a maximum strength of 250 MPa (40 wt% rCF, cross-plied) compared to 177 MPa measured for IM56R/PP. Averaging the obtained results from both years showed an increase of 44 %. With a further increase in MA content, the strength properties decrease. The mathematical polynomial fit estimated the maximum possible composite strength at 5.5 wt% MA content.
- The composite stiffness (tensile modulus) seemed unaffected by the addition of anhydride concentration for levels from 0.5 wt% to 4.6 wt%, but this could also be related to the supplied polymer type with a lower dispersion level. An increase in stiffness is noted from 5 wt% onwards and could be related to a better compatibly with polymer type 2, containing fewer longer chains, to create a compact network around the reinforcement. After an obtained maximum at 7 wt% additive, a decrease in tensile modulus is observed. The highest noted increase in stiffness was averaged to 21.2 %.

Overall, the addition of MAPP enhanced the composite properties of panels manufactured under isothermal conditions at a laboratory scale as desired and was ranked in the mid-range of all comparable rCF applications (Figure 5-9). When considering a potential increase in

performance by 80% from cross-ply to oriented fibre direction, the quality is expected to further improve.

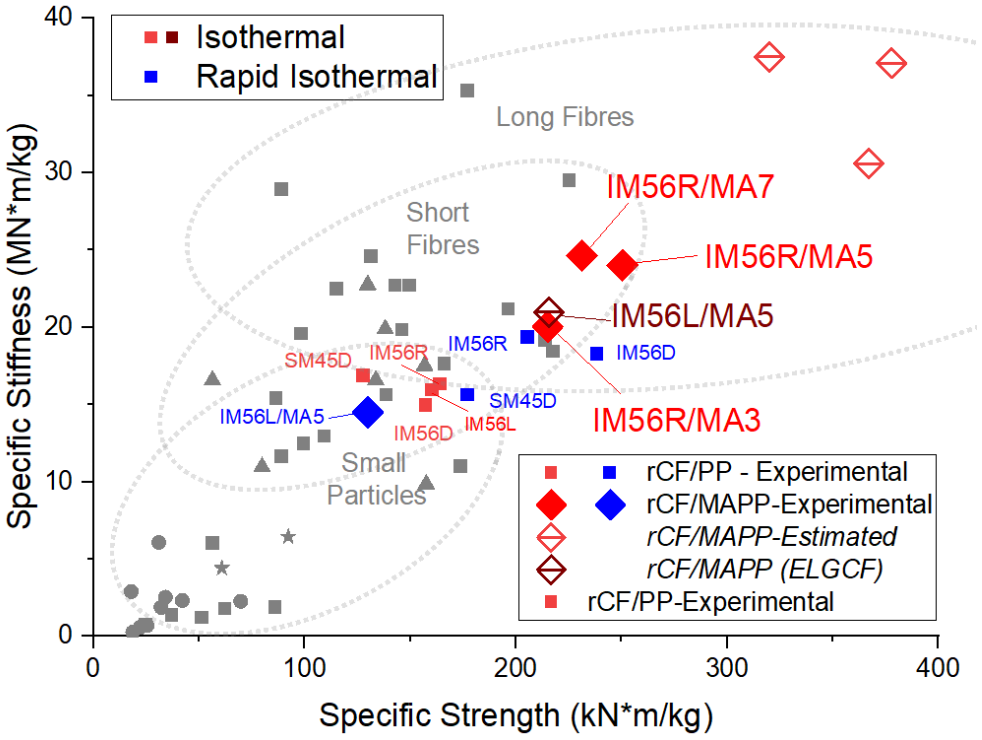

Figure 5-9: Obtained composite properties of IM56R/MAPP processed isothermally (■◆, cross-plied), including estimation for performance when tested in fibre direction (◇) and processed isothermally in-house at ELGCF (◇). In comparison, processed rapid isothermally (◆) compared to rCF/PP composites (■), which were all tested along the transverse direction.

However, with an upscale of the process and investigation of rapid isothermal and non-isothermal processing, limitations were detected regarding the base material quality and application for faster processing. The case study showed the need to maintain good quality feedstock throughout the recycling procedure, to ensure a good level of composite quality when reusing the recyclates. It was shown that over-pyrolysed feedstock lacks in performance during process and cannot reach comparable composite strength and stiffness with composites processed on a laboratory scale. This highlights the importance of the control of the feedstock in recycling and that the source of material is crucial for the quality of the recyclates.

With regard to the manufacturing procedure, the feasibility of reducing the processing time from 25 minutes to 7 minutes was demonstrated. However, a further reduction to a 1 – 2 minute total cycle time, when applying a non-isothermal process type, failed. The material solidified before impregnation and moulding. Further investigation of the process window of different MAPP types needs to be considered. A lack in polymer flow could be

prevented with an adjustment of the polymer type (e.g. change in molecular weight, melt flow index) in further studies.

When comparing the obtained experimental data and applied estimate, as indicated in Figure 5-9, the reference value for the IM56L/MA5 composite material obtained from ELGCF is located in the middle of the gathered data. The in-house production by project partner ELGCF obtained similar mechanical performance for IM56L/MAPP composites tested in the transverse direction as experimental methods showed with cross-ply for the IM56R/MA3 sample. A further increase in composite stiffness and strength properties for IM56R/MA3 could be expected when repeating and extending the experimental study and testing the material in a transverse direction, but this was paused due to time constraints. However, this effect has been shown previously, as stated in Section 4.1.4 where the fibre orientation was investigated. Overall, this shows the potential of applying similar isothermal conditions in terms of moulding temperature level but a shorter cycle time to obtain similar or improved composite performance. Therefore, the material tested in the experimental study conducted at WMG could outperform the material processed in a larger process window (110 minute) at ELGCF. This shows an improvement in ELGCF's process and productivity in terms of composite quality and enhanced business practice.

5.2 FIBRE TREATMENT

The previous studies highlighted possibilities to modify the polymer to enhance the interfacial properties on a micro level with the overall target to boost the final composite performance. An additional area of study was the surface treatment that recycled fibres require to chemically alter their fibre surface before interacting with the target matrix system. The research work described in the following involved administering an alternative fibre enhancement: selective reductive electrochemical treatment using different types of diazonium salt (depending on the organic group attached) for possible electrochemical treatment(grafting). Bélanger & Pinson describe this as an organic layer bonded covalently on the carbon fibre surface [222]. This was expected to modify the rCF surface, following from previous work achieved at Carbon Nexus, Deakin University [137], who have seen successful grafts using pristine carbon fibre. The validation of successful grafting with pure and commingled thermoplastic textile mats applicable for thermoplastic composites was the primary aim and scope of this work.

5.2.1 OVERVIEW

This experimental work focused on administering an alternative, yet selective, reductive electrochemical treatment using diazonium salts. Focusing on sustainable methods applicable for the nonwoven textiles, a solvent and water-based treatment were the focus of this work. Both methods follow the same principle, which is schematically shown in Figure 5-10, where functional groups (R) are attached to the carbon fibre surface, which reacts as the electrode.

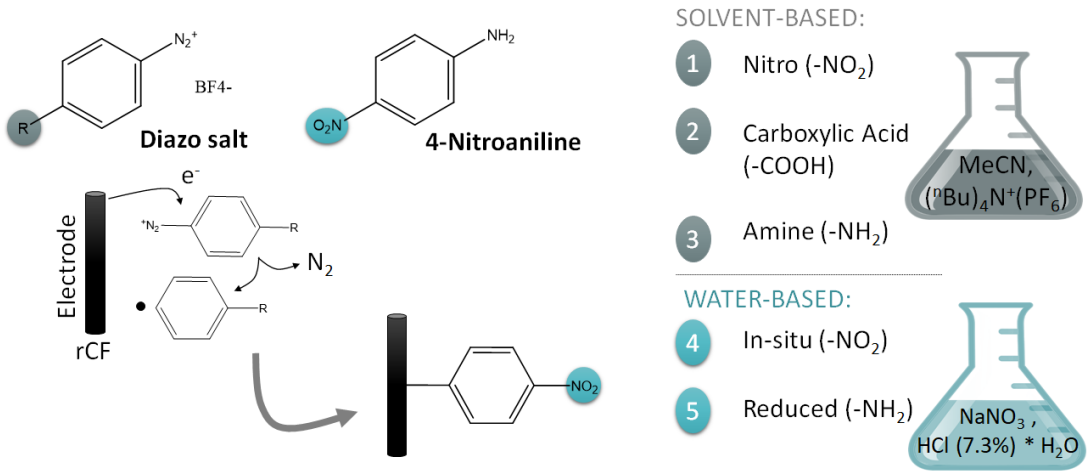

Figure 5-10: Schematic of solvent-based and water-based electrochemical treatment including applied chemicals.

In the case of the solvent-based method, commercially available types of diazonium salt were used with acetonitrile (CH_3CN) functioning as solvent and tetra-n-butylammonium hexafluorophosphate ($TBAPF_6$) as electrolyte, which would be rinsed out after the reaction took place. The second application method was carried out using water. The in-situ reaction describes a synthesis and formation of the diazonium salt spontaneously in aqueous solution. In this case, a hydrogen chloride solution (HCl 7.3%) acts as the electrolyte and sodium nitrate ($NaNO_3$) as the catalyst, with simultaneous grafting of nitro groups to the carbon fibre taking place during an electrochemical treatment [223]. The goal is the same as for the other method, to form a functionalised grafted layer on the carbon fibre surface which enables improved adhesion to the target matrix system. For this purpose an aromatic amine, here 4-nitroaniline, as base is mixed with sodium nitrate, as catalyst, to initiate the reaction in the solution [222]. Mixing and stirring are set to 60 minutes to give time to fully dissolve in the solution. Overall, this is an example of a more sustainable alternative to standard research procedures, but also shows similarity to the procedure applied at industrial scale to save cost and the amount and number of chemicals used.

Regarding the diversity of the waste origin and the sensitivity of the characterisation methods, it was decided that IM56L fibres (derived from cured laminates, pyrolysed) from the same batch (Figure 5-11) would be used for treatment and evaluation. By doing so, it was possible at this stage to get a relative comparison with the same fibre conditions focusing on the difference in treatment only.

Figure 5-11: Sample selection for SFTS and XPS analysis , showing different pieces (a, b) of recycled woven textiles of fibre type IM56L from the same batch, as well as the gathered fibre tows (~12 cm) for treatment and following evaluation (c).

Nonwoven mats of different thickness (100, 200 and 400 gsm) were treated to study the efficiency of the treatment correlated to the size of the sample. Nonwoven mats of 100 gsm and 200 gsm are more intensely covered by functional groups than 400 gsm mats in an identical treatment time and treatment solution volume. Fibre probes were taken from the inside outside of the mats to obtain an average result.

A project plan was developed with set milestones throughout the evaluation of the effect of the applied methods (Figure 5-12). The milestones highlight intermediate steps of the project, which were targeted to prove the concept prior to further investigations. The validation of a successful grafting method was given by the cyclic voltammogram scan monitoring the electron transfer. After optimising the grafting method, the treatment was applied to fibre tows and textiles for further characterisation.

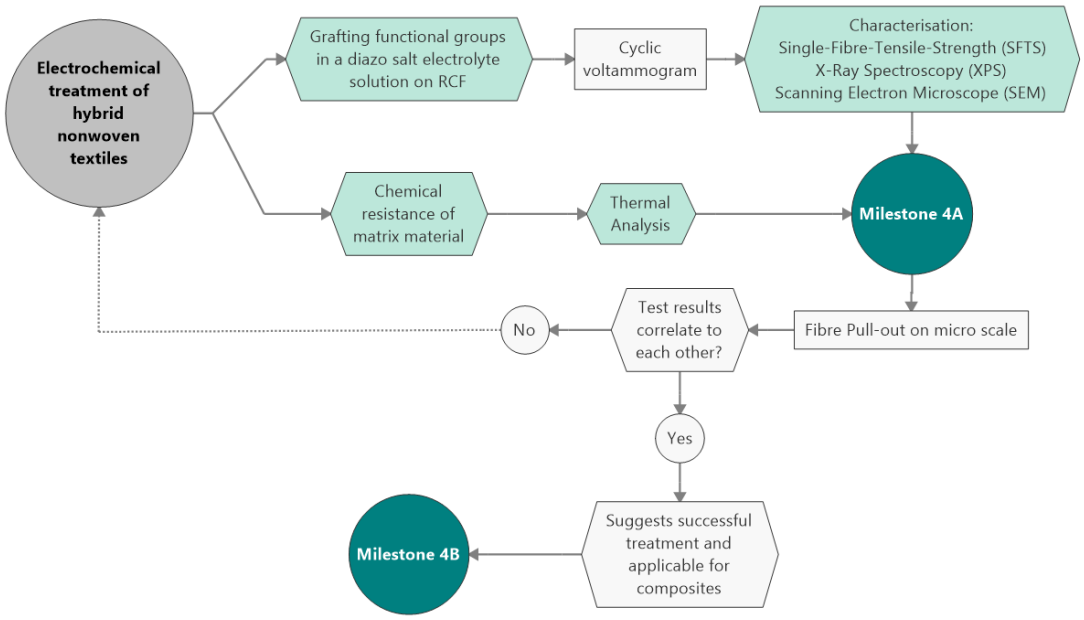

Figure 5-12: Schematic approach for the project to be conducted using several characterisation methods to prove the success of the treatment.

The marked milestones highlight the intermediate steps of the research, which were targeted to prove the concept prior to further investigations. The following process steps were conducted to evaluate the material:

- Check the chemical resistance of polymer filaments in proposed electrolytes and other solvents
- SFTS testing on FAVIMAT machine before/after treatment (Comparison to standard commercial treatment & untreated fibres)
- XPS & SEM characterisation of the single fibres before/ after treatment (Swinburne University)
- Treatment of textiles, and evaluating continuity and efficiency of the treatment

In addition to this, the interfacial adhesion was examined as follows:

- Evaluating the Interfacial Shear Strength (IFSS) with the SFPT in MAPP on micro-scale
- Evaluating possible upscale to composite tests to evaluate resulting tensile strength/ fracture toughness performance on macro-scale.

The fibres in mat or tow form were functionalised applying either cyclic voltammetry (CV) or chronoamperometry (CA). CV describes a method to apply a specific potential window, e.g. -1 V to 1 V, with a set scan rate where the current is measured simultaneously. Whereas, CA applies a constant potential over time. Both methods are common practice for electrochemical grafting on a laboratory scale [37, 43, 44]. To begin with a standard method, CV scans from a positive to negative voltage range ensure maximum surface grafting coverage, where the potential window and scan rate can be modified. The treatment time can be further reduced by applying CA scans and promises industrial applicability due to the negative voltage range, compared to continuous change with CV scans. No matter which method is applied, each treatment is followed by a CV scan for monitoring purposes and to evaluate the efficiency of the reduction process and to allow prompt action to be taken when reduction occurs. The bottom diagram (Figure 5-13) shows an example of an expected reduction of nitro species onto the surface.

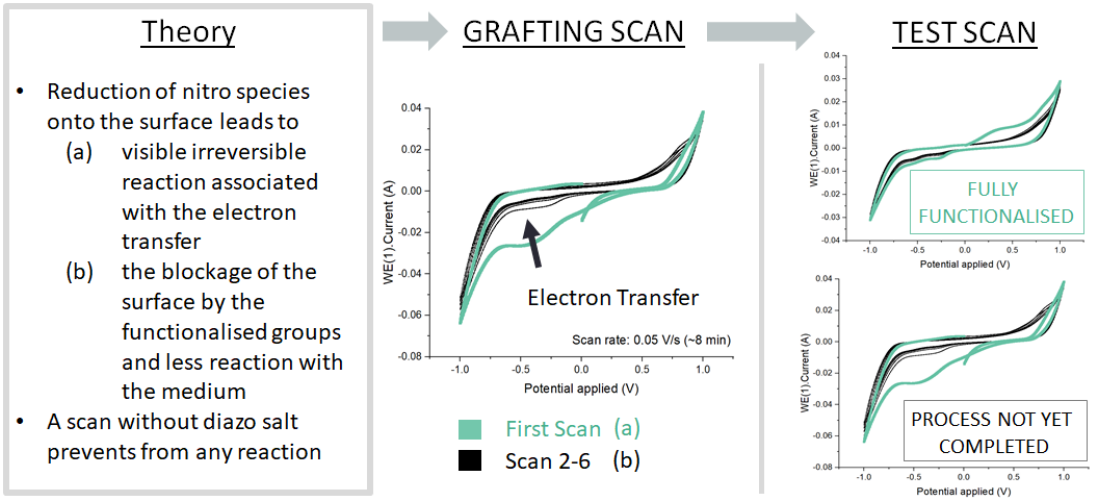

Figure 5-13: Reduction visible in cyclic voltammetry scan with irreversible reaction associated with the electron transfer (modified from [224]**).**

The visible irreversible reaction is associated with the electron transfer, which is followed by a blockage of the surface by the functionalised groups [224]. This means that less or insufficient reaction with the medium and scans without diazo salt prevent from any reaction, as shown in Figure 5-13.

5.2.2 OPTIMISED ELECTRO-CHEMICAL GRAFTING METHOD

In this set of experiments, aprotic electrochemical grafting, reduction and in situ reactions were conducted. The nitro samples were treated first as these represent the simplest method of the whole set of treatment variations.

Initially, a standard method of CV was applied to 100 gsm IM56L nonwoven textile stripes in a solvent-based solution using nitrobenzene diazonium salt. Starting with a potential window from -1V-1V, a scan rate 0.1 V/s and two treatments of 6 scans, the total treatment time lasted 4.5 minutes (Figure 5-14 left). The blue marked line indicates the first scan, which shows the current prior to reduction of nitro species onto the surface. The following 5 scans, marked black, show the reduction and following blockage of the surface by functionalised groups and reduced reaction to the medium after saturation.

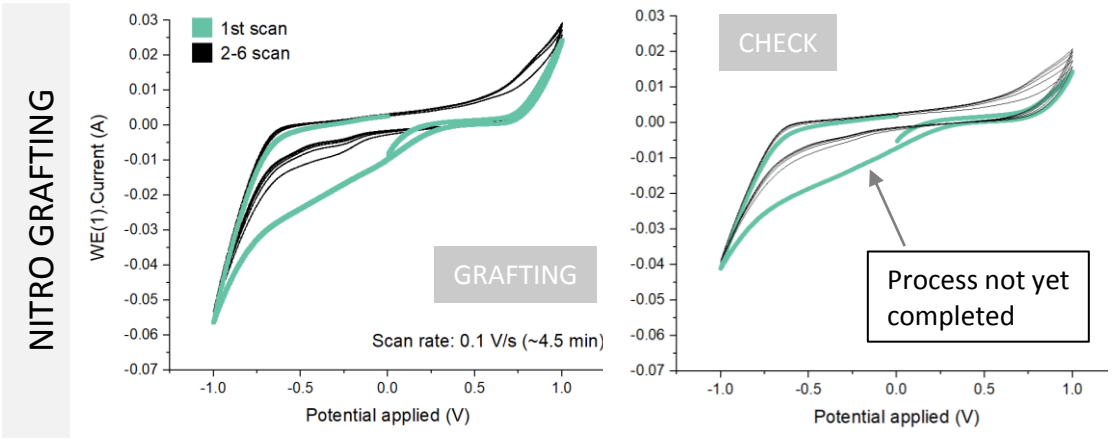

Figure 5-14: Cyclic voltammogram with process window from -1 V to 1 V (scan rate 0.1 V/s) of nitro functionalised fibres for actual electro grafting (left) and the subsequent check (right).

The goal was to fully functionalise the fibre surface, and show high current response, which indicates an efficient treatment. The actual grafting is followed by a “check scan”, another CV scan, to see if reduction still takes place (Figure 5-14 right). An ongoing reduction can be detected after 4.5 min, as there is still a shift from the first scan (green) to the second scan (marked black) indicating continuing electron transfer. Another sample was exposed to the same potential (-1 V, + 1V) but with a reduced scan rate of 0.05 V/s to give more time for the actual functionalisation, which simultaneously results in lower current response (Figure 5-15).

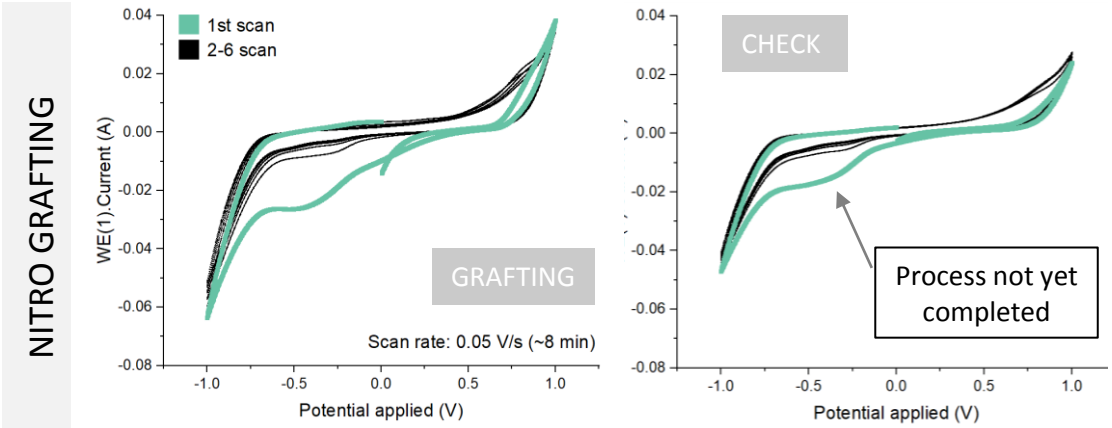

Figure 5-15: Cyclic voltammogram with process window from -1 V to 1 V (scan rate 0.05 V/s) of nitro functionalised fibres for actual electro grafting (left) and the subsequent check (right).

The treatment time has doubled to approximately 8 min. Looking at the graphs below demonstrates that the sample treated for 8 min was also not yet fully functionalised because the reduction process was still taking place as visible in the CV check scan (Figure 5-15 right).

The time taken for completion is too long for an industrial process and as such, alternative treatments were investigated. CA describes a more radical treatment without relaxation which is more industrially applicable due to the single voltage range (only negative type applied). For the following experiment, a negative voltage of -1 V was applied for 3 min (Figure 5-16 left). The CA type of treatment produces a successfully completed reaction where the treatment time is lower than the previous attempts (Figure 5-16 right).

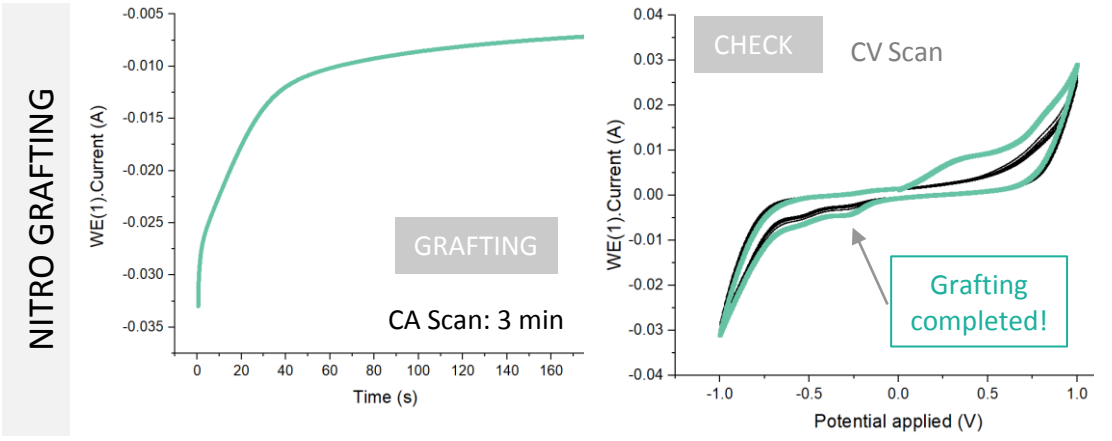

Figure 5-16: Chronoamperogram for treatment at -1 V (3 min) of nitro functionalised fibres for the actual electro grafting (left) and the subsequent cyclic voltammogram as check (right).

The process was chosen for the following experiments and was not shorten further to ensure also thicker nonwoven mats will be efficiently treated. This could be further optimised in later studies to reduce the actual treatment time. The optimised treatment method of 3 min

at a constant potential of -1 V was applied for all 5 different grafting types, except the reduction, which was treated at -1.5 V. The corresponding cyclic voltammogram for the nitro, carboxylic acid and the reduced amine groups are shown in [Appendix D]. A completed reaction was detectable with CV after optimised electrochemical treatment for all treatments, apart from the nitro grafting in water, where the process was not fully completed.

5.2.3 EFFECT OF GRAFTING ON FIBRE SURFACE CHARACTERISTIC

5.2.3.1 PHYSICAL FIBRE PROPERTIES

The SFTS of unmodified and modified fibres using the solvent-based grafting method was evaluated and the results are summarised in Figure 5-17. The control fibre IM56L (pyrolysed and chopped dry fibre) was compared to the modified fibres with carboxylic acid groups (IM56L/Carboxyl), nitro groups (IM56L/nitro) and amine groups (IM56L/amine), which were tested for their strength and modulus properties to see the potential impact of the treatment.

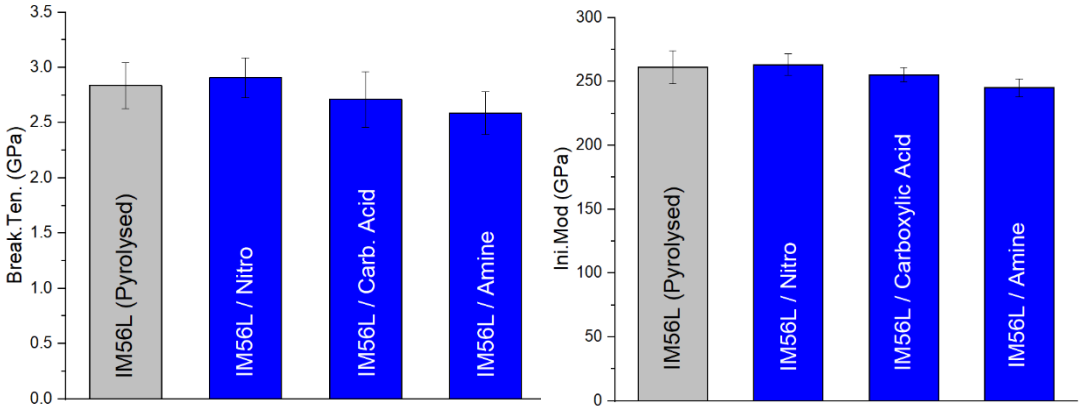

Figure 5-17: Measured single fibre tensile strength & modulus of control and modified (solvent-based) fibres.

The electrochemical treatment seemed to affect the fibre strength and stiffness, where a slight decrease in fibre properties was visible for carboxyl and amine treatment types compared to its control. A statistical verification was conducted in OriginPro using the T-test where a 95 % confidence level was allowed ($P > 0.05$). If the p-value drops below 0.05, it can be concluded that with 95% confidence there are significant differences between the measured fibre properties. However, all three tests indicated that there is no significant evidence for a difference in treatment effects on the tensile strength with p-values of 0.6833, 0.5367 and 0.2038 for the nitro, carboxylic acid and amine functionalisation respectively. A similar outcome was evaluated for the tensile modulus of control 1 and the treated fibres where all calculated p-values exceeded 0.05.

Additionally, a Weibull analysis was performed to further understand the effect of fibre treatment on failure and fibre characteristic. Researchers showed that more aggressive treatment procedures of carbon fibre, e.g. thermal [4] or chemical treatment [110], led to a weaker and less homogeneous fibre characteristic correlating to a higher variability in fibre strength and consequent drop in Weibull modulus. Figure 5-18 (left) shows the Weibull plots for the control and treated fibres, with its probability of failure at varied level of fibre tensile strength (Figure 5-18, right).

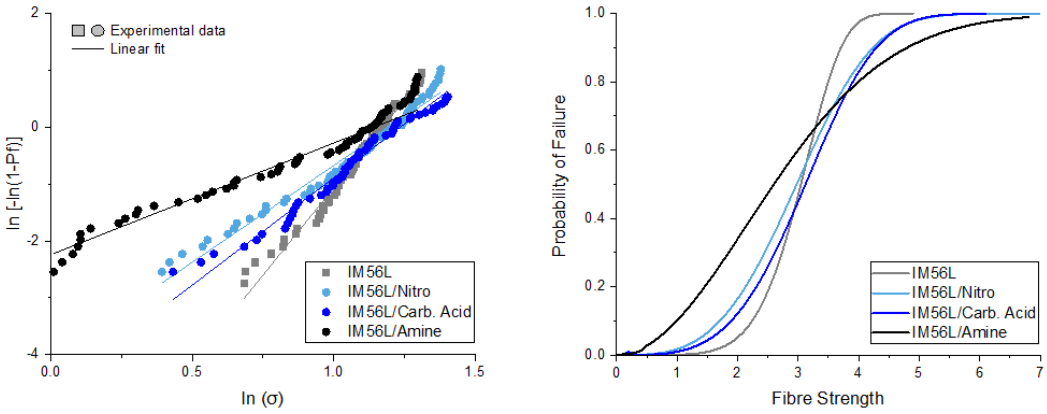

Figure 5-18: Weibull analysis on control (IM56L) and treated fibre samples (IM56L/Nitro, IM56L/Carb. Acid, IM56L/Amine).

The determined values from the Weibull analysis are summarised in Table 5-4. All of the plots showed good agreement between experimental data points and its fitted curve plot with coefficients of determination (R^2) close to 100 % and similar level of experimentally obtained strength values and the scale parameter.

Table 5-4: Determined values of Weibull Analysis compared to experimental data.

Fibre Type	Weibull Modulus (m)	Tensile Strength (GPa)	Scale Parameter (σ_0)	R^2 (%)	Fibre Diameter [µm]
Control: IM56L	6.14	2.84 ± 0.21	3.23	98.4	4.63 ± 0.33
IM56L/Nitro	3.39	2.91 ± 0.18	4.04	97.3	4.17 ± 0.14
IM56L/Carb. Acid	3.77	2.71 ± 0.24	3.44	97.8	4.48 ± 0.06
IM56L/Amine	2.18	2.59 ± 0.19	2.95	96.0	4.50 ± 0.07

The Weibull moduli divers comparing the control fibre and the electrochemically treated fibres. The highest Weibull modules was reported for the control fibre and drops with treatment. The reduction relative to the control fibre could be a sign of decreased fibre homogeneity caused by the treatment or the nature of the material source. Furthermore, a

different distribution in fibre strengths in regard to the probability of failure and a smaller gradient could be related to a change in failure mechanism and a subsequent reduction in performance for the treated fibre types. However, in this case, the overall small drop in tensile strength performance and statistically insignificant change ($P > 0.05$) does not confirm the observation and were therefore neglected at that stage.

The small shrinkage in diameter (Table 5-19) from control fibre IM56L to the modified ones, which were electrochemically treated, can be attributed to a possible char removal. The fibres were also analysed optically to confirm no damage to the fibres during the treatment (Figure 5-19). The IM56L fibres are visibly covered by remaining char. The treated fibres show less coverage where the carbon fibre surface is visible occasionally.

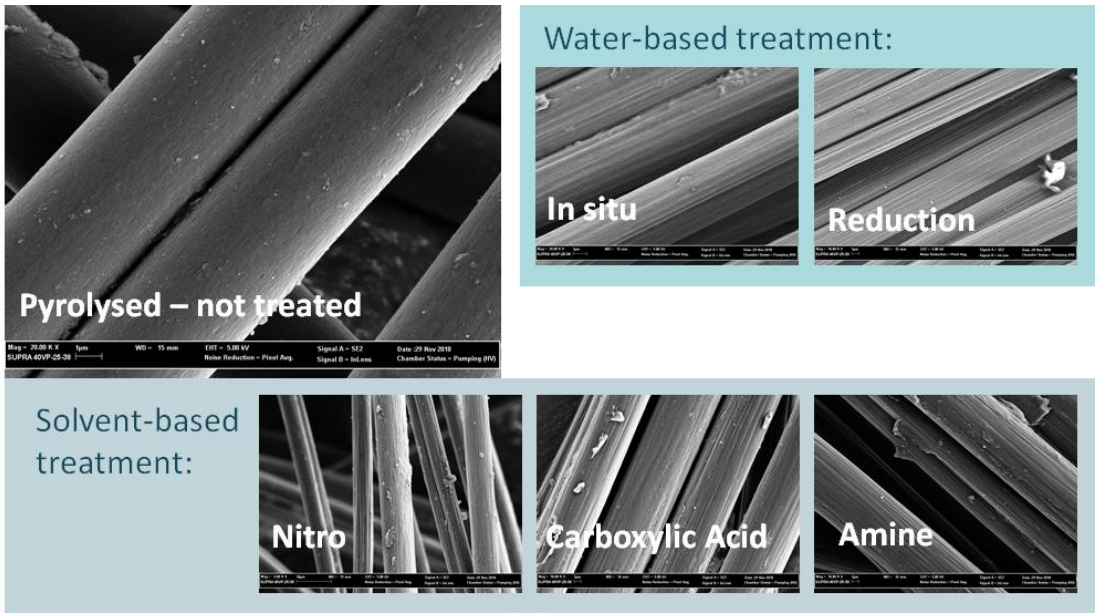

Figure 5-19: SEM images of control and treated fibre samples.

The dust which is visible in the above images can be explained by electrostatic loading suggesting a more polar surface due to successful functionalisation. In general, no visible damage to the fibres is observable as a result of the treatment.

5.2.3.2 FIBRE SURFACE CHEMISTRY

Fibre surface chemistry is one of the main characterisation methods used to analyse efficient grafting. With the control fibres, detection of oxygen containing groups such as alcohol or ether groups (C-O), carbonyl groups (C=O) and carboxylic acid groups (COOH) are assumed to be detected on the fibre surface due to sizing or residual char. However, the evaluation of the modified fibres shows a presence of nitro groups (NO_2), further carboxylic acid (COOH) and amine groups (NH_2), which simultaneously results in a general increase of nitrogen and oxygen. The elemental composition values of the rCF surfaces are summarised in Table 5-5.

Table 5-5: Elemental composition of survey spectra of all samples.

Fibre Type	C (at. %)	O (at. %)	N (at. %)	O/C ratio	N/C ratio
Control: IM56L	83.68 ± 0.59	11.23 ± 0.62	1.09 ± 0.18	0.13	0.01
IM56L/Nitro	92.12 ± 0.57	6.53 ± 0.33	0.68 ± 0.39	0.07	0.01
IM56L/Carb. Acid	92.71 ± 0.44	5.72 ± 0.37	0.79 ± 0.00	0.06	0.01
IM56L/Amine	91.39 ± 2.31	6.27 ± 0.72	1.00 ± 0.22	0.07	0.01
IM56L/Nitro (In situ)	81.91 ± 1.37	11.33 ± 0.36	0.39 ± 0.14	0.14	0.01
IM56L/Amine	83.31 ± 0.63	11.90 ± 0.41	1.21 ± 0.47	0.14	0.02

The char covered IM56L fibre contained a higher amount of oxygen and nitrogen content than the samples treated in a solvent-based electrolyte solution. For all three treatment types increased oxygen was expected as well as an increase in nitrogen specifically for nitro and amine groups. The low number of elements detected in all the samples was unexpected and questions the success of the applied grafting method. Whereas the amount of approximately 1 at% of nitrogen detected in all the samples is very small and less than assumed, the change in oxygen content is rather surprising. The amount of oxygen detected drops from 11.26 at% (Control: IM56L) to 6.53 at%, 5.72 at% and 6.27 at% for nitro, carboxylic acid and amine functionalised fibres respectively, treated in acetonitrile and $TBAPF_6$ solution using a compact diazonium salt (Figure 5-20). The reduction in oxygen present on the surfaces of the fibres could be due to a cleaning of the fibres when applying the solvent-based method, which may lead to the removal of the char from the fibre surfaces.

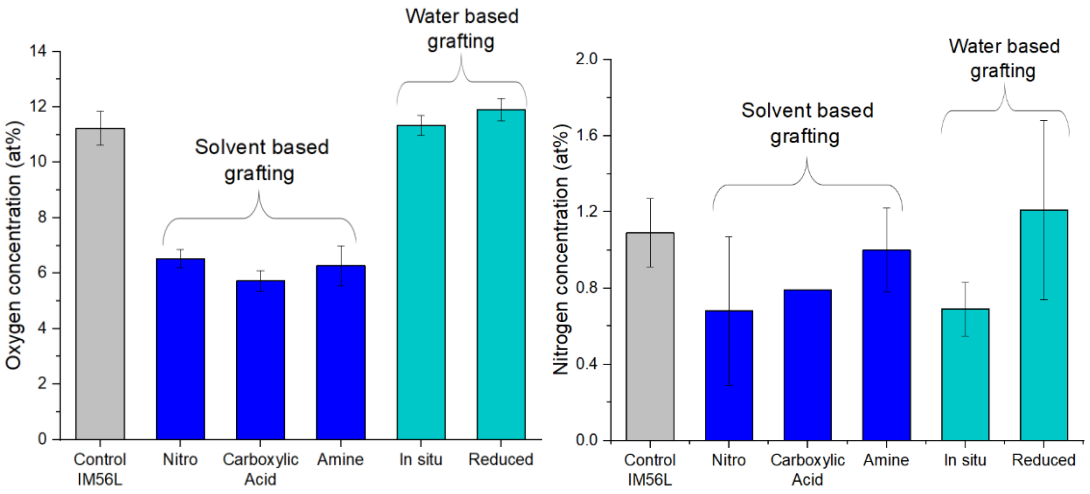

Figure 5-20: Oxygen and nitrogen concentration of the control and treated fibres (evaluated from the survey spectra).

However, a similar or slightly high oxygen content of 11.33 at% and 11.90 at% was detected on the fibres treated in the water-based electrolyte solution compared to the control, where an in-situ reaction and the subsequent reduction was applied. Reviewing the reported grafting scans, they showed an ongoing reaction for the in-situ treatment but a fully completed one for the subsequent reduction when applying the 3-minute CA scan. Comparing these to the results from microscopic analysis and the obtained chemical composition, less visible char and similar levels of oxygen and nitrogen elements suggest a successful but not yet optimised grafting in aqueous solution. The following evaluation of different functional groups being present on the rCF surfaces was confirmed (Figure 5-21).

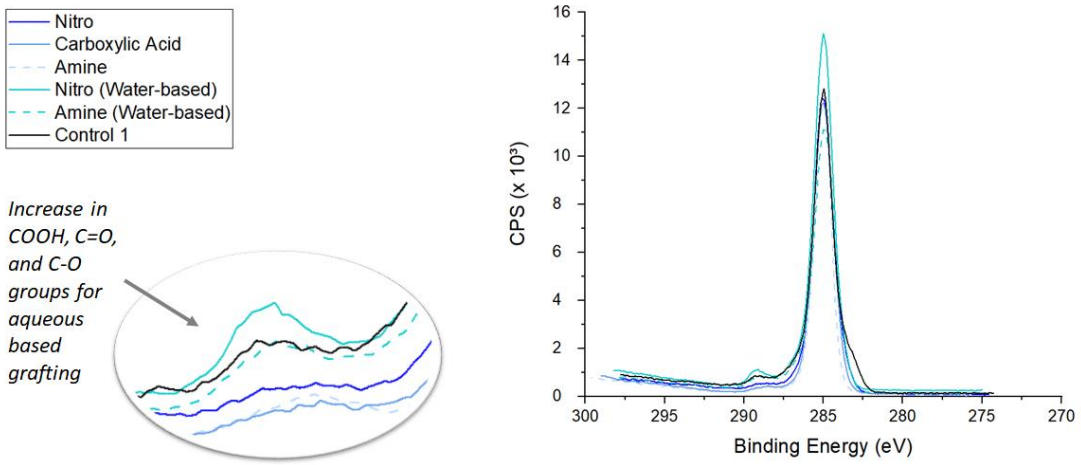

Figure 5-21: Carbon related peak intensity as observed by XPS for control and treated fibres highlighting the presence of COOH, C-O and C=O groups.

The higher peak visible in the C1s scan, suggesting an increase in functional groups for the water-based treatment, can be related to a slighter higher amount of carboxylic acid groups detected on the IM56L/Nitro (in situ) surface. The amount of carbonyl and ether groups are lower than to the control (Table 5-6).

Table 5-6: Detailed breakdown of evaluated functional groups detected on the fibres by XPS with performed curve-fitting on the C1s spectra.

Fibre Type	C-C, C-H [at.%]	C-O [%]	C=O [%]	COOH [%]
Control: IM56L	86.33 ± 0.17	8.01 ± 0.99	3.02 ± 1.36	2.64 ± 0.21
IM56L/Nitro	92.03 ± 3.70	5.13 ± 3.57	2.01 ± 0.25	0.83 ± 0.40
IM56L/Carb. Acid	94.39 ± 1.57	3.28 ± 1.9	1.02 ± 0.70	1.32 ± 0.32
IM56L/Amine	94.29 ± 0.73	2.94 ± 0.59	1.28 ± 0.10	1.48 ± 0.19
IM56L/Nitro (In situ)	90.25 ± 1.40	4.33 ± 1.51	2.31 ± 0.08	3.12 ± 0.07
IM56L/Amine	89.73 ± 1.39	5.20 ± 1.23	2.54 ± 0.86	2.53 ± 0.27

With the data obtained, it cannot be confirmed if the grafting led to a covalently bond of functional groups to the surface which is a stronger bond than, for example, char detached to the fibre surface by Van-der-Waals forces. Nevertheless, the total amount of functional groups detected on fibres treated in water was in general higher than compared to the solvent-based treatment. Therefore, future treatment of rCF should focus on water-based alternatives to achieve a higher success rate and to reduce the environmental impact of production.

The functionality of the char can be traced back to the previous sizing or matrix system the fibre was in contact with before the recycling process took place. It can be noted, that the IM56L control fibre showed similar surface chemistry to the water-based treated fibres. A fibre pull-out test could reveal a possible difference in the bonding type.

5.2.3.3 INTERFACIAL TESTING

A test procedure using the SFPT method was performed by the Leibniz Institute Dresden. Unfortunately, only control fibres (selection of ELGCF feedstock) were able to be mounted in the test device (Table 5-7). A slightly higher IFSS was obtained for the pyrolysed feedstocks IM56L and IM56R which may be due to the char on the fibres containing a higher amount of carbonyl (C=O) and ester (COOH) groups detected before by the XPS. This shows that pyrolysed fibres have better adhesion to the MAPP matrix than sized fibres.

Table 5-7: Overview of interfacial parameters obtained for control fibres.

ELGCF Fibre	Type	τ_{app} [N/mm²]	τ_{d} [N/mm²]	W_{debond} [mN*mm]	$W_{pullout}$ [mN*mm]
IM56L	Pyrolysed from laminate	5.3 ± 1.9	22.9 ± 8.4	0.4 ± 0.4	7.1 ± 3.0
IM56R	Pyrolysed from chopped tow	5.2 ± 2.1	26.8 ± 12.6	0.2 ± 0.2	5.7 ± 3.1
IM56D	Sized (sizing 1)	4.9 ± 1.9	22.6 ± 11.1	0.2 ± 0.2	6.9 ± 3.8
SM45D	Sized (sizing 2)	4.3 ± 1.9	16.8 ± 7.4	0.3 ± 0.2	8.0 ± 3.2

All modified fibres, which were treated by electrochemical grafting were very brittle and difficult to handle, which resulted in fibre breakage before the testing could be carried out. The failed testing could have happened for various reasons:

- Firstly, the test institute recorded fibre diameter as low as 2.5 µm. It is not clear if the shrinkage in fibre diameter was caused by the treatment, which was previously excluded from the SFTS test.

- Secondly, the origin of the fibre, a classified waste product, could be a reason for the deviation in fibre properties. The fibres derived from laminates and were pyrolysed. A difference in matrix thickness (referring to component thickness) could lead to a different level of pyrolysis treatment which could result in infrequently over-pyrolysed feedstock, which was not selected for testing.

The contact angle method was applied to determine any potential trends towards an increase or decrease in interfacial bonding when applying the selected grafting methods. All feedstock from ELGCF was tested to compare the interfacial tension and work of adhesion with the obtained pull-out results, before the modified fibres were analysed. Table 5-8 summarises the experimental data. The highest surface energy and polarity was measured for the SM45D feedstock, which also recorded the highest interfacial tension. This means that this fibre is less favourable to bond to the MAPP matrix system than the others (IM56D, IM56R, IM56L).

Table 5-8: Surface energies γ of all fibres, including the polarity X^p, interfacial tension σ_{SL} and adhesion energy ψ_{SL} given in relation to MAPP (5 wt% MA, Chapter 5.1.1).

Fibre Type	Surface Energy γ [mJ/m²]	Polarity X^p [%]	Interfacial Tension σ_{SL} [mN/m]	Adhesion Energy ψ_{SL} [mJ/m²]
SM45D	74.95 ± 0.16	53.34 ± 0.23	38.52 ± 0.43	65.10 ± 1.52
IM56D	54.35 ± 3.36	21.04 ± 0.51	11.94 ± 1.50	71.09 ± 1.21
IM56R	50.81 ± 2.19	5.17 ± 0.84	4.71 ± 1.07	74.77 ± 0.99
IM56L	52.06 ± 0.37	13.12 ± 0.42	7.99 ± 0.49	72.73 ± 0.54
IM56L/Nitro	50.93 ± 0.43	0.25 ± 0.01	3.19 ± 0.60	78.09 ± 0.85
IM56L/Amine	55.06 ± 3.30	7.73 ± 0.29	6.84 ± 0.72	81.35 ± 0.77
IM56L/Nitro (In situ)	50.74 ± 0.17	0.12 ± 0.03	3.13 ± 0.17	77.78 ± 0.81
IM56L/Amine	51.21 ± 0.50	0.80 ± 0.02	3.39 ± 0.56	78.62 ± 1.02

The interfacial tension is less when the compatibility between the fibre and the matrix is given, which seemed to be more the case for the pyrolysed feedstock, then the sized fibres. The interfacial tension of the ELGCF feedstock is indirectly related to the interfacial bonding characteristic obtained by the fibre pull-out test, which agrees with other findings in the literature [127].

These findings support the following conclusions:

- The amine grafting on solvent-base is not recommended for this fibre-matrix system, as it did not produce any improvement in the interfacial characteristic.
- The contact angle method applied to fibre bundles did not produce definitive results for the characterisation of pyrolysed feedstock. Here, a pull-out test method may be more appropriate to understand the change in surface characteristic and should be confirmed with other methods if applicable. However, relating these results to the chemical analysis from the previous section, water-based treatment methods are recommended for future investigations as a trend in improved interfacial characteristic is given.
- The interfacial tension level was lowest for the nitro grafting in solvents and water, as well as the amine grafting in water. Even though the decrease is very small, interfacial bonding could be improved by optimising these methods in future research studies.

Nevertheless, due to the unsuccessful interfacial testing, it could not be determined if a possible difference in the bonding type of untreated and treated fibres was present. Therefore, no final conclusion can be made about the effect and potential success of the grafting method to increase the interfacial adhesion due to covalent bonded functional groups (potentially) present on the surface.

The brittleness observed in some materials may be a result of the recycling process and further electrochemical treatment. When fibres are used to manufacture composites, a considerable degradation in fibre length occurs, as reported before by Oliveux *et al.* [5], which results in low composite properties. A similar phenomenon was also detected when working with MAPP (Chapter 5.1.3). In this case, over-pyrolysed IM56L feedstock showed low composite properties due to low fibre quality. For that reason, IM56L is unsuitable for further treatment and handling at the time of research. Future research could focus on its characteristic sensitivity and how to efficiently repurpose fibres derived from laminates.

An alternative would be a change in characterisation method of the micro bond test. However, the challenges in handling the fibres would also create difficulties for that method because the preparation task is similar to that which is carried out for the pull-out method.

5.2.4 SUITABLE FOR COMPOSITE MANUFACTURING?

A significant part of this project was to determine whether the grafting method is suitable for composite manufacturing and was investigated as follows:

- Polymer fibres were tested separately for its chemical resistance to applied solvents (≤ 48h)
- Nonwovens of different textile weight (100 gsm, 200 gsm, 400 gsm) were tested for the level of consistent treatment throughout the web (through-thickness) by XPS
- Treated nonwoven textiles were processed on laboratory scale under the same conditions as the benchmark (Milestone 1, Section 4.1.6) and moulded to composites

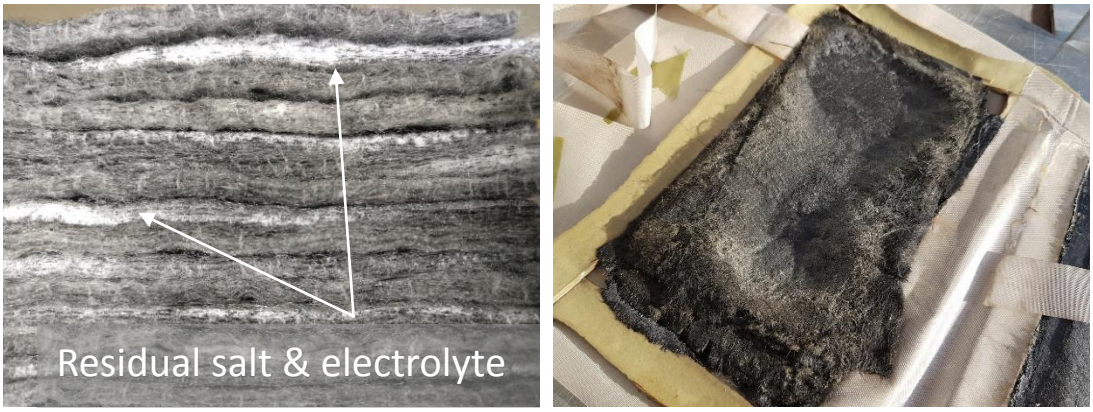

Figure 5-22: Treated nonwoven mats showed an excess of residual electrolytes (left) which caused drop in process window and subsequent degradation of the material when applying the not adjusted processing conditions (right).

The polymers were shown to be chemically resistant to all used solvents, which is an advantage for future composite applications. The chemical analysis (here XPS) of the textiles of different thickness showed successful treatment through the thickness. Additionally, a drop in the level of treatment with increased textile thickness could be positively excluded. However, the treatment required a high amount of solvents (4.4 l/m^2 ethanol and 2.2 l/m^2 water) to wash out the salts introduced into the textiles in the first instance.

With the applied rinsing method, no composites could be successfully produced for the final testing. The processing was stopped after smoke formation at standard processing conditions which was traced back to the salt still present in the textiles (Figure 5-22). Subsequent thermal analysis (TGA, DSC) detected no difference in melting or crystallisation temperature, but a significant drop in the onset of degradation from an initial unmodified system at 207 ± 7.1 °C to 178 ± 2.5 °C and 175 ± 1.2 °C for IM56L-nitro/MAPP and IM56L-amine/MAPP textiles respectively.

5.2.5 MILESTONE 4: NOVEL TREATMENT WITH DRAWBACKS

The fibre treatment, reductive electrochemical treatment using diazonium salts, offers a way forward for combining electrochemical treatments on recycled carbon fibres. Initial results were promising and consistent with data achieved prior acquisitions for pristine fibres (benchmark) when looking at the physical and chemical properties of unmodified and modified fibres. No damage to the recycled feedstock was visible nor measurable for all electrochemical treatments. Furthermore, the polymers showed suitability for electrochemical treatment applied to commingled nonwovens. High functionality detected in char-covered recycled carbon feedstock shows suitability for interface formation with the target matrix system.

In the first stage of this research an efficient treatment was demonstrated for a variety of textile thicknesses, assessed by chemical analysis. The fibres prepared using the water-based treatment gave the same elemental composition as the unmodified control. However, it cannot be clearly concluded if the final functional groups are bonded covalently on the fibres as targeted. The only evidence is given from the CV and CA scans, which showed no full completion for the nitro grafting, but did so for amine grafting in the aqueous solution. The final interfacial characterisation applying the SFPT was not possible (due to weak fibre quality) to prove the principle. Alternatively, the contact angle method shows a trend towards a slight improvement in interfacial properties applying the water-based method. However, further characterisation requires further investigations before a final conclusion can be drawn. Difficulties in handling the feedstock could be a result of the combination of the pyrolysis and electrochemical treatment. Low mechanical composite properties in regard to tensile strength and modulus of IM56L/PP and IM56L/MAPP composites were reported before in Section 5.1. It is suggested that IM56R fibres are more robust and therefore this fibre type is recommended for further treatment trials.

In contrast, a completed reaction during the electrochemical treatment was detectable with CV after optimised electrochemical grafting for solvent-based treatments, but the XPS does not confirm an increase in nitrogen or oxygen content. This may be because the solvents removed the char and cleaned the fibres instead of functionalising them. Therefore, water-based treatments are suggested for further investigations. Overall, a successful applied fibre treatment cannot be confirmed, and the project was paused at that stage. However, a newly established collaboration between ELGCF and Deakin University will further focus on this topic to see if there are sustainable ways to re-functionalise rCF feedstock.

6 REVIEW OF RESEARCH CONTRIBUTION

This section shows how this research has supported the development of knowledge and expertise within the industrial sponsor and its performance in a competitive market environment. This EngD project improved the understanding of commingled nonwoven material at ELGCF, in terms of the handling and processing, and was able to demonstrate that the material can compete in a competitive market when processed on a pilot scale using specific recyclate material.

The project was conducted at WMG's research facilities and investigated a variety of thermoplastic process types to determine the best possible re-utilisation of recycled carbon fibres (supplied by ELGCF in the form of nonwoven textiles) in semi-structured components. Preliminary process studies, on a laboratory scale press, assessed the effect of temperature, time and pressure on the processability of the nonwoven textiles under isothermal conditions (where the material is heated and cooled in the tool before de-moulding). This process simulates the technique of the industrial sponsor (static pressing). The research focussed initially on one feedstock type, SM45D, which represented mechanically chopped dry fibre and was the main rCF type at the time of research. At the end of this study, the optimised manufacturing conditions, on a laboratory scale, were applied to other recyclate types to understand the effect on material behaviour and impact on composite quality. At this stage of research, it was observed that the fibre type had a significant effect on the composite performance though which could not be specified. The isothermal processing conditions indicated limitations in cycle time, which was previously identified as the main barrier towards more viable thermoplastic composite applications using rCF and its ability to be processed on an industrial scale.

Therefore, a comprehensive study comparing different types of thermoforming was developed to understand how the textiles could be processed and utilised with a significant reduction in cycle time, whilst retaining their mechanical properties. In particular, a rapid-isothermal process was compared to the conventional non-isothermal (stamp forming) process on a pilot scale. The assessment of composite quality was related to the level of impregnation, mechanical performance and level of porosity of the manufactured composite panels. A balance between achieving the fastest process for industry applications, while simultaneously demonstrating optimum performance in tested mechanical characteristic was targeted.

The rapid-isothermal process showed relatively good processability for all fibre types, but the stamping process was only suitable for the SM45D/PP commingled mats. The results showed that the level of processability was directly dependent on the fibre type and its surface characteristic, which in the case of SM45D feedstock is the type of sizing. Although a variety in FWF was detected throughout processing both within and between batches, a significant effect on the processability was eliminated by comparing the textile's loft factor and impregnation level of the manufactured panels.

However, a direct link between the processability of the textiles and the surface characteristic of the recyclate was detected when analysing the fibre's surface energy and level of wettability. The lack of wetting was a problem in certain material combinations, though this is also a common problem in thermoplastic composites using virgin feedstock. Currently, common practice in industry is for virgin carbon fibres, which have a chemically inert surface, are subsequently treated with adjusted sizing to tune the surface characteristic (chemically and physically) to match with the target matrix system. When using rCF the original surface treatment applied to the virgin fibres is unknown; this research project identified the original treatment as essential information.

The isothermal process used as a benchmark at laboratory scale was later outperformed, in terms of cycle time, by the rapid-isothermal process (on a pilot scale). A reduction in cycle time from 27 minutes to 13-18 minutes (under 10 minutes moulding time) was possible and mechanical properties on industry-standard between all applied process methods were demonstrated. The enhanced performance was related to a more suitable process window adjusted to each recyclate type, where shorter cycle times can eliminate any polymer degradation. A difference in pressure application and distribution on larger tooling led to optimum impregnation levels. In terms of part-cost, the maximum number of parts processable per annum is directly relating to the achievable cycle time. Within this context, the isothermal process showed limitations in application above the level of low volume production, whereas the rapid-isothermal process and stamping process both demonstrated suitability for mid-volume production and simultaneously lower final part-cost.

The following conclusions were made for different mechanically and thermally recycled feedstock based on the results from the experimental work:

- The application of the stamping process to the SM45D/PP commingled textiles to manufacture good quality composites, in regard to low or no measured porosity, within 60 s exceeded expectations. The process demonstrated the shortest cycle times compared to previously reported process studies of rCF composites. The processability can be related to the polar and therefore hydrophilic surface characteristic of the fibre, giving the polymer the best ability to flow throughout the textile when moulding
- IM56R/PP type textile was only suitable for longer process types in terms of cycle time and obtained the highest strength values when processed rapid- isothermally. It was assumed that the level of polymer flow was hindered due to mechanical friction due to roughness from residual char, which could be resolved with a higher applied pressure. However, due to machine breakage, further evaluation was paused.
- The application of IM56D/PP was evaluated, and a high porosity level demonstrated the unsuitability and incompatibility of this material mix for thermoplastic applications. The material might be most suited for thermoset applications.

Further investigations evaluated the matrix modification and its effect on the interfacial adhesion between the matrix and fibre, and the subsequent enhancement of the composite quality. Applying MAPP to enhance composite properties, regarding tensile strength and stiffness, was proven to clearly outperform the neat PP based material, on a laboratory scale. A process upscale to pilot scale processing was applicable, however, low recyclate quality hindered a detailed analysis for a final conclusion in terms of suitability. Future studies should investigate the material performance with better recyclate quality, as the cycle time was able to be reduced, and hence there are possible environmental and economic benefits. In this case, MAPP as a matrix system would provide a sustainable counterpart to the recycled fibre reinforcement. In addition, the applied electrochemical fibre treatment showed progress in this area of research, where electrochemical grafting is applied to pyrolysed feedstock. A newly established partnership with Deakin University will conduct further research in that field.

7 CONCLUSION

7.1 KEY INNOVATIONS

A summary of the key innovations is highlighted in the following more in detail.

- Innovation 1: Established material knowledge

The research study investigated the processability of the commingled rCF/PP and rCF/MAPP nonwovens and a comprehensive dataset was established. Using a systematic approach and applying advanced process types generated new knowledge about the material performance, demonstrated the processability and improved the understanding of how to handle the material. This project also extended the range of ELGCF`s research focus. As a result, the commingled nonwoven textile material is now part of ELGCF`s product range (Figure 7-1).

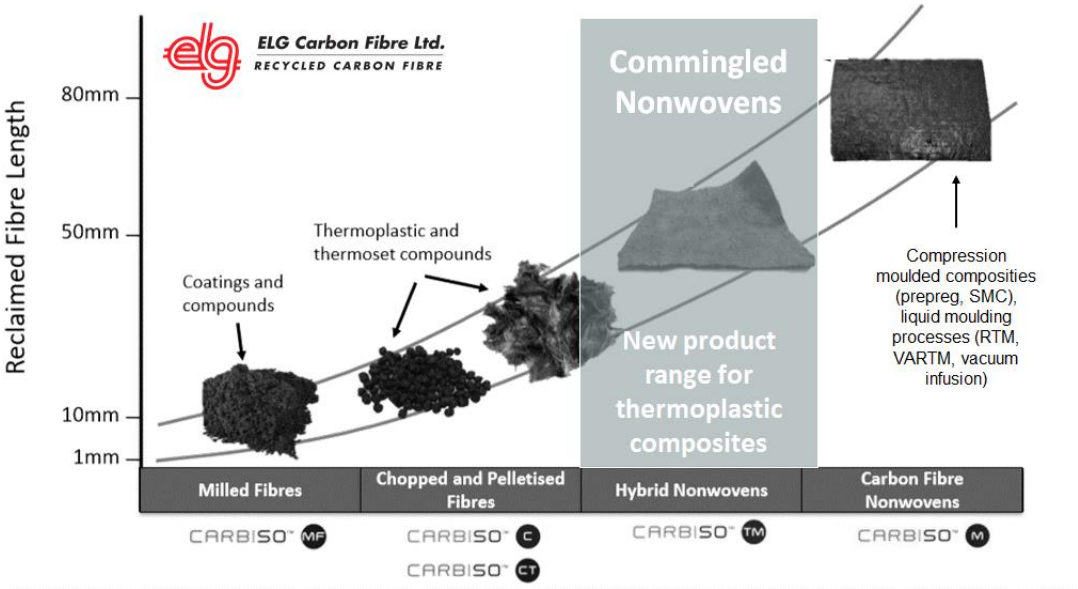

Figure 7-1: Product range of recycled carbon fibres in the form of milled or chopped fibres, as well as nonwoven textiles as semi-finished products developed by ELGCF Ltd [6].

The obtained material characteristics were benchmarked, and it was demonstrated that the PP and MAPP based textiles can compete in a competitive market environment. The work presented in this entire portfolio has been continuously exchanged with the project partner and has served ELGCF as an essential database.

- Innovation 2: Proven suitability for mid-volume production

The aim of this project was to valorise recycled carbon fibres and show potential applications of thermoplastic composites for thermoforming processing. Lengthy processing times were identified as the main barrier for upscaling thermoplastic composite manufacturing using rCF feedstock. Experimental work on a laboratory scale led to an optimised cycle time of 27 minutes when processing the material isothermally. In a subsequent study, the rapid-isothermal, stamping and conventional non-isothermal approaches were investigated on a pilot-scale. This enabled a more advanced case study of processing conditions in contrast to the previous isothermal process on a laboratory scale. Demonstrating possible cycle times in a range of 18 to 1 minute(s) for thermoforming commingled nonwoven textiles in this research project relied on state-of-the-art production applied to new material and showcased the efficient repurposing of recycled carbon fibres. The cycle times achieved for different material are highlighted in Figure 7-2. The reduction in cycle time, from 110 minutes (in-house production at ELGCF as the starting point of the project) to 1 minute, improved the productivity and highlighted a potential enhancement of the business practice of ELGCF. The advanced processing conditions were then tailored to a range of ELGCF`s recycled material.

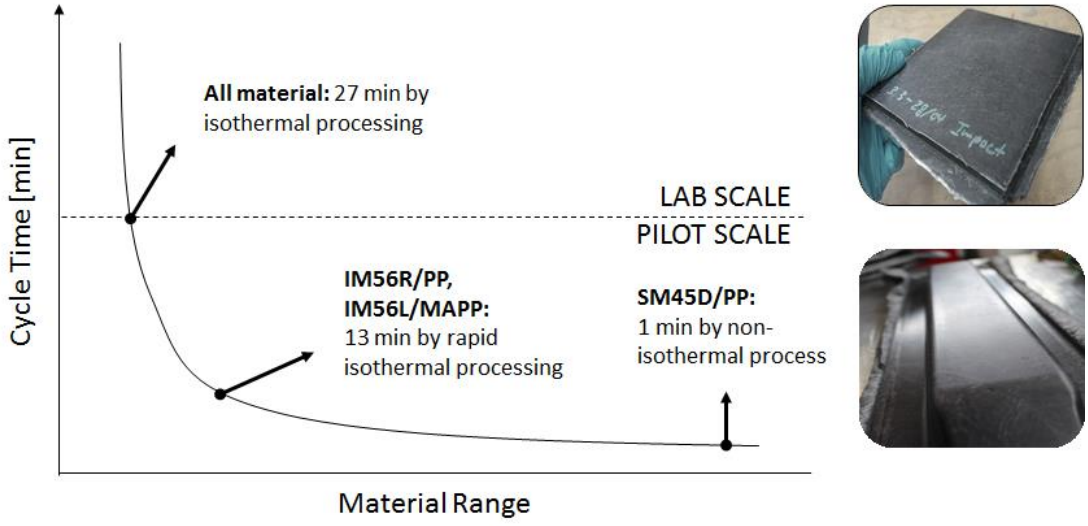

Figure 7-2: Schematic of processing level highlighting the reduction in cycle time when moving from laboratory to pilot scale and involved limitation of application for only certain material.

The significant reduction in cycle time reduces the overall energy consumption. The carbon footprint of composite manufacturing can be drastically reduced with the use of rCF feedstock instead of virgin material. Applying efficient processing methods showed potential for further reductions in CO_2 emissions.

Shorter cycle times also had a significant impact on the production costs of the composite. Applying stamping procedures as well as rapid-isothermal conditions enabled and proved the possibility of a growth in volume production from low-volume (part number limited to 3876 per annum using one press), to mid-volume of up to 30 000 parts per annum. An increase in part volume led to a subsequent reduction in price from £ 35.86 to £20.56 applying the rapid isothermal process, and £ 8.01 applying the stamping method. In particular, the stamping procedure achieved a cost reduction of 78 % and demonstrated an economically and ecologically viable process. The achievement gained great interest from delegates and companies at international conferences, where part of the work was presented [227], [228].

In terms of the composite properties, it can be concluded that the properties can outperform GF applications in terms of composite strength and stiffness, and weight. In addition, the technical benchmarking proved better properties specifically in terms of strength compared to aluminium and thereby demonstrates the suitability of the composites in the field of semi-structural applications, for example in the automotive industry.

- ## Innovation 3: Identified significant process factors

The comprehensive process study revealed crucial information about the feedstock type-dependent processing and identified significant factors for processing the new material. For example, with regard to the recyclate characteristic versus impregnation level, a direct dependency on the surface characteristic of rCF on the level of processability was detected which underlines the need for establishing single-origin recycling routes. The impregnation level with the target matrix system during moulding and interfacial bonding was evaluated. The base material assessment on micro-scale directly correlated to the composite performance on a macro-scale. For first estimates on the interfacial fibre-matrix characteristic, the contact angle method is recommended. Using this method, the surface energy was successfully determined on fibre bundles. This quick, simple and cost-efficient technique enables fibre testing for rapidly changing customer and consumer demands. The surface energy characterisation supported the differentiation of waste types due to a varied surface characteristic e.g. sizing and char covered fibres.

The wetting behaviour of the target matrix system and related impregnation level when moulding the textiles, were able to be assessed. Using the surface energy values, the interfacial tension and work of adhesion was calculated, where an indirect correlation to the interfacial bonding affinity was shown. After the in-depth constituent analysis, the

processing window was reduced by the thermal analysis of the applied polymers simulating process conditions on standard TGA test equipment. In combination with the microscopic analyses and the identification of the melt level of the polymer throughout the textile when moulding, the optimum process window (using adaptable and repeatable methods) was established.

By applying the sequence of characterisation methods, the most suitable processing methods can be identified for different recyclate and polymer types. The classification of rCF and the process type allocation is recommended in order to utilise the feedstock, guarantee sufficient interfacial properties and ensure the best possible mechanical composite properties. Extra care needs to be taken when doing material or process studies on different material batches. The material properties can vary significantly, and which makes an evaluation of the effect of potential material or process modifications challenging.

- Innovation 4: Modified matrix was moved from lab to pilot scale

To overcome insufficient interfacial adhesion between rCF and the thermoplastic polymers, chemical modification of the interfacial characteristic was undertaken. MAPP was successfully deployed to enhance material performance when processed isothermally on a laboratory scale. A wide range of characterisation methods was used to identify the optimum MA amount and the effect of MA on the interfacial characteristic and subsequent composite performance. The most improved composite properties were obtained with a material fraction of 5wt% of MA, which also produces a cost-efficient material combination compared to its control. An enhancement of 44% in composite strength and 19% in stiffness were obtained with a simultaneous increase in cost of 9% compared to conventional IM56R/PP commingled textiles. Furthermore, processing of the modified matrix material was moved from laboratory to pilot scale applying the rapid-isothermal process which demonstrated process times of 7 min, a significant reduction compared to ELGCF`s in-house trials as mentioned earlier. However, it should be noted that when processing this material on a pilot scale with new feedstock the composite performance did not demonstrate the same effect of advance composite properties. Due to a difference in recycling procedure the material performance was adversely affected, which highlights another key conclusion - the control of feedstock in recycling by the recycler is crucial.

7.2 FUTURE RESEARCH OPPORTUNITIES

This study identified opportunities for further research:

- Additional adjusted material processing required when processing modified matrix material (MAPP stamping did not work due to frozen state after pre-heating) or nonwovens including treated fibres (requires further work on the effect of treatment on process conditions, e.g. possible degradation of the material)
- Further information is required for the recycler so that they can produce recyclates which match specific matrix systems. For example, would be useful to implement an intelligent waste tracking system in the development stage of new products
- It might be possible to adapt the developed test procedures to other systems, e.g. polyamide
- Life Cycle Assessment (LCA) could be used to support the decision making and to check how the applied processing techniques relate to their environmental impact

7.2.1 SUPPLEMENT MATERIAL CHARACTERISATION & PROJECT TRIALS

Future work should focus on additional interfacial tests to identify the simplest and most accurate quantitative analysis. It would also be beneficial to establish if there is a direct correlation between the estimated and evaluated interfacial adhesion properties and the macro-mechanical performance, obtained in the sub-project, when considering the fibre treatment.

A now discontinued fibre treatment process consumed a high volume of solvents which made it unsuitable for upscaling, as shown in this project on a laboratory scale. The process now in place is more efficient and shows potential suitability for this upscaling. When it comes to upscale of the system, the water-based solution can be prepared continuously alongside the actual grafting process. This continuous process has the advantage of short treatment cycles, which require an efficient functionalising process to achieve the target treatment quality [229]. Combining the continuous carding process on a high production rate with additional continuous water-based surface treatment would lead to an efficient production cycle for high volume production.

High void content was observed for materials IM56R/PP and IM56D/PP which related to pyrolysed and mechanical recycled feedstock respectively. Further processing trials should be performed utilising higher pressure to understand the effect on mechanical properties.

This project focused on PP and MAPP based composites, which represent a cost-efficient polymer for semi-structural properties. However, more advanced polymers such as PA6 and PPS could outperform the tested material combinations, and cost-benefit needs to be evaluated with regards to possible low cycle times. A change in cooling rates when using the same tooling should be expected when working on higher moulding temperatures which help to produce shorter cycle times. Extra care should be taken when processing PA6, which need to be pre-dried prior to processing. The same procedure developed for the processing conditions using PP and MAPP can be applied for new material combinations. The polymer process window can be limited by the thermal analysis:

- DSC running in nitrogen atmosphere gives information about the lowest process temperature of the polymer ($\geq T_m + 20$ K) and de-moulding temperature ($\geq T_C$)
- Maximum process temperature sits below the determined onset of degradation temperature, which must be evaluated in air atmosphere using TGA.

Possible fibre breakage could be one limitation of other process conditions but could not be eliminated at this stage.

7.2.2 MATERIAL SELECTION & TREATMENT

Several processes and material modifications were presented in this research project. Nevertheless, the material composition and level of impact vary with the type of recyclate quality and manufacturing type and further investigation needs to be done before adopting the knowledge to a new composite system. Whereas this project focused on the most cost-effective thermoplastic polymer types, further studies should investigate more advanced versions and analyse their cost-benefits. In addition, more sustainably derived polymers e.g. PA11, PA12 and PA66 bio-based polymers, could lead to lower energy consumption during the process, due to lower processing temperatures, and could decrease the carbon footprint when produced and utilised efficiently [230], [231]. However, a life cycle assessment should be considered to determine the environmental and economic impact of all stages of the product's life [1], [232]–[234].

Where the matrix modification has proven the approach taken from literature, the fibre treatment was a novel approach, applying electrochemical grafting on rCF feedstock. The aim was to develop an industrially applicable method for pyrolysed feedstock where functional groups can be covalently bonded to the fibre surface. The success of this treatment could not be confirmed in this research project. The research on the fibre treatment was very interesting and also suggests that there are substantial obstacles to

overcome to successfully re-functionalise recyclates. In general, water-based treatments show great potential for upscale to pilot and industrial level but require further investigation to produce optimum treatments. The experimental study was paused at this stage, but a newly established collaboration between ELGCF and Deakin University will develop this topic.

7.2.3 CLOSING THE LOOP

This study has not investigated the potential to re-recycle manufactured parts by re-moulding or shredding and subsequent moulding. This should be considered in further work, also simulating several loops and evaluating the change in performance with each process cycle.

The main focus of this study was how to overcome the challenge of working with rCF feedstock with unknown surface characteristics and the unknown effect of these on processability. Both were successfully resolved through the research. However, smart waste tracking [235] or material codes [236] could potentially support the recycler to match new processes effectively to the incoming (and increasing amount of) carbon fibre by-products or EoL parts and to define the best re-use route for each recyclate type. This could be integrated into the design new parts by using design for disassembly [237] or design for second life strategies [238], or when classifying as a waste product at the manufacturer or user end-stage. The main challenge here is to protect the intellectual property rights of the manufacturer whilst giving the recycler enough information for further processing. A more transparent system would facilitate a step closer to a circular economy, where waste is completely out designed and the material flow is a closed loop [239].

8 REFERENCES

[1] F. Meng, J. McKechnie, and S. J. Pickering, “An assessment of financial viability of recycled carbon fibre in automotive applications,” *Compos. Part A Appl. Sci. Manuf.*, vol. 109, pp. 207–220, Jun. 2018.

[2] A. Stevenson, “Recycling carbon fibre: State of the art and future developments,” *International Textile Conference Dresden April 2016*. Dresden, 2016.

[3] R. A. Witik, R. Teuscher, V. Michaud, C. Ludwig, and J. A. E. Månson, “Carbon fibre reinforced composite waste: An environmental assessment of recycling, energy recovery and landfilling,” *Compos. Part A Appl. Sci. Manuf.*, vol. 49, pp. 89–99, 2013.

[4] S. Pimenta and S. T. Pinho, “The effect of recycling on the mechanical response of carbon fibres and their composites,” *Compos. Struct.*, vol. 94, pp. 3669–3684, 2012.

[5] G. Oliveux, L. O. Dandy, and G. A. Leeke, “Current Status of Recycling of Fibre Reinforced Polymers: Review of Technologies, Reuse and Resulting Properties,” *Prog. Mater. Sci.*, vol. 72, pp. 61–99, 2015.

[6] “ELG Carbon Fibre Ltd.” [Online]. Available: http://www.elgcf.com/. [Accessed: 19-Aug-2016].

[7] R. Brooks, “Forming technology for thermoplastic composites,” in *Composites Forming Technologies*, Woodhead Publishing Limited, 2007, pp. 256–276.

[8] P. Mitschang and K. Hildebrandt, “Polymer and composite moulding technologies for automotive applications,” in *Advanced Materials in Automotive Engineering*, 2012, pp. 210–229.

[9] M. Selezneva *et al.*, “Compression moulding of Discontinous fibre carbon / PEEK composites: Study of mechanical properties,” in *SAMPE 2012*, 2012, pp. 1–10.

[10] F. Gnädinger, P. Middendorf, and B. L. Fox, “Interfacial shear strength studies of experimental carbon fibres, novel thermosetting polyurethane and epoxy matrices and bespoke sizing agents,” *Compos. Sci. Technol.*, vol. 133, pp. 104–110, 2016.

[11] M. Szpieg, M. Wysocki, and L. Asp, “Mechanical performance and modelling of a fully recycled modified CF/PP composite,” *J. Compos. Mater.*, vol. 46, no. 12, pp. 1503–1517, 2012.

[12] K. H. Wong, D. Syed Mohammed, S. J. Pickering, and R. Brooks, “Effect of coupling

agents on reinforcing potential of recycled carbon fibre for polypropylene composite," *Compos. Sci. Technol.*, vol. 72, no. 7, pp. 835–844, 2012.

[13] H.-I. Kim, W. Han, W.-K. Choi, S.-J. Park, K.-H. An, and B.-J. Kim, "Effects of maleic anhydride content on mechanical properties of carbon fibers-reinforced maleic anhydride-grafted-poly-propylene matrix composites," *Carbon Lett.*, vol. 20, pp. 39–46, 2016.

[14] M. Harris, "Carbon fibre: the wonder material with a dirty secret," *The Guardian*, 22-Mar-2017.

[15] M. Sauer, "Carbon Composites e.V.: Composites Market Report 2019," 2019.

[16] D. Hull and T. W. Clyne, *An Introduction to Composite Materials*, 2nd ed. Cambridge University Press, 1996.

[17] S. Rana and R. Fangueiro, *Fibrous and Textile Materials for Composite Applications*. SpringerNature, 2016.

[18] J. Summerscales, "Composites Design and Manufacture," *Plymouth University teaching support materials*, 2018. [Online]. Available: https://www.fose1.plymouth.ac.uk/sme/MATS347/MATS347A2 E-G-nu.htm#fodf. [Accessed: 06-Jun-2019].

[19] V. Goodship, *Management, recycling and reuse of waste composites*. .

[20] S. Thomas, K. Joseph, S. K. Malhotra, K. Goda, and M. S. Sreekala, *Polymer Composites - vol. 1: Macro- and Microcomposites*. Wiley-VCH Verlag GmbH & Co. KGaA, 2012.

[21] JEC Composites, "Sound fundamentals and fierce competition," *JEC Magazine - Wind energy No. 108*, pp. 38–39, 2016.

[22] MHI Vestas Offshore Wind A/S, "V164-8.0 MW® breaks world record for wind energy production | MHI Vestas Offshore," *MHI Vestas Offshore Wind*, 2014. [Online]. Available: https://mhivestasoffshore.com/v164-8-0-mw-breaks-world-record-for-wind-energy-production/. [Accessed: 12-Aug-2020].

[23] A. Wilson, "Developments in nonwovens for automotive textiles," in *Advances in Technical Nonwovens*, 2016, pp. 257–271.

[24] A. Kelly and C. Zweben, "Fiber Reinforcements and General Theory of Composites," in *Comprehensive Composite Materials*, Elsevier, 2000.

[25] Black Country Bullet, "ELG Carbon Fibre Ltd.," 2016. [Online]. Available:

https://blackcountrybullet.co.uk/company/671/e-l-g-carbon-fibre-limited.html. [Accessed: 15-Nov-2016].

[26] "Teijin Carbon – What is Carbon Fiber?," *Teijin Carbon Europe GmbH*, 2019. [Online]. Available: https://www.teijincarbon.com/products/what-is-carbon-fiber?r=1. [Accessed: 19-Oct-2019].

[27] C. Cherif, *Textile Materials for Lightweight Constructions*. Berlin: Springer, 2016.

[28] Y. S. Song, J. R. Youn, and T. G. Gutowski, "Life cycle energy analysis of fiber-reinforced composites," *Compos. Part A Appl. Sci. Manuf.*, vol. 40, no. 8, pp. 1257–1265, 2009.

[29] R. Thevenin, "Composites in Airbus," in *Global Investor Forum*, 2008, pp. 1–26.

[30] J. Hale, "Boeing Aeromagazine (04/2006) - Boeing 787 from the Ground Up," 2006.

[31] D. Brosius, "Composites recycling — no more excuses," *CompositesWorld*, 2019. [Online]. Available: https://www.compositesworld.com/blog/post/composites-recycling-no-more-excuses. [Accessed: 19-Oct-2019].

[32] A. Hohmann and B. Schwab, "MAI ENVIRO. Vorstudie zur Lebenszyklusanalyse mit ökobilanzieller Bewertung relevanter Fertigungsprozessketten für CFK-Strukturen," 2015.

[33] E. Witten, M. Thomas, and K. Michael, "Composites Market Report 2015," *Ind. Verstärkte Kunstoffe*, pp. 1–44, 2015.

[34] B. Zhang, "United Airlines CEO explains why the Boeing 747 will soon go away," *Business Insider*, 2017. [Online]. Available: https://www.businessinsider.com/united-airlines-ceo-why-boeing-747-jumbo-jet-retire-2017-3?r=US&IR=T. [Accessed: 23-Oct-2019].

[35] D. Sander, "Emirates Begins Initial Airbus A380 Retirement," *Airways Magazine*, 2019. [Online]. Available: https://airwaysmag.com/airlines/emirates-begins-initial-airbus-a380-retirement/. [Accessed: 23-Oct-2019].

[36] European Commission, "A380 takes first passengers," *EU Publications Office*, 2006. [Online]. Available: https://cordis.europa.eu/article/rcn/26285/en. [Accessed: 23-Oct-2019].

[37] J. Davidson and R. Price, "Recycling Carbon Fibre (European Patent 2152487B1)," 2011.

[38] W. Carberry, "Aerospace's role in the development of the recycled carbon fibre

supply chain.," in *Carbon Fibre Recycling and Reuse. IntertechPira*, 2009.

[39] AIRBUS S.A.S., "Airbus forecasts need for over 39,000 new aircraft in the next 20 years - Commercial Aircraft - Airbus," *Airbus Media*, 2019. [Online]. Available: https://www.airbus.com/newsroom/press-releases/en/2019/09/airbus-forecasts-need-for-over-39000-new-aircraft-in-the-next-20-years.html. [Accessed: 06-Oct-2019].

[40] K. Wood, "Carbon fiber reclamation : Going commercial," pp. 1–6, 2010.

[41] S. Pimenta and S. T. Pinho, "Recycling carbon fibre reinforced polymers for structural applications: Technology review and market outlook," *Waste Manag.*, vol. 31, no. 2, pp. 378–392, 2011.

[42] European Commisssion, "Waste Framework Directive (2008/98/EC)," 2008.

[43] J. Rybicka, A. Tiwari, and G. A. Leeke, "Technology readiness level assessment of composites recycling technologies," *J. Clean. Prod.*, vol. 112, 2016.

[44] European Commisssion, "Council Directive on the Landfill and Waste (1999/31/EC)," 1999.

[45] European Commission, "Council Directive on the Incineration of Waste (2000/76/EC)," *Off. J. Eur.*, no. 2000, 2000.

[46] N. A. Shuaib and P. T. Mativenga, "Energy Intensity and Quality of Recyclate in Composite Recycling," pp. 1–11, 2015.

[47] European Commission, "Council Directive on End-of Life Vehicles (2000/53/EC)," *Off. J. Eur.*, 1999.

[48] S. Job, G. Leeke, P. T. Mativenga, G. Oliveux, S. J. Pickering, and N. A. Shuaib, "COMPOSITES RECYCLING : Where are we now ?," p. 11, 2016.

[49] S. Halliwell, "Best Practice Guide - End of Life Options for Composite Waste," 2006.

[50] J. Hopewell, R. Dvorak, and E. Kosior, "Plastics Recycling: Challenges and Opportunities," *Philos. Trans. R. Soc. B Biol. Sci.*, vol. 364, no. 1526, pp. 2115–2126, 2009.

[51] S. J. Pickering, "Recycling technologies for thermoset composite materials-current status," *Compos. Part A Appl. Sci. Manuf.*, vol. 37, no. 8, pp. 1206–1215, 2006.

[52] R. Cherrington *et al.*, "Producer responsibility: Defining the incentive for recycling

composite wind turbine blades in Europe," *Energy Policy*, vol. 47, pp. 13–21, 2012.

[53] Y. Yang, R. Boom, B. Irion, D. J. Van Heerden, P. Kuiper, and H. De Wit, "Recycling of composite materials," *Chem. Eng. Process. Process Intensif.*, vol. 51, no. 2012, pp. 53–68, 2012.

[54] A. Conroy, S. Halliwell, and T. Reynolds, "Composite recycling in the construction industry," *Compos. Part A Appl. Sci. Manuf.*, vol. 37, no. 8, pp. 1216–1222, 2006.

[55] L. O. Meyer, K. Schulte, and E. Grove-Nielsen, "CFRP-Recycling Following a Pyrolysis Route: Process Optimization and Potentials," *J. Compos. Mater.*, vol. 43, no. 9, pp. 1121–1132, 2009.

[56] E. H. Lester, S. Kingman, K. H. Wong, C. Rudd, S. J. Pickering, and N. Hilal, "Microwave heating as a means for carbon fibre recovery from polymer composites: A technical feasibility study," *Mater. Res. Bull.*, vol. 39, no. 10, pp. 1549–1556, 2004.

[57] S. J. Pickering, R. M. Kelly, J. R. Kennerley, C. D. Rudd, and N. J. Fenwick, "Fluidized-bed process for the recovery of glass fibres from scrap thermoset composites," *Compos. Sci. Technol.*, vol. 60, no. 4, pp. 509–523, 2000.

[58] S. J. Pickering *et al.*, "Developments in the Fluidised Bed Process for Fibre Recovery From Thermoset Composites," in *2nd Annual Composites and Advanced Materials Expo, (CAMX)*, 2015.

[59] S. Job, "Composite Recycling - Summary of recent research and development," 2010.

[60] K. H. Wong, T. A. Turner, and S. J. Pickering, "Challenges in Developing Nylon Composites Commingled With Discontinuous Recycled Carbon Fibre," in *ECCM16 - European Conference on Composite Materials*, 2014, no. June.

[61] M. H. Akonda, C. A. Lawrence, and B. M. Weager, "Recycled carbon fibre-reinforced polypropylene thermoplastic composites," *Compos. Part A Appl. Sci. Manuf.*, vol. 43, no. 1, pp. 79–86, 2012.

[62] G. Jiang and S. J. Pickering, "Structure-property relationship of recycled carbon fibres revealed by pyrolysis recycling process," *J. Mater. Sci.*, vol. 51, no. 4, pp. 1949–1958, 2016.

[63] M. Roux, N. Eguémann, C. Dransfeld, F. Thiébaud, and D. Perreux, "Thermoplastic carbon fibre-reinforced polymer recycling with electrodynamical fragmentation," *J. Thermoplast. Compos. Mater.*, vol. 30, no. 3, pp. 381–403, 2017.

[64] Y. Bai, Z. Wang, and L. Feng, “Chemical recycling of carbon fibers reinforced epoxy resin composites in oxygen in supercritical water,” *Mater. Des.*, vol. 31, no. 2, pp. 999–1002, 2010.

[65] J. Li, P.-L. Xu, Y.-K. Zhu, J.-P. Ding, L.-X. Xue, and Y.-Z. Wang, “A promising strategy for chemical recycling of carbon fiber/thermoset composites: self-accelerating decomposition in a mild oxidative system,” *Green Chem.*, vol. 14, no. 12, p. 3260, 2012.

[66] J. R. Hyde, E. H. Lester, S. Kingman, S. J. Pickering, and K. H. Wong, “Supercritical propanol, a possible route to composite carbon fibre recovery: A viability study,” *Compos. Part A*, vol. 37, no. 11, pp. 2171–2175, 2006.

[67] K. Ogi, T. Nishikawa, Y. Okano, and I. Taketa, “Mechanical properties of ABS resin reinforced with recycled CFRP,” *Adv. Compos. Mater. Off. J. Japan Soc. Compos. Mater.*, vol. 16, no. 2, pp. 181–194, 2007.

[68] J. Takahashi, N. Matsutsuka, and T. Okazumi, “Mechanical Properties of Recycled CFRP by Injection Molding Method,” in *16Th International Conference on Composite Materials*, 2007, pp. 1–6.

[69] T. McNally *et al.*, “Recycled carbon fiber filled polyethylene composites,” *J. Appl. Polym. Sci.*, vol. 107, no. 3, pp. 2015–2021, Feb. 2008.

[70] E. Uhlmann and P. Meier, “Carbon Fibre Recycling from Milling Dust for the Application in Short Fibre Reinforced Thermoplastics,” *Procedia CIRP*, vol. 66, pp. 277–282, 2017.

[71] L. Altay *et al.*, “Manufacturing of Recycl ed Carbon Fiber ReinforcedPolypropylene Composites by High Speed Thermo-Kinetic Mixing for Lightweight Applications,” *Polym. Compos.*, 2017.

[72] K. Stoeffler, S. Andjelic, and N. Legros, “Polyphenylene sulfide (PPS) composites reinforced with recycled carbon fiber,” *Compos. Sci. Technol.*, vol. 84, pp. 65–71, 2013.

[73] G. Schinner, J. Brandt, and H. Richter, “Recycling Carbon-Fiber-Reinforced Thermoplastic Composites,” *Thermoplast. Compos. Mater.*, vol. 9, 1996.

[74] M. Mihai, K. Stoeffler, E. Lee, H. Lobo, and D. Houston, “Injection-Molded Composites Based on Recycled Carbon Fibers and Cellulosic Fibers Mihaela Mihai & Karen Stoeffler Automotive and Surface Transportation , National Research Council

Canada," in *Plastics-in-Motion*, 2017.

[75] M. Tomioka, T. Ishikawa, K. Okuyama, and T. Tanaka, "Recycling of carbon-fiber-reinforced polypropylene prepreg waste based on pelletization process," *J. Compos. Mater.*, vol. 51, no. 27, pp. 3847–3858, 2017.

[76] H. Lee, I. Ohsawa, and J. Takahashi, "Effect of plasma surface treatment of recycled carbon fiber on carbon fiber-reinforced plastics (CFRP) interfacial properties," *Appl. Surf. Sci.*, vol. 328, pp. 241–246, 2015.

[77] M. Hengstermann, N. Raithel, A. Abdkader, and C. Cherif, "Spinning of Staple Hybrid Yarn from Carbon Fiber Wastes for Lightweight Constructions," *Mater. Sci. Forum*, vol. 825–826, pp. 695–698, 2015.

[78] R. Lützkendorf, T. Reussmann, and M. Danzer, "Hybrid Composites with Recycled Carbon Fibres," *Light. Des.*, vol. 10, no. 2, pp. 16–19, 2017.

[79] J. Wölling, M. Schmieg, F. Manis, and K. Drechsler, "Nonwovens from recycled carbon fibres – comparison of processing technologies," *Procedia CIRP*, vol. 66, pp. 271–276, 2017.

[80] M. Hengstermann, N. Raithel, A. A. M. Science, and T. T. Publ, "Spinning of staple hybrid yarn from carbon fiber wastes for lightweight constructions Development of new hybrid yarn construction from recycled carbon fibers for high performance composites . Part - I : basic processing of hybrid carbon fiber / polyamide ," vol. 6, no. Pa 6, pp. 2016–2017, 2017.

[81] M. D. Wakeman, T. a. Cain, C. D. Rudd, R. Brooks, and A. C. Long, "Compression moulding of glass and PP composites for optimised macro- and micro- mechanical properties—1 commingled glass and polypropylene," *Compos. Sci. Technol.*, vol. 58, no. 98, pp. 1879–1898, 1998.

[82] A. C. Long, *Design and manufacture of Textile Composites*. Woodhead Publishing Limited, 2005.

[83] A. C. Caba, "Characterization of Carbon Mat Thermoplastic Composites : Flow and Mechanical Properties," Virginia Polytechnic Institute and State University, 2005.

[84] A. Arbelaiz, B. Fernández, J. A. Ramos, and I. Mondragon, "Thermal and crystallization studies of short flax fibre reinforced polypropylene matrix composites: Effect of treatments," *Thermochim. Acta*, vol. 440, no. 2, pp. 111–121, 2006.

[85] M. H. B. Snijder and H. L. Bos, “Reinforcement of polypropylene by annual plant fibers: Optimisation of the coupling agent efficiency,” *Compos. Interfaces*, vol. 7, no. 2, pp. 69–75, 2000.

[86] W. Thielemans, E. Can, S. S. Morye, and R. P. Wool, “Novel applications of lignin in composite materials,” *J. Appl. Polym. Sci.*, vol. 83, no. 2, pp. 323–331, 2002.

[87] T. J. Keener, R. K. Stuart, and T. K. Brown, “Maleated coupling agents for natural fibre composites,” *Compos. Part A*, vol. 35, pp. 357–362, 2004.

[88] A. Hassan, N. A. Rahman, and R. Yahya, “Extrusion and injection-molding of glass fiber/MAPP/polypropylene: Effect of coupling agent on DSC, DMA, and mechanical properties,” *J. Reinf. Plast. Compos.*, vol. 30, no. 14, pp. 1223–1232, 2011.

[89] S. Enoki and K. Kojima, “High-speed compression molding of continuous carbon fiber reinforced polypropylene,” *WIT Trans. State-of-the-art Sci. Eng.*, vol. 88, pp. 93–97, 2014.

[90] D. T. Burn *et al.*, “The usability of recycled carbon fibres in short fibre thermoplastics: interfacial properties,” *J. Mater. Sci.*, vol. 51, no. 16, pp. 7699–7715, 2016.

[91] B. Nagy, “Influence of Novel Types of Olefin-Maleicanhydride Copolymer Based Additives in Blends of PA and Recycled PET,” in *ICCM22*, 2019.

[92] J. Parameswaranpillai, G. Joseph, R. V. Chellappan, A. K. Zahakariah, and N. Hameed, “The effect of polypropylene-graft-maleic anhydride on the morphology and dynamic mechanical properties of polypropylene/polystyrene blends,” *J. Polym. Res.*, vol. 22, no. 2, 2015.

[93] S. Jose, S. Thomas, J. Parameswaranpillai, A. S. Aprem, and J. Karger-Kocsis, “Dynamic mechanical properties of immiscible polymer systems with and without compatibilizer,” *Polym. Test.*, vol. 44, pp. 168–176, 2015.

[94] J. D. H. Hughes, “The Carbon Fibre / Epoxy Interface - A Review,” *Compos. Sci. Technol.*, vol. 41, pp. 13–45, 1991.

[95] S. Park and G. Heo, *Carbon Fibers*. 1985.

[96] K. M. Beggs *et al.*, “Rapid surface functionalization of carbon fibres using microwave irradiation in an ionic liquid,” *RSC Adv.*, vol. 6, no. 39, pp. 32480–32483, 2016.

[97] K. Mason, “Advances in sizings and surface treatments for carbon fibers : CompositesWorld,” *Composites World*, 2004. [Online]. Available:

https://www.compositesworld.com/articles/advances-in-sizings-and-surface-treatments-for-carbon-fibers. [Accessed: 08-Oct-2018].

[98] N. Feng, X. Wang, and D. Wu, “Surface modification of recycled carbon fiber and its reinforcement effect on nylon 6 composites: Mechanical properties, morphology and crystallization behaviors,” *Curr. Appl. Phys.*, vol. 13, no. 9, pp. 2038–2050, 2013.

[99] E. Giebel, T. Herrmann, F. Simon, A. Fery, and M. R. Buchmeiser, “Surface Modification of Carbon Fibers by Free Radical Graft-Polymerization of 2-Hydroxyethyl Methacrylate for High Mechanical Strength Fiber-Matrix Composites,” *Macromol. Mater. Eng.*, vol. 302, no. 12, p. 1700210, 2017.

[100] M. Sharma, S. Gao, E. Mäder, H. Sharma, L. Y. Wei, and J. Bijwe, “Carbon Fiber Surfaces and Composite Interphases,” *Compos. Sci. Technol.*, vol. 102, pp. 35–50, 2014.

[101] A. Bismarck, M. Pfaffernoschke, J. Springer, and E. Schulz, “Polystyrene-grafted carbon fibers: Surface properties and adhesion to polystyrene,” *J. Thermoplast. Compos. Mater.*, vol. 18, no. 4, pp. 307–331, 2005.

[102] R. L. Clark, R. G. Kander, and B. B. Sauer, “Nylon 66 / poly (vinyl pyrrolidone) reinforced composites : 1 . Interphase microstructure and evaluation of fiber – matrix adhesion,” *Compos. Part A Appl. Sci. Manuf.*, vol. 30, pp. 27–36, 1999.

[103] Y. Xie, C. A. S. Hill, Z. Xiao, H. Militz, and C. Mai, “A Silane coupling agents used for natural fiber / polymer composites : A review,” *Compos. Part A*, vol. 41, no. 7, pp. 806–819, 2010.

[104] K. L. Pickering, M. G. A. Efendy, and T. M. Le, “A review of recent developments in natural fibre composites and their mechanical performance,” *Compos. Part A Appl. Sci. Manuf.*, vol. 83, pp. 98–112, 2015.

[105] V. Gupta, S. Kumar, and U. Vihar, “The Superior Coupling Agent for Glass Filled Polypropylene Composites.”

[106] E. Mäder, H. J. Jacobasch, K. Grundke, and T. Gietzelt, “Influence of an optimized interphase on the properties of polypropylene/glass fibre composites,” *Compos. Part A Appl. Sci. Manuf.*, vol. 27, no. 9 PART A, pp. 907–912, 1996.

[107] Carbon Composites, “Carbon Composites Magazin (German, Issue 2|2016),” 2016.

[108] a M. Rodrigues, S. Franceschi, E. Perez, J. Garrigues, J. Fitremann, and I. Giraud,

"Sustainable and recyclable thermoplastic sizing based on aqueous dispersion," *ICCM20, Int. Conf. Compos. Mater.*, no. July, pp. 19–24, 2015.

[109] I. Giraud *et al.*, "Preparation of aqueous dispersion of thermoplastic sizing agent for carbon fiber by emulsion / solvent evaporation To cite this version : HAL Id : hal-00835632," 2013.

[110] D. J. Eyckens *et al.*, "Synergistic interfacial effects of ionic liquids as sizing agents and surface modified carbon fibers," *J. Mater. Chem. A*, vol. 6, no. 10, pp. 4504–4514, 2018.

[111] B. K. Price, J. L. Hudson, and J. M. Tour, "Green Chemical Functionalization of Single-Walled Carbon Nanotubes in Ionic Liquids," pp. 14867–14870, 2005.

[112] B. Török and T. Dransfield, *Green chemistry : an inclusive approach*. .

[113] S. King, N. J. Boxall, and A. I. Bhatt, "Lithium battery recycling in Australia | CSIRO Report EP181926," 2018.

[114] J. F. Fernández, R. Bartel, U. Bottin-Weber, S. Stolte, and J. Thöming, "Recovery of Ionic Liquids from Wastewater by Nanofiltration," *J. Membr. Sci. Technol.*, no. 4, pp. 1–8, 2011.

[115] L. Thi, P. Trinh, Y. Ju, J. Lee, H. Bae, and H. Lee, "Recovery of an ionic liquid [BMIM] Cl from a hydrolysate of lignocellulosic biomass using electrodialysis," *Sep. Purif. Technol.*, vol. 120, pp. 86–91, 2013.

[116] R. Brooks, "Composites in Automotive Applications: Design," in *Comprehensive Composite Materials*, Elsevier Ltd., 2000.

[117] Gogoro, "Gogoro VIVA," *Gogoro Smart Scooter*, 2019. [Online]. Available: https://www.gogoro.com/smartscooter/viva/. [Accessed: 06-Oct-2019].

[118] EAV Cargo, "Home | EAV," *Electric Assisted Vehicles Ltd.*, 2019. [Online]. Available: https://www.eavcargo.com/. [Accessed: 06-Oct-2019].

[119] "Composites Solutions for Mobility – NetComposites," *NetComposites*, 2019. [Online]. Available: https://netcomposites.com/news/jec-group-composites-solutions-for-mobility/. [Accessed: 20-Oct-2019].

[120] S. T. Jespersen *et al.*, "Rapid processing of net-shape thermoplastic planar-random composite preforms," *Appl. Compos. Mater.*, vol. 16, no. 1, pp. 55–71, 2009.

[121] S. R. Coles *et al.*, "A Design of Experiments (DoE) Approach to material Properties

Optimization of Electrospun Nanofibers," *J. Appl. Polym. Sci.*, vol. 117, no. 5, pp. 2251–2257, 2010.

[122] R. M. Khan, *Problem Solving and Data Analysis using Minitab*. Loughborough: Wiley-VCH Verlag GmbH & Co. KGaA, 2013.

[123] J. Antony, *Design of Experiments for Engineers and Scientists*, 2nd ed. Elsevier Ltd., 2014.

[124] ELG Carbon Fibre Ltd., "Technical Note 1702 : Product Nomenclature," 2017. [Online]. Available: http://www.elgcf.com/presentations-and-papers. [Accessed: 16-May-2018].

[125] A. Gillet, O. Mantaux, and G. Cazaurang, "Characterization of composite materials made from discontinuous carbon fibres within the framework of composite recycling," *Compos. Part A*, vol. 75, pp. 89–95, 2015.

[126] A. K. Saelhoff *et al.*, "Matrix/fibre boundary layer in fibre reinforced plastics: Characterization of the adhesion," *Chem. Eng. Trans.*, vol. 32, pp. 1633–1638, 2013.

[127] E. Mäder, K. Grundke, H.-J. Jacobasch, and G. Wachinger, "Surface, Interphase and Composite Property Relations in Fibre-Reinforced Polymers," *Composites*, vol. 25, no. 7, pp. 739–744, 1994.

[128] M. Connor, P. H. Harding, J. A. E. Månson, and J. C. Berg, "Influence of the fiber surface properties on the mechanical strength of unidirectional fiber composites," *J. Adhes. Sci. Technol.*, vol. 9, no. 7, pp. 983–1004, 1995.

[129] J. H. Kamps *et al.*, "Electrolytic surface treatment for improved adhesion between carbon fibre and polycarbonate," *Materials (Basel).*, vol. 11, no. 11, 2018.

[130] B. Fernández, A. Arbelaiz, A. Valea, F. Mujika, and I. Mondragon, "A comparative study on the influence of epoxy sizings on the mechanical performance of woven carbon fiber-epoxy composites," *Polym. Compos.*, vol. 25, no. 3, pp. 319–330, 2004.

[131] Kruess, "Adhesion Energy and Interfacial Tension (AR232e)," 2003.

[132] M. Connor, S. Toll, and J.-A. E. Manson, "On the surface energy effects in composite impregnation," *Compos. Manuf.*, vol. 6, no. 3, pp. 289–295, 1995.

[133] N. Bernet, V. Michaud, P.-E. Bourban, and J.-A. E. Manson, "An Impregnation Model for the Consolidation of Thermoplastic Composites Made from Commingled Yarns," *Compos. Mater.*, vol. 33, no. 8, p. 22, 1999.

[134] K. S. Birdi, *Handbook of Surface and Colloid Chemistry*, 4th ed. CRC Press, 2016.

[135] J. Li, "The effect of surface modification with nitric acid on the mechanical and tribological properties of carbon fiber-reinforced thermoplastic polyimide composite," *Surf. Interface Anal.*, vol. 41, pp. 759–763, 2009.

[136] F. Su, Z. Zhang, K. Wang, W. Jiang, and W. Liu, "Tribological and mechanical properties of the composites made of carbon fabrics modified with various methods," *Compos. - Part A Appl. Sci. Manuf.*, vol. 36, pp. 1601–1607, 2005.

[137] L. Servinis *et al.*, "Electrochemical surface modification of carbon fibres by grafting of amine, carboxylic and lipophilic amide groups," *Carbon N. Y.*, vol. 118, pp. 393–403, 2017.

[138] J. C. Vickerman and I. S. Gilmore, *Surface Analysis - The Principal Techniques*. Wiley-VCH Verlag GmbH & Co. KGaA, 2009.

[139] ASTM Internationalcal, "Standard Test Method for Thermal Stability by Thermogravimetry (ASTM E2550 − 11: 2011)." ASTM International, pp. 2–6, 2011.

[140] BSI Standards Publication, "Plastics — Differential scanning calorimetry (DSC) Part 2 : Determination of glass transition temperature and glass transition step height (BS EN ISO 11357-2:2014)," 2014.

[141] BSI Standards Publication, "Plastics — Differential scanning calorimetry (DSC) Part 3 : Determination of temperature and enthalpy of melting and crystallization (ISO 11357-3:2011)," 2013.

[142] B. Mohebby, P. Fallah-Moghadam, A. R. Ghotbifar, and S. Kazemi-Najafi, "Influence of maleic-anhydride-polypropylene (MAPP) on wettability of polypropylene/wood flour/glass fiber hybrid composites," *J. Agric. Sci. Technol.*, vol. 13, no. 6, pp. 877–884, 2011.

[143] R. Rengarajan, V. R. Parameswaran, S. Lee, M. Vicic, and P. L. Rinaldi, "N.m.r. analysis of polypropylene-maleic anhydride copolymer," *Polymer (Guildf).*, vol. 31, no. 9, pp. 1703–1706, 1990.

[144] G. Wypych, "PP polypropylene," in *Handbook of Polymers*, vol. 5, 2016, pp. 497–504.

[145] G. Wypych, "PPMA polypropylene, maleic anhydride modified," *Handb. Polym.*, vol. 100, pp. 520–521, 2016.

[146] B. De Roover, M. Sclavons, V. Carlier, J. Devaux, R. Legras, and A. Momtaz, "Molecular

characterization of maleic anhydride-functionalized polypropylene," *J. Polym. Sci. Part A Polym. Chem.*, vol. 33, no. 5, pp. 829–842, 1995.

[147] A. Watzl, "Thermofusion, Thermobonding und Thermofixierung f€ur Nonwovens-Theoretische Grundlagen, Praktische Erfahrungen, Marktentwicklung (German)," *Melliand-Textilberichte*, vol. 75, no. 11, pp. 933–940, 1994.

[148] F. A. Tester, "Fibre-Matrix Adhesion Tester."

[149] Mm. Mäder, Edith; Mörschel, Ulrich; Effing, "Quality assessment of composites," *JEC Compos. Mag.*, vol. 102, no. February, pp. 49–51, 2016.

[150] S. F. Zhandarov, E. Mäder, and O. R. Yurkevich, "Indirect estimation of fiber/polymer bond strength and interfacial friction from maximum load values recorded in the microbond and pull-out tests. Part I: Local bond strength," *J. Adhes. Sci. Technol.*, vol. 16, no. 9, pp. 1171–1200, 2002.

[151] J. A. Nairn, "Analytical fracture mechanics analysis of the pull-out test including the effects of friction and thermal stresses," *Adv. Compos. Lett.*, vol. 9, no. 6, pp. 373–383, 2000.

[152] BSI Standards Publication, "Plastics - Determination of Tensile Properties - Part 4: Test conditions for isotropic and orthotropic fibre-reinforced plastic composites (BS EN ISO 527-4)," 1997.

[153] BSI Standards Publication, "Fibre-reinforced plastic composites — Determination of flexural properties (BS EN ISO 14125)," 2011.

[154] J. H. Kamps *et al.*, "Electrolytic surface treatment for improved adhesion between carbon fibre and polycarbonate," *Materials (Basel).*, vol. 11, no. 11, pp. 1–20, 2018.

[155] K. Tsutsumi, S. Ishida, and K. Shibata, "Determination of the surface free energy of modified carbon fibers and its relation to the work of adhesion," *Colloid Polym. Sci.*, vol. 268, no. 1, pp. 31–37, 1990.

[156] C. Unterweger, J. Duchoslav, D. Stifter, and C. Fürst, "Characterization of carbon fiber surfaces and their impact on the mechanical properties of short carbon fiber reinforced polypropylene composites," *Compos. Sci. Technol.*, vol. 108, pp. 41–47, 2015.

[157] M. Gonçalves, M. Molina-Sabio, and F. Rodriguez-Reinoso, "Modification of activated carbon hydrophobicity by pyrolysis of propene," *J. Anal. Appl. Pyrolysis*, vol. 89, no. 1,

pp. 17–21, 2010.

[158] L. Y. Meng and S. J. Park, “Effect of fluorination of carbon nanotubes on superhydrophobic properties of fluoro-based films,” *J. Colloid Interface Sci.*, vol. 342, no. 2, pp. 559–563, 2010.

[159] R. Blossey and C. Scientifique, “Self-cleaning surfaces — virtual realities,” *Nat.*, vol. 2, pp. 301–306, 2003.

[160] B. Davis, P. Gramann, T. A. Osswald, and A. Rios, *Compression Molding*. Munich: Hanser Gardner Publications, Inc., 2003.

[161] D. C. Montgomery, *Design and analysis of experiments*, 7th ed. John Wiley & Sons Ltd, 2009.

[162] K. Giannadakis, M. Szpieg, and J. Varna, “Mechanical Performance of a Recycled Carbon Fibre/PP Composite,” *Exp. Mech.*, vol. 51, no. 5, pp. 767–777, 2011.

[163] BSI Standards Publication, “Plastics - Polypropylene (PP) moulding and extrusion materials - Part 2: Preparation of test specimens and determination of properties (BS EN ISO 1873-2),” 2007.

[164] BSI Standards Publication, “Plastics - Compression moulding of test specimens of thermoplastic materials (BS EN ISO 293),” 2005.

[165] D. Rosato, D. Rosato, and M. Rosato, *Plastic Product Material and Process Selection Handbook*. Elsevier, 2004.

[166] S. Lunau, *Six Sigma Toolset: Executing Improvement Projects Successfully*. Heidelberg: Springer, 2008.

[167] N. Reynolds, S. Awang-Ngah, G. Williams, and D. Hughes, “Structural thermoplastic composites via the direct processing of hybrid textiles using rapid isothermal stamp forming,” *Prog.*

[168] D. T. Burn, “Long Discontinuous Carbon Fibre / Polypropylene Composites for High Volume Automotive Applications,” University of Nottingham, 2016.

[169] M. D. Wakeman, P. Blanchard, and J. A. E. Månson, “Void evolution during stamp-forming of thermoplastic composites,” *Proc. of*, vol. 1001, no. July, p. 15, 2005.

[170] D. Trudel-Boucher, B. Fisa, J. Denault, and P. Gagnon, “Experimental investigation of stamp forming of unconsolidated commingled E-glass/polypropylene fabrics,” *Compos. Sci. Technol.*, vol. 66, no. 3–4, pp. 555–570, 2006.

[171] C. Santulli, R. Brooks, C. D. Rudd, and A. C. Long, “Influence of microstructural voids on the mechanical and impact properties in commingled E-glass/polypropylene thermoplastic composites,” *Proc. I MECH E Part L J. Mater. Appl.*, vol. 216, no. 2, pp. 85–100, 2002.

[172] M. D. Wakeman and J.-A. E. Manson, “Stamp-forming of Reactive-Thermoplastic Carbon fibre PA12 composite Sheet.” .

[173] M. Biron, “Thermoplastic Composites,” in *Thermoplastics and Thermoplastic Composites*, 2013, pp. 767–828.

[174] W. Grzesik, *Advanced machining processes of metallic materials : theory, modelling and applications*. Elsevier, 2008.

[175] W. Albrecht, H. Fuchs, and W. Kittelmann, *Nonwoven Fabrics*. Wiley-VCH Verlag GmbH & Co. KGaA, 2003.

[176] N. O. Cabrera, C. T. Reynolds, B. Alcock, and T. Peijs, “Non-isothermal stamp forming of continuous tape reinforced all-polypropylene composite sheet,” *Compos. Part A Appl. Sci. Manuf.*, vol. 39, no. 9, pp. 1455–1466, 2008.

[177] A. G. Gibson and J.-A. E. Manson, “Impregnation technology for thermoplastic matrix composites,” *Compos. Manuf.*, vol. 3, no. 4, 1992.

[178] E. Chibowski, “On some relations between advancing, receding and Young’s contact angles,” *Adv. Colloid Interface Sci.*, vol. 133, no. 1, pp. 51–59, 2007.

[179] A. Kaminska, H. Kaczmarek, and J. Kowalonek, “The influence of side groups and polarity of polymers on the kind and effectiveness of their surface modification by air plasma action,” *Eur. Polym. J.*, vol. 38, pp. 1915–1919, 2002.

[180] R. Mahlberg, H. E. M. Niemi, F. Denes, and R. M. Rowell, “Effect of oxygen and hexamethyldisiloxane plasma on morphology, wettability and adhesion properties of polypropylene and lignocellulosics,” *Int. J. Adhes. Adhes.*, vol. 18, no. 4, pp. 283–297, 1998.

[181] C. Rulison, “Interfacial Tension as a Predictor of the Completeness of Pore Wetting in Epoxy Resin Impregnated Non-Woven Glass (AR248e),” *Kruess - Application Report*, vol. 101, no. 10. p. 87, 2005.

[182] G. Zitzenbacher, H. Dirnberger, M. Laengauer, and C. Holzer, “Calculation of the Contact Angle of Polymer Melts on Tool Surfaces from Viscosity Parameters,”

Polymers (Basel)., vol. 10, no. 38, 2018.

[183] D. Y. Kwok, L. K. Cheung, C. B. Park, and A. W. Neumann, "Study on the surface tensions of polymer melts using axisymmetric drop shape analysis," *Polym. Eng. Sci.*, vol. 38, no. 5, 1998.

[184] M. Åkermo and B. T. Åström, "Modelling component cost in compression moulding of thermoplastic composite and sandwich components," *Compos. Part A Appl. Sci. Manuf.*, vol. 31, no. 4, pp. 319–333, 2000.

[185] M. D. Wakeman and J.-A. E. Manson, "Cost Analysis," in *Design and Manufacture of Textile Composites*, Cambridge: Woodhead Publishing Limited, 2005.

[186] K. Kendall, C. Mangin, and E. Ortiz, "Discrete event simulation and cost analysis for manufacturing optimisation of an automotive LCM component," *Compos. Part A Appl. Sci. Manuf.*, vol. 29, no. 7, pp. 711–720, 1998.

[187] T. Gutowski *et al.*, "Development of a theoretical cost model for advanced composite fabrication," *Compos. Manuf.*, vol. 5, no. 4, pp. 231–239, 1994.

[188] M. D. Wakeman, L. Zingraff, P. E. Bourban, J. A. E. Månson, and P. Blanchard, "Stamp forming of carbon fibre/PA12 composites - A comparison of a reactive impregnation process and a commingled yarn system," *Compos. Sci. Technol.*, vol. 66, no. 1, pp. 19–35, 2006.

[189] T. A. Turner, L. T. Harper, N. A. Warrior, and C. D. Rudd, "Low cost carbon fibre based automotive body panel systems: a performance and manufacturing cost comparison," *Proc. Inst. Mech. Eng. Part D J. Automob. Eng.*, vol. 222, pp. 53–63, 2008.

[190] L. T. Harper, "Discontinuous Carbon Fibre Composites for Automotive Applications," University of Nottingham, 2006.

[191] Thomas Schalm | ELKOM, *Quote: Mikutherm Optimal 2111*. Oeynhausen, 2019.

[192] UK Power, "Compare Energy Prices Per kWh | Gas & Electric Per Unit | UKPower." [Online]. Available: https://www.ukpower.co.uk/home_energy/tariffs-per-unit-kwh. [Accessed: 13-Oct-2019].

[193] Mitsubishi Chemical Advanced Materials Composites, "GMT Glass Mat D100F40-F1 (Technical Datasheet)," Lenzburg, Switzerland, 2019.

[194] Mitsubishi Chemical Advanced Materials Composites, "GMT Glass Mat G100F40-F6

(Technical Datasheet)," Lenzburg, Switzerland, 2019.

[195] Mitsubishi Chemical Advanced Materials Composites, "GMT Glass Mat 0/90 X121F42-4/1 (Technical Datasheet)," Lenzburg, Switzerland, 2019.

[196] P. K. Mallick, "Thermoset-matrix composites for lightweight automotive structures," in *Materials, Design and Manufacturing for Lightweight Vehicles*, Woodhead Publishing Limited, 2010, pp. 208–231.

[197] M. Karlsson, "The development of a technical cost model for composites," KTH Stockholm, 2013.

[198] S. Kalpakjian and R. S. Schmid, "Physical Properties of Materials," in *Manufacturing Engineering and Technology*, 7th ed., Singapore: Pearson Education South Asia Pte Ltd, 2014.

[199] "StrongLite(GMT), Light and Str... | Hanwha." [Online]. Available: https://www.hanwha.com/en/news_and_media/business_highlights/gmt_light_and_strong_the_realistic_answer_for_shedding_car_weight.html. [Accessed: 20-Oct-2019].

[200] H. Boyle, "Improving the Fibre-Matrix Interface of Recycled Carbon Fibre Composites," Bachelor Thesis, University of Warwick, 2019.

[201] F. Gray, "Investigating the Effect of Maleic Anhydride on Recycled Carbon Fibre-Reinforced Polypropylene Composites," Bachelor Thesis, University of Warwick, 2018.

[202] M. Sclavons *et al.*, "Quantification of the maleic anhydride grafted onto polypropylene by chemical and viscosimetric titrations, and FTIR spectroscopy," *Polymer (Guildf).*, vol. 41, no. 6, pp. 1989–1999, 2000.

[203] E. Schröder, G. Müller, and K.-F. Arndt, *Polymer Characterisation*. New York: Oxford University Press, 1989.

[204] C. Maier and T. Calafut, *Polypropylene: The Definitive User's Guide and Databook*. New York: Plastics Design Library, 1998.

[205] M. P. Stevens, *Polymer Chemistry: An Introduction*, 3rd ed. New York: Oxford University Press, 1999.

[206] "Chapter 3 – Solid-Liquid Interface," in *Interface Science and Technology*, vol. 18, 2011, pp. 147–252.

[207] I. Novák, E. Borsig, L. Hrčková, A. Fiedlerová, A. Kleinová, and V. Pollák, "Study of surface and adhesive properties of polypropylene grafted by maleic anhydride," *Polym. Eng. Sci.*, vol. 47, no. 8, pp. 1207–1212, 2007.

[208] A. R. Sanadi, D. F. Caulfield, R. E. Jacobson, and R. M. Rowell, "Renewable Agricultural Fibers as Reinforcing Fillers in Plastics: Mechanical Properties of Kenaf Fiber-Polypropylene Composites," *Ind. Eng. Chem. Res.*, vol. 34, no. 5, pp. 1889–1896, 1995.

[209] M. D. Tabone, J. J. Gregg, E. J. Beckman, and A. E. Landis, "Sustainability metrics: Life cycle assessment and green design in polymers," *Environ. Sci. Technol.*, vol. 44, pp. 8264–8269, 2010.

[210] Franklin Associates, "Cradle-To-Gate Life Cycle Inventory of Nine Plastic Resins and four Polyurethane Precursors," *Am. Chem. Counc.*, pp. 1–198, 2011.

[211] G. P. Thomas, "Recycling of Polypropylene (PP)," *AZoNetwork*, 2012. [Online]. Available: https://www.azocleantech.com/article.aspx?ArticleID=240. [Accessed: 02-Sep-2019].

[212] S. Zande, "The UV resistance of polypropylene and polyester explained," *Service Thread*, 2015. [Online]. Available: https://www.servicethread.com/blog/the-uv-resistance-of-polypropylene-and-polyester-explained. [Accessed: 03-Sep-2019].

[213] A. Gupta, "Improving UV resistance of high strength fibers," North Carolina State University, 2005.

[214] V. H. Grassian, *Environmental Catalysis*. New York: Taylor & Francis Group, 2005.

[215] H. Althaus *et al.*, "Life cycle inventories of chemicals. ecoinvent report No.8, v2.0.," *Final Rep. ecoinvent data …*, no. 8, pp. 1–957, 2007.

[216] J. A. Kent, *Handbook of Industrial Chemistry and Biotechnology*, 12th ed. Springer, 2012.

[217] Sigma Aldrich, "Maleic anhydride (Safety Data Sheet)," no. 1907. pp. 1–9, 2018.

[218] M. L. Hendewerk, "Polypropylene Composition and Method for Functionalization of Polypropylene," US5001197, 1989.

[219] T. D. Roberts and S. W. Coe, "Maleated high acid number high molecular weight polypropylene of low color," US7683134B2, 21-Jul-2008.

[220] H. Huang, V. Singh, and N. Qureshi, "Butanol production from food waste: a novel process for producing sustainable energy and reducing environmental pollution,"

Biotechnol. Biofuels, vol. 8, no. 1, pp. 1–12, 2015.

[221] B. Ndaba, I. Chiyanzu, and S. Marx, "N-Butanol derived from biochemical and chemical routes: A review," *Biotechnol. Reports*, vol. 8, pp. 1–9, 2015.

[222] D. Bélanger and J. Pinson, "Electrografting: A powerful method for surface modification," *Chem. Soc. Rev.*, vol. 40, no. 7, pp. 3995–4048, 2011.

[223] S. Baranton and D. Bélanger, "Electrochemical Derivatization of Carbon Surface by Reduction of in Situ Generated," *Phys. Chem. B*, vol. 109, pp. 24401–24410, 2005.

[224] J. Pinson and F. Podvorica, "Attachment of organic layers to conductive or semiconductive surfaces by reduction of diazonium salts," *Chem. Soc. Rev.*, vol. 34, no. 5, pp. 429–439, 2005.

[225] M. Delamar, G. Désarmot, O. Fagebaume, R. Hitmi, J. Pinson, and J.-M. Savéant, "Modification of Carbon Fibre Surfaces by Electrochemical Reduction of Aryl Diazonium Salts: Application to Carbon Epoxy Composites," *Carbon N. Y.*, vol. 35, no. 6, pp. 801–807, 1997.

[226] K. M. Beggs, "Optimising Surface Functionalisation of Carbon Fibre to Enhance Interfacial Adhesion By," Deakin University, 2017.

[227] C. Froemder, K. Kirwan, S. R. Coles, N. Reynolds, P. R. Wilson, and F. C. Fernandes, "Investigation of the Processability of Hybrid Thermoplastic Nonwoven Including Recycled," *SAMPE Eur. Conf. 2018*, no. September, 2018.

[228] C. Froemder, F. Stojcevski, L. C. Henderson, J. Randall, and S. R. Coles, "Investigation of the Process Resistance of Fibre Surface Treatments for Thermoplastic Composites using Recycled Carbon Fibre," in *International Conference on Composite Materials (ICCM22)*, 2019, no. September, pp. 4–6.

[229] N. Le Moigne, B. Otazaghine, S. Corn, H. Angellier-Coussy, and A. Bergeret, "Modification of the Interface/Interphase in Natural Fibre Reinforced Composites: Treatments and Processes," in *Surfaces and Interfaces in Natural Fibre Reinforced Composites*, Alès: Springer, 2018, p. 149.

[230] European Comission, "Top emerging bio-based products, their properties and industrial applications," Berlin, 2018.

[231] S. Armioun, S. Panthapulakkal, J. Scheel, J. Tjong, and M. Sain, "Biopolyamide hybrid composites for high performance applications," vol. 43595, pp. 1–9, 2016.

[232] R. Nealer, D. Reichmuth, and D. Anair, “Cleaner Cars from Cradle to Grave,” *Union of Concerned Scientists*, 2015. [Online]. Available: https://www.ucsusa.org/clean-vehicles/electric-vehicles/life-cycle-ev-emissions. [Accessed: 30-Jul-2018].

[233] J. Howarth, S. S. R. Mareddy, and P. T. Mativenga, “Energy intensity and environmental analysis of mechanical recycling of carbon fibre composite,” *J. Clean. Prod.*, vol. 81, pp. 46–50, 2014.

[234] J. Clavreul, H. Baumeister, T. H. Christensen, and A. Damgaard, “An environmental assessment system for environmental technologies,” *Environ. Model. Softw.*, vol. 60, pp. 18–30, 2014.

[235] ATF Professional LLP, “£1 million boost for UK smart waste tracking | ATF Professional,” *ATF Professional LLP Online Magazine*, 2019. [Online]. Available: https://atfpro.co.uk/1-million-boost-for-uk-smart-waste-tracking/. [Accessed: 22-Oct-2019].

[236] Defra & UK Government, “Classify different types of waste,” 2019. [Online]. Available: https://www.gov.uk/how-to-classify-different-types-of-waste. [Accessed: 22-Oct-2019].

[237] J. M. Allwood, “Squaring the Circular Economy: The Role of Recycling within a Hierarchy of Material Management Strategies,” in *Handbook of Recycling: State-of-the-art for Practitioners, Analysts, and Scientists*, Elsevier Inc., 2014, pp. 445–477.

[238] G. A. Pauli, *The Blue Economy: 10 Years, 100 Innovations, 100 Million Jobs*. New Mexico: Redwing Book Company, 2010.

[239] M. Charter, *Designing for the Circular Economy*. New York: Apex CoVantage LLC, 2019.

APPENDIX A: DATA SET OF RCF THERMOPLASTIC APPLICATIONS

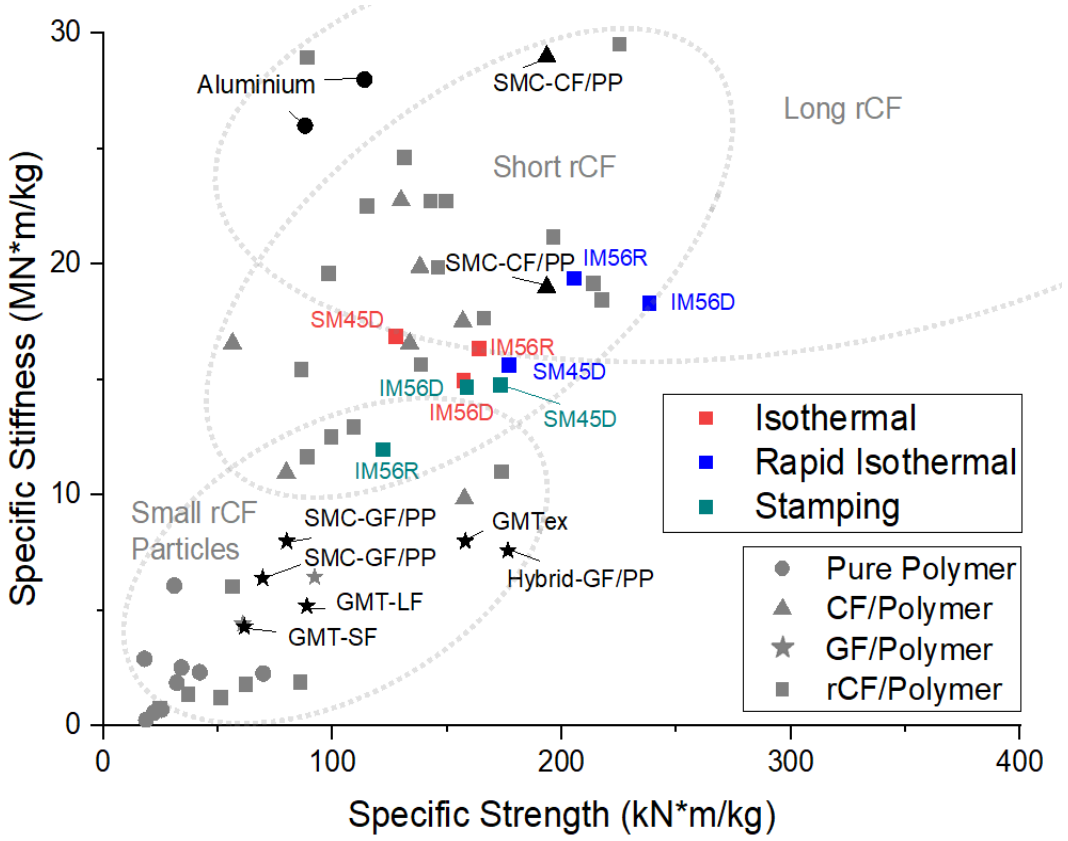

The data shown in this figure derived from a systematic literature review (CF – carbon fibre reinforced thermoplastics, GF – glass fibre reinforced thermoplastics, rCF – recycled fibre reinforced thermoplastics) and also include the experimental results.

APPENDIX B: DESIGN OUTCOME (DOE, DOE2)

Table 0-1: Experimental test matrix of DOE showing combinations of applied input factors investigating two levels, with its low level for a screening design based on a ½ factorial model. Response values and quality control is given by tensile strength, tensile modulus and porosity respectively.

NO.	INPUT FACTORS					RESPONSE VALUES		QUALITY
Run	Moulding Temperature [°C]	Moulding Time [min]	Cooling Rate [K/min]	Moulding Pressure [bar]	Mould Fill [%]	Tensile Strength [MPa]	Tensile Modulus [GPa]	Porosity [vol%]
1	200	2	5	5.21	130	**99.54 ± 2.08**	**7.68 ± 0.04**	**14.10 ± 1.28**
2	200	2	5	15.62	100	**179.49 ± 6.64**	**16.03 ± 1.58**	**7.07 ± 0.90**
3	200	2	20	5.21	100	**157.70 ± 4.34**	**11.80 ± 0.74**	**11.03 ± 0.73**
4	200	2	20	15.62	130	**184.13 ± 2.41**	**15.24 ± 0.18**	**8.13 ± 0.84**
5	200	10	5	5.21	100	**154.51 ± 4.70**	**14.48 ± 0.90**	**13.49 ± 0.86**
6	200	10	5	15.62	130	**201.60 ± 1.50**	**16.19 ± 0.52**	**6.55 ± 0.48**
7	200	10	20	5.21	130	**113.81 ± 1.77**	**8.74 ± 0.32**	**16.91 ± 0.96**
8	200	10	20	15.6	100	**120.69 ± 0.88**	**10.41 ± 1.25**	**10.32 ± 0.10**
9	240	2	5	5.21	100	**138.90 ± 7.49**	**12.01 ± 1.04**	**14.54 ± 1.02**
10	240	2	5	15.62	130	**176.21 ± 1.43**	**14.64 ± 0.37**	**5.49 ± 0.25**
11	240	2	20	5.21	130	**164.90 ± 4.59**	**13.84 ± 0.21**	**8.66 ± 0.21**
12	240	2	20	15.62	100	**128.60 ± 0.06**	**10.06 ± 0.39**	**8.04 ± 1.88**
13	240	10	5	5.21	130	**168.45 ± 6.52**	**15.53 ± 1.51**	**9.09 ± 1.02**
14	240	10	5	15.62	100	**108.38 ± 0.11**	**9.33 ± 0.09**	**10.76 ± 0.25**
15	240	10	20	5.21	100	**167.99 ± 4.80**	**14.05 ± 0.72**	**11.55 ± 0.96**

16	240	10	20	15.62	130	**121.83 ± 3.71**	**10.87 ± 0.72**	**9.36 ± 0.13**

Table 0-2: Experimental test matrix of DOE2 showing combinations of applied input factors investigating two levels, with its low level for a screening design based on a ½ factorial model. Response values and quality control is given by tensile strength, tensile modulus and porosity respectively.

NO.	INPUT FACTORS					RESPONSE VALUES		QUALITY
Run	Moulding Temperature [°C]	Moulding Time [min]	Cooling Rate [K/min]	Moulding Pressure [bar]	Mould Fill [%]	Tensile Strength [MPa]	Tensile Modulus [GPa]	Porosity [vol%]
1	200	2	5	5.21	130	**99.54 ± 2.08**	**7.68 ± 0.04**	**14.10 ± 1.28**
2	200	2	5	15.62	100	**213.26 ± 7.96**	**14.82 ± 1.15**	**12.18 ± 0.70**
3	200	2	20	5.21	100	**157.70 ± 4.34**	**11.80 ± 0.74**	**11.03 ± 0.73**
4	200	2	20	15.62	130	**127.11 ± 4.10**	**10.10 ± 0.33**	**8.23 ± 0.60**
5	200	10	5	5.21	100	**154.51 ± 4.70**	**14.48 ± 0.90**	**13.49 ± 0.86**
6	200	10	5	15.62	130	**144.17 ± 2.82**	**10.72 ± 0.35**	**8.87 ± 0.26**
7	200	10	20	5.21	130	**113.81 ± 1.77**	**8.74 ± 0.32**	**16.91 ± 0.96**
8	200	10	20	15.6	100	**131.85 ± 4.93**	**9.88 ± 0.45**	**11.79 ± 1.32**
9	240	2	5	5.21	100	**138.90 ± 7.49**	**12.01 ± 1.04**	**14.54 ± 1.02**
10	240	2	5	15.62	130	**149.37 ± 3.01**	**10.51 ± 1.19**	**7.95 ± 0.65**
11	240	2	20	5.21	130	**164.90 ± 4.59**	**13.84 ± 0.21**	**8.66 ± 0.21**
12	240	2	20	15.62	100	**150.85 ± 2.16**	**10.06 ± 0.39**	**8.00 ± 0.59**
13	240	10	5	5.21	130	**168.45 ± 6.52**	**15.53 ± 1.51**	**9.09 ± 1.02**
14	240	10	5	15.62	100	**133.37 ± 3.04**	**10.97 ± 0.18**	**13.76 ± 0.43**
15	240	10	20	5.21	100	**167.99 ± 4.80**	**14.05 ± 0.72**	**11.55 ± 0.96**

16	240	10	20	15.62	130	**138.72 ± 2.02**	**10.30 ± 0.15**	**7.85 ± 1.02**

APPENDIX C: XPS ANALYSIS - C1S SPECTRA OF ELGCF FEEDSTOCK

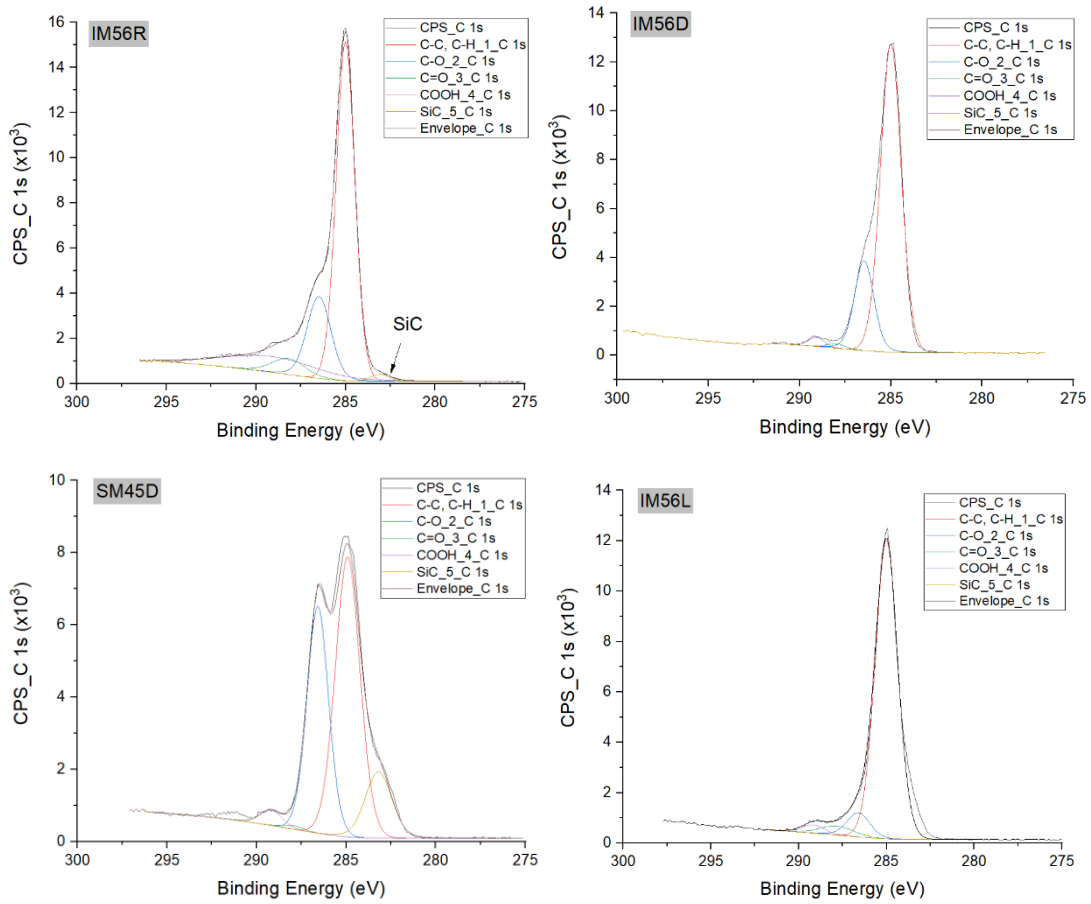

Figure 0-1: C1s spectra of SM45D, IM56D, IM56R and IM56L fibre type as developed using the CasaXPS Software.

APPENDIX D: SOLVENT VERSUS WATER-BASED TREATMENT

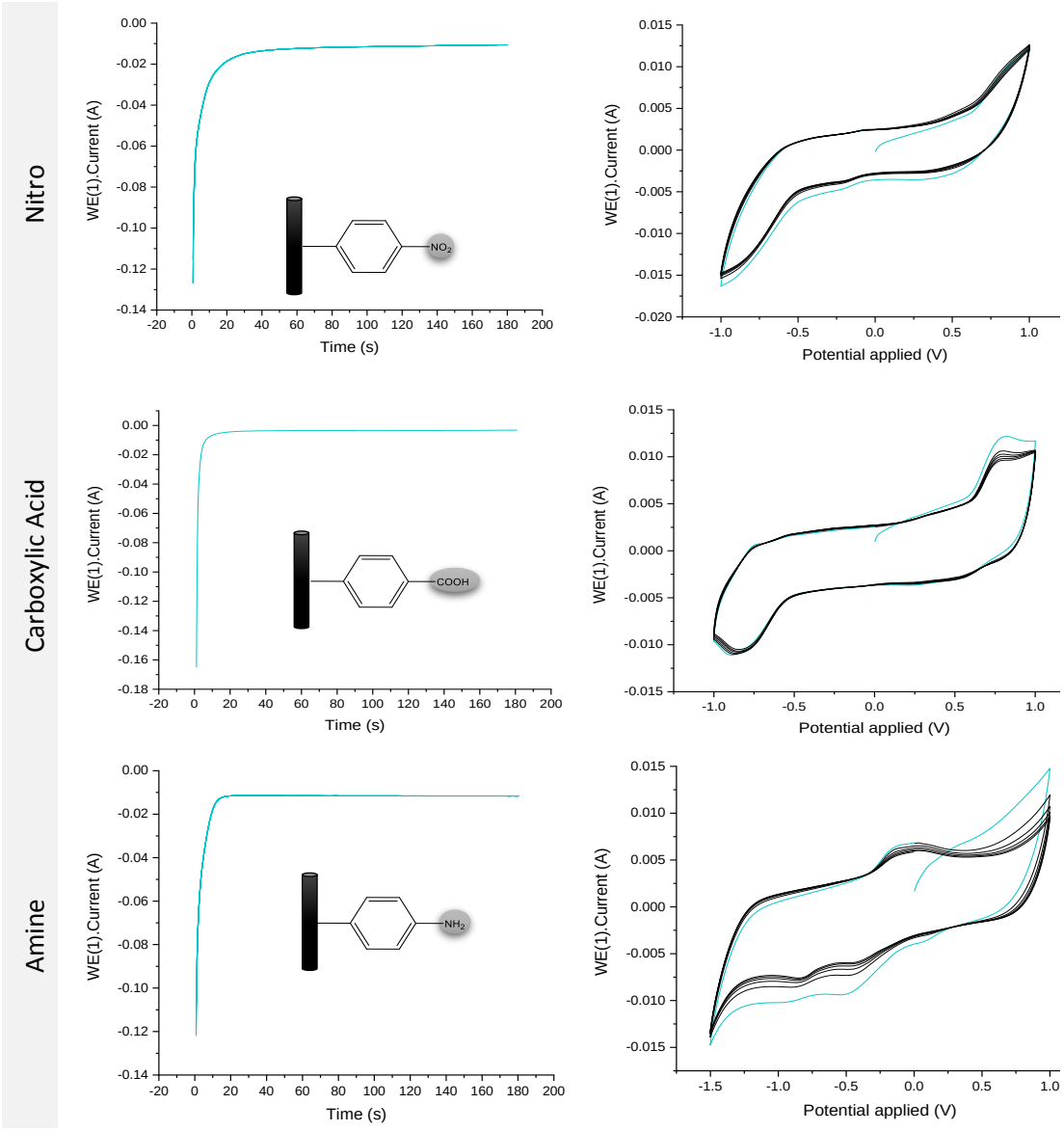

Figure 0-1: CA treatment at -1 V (3 min) is shown targeting nitro (0.1A) and carboxylic acid (0.2A) and the subsequent CV as check (right). Reduction was conducted at -1.5 V.

All scans show a typical course of the reaction as is typical for this system suggesting the grafting was completed within the given time frame. In comparison to the previous solvent-based treatment, a water-based treatment was applied where the same potential of -1V was applied continuously for 3 min to graft nitro groups in suit onto the fibre surface. The subsequent reduction was performed at -1.5V. The more sustainable treatments were investigated as alternative and potential future application in industry.

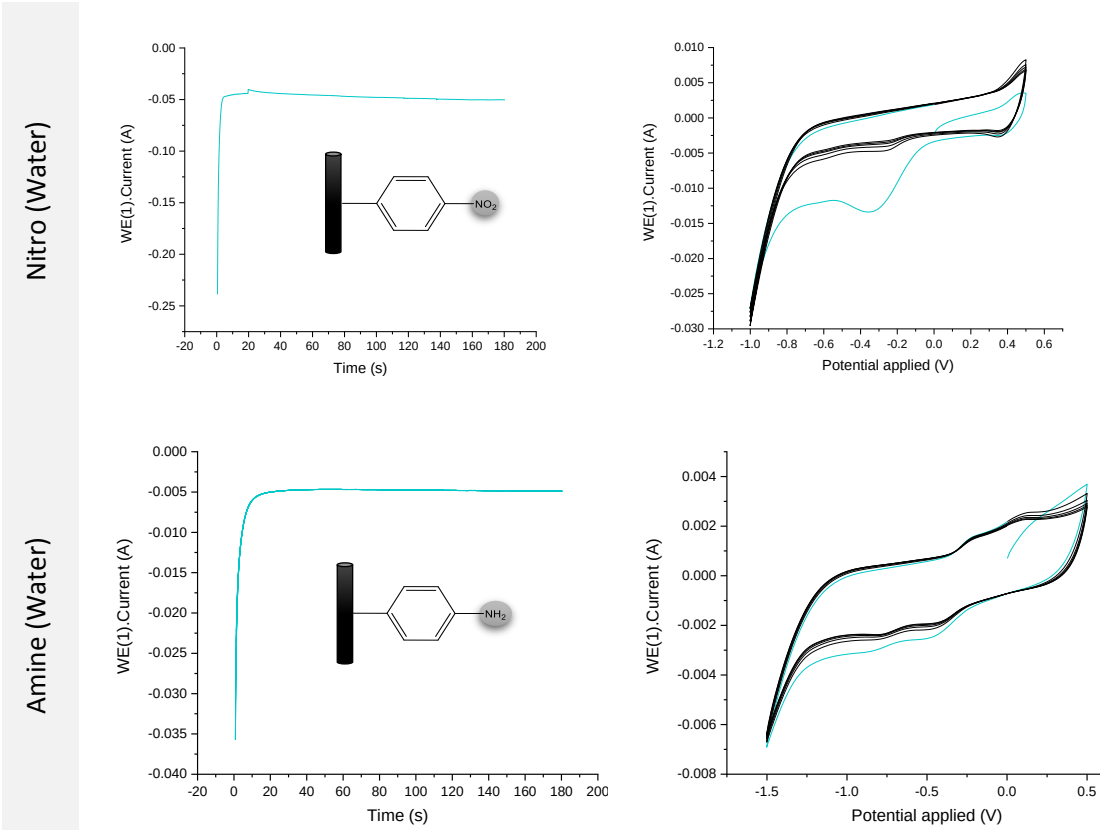

Figure 0-2: Chronoamperogram for treatment at -1 V (3 min) of nitro functionalised fibres for the actual electro grafting (left) and the subsequent cyclic voltammogram as check (right) with the subsequent reduction occurring at a treatment of 3 min at -1.5V.

The cyclic voltammogram taken after the grafting shows that the process was not yet completed within the 3 min time frame. No further adjustment has been carried out to have a straight comparison to the other treatments. The reduction from nitro to amine groups shows similar reduction peaks as the solvent-based treatment suggesting a comparable quality. The generally lower measured current was suggesting a limited reaction due to a lower number of available and reducible nitro groups as previously mentioned.